

Technical Report

TR-99-07

**Background report
to SR 97**

SR 97

**Processes in the
repository evolution**

November 1999

Svensk Kärnbränslehantering AB

Swedish Nuclear Fuel
and Waste Management Co
Box 5864

SE-102 40 Stockholm Sweden

Tel 08-459 84 00

+46 8 459 84 00

Fax 08-661 57 19

+46 8 661 57 19



**Background report
to SR 97**

SR 97

Processes in the repository evolution

November 1999

Foreword

This report describes, in a comprehensive and coherent fashion, all identified internal processes of importance for the post-closure evolution and safety of a KBS-3 repository for spent nuclear fuel.

The report has been written to be used in the SR 97 project, which has limited the time available for its preparation. Differences in the level of detail in descriptions of different processes do not always reflect differences in the significance of the processes. Discussions of different types of uncertainties could in many cases be broadened and deepened, and the stylistic quality could sometimes be improved.

Like other background material for the safety assessments, the process report is also expected to require revision as site-specific conditions are progressively clarified.

Today's version of the process report is therefore the first version of a report that will be revised prior to every safety report. The intention is to perform the first revision of the report after scrutiny of SR 97. The material will then also be linked to SKB's FEP database.

Many authors inside and outside SKB have contributed to this version:

Processes in fuel and canister: Lars Werme, SKB

Processes in buffer/backfill: Harald Hökmark, Clay Technology (thermal processes); Lennart Börgesson, Clay Technology (hydraulic and mechanical processes); Ola Karnland, Clay Technology (chemical processes) and Patrik Sellin, SKB (radionuclide transport). Roland Pusch, Geodevelopment AB, has also contributed to the buffer section.

Processes in the geosphere: Harald Hökmark, Clay Technology (T, M); Ingvar Rhén, VBB Viak (H); Peter Wikberg and Jan-Olof Selroos, SKB (C and radionuclide transport, respectively).

Furthermore, Karsten Pedersen of the Department of General and Marine Microbiology at Göteborg University has contributed material on bacterial processes in buffer and geosphere.

The material has been discussed with the authors in a group consisting of Johan Andersson, Golder Grundteknik, Patrik Sellin, SKB (processes in fuel, canister and buffer/backfill), Jan-Olof Selroos, SKB (processes in geosphere) and the undersigned.

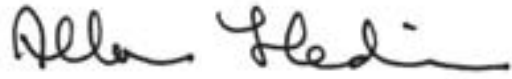
Kristina Skagius, Kemakta Konsult AB, has checked the contents of the report against the documentation of the interaction matrices used to select the processes.

The undersigned is responsible for the format of the process descriptions, as well as for editing the text. Karin Pers, Kemakta Konsult AB, assisted in the final phase of the editing.

We would like to express our sincere gratitude to all those who have contributed material and then, often with great patience, answered countless questions and accommodated sometimes extensive requests for reworking.

SKB is responsible for the material and conclusions presented in the report.

Stockholm in October 1999

A handwritten signature in black ink, appearing to read "Allan Hedin". The signature is written in a cursive style with a long horizontal stroke at the end.

Allan Hedin

Contents

| | Page |
|--|-------------|
| 1 Introduction | 9 |
| 1.1 References | 10 |
| 2 Fuel/cavity in canister | 11 |
| 2.1 Description of fuel/cavity | 11 |
| 2.1.1 General | 11 |
| 2.1.2 Overview of variables | 12 |
| 2.1.3 Detailed description of fuel structure and radionuclide distribution in the structure | 13 |
| 2.2 Overview of processes | 18 |
| 2.3 Radiation-related processes | 20 |
| 2.3.1 Radioactive decay | 20 |
| 2.3.2 Radiation attenuation/heat generation | 21 |
| 2.3.3 Induced fission (criticality) | 23 |
| 2.4 Thermal processes | 24 |
| 2.4.1 Heat transport | 24 |
| 2.5 Hydraulic processes | 26 |
| 2.5.1 Water and gas transport in canister cavity, boiling/condensation | 26 |
| 2.6 Mechanical processes | 29 |
| 2.6.1 Thermal expansion/cladding failure | 29 |
| 2.7 Chemical processes | 30 |
| 2.7.1 Advection and diffusion | 30 |
| 2.7.2 Residual gas radiolysis/acid formation | 30 |
| 2.7.3 Water radiolysis | 32 |
| 2.7.4 Metal corrosion | 33 |
| 2.7.5 Fuel dissolution | 36 |
| 2.7.6 Dissolution of gap inventory | 39 |
| 2.7.7 Speciation of iron corrosion products | 40 |
| 2.7.8 Speciation of radionuclides, colloid formation | 42 |
| 2.7.9 Helium production | 48 |
| 2.8 Radionuclide transport | 49 |
| 2.9 References | 52 |
| 3 Cast iron insert/copper canister | 57 |
| 3.1 Description of cast iron insert and copper canister | 57 |
| 3.1.1 General | 57 |
| 3.1.2 Overview of variables | 58 |
| 3.2 Overview of processes | 58 |
| 3.3 Radiation-related processes | 60 |
| 3.3.1 Radiation attenuation/heat generation | 60 |
| 3.4 Thermal processes | 61 |
| 3.4.1 Heat transport | 61 |
| 3.5 Hydraulic processes | 63 |

| | | |
|----------|---|-----------|
| 3.6 | Mechanical processes | 63 |
| 3.6.1 | Introduction | 63 |
| 3.6.2 | Deformation of cast iron insert | 64 |
| 3.6.3 | Deformation of copper canister from external pressure | 68 |
| 3.6.4 | Thermal expansion (both cast iron insert and copper canister) | 70 |
| 3.6.5 | Deformation from internal corrosion products | 71 |
| 3.7 | Chemical processes | 73 |
| 3.7.1 | Corrosion of cast iron insert | 73 |
| 3.7.2 | Galvanic corrosion | 76 |
| 3.7.3 | Stress corrosion cracking of cast iron insert | 78 |
| 3.7.4 | Radiation effects | 79 |
| 3.7.5 | Corrosion of copper canister | 81 |
| 3.7.6 | Stress corrosion cracking, copper canister | 86 |
| 3.8 | Radionuclide transport | 87 |
| 3.9 | References | 87 |
| 4 | Buffer/backfill | 91 |
| 4.1 | Description of buffer and backfill | 91 |
| 4.1.1 | General | 91 |
| 4.1.2 | Overview of variables | 92 |
| 4.2 | Overview of processes | 94 |
| 4.3 | Radiation-related processes | 96 |
| 4.3.1 | Radiation attenuation/heat generation | 96 |
| 4.4 | Thermal processes | 97 |
| 4.4.1 | Heat transport | 97 |
| 4.5 | Hydraulic processes | 102 |
| 4.5.1 | Water transport under unsaturated conditions | 102 |
| 4.5.2 | Water transport under saturated conditions | 107 |
| 4.5.3 | Gas transport/dissolution | 110 |
| 4.6 | Mechanical processes | 115 |
| 4.6.1 | Swelling | 115 |
| 4.6.2 | Mechanical interaction buffer/backfill | 120 |
| 4.6.3 | Mechanical interaction buffer/canister | 122 |
| 4.6.4 | Mechanical interaction buffer/near-field rock | 125 |
| 4.6.5 | Mechanical interaction backfill/near-field rock | 127 |
| 4.6.6 | Thermal expansion | 129 |
| 4.7 | Chemical processes | 131 |
| 4.7.1 | Introduction, cementation | 131 |
| 4.7.2 | Advection | 131 |
| 4.7.3 | Diffusion | 133 |
| 4.7.4 | Ion exchange/sorption | 134 |
| 4.7.5 | Montmorillonite transformation | 138 |
| 4.7.6 | Dissolution/precipitation of impurities | 144 |
| 4.7.7 | Colloid release/erosion | 147 |
| 4.7.8 | Radiation-induced montmorillonite transformation | 150 |
| 4.7.9 | Radiolysis of pore water | 151 |
| 4.7.10 | Microbial processes | 152 |

| | | |
|----------|--|------------|
| 4.8 | Radionuclide transport | 154 |
| 4.8.1 | Overview | 155 |
| 4.8.2 | Advection | 155 |
| 4.8.3 | Colloid transport | 155 |
| 4.8.4 | Speciation of radionuclides | 156 |
| 4.8.5 | Sorption | 157 |
| 4.8.6 | Diffusion | 159 |
| 4.8.7 | Decay | 162 |
| 4.9 | References | 162 |
| 5 | Geosphere | 169 |
| 5.1 | Description of the geosphere | 169 |
| 5.1.1 | General | 169 |
| 5.1.2 | Overview of variables | 169 |
| 5.2 | Overview of processes | 170 |
| 5.3 | Radiation-related processes | 172 |
| 5.4 | Thermal processes | 172 |
| 5.4.1 | Heat transport | 172 |
| 5.5 | Hydraulic processes | 178 |
| 5.5.1 | Groundwater flow | 178 |
| 5.5.2 | Gas flow/dissolution | 189 |
| 5.6 | Mechanical processes | 191 |
| 5.6.1 | Introduction | 191 |
| 5.6.2 | Movements in intact rock | 197 |
| 5.6.3 | Thermal movement | 199 |
| 5.6.4 | Reactivation – Movement along existing fractures | 201 |
| 5.6.5 | Fracturing | 211 |
| 5.6.6 | Time-dependent deformations | 215 |
| 5.7 | Chemical processes | 218 |
| 5.7.1 | Introduction | 218 |
| 5.7.2 | Advection/mixing | 222 |
| 5.7.3 | Diffusion | 228 |
| 5.7.4 | Reactions groundwater/rock matrix | 229 |
| 5.7.5 | Dissolution/precipitation of fracture-filling minerals | 233 |
| 5.7.6 | Microbial processes | 237 |
| 5.7.7 | Decomposition of inorganic engineering material | 240 |
| 5.7.8 | Colloid formation | 242 |
| 5.7.9 | Gas formation/dissolution | 244 |
| 5.7.10 | Methane ice formation | 245 |
| 5.7.11 | Salt exclusion | 247 |
| 5.8 | Radionuclide transport | 248 |
| 5.8.1 | Advection and dispersion | 248 |
| 5.8.2 | Sorption | 251 |
| 5.8.3 | Molecular diffusion and matrix diffusion | 253 |
| 5.8.4 | Colloid transport | 257 |
| 5.8.5 | Speciation | 258 |
| 5.8.6 | Transport in gas phase | 258 |
| 5.8.7 | Radioactive decay | 259 |
| 5.9 | References | 260 |

1 Introduction

This report describes the internal processes which over time lead to changes in a KBS-3 repository for spent nuclear fuel. The context of the material in the report is described in Chapter 4 in SR 97 Main Report and briefly entails the following:

The repository has in SR 97 been divided into four subsystems: fuel/cavity, cast iron insert/copper canister, buffer/backfill and geosphere. A number of processes of importance for the post-closure evolution of the repository have been identified within each subsystem. This has been done with the aid of material in the so-called interaction matrices previously developed by SKB /see e.g. Skagius et al, 1995/. The processes have been divided into the categories thermal, hydraulic, mechanical and chemical. Furthermore, there are processes related to radiation and radionuclide transport. The coupling between the material in the interaction matrices and this report is described in /Pers et al, 1999/.

The identified processes are documented in this report. Each subsystem has its own chapter, and each chapter is divided into radiation related, thermal, hydraulic, mechanical and chemical processes as well as radionuclide transport. Each chapter begins with a description of the subsystem in question plus an overview of the processes treated in the chapter.

All processes are then described in a standard format with the following subheadings:

Overview

Brief description of the process, what it is influenced by and influences, and its importance for safety.

General description

More detailed description of the process and the mechanisms involved.

Model studies/experimental studies

Description of model studies and/or experimental studies that have been performed to quantify the process.

Time perspective

If possible to specify: On what timescale does the process lead to relevant changes? Sometimes several time perspectives need to be defined.

Natural analogues

Where applicable.

Summary of uncertainties

Both uncertainties in understanding (conceptual uncertainty) and data uncertainties are discussed here.

Handling in the safety assessment

How the process can be handled in the safety assessment for four important scenarios analyzed in SR 97 is described here.

1.1 References

Pers K, Skagius K, Södergren S, Wiborgh M, Bruno J, Pusch R, Hedin A, Morén L, Sellin A, Ström A, 1999. SR 97 – Identification and structuring of process. SKB TR 99-20, Svensk Kärnbränslehantering AB.

Skagius K, Ström A, Wiborgh M, 1995. The use of interaction matrices for identification, structuring and ranking of FEPs in a repository system. Application on the far-field of a deep geological repository for spent fuel. SKB TR 95-22, Svensk Kärnbränslehantering AB.

2 Fuel/cavity in canister

2.1 Description of fuel/cavity

2.1.1 General

Fuel types

Several kinds of fuel will be disposed of in the repository. For an alternative with 25 years' reactor operation, the quantity of BWR fuel is estimated to be about 5,000 tonnes and the quantity of PWR fuel about 1,500 tonnes /PLAN 98/. In addition, 23 tonnes of MOX fuel and 20 tonnes of fuel from the reactor in Ågesta will be disposed of.

BWR fuel of type SVEA 96 with a burnup of 38 MWd/tU is used as a reference fuel for SR 97.

PWR fuel differs marginally from BWR fuel as far as content of radionuclides is concerned. Other aspects of importance in the safety assessment, for example the geometry of the fuel cladding tubes, are as a rule dealt with so pessimistically in analyses of radionuclide transport that differences between different fuel types are irrelevant. The difference between MOX fuel and uranium fuel is discussed in /Forsström, 1982/. MOX fuel has a higher decay heat, which means that less fuel can be disposed of in each canister.

Differences between different fuel types are more important in criticality assessments. In this case, BWR fuel of type SVEA-64 and PWR fuel of type FA17x17 are dealt with in SR 97, since these types are the most unfavourable in terms of criticality.

Structure of the fuel assemblies

Nuclear fuel consists of cylindrical pellets of uranium dioxide. The pellets are 11 mm long and have a diameter of 8 mm. In fuel of the SVEA 96 type, the pellets are stacked in approximately 4-metre-long cladding tubes or "cans" of Zircaloy, a durable zirconium alloy. The cladding tubes are sealed with welds and assembled into fuel assemblies. Each assembly contains 96 cladding tubes. A fuel assembly also contains channel, handle, spacers etc. These parts are made of the nickel alloys Inconel and Incoloy as well as of stainless steel.

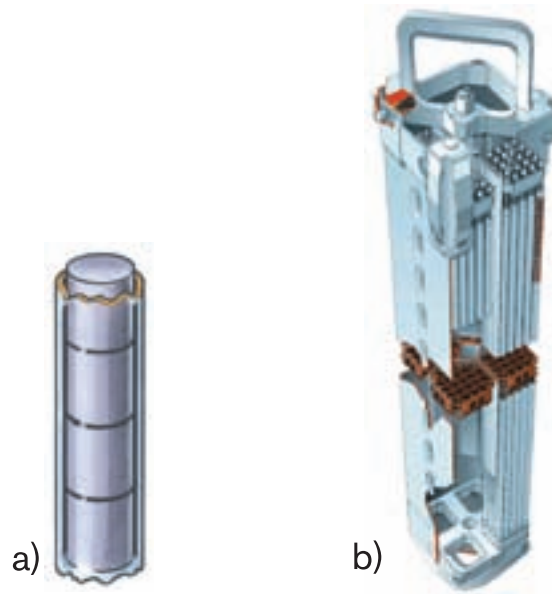


Figure 2-1.

- a. Cylindrical fuel pellets in cladding tubes of Zircaloy. The pellets have a diameter of about one centimetre.
- b. Fuel assembly of type SVEA 96. The assembly consists of 96 fuel tubes and is about 4 metres long.

Radionuclides

Radionuclides are formed during reactor operation by fission of nuclei of uranium-235 and plutonium-239 in particular and by capture of neutrons by nuclei in the metal parts of the fuel. The former are called *fission products*, the latter *activation products*. Moreover, uranium can form plutonium and other heavier elements by absorbing one or more neutrons. These and other elements (including uranium) are called *actinides* and decay to radioactive *actinide daughters* in several steps, finally forming stable isotopes of the metals lead or bismuth.

Most of the radionuclides lie embedded in the fuel matrix of uranium dioxide. A few fission products are relatively mobile in the fuel and may migrate to the surface of the fuel pellets during operation. The distribution of radionuclides in the fuel is discussed in detail in section 2.1.3.

2.1.2 Overview of variables

For the safety assessment, the fuel is described by means of a set of variables which together characterize the fuel in a suitable way for the assessment. The description applies not only to the fuel itself, but also the cavities in the canister, into which water can penetrate in the event of a defect in the copper canister. Processes will then take place in the cavity, such as fuel dissolution and corrosion of the cast iron insert. The cavity could thus be included in either the fuel or the canister part of the system, and has been included in the fuel here.

The fuel is characterized with respect to radiation by the **intensity** of α -, β -, γ - and neutron radiation and thermally by the **temperature**. Hydraulically, it is interesting to characterize the cavity if the copper canister should be damaged and water should enter. Hydraulically, the cavity is characterized by water flows and water pressure as well as by gas flows and gas pressures, which are jointly termed **hydrovariables** in the system description. Mechanically, the fuel is characterized by **stresses** in the materials. Chemically, the fuel is characterized by the **material composition** of the fuel matrix and metal parts, and by the **radionuclide inventory**. If water enters the canister, **water composition** and **gas composition** are also included in the description.

All variables are defined in Table 2-1.

Table 2-1. Variables in fuel/cavity.

| | |
|-------------------------------|--|
| Geometry | Geometric dimensions of all components of the fuel assembly, such as fuel pellets and Zircaloy cladding. Also includes the detailed geometry, including cracking, of the fuel pellets. |
| Radiation intensity | Intensity of α -, β -, γ - and neutron radiation as a function of time and space in the fuel assembly. |
| Temperature | Temperature as a function of time and space in the fuel assembly. |
| Hydrovariables | Flows and pressures of water and gas as a function of time and space in the cavities in the fuel and the canister. |
| Mechanical stresses | Mechanical stresses as a function of time and space in the fuel assembly. |
| Radionuclide inventory | Occurrence of radionuclides as a function of time and space in the different parts of the fuel assembly. The distribution of the radionuclides in the pellets between matrix and surface is also described here. |
| Material composition | The materials of which the different components in the fuel assembly are composed, <i>excluding radionuclides</i> . |
| Water composition | Composition of water (including any radionuclides and dissolved gases) in the cavities in the fuel and canister. |
| Gas composition | Composition of gas (including any radionuclides) in the cavities in the fuel and canister. |

2.1.3 Detailed description of fuel structure and radionuclide distribution in the structure

The nuclear fuel consists of centimetre-sized cylindrical pellets of sintered ceramic uranium dioxide. The pellets are stacked in cladding tubes to form fuel rods, which are in turn assembled into fuel assemblies. The fuel assemblies for a Swedish BWR reactor consist of 64 to 100 rods, arranged in a square array of 8x8 or 10x10 rods. These are in turn enclosed by a square fuel channel with a cross-sectional area of approximately 14x14 cm. The total length of a BWR assembly can be up to 4.4 m. The length of the column of nuclear fuel is approximately 3.7 m. The Swedish BWR waste also contains small quantities of MOX fuel and fuel from the decommissioned Ågesta reactor.

In the case of the PWR fuel, the array of fuel rods in a fuel assembly is 15x15 or 17x17, giving a cross-sectional area of 21.4x21.4 cm. The PWR fuel assembly lacks a fuel channel and is also a decimetre or so shorter than the BWR assembly.

Most of the radioactivity in the fuel assembly is located in or on the uranium dioxide; smaller quantities are also present as activation products in the cladding tubes and other metal parts. The cladding tubes for the fuel consist of Zircaloy. Other structural elements in the fuel are made of stainless steel, Inconel, Incoloy or Zircaloy.

Fuel

The nuclear fuel consists of very nearly stoichiometric uranium dioxide in the form of cylindrical pellets approximately 1 cm in diameter and 1 cm in length. The grain size is normally a micron or so. The uranium in the fuel has been enriched in the isotope ^{235}U from the naturally occurring concentration of 0.7 percent up to 3.6 percent in BWR fuel (4.2 percent in gadolinium-bearing fuel) and 4.2 percent in PWR fuel.

The fuel typically develops a power of 15 to 25 kW per metre of fuel rod during operation, which corresponds to a centre temperature in the fuel pellet in of 800 to 1200°C. After use in the reactor, the fuel contains 3–5 percent fission products, depending on the burnup, and approximately 1 percent higher actinides formed by neutron capture and radioactive decay. The average burnup for Swedish nuclear fuel is currently (1998) 40 MWd/kg U, but the average burnup has gradually increased and will be in the range 50–60 MWd/kg U in newer fuel.

The majority of the fission products and the higher actinides are present as a solid solution in the uranium dioxide matrix. Besides the chemical alteration of the uranium dioxide this entails, the fuel has also been altered physically during operation in the reactor.

Geometry of fuel pellets

During operation, the originally cylindrical fuel pellets crack, resulting in surface area enlargement. The scope of this surface area enlargement, which can be of importance if the fuel comes into contact with water in a deep repository, is not fully known. Geometric estimates lie in the order of a few square centimetres per gram of fuel. Johnson /1982/ estimates the area to be 2 cm²/g. Gray et al /1992/ arrive at roughly the same result (2.1 cm²/g) for fuel particles in the size range 0.5 to 5 mm, but set a value of 6.4 cm²/g after taking in account surface roughness and porosity. For fuel particles in the size range 700 to 1700 nm, Gray et al /1993/ arrive at an area of 17 cm²/g, equivalent here as well to the geometric area multiplied by a factor of 3 in order to take surface roughness into account. This agrees well with areas measured on unirradiated fuel in a similar size range (900–1100 nm) by means of gas adsorption (the Braunauer-Emmett-Teller method, BET method), where Torrero /1995/; Casas et al /1993/ determined the area to be 16 cm²/g. Torrero reports an area of 1.9 cm²/g for a whole fuel pellet. In both of these size ranges of fuel, the BET area is three times the geometric area.¹

One measurement series is known where an attempt has been made to measure the area of spent fuel using the BET method /Lundström et al, 1997/. The results lay in the range 59 to 121 cm²/g with a mean value of around 80 cm²/g. Areas of the same order of magnitude were measured for unused fuel, to be compared with Torrero's much lower values for equivalent size ranges. It is uncertain whether these areas are representative of the fuel area over which oxidation/dissolution would occur if the fuel came into contact with water.

¹ It should be noted that Casas et al, calculate the geometric area by assuming that the fuel particles can be regarded as spheres, while Gray et al, /1993/ regard them as cubes. This gives a difference of roughly a factor of two for estimated geometric area.

Results from the BET method must also be regarded critically. The measurement, which usually yields reproducible results, gives a measure of the area on which an inert gas adsorbs and also gives good relative measures of the areas of different materials in the same size fractions. However, it cannot simply be assumed that this method gives a measure of the wetted area of spent fuel in contact with water. The method probably overestimates the area of the sample that is in contact with water. Furthermore, the heat output and ionizing radiation in the spent fuel can affect the area determination. Gray et al /1994/ also conclude that it is probably more appropriate to use some form of geometric area for fuel than a BET area.

The porosity and grain size of the fuel can be of importance for the specific area of the fuel. These parameters vary over a wide range, depending on factors such as fabrication, burnup and irradiation history, but also vary along the radius within the same fuel pellet.

Enrichment on pellet surface

In the case of fuel that has been irradiated at a relatively low temperature, the radial variation in grain size and porosity is small, with moderate grain growth in the centre of the pellet. An exception from this rule is the sharp increase in porosity in the pellet rim. On an area a few microns in depth on the rim of the pellet, the porosity is several times higher than inside the fuel. This rim zone also deviates in microstructure from the rest of the pellet in that the original grains have been subdivided into many smaller grains. The reason for this lies in local variations in the fission rate across the diameter of the fuel.

Self-shielding in the fuel leads to increased formation and fission of plutonium isotopes, increased formation of other actinides and increased frequency of ^{235}U fissions in the rim of the fuel pellet. The result is sharp variations in both burnup and alpha activity increases at the periphery of the fuel pellets. The increased burnup is also accompanied by a higher content of fission products. At an average burnup of about 40 MWd/kg U, the surface layer can have up to twice the burnup as well as more than four times the alpha activity /Forsyth, 1995/.

Radionuclides in the fuel-clad gap

Some fission products are gaseous at the temperatures the fuel has had during operation. This is true of the inert gases krypton and xenon, but can also apply to volatile fission products such as caesium and iodine. A fraction of these fission products can leave the fuel matrix during irradiation and migrate to the voids that exist between the fuel and the cladding. Most of the fuel has a fission gas release of less than 1 percent, but the maximum value can be tens of percent /Johnson and Tait, 1997/. It is generally assumed that the release of caesium and iodine is of the same magnitude as the fission gas release. This has been shown for CANDU fuel /Stroes-Gascoyne et al, 1987/. It has not been established that the same correlation exists for light water reactor fuel, even though the results of SKB's fuel studies seem to support this for Cs (BWR, 42 MWd/kg U: fission gas release 0.7 percent, Cs release approximately 1 percent; PWR, 43 MWd/kg U: fission gas release 1.05 percent, Cs release approximately 1 percent /Forsyth and Werme, 1992/). However, results from fuel with a high fission gas release rate (up to 18 percent) show a caesium release that corresponds to only one-fourth of the fission gas release /Gray et al, 1992/. Gray /1998/ has made similar observations for iodine.

There are large uncertainties concerning the fraction of fission products that may have been released from the fuel matrix during operation in the reactor. The irradiation history of the fuel is of great importance, and the trend is towards higher burnup and even higher power ratings. Barner et al /1993/ show that for burnups lower than 20 MWd/kg U, the fission gas release is less than 1 percent, and for most of fuel with a higher burnup the fission gas release is less than around 5 percent. Studies by Koizumi et al /1991/ suggest that the fission gas release rate is dependent more on the maximum linear power density than on the burnup.

Models have been developed for calculation of important fuel parameters, such as build-up of internal gas pressure and fission gas release /Forsberg et al, 1996/.

The models were used for calculations of the fission gas release in BWR SVEA-64 fuel, and the results showed that at 100 percent power output the maximum fission gas release was nearly 20 percent, and at 106 percent power output it was over 23 percent; the median was 2 percent and 1 percent, respectively /based on information from Massih /1997/. The mean fission gas release was 4.5 percent and 2.5 percent, respectively. 95 percent of all rods have a fission gas release of less than 14 percent and 8 percent, respectively, for the two cases. The maximum fission gas release rate may be tens of percent, but only for an insignificant fraction of the core equivalent to 0.001 to 0.01 percent of all fuel.

Hallstadius and Grapengiesser /1991/ have made an analysis of the fission gas release for a number of 8x8 array ABB fuel rods and found that the fission gas release was dependent on the position of the fuel assemblies in the core in relation to the control rods, the highest values being from 8 percent to over 20 percent. The majority of the analyzed fuel assemblies had a fission gas release of less than 5 percent, even at such high burnups as 50 MWd/kgU. The estimated mean for Hallstadius and Grapengiesser's data is approximately 3.5 percent.

Schrire et al /1997/ measured the fission gas release of over 100 10x10 SVEA fuel assemblies with a burnup of up to 50 MWd/kgU. The fission gas release was at most 5 percent, despite the fact that they chose assemblies which experience has shown have a high fission gas release. The estimated mean fission gas release was 1 percent.

The variation between different fuel rods is thus great, which leads to large uncertainties for the fission gas release. Since modellings show that more than 50 percent of the rods, even under extreme conditions, have a release of less than 2 percent, and recently completed studies /Schrire et al, 1997/ give a mean of 1 percent for modern fuel, it may be reasonable to choose 2 percent as a reference value.

Even though no systematic investigations of correlations between the release of fission gases and water-soluble fission products have been done for light water reactor fuel, it may be pessimistic to use Canadian data for CANDU fuel /Stroes-Gascoyne, 1996/. It is probably very pessimistic for most of the present-day fuel inventory, but the trend towards irradiation with higher peak linear power density is increasing the tendency towards segregations of fission products to the gap and is leading to a decrease in the differences between light water fuel and CANDU fuel. This means that 2 percent of the fraction of caesium and iodine can pessimistically be assumed to be present in the fuel-clad gap for Swedish light water fuel.

Radionuclides at grain boundaries; segregations

In addition to the release of gaseous fission products, solid elements that are incompatible with the structure of the uranium oxide are also segregated and form separate phases. Light water reactor fuel contains inclusions of metal alloys of Mo-Tc-Ru-Rh-Pd (4d metals), also called ϵ -Ru phases. In normal fuel, these particles can be seen with sizes of 0.5 to 1 μm , equivalent to the resolution of optical microscopes /Forsyth 1995, Forsyth, 1996/. The fraction of 4d metals which Forsyth was able to determine by optical microscopy corresponded to less than 2 percent of their total inventory in the fuel. By electron microscopy, it has been possible to determine that ϵ -Ru phases also occur in the size range 1 to 100 nm /Thomas and Guenther, 1989/. When fuel is dissolved in nitric acid, the 4d metals form an insoluble residue. By analyzing these residues, Forsyth was able to conclude that at least 80 percent of the inventory was present as spherical inclusions in the size range 0.1 to 0.5 μm .

Besides these known segregations in irradiated fuel, the possibilities that certain fission products have segregated to the grain boundaries in the uranium dioxide have been discussed. For CANDU fuel, which is irradiated with higher linear power density (20–55 kW/m) than light water fuel, it has been established by photoelectron spectroscopy that caesium, rubidium, tellurium and barium are present in the grain boundaries, often with high surface enrichments /Hocking et al, 1994/. Gray et al /1992/ determined the grain boundary inventory of caesium to be less than 1 percent. The values of gap and grain boundary inventories for technetium and strontium were near the detection limits and were found to be less than 0.2 percent of the total inventory. A study of grain boundaries by Auger spectroscopy by Thomas et al /1988/ on fuels with moderate burnup and low fission gas release showed no detectable amount of caesium, strontium and technetium. On a PWR fuel with high fission gas release (18 percent; equivalent fuel was also included in Gray's et al, study /1992/), Thomas et al, found ϵ -phases with high surface concentrations of caesium, tellurium and palladium. This observation was interpreted as indicating that caesium and other fission products are mainly associated with the ϵ -phases and thereby indirectly with the grain boundaries that contain them. Since no detectable quantities of caesium, strontium and technetium could be detected in the grain boundaries, Thomas et al, drew the conclusion that the grain boundary inventory is small and can therefore hardly be regarded as a source of release of these elements from the fuel.

The question of strontium segregations and the differences between strontium and uranium release from spent fuel in experiments at Studsvik has been discussed a great deal. Werme and Forsyth /1988/ offer the hypothesis that most of the strontium that is released comes from selective leaching of cracks and grain boundaries. Attempts have been made to determine grain boundary inventories by microprobe analysis in a fuel with a burnup of 37 MWd/kg U (linear power density <20 kW/m) that has been subjected to controlled power ramping to 43 kW/m in the Studsvik R2 reactor /Forsyth et al, 1988/. The rod had an appreciable release of krypton and xenon, as well as redistribution of caesium to the fuel-clad gap during the power increase. Sharp concentration gradients within the individual grains could be observed for xenon and caesium, but not for neodymium. In the case of strontium, the concentrations were far too close to the detection limit to yield reliable data. In a subsequent corrosion experiment with a fuel with a burnup of 44–48 kWd/kg U (linear power density <15 kW/m), a similar power ramping to a peak of 43 kW/m was performed /Forsyth et al, 1994/. A significant increase in the release of caesium and rubidium was observed, and some effect for barium and technetium as well as possibly also for molybdenum. No significant redistribution of strontium was found.

Available data thus suggest that in contrast to CANDU fuel, light water reactor fuel irradiated with moderate power densities has at most a few tenths of a percent of the inventory of radionuclides in the grain boundaries. Aside from the ϵ -Ru phases, there are probably no segregations in the fuel that would be of any significance. The grain boundary inventory is, within the margin of error, equal or close to zero. A possible contribution from the grain boundaries will be small compared with the inventory in the gap and can be modelled with a slight increase of the expected gap inventory for the fuel. Some uncertainty comes, in the same way as for the gap inventory, from the trend towards irradiation with higher peak linear power density. Pessimistically, the grain boundary inventory can be set equal to what has been determined for CANDU fuel /Stroes-Gascoyne, 1996/ and what is discussed by Johnson and Tait /1997/.

2.2 Overview of processes

A number of processes will with time alter the state in the fuel and in the canister's cavity. Some take place in any circumstances, while many others only occur if the isolation of the copper canister is broken and water enters the canister.

The radionuclides in the fuel will eventually be transformed into non-radioactive substances by means of *radioactive decay*. This process gives rise to α , β , γ and neutron radiation which, by interaction with the fuel and surrounding materials, is *attenuated* and converted to thermal energy. The temperature in the fuel is changed by means of *heat transport* in the form of heat conduction and heat radiation, and heat is transferred to the surroundings. The temperature change will lead to some *thermal expansion* of the constituents of the fuel. In combination with the *helium formation* to which the α radiation gives rise, this can lead to *mechanical failure of the cladding tubes* in the fuel.

In an intact canister, *radiolysis of residual gases* in the cavity will lead to the formation of small quantities of corrosive gases, which could contribute to stress corrosion cracking (SCC) of the cast iron insert.

If the copper canister is penetrated, *water and gas may be transported* into the canister cavity, radically altering the chemical environment. *Radiolysis* of the water in the cavity will further alter the chemical environment. The water in the canister causes *corrosion of cladding tubes and other metal parts* in the fuel. If the cladding tubes' isolation should be broken initially or later by corrosion or mechanical stresses, the fuel will come into contact with water. This leads to dissolution of radionuclides that have collected on the surface of the fuel matrix and *dissolution or transformation of the fuel matrix* with release of radionuclides. The radionuclides may either be dissolved in the water, rendering them accessible for transport, or precipitate in solid phases in the canister void. This is determined by the *chemical speciation of radionuclides* in the canister cavity. On dissolution of the fuel, microscopic particles (colloids) with radionuclides may also form.

Radionuclides dissolved in water can be transported with mobile water in the canister, *advection*, or by *diffusion* in stagnant water. Fuel colloids carrying radionuclides can be transported in the same way. Nuclides dissolved in water can be *sorbed* to the different materials in the canister. Certain nuclides can also be *transported in the gas phase*.

Finally, water can attenuate the energy of neutrons in the canister cavity. Low-energy neutrons can subsequently cause *fission* of certain nuclides in the fuel, releasing more neutrons. If conditions are unfavourable, criticality may be achieved, i.e. the process becomes self-sustaining.

The THMC diagram for fuel/cavity is given in figure 2-2.

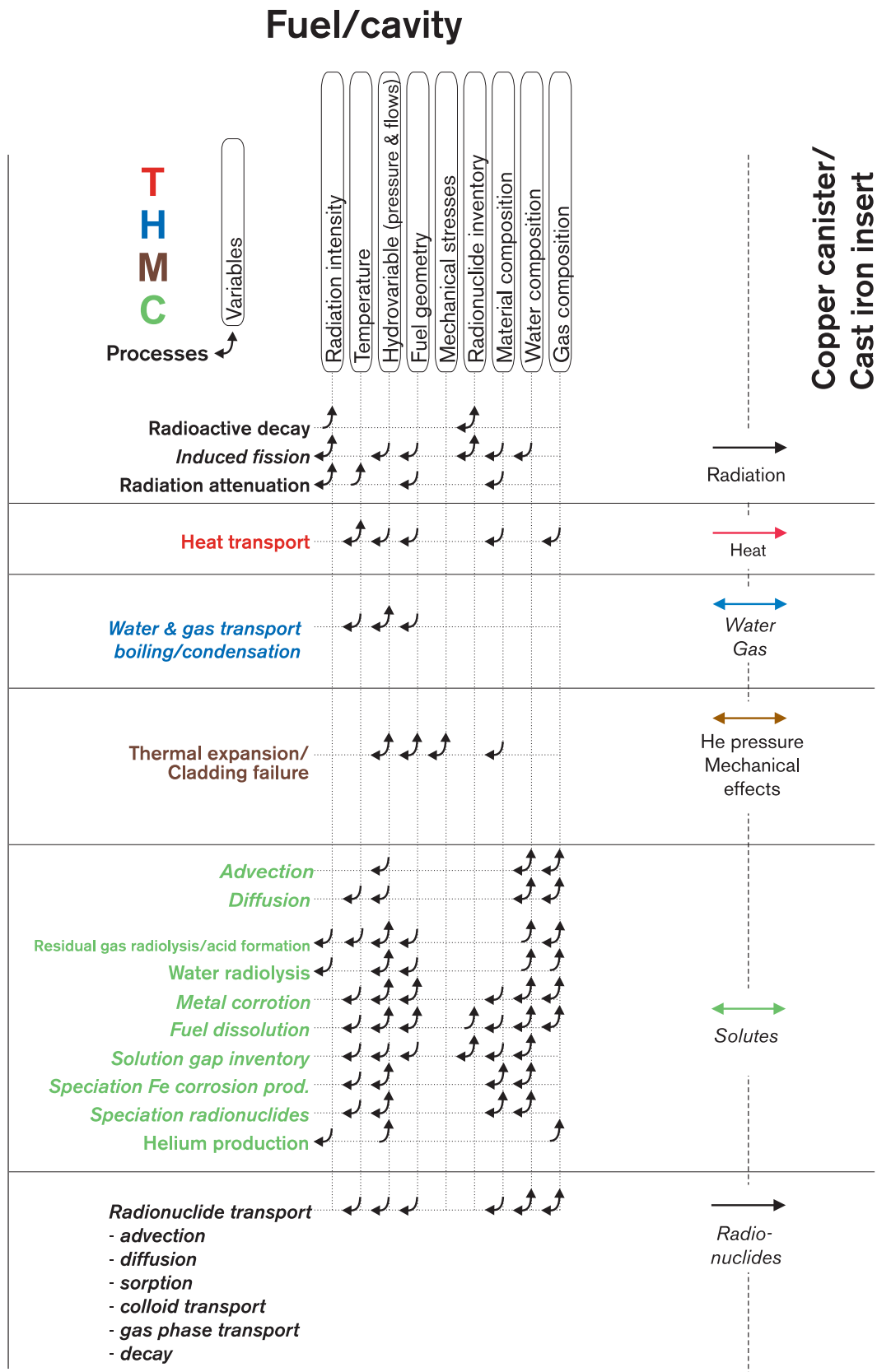


Figure 2-2. THMC diagram for fuel/cavity. Processes in italics only occur when the isolation of the copper canister is broken.

2.3 Radiation-related processes

2.3.1 Radioactive decay

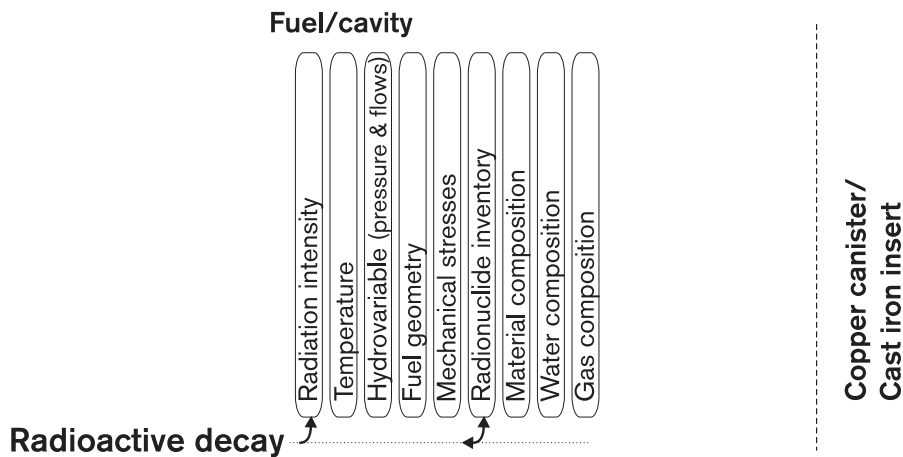


Figure 2-3. Radioactive decay.

Overview, general description

The process of radioactive decay transforms the radionuclide content of the fuel and of those parts of the canister cavity to which radionuclides have spread. The radioactive disintegrations generate α -, β -, γ - and neutron radiation plus new nuclides. These may also be radioactive and decay until a stable nuclide is created.

The process is of fundamental importance, especially since it describes how the radiotoxicity and composition of the fuel evolves over time. The energy that is liberated is converted for the most part into heat (section 2.3.2), and the process thereby also constitutes the basis for the description of the repository's thermal evolution.

Model studies/experimental studies

Radioactive decay has been thoroughly studied experimentally over a long period of time, and our theoretical understanding of the process is very good.

Time perspective

The time it takes for half of all radioactive atoms to decay is called the half-life of the radionuclide. The half-lives of various radionuclides vary from fractions of a second up to millions of years.

Natural analogues

Radioactive substances occur naturally, and it is by studies of such natural analogues that our knowledge of radioactivity grew during the first few decades of this century.

Summary of uncertainties

Uncertainties in understanding: Our understanding of the process is sufficient for the needs of the safety assessment.

Uncertainties in data: The half-lives of the concerned radionuclides are generally known with good accuracy.

New data have been gathered on the half-lives of Se-79 and Sn-126. This is discussed in section 2.7.8.

Uncertainties concerning the inventory at deposition are discussed by /Andersson, 1999/.

Handling in the safety assessment

Base scenario: The process is handled by model calculations.

Canister defect scenario: See base scenario.

Climate change: See base scenario.

Earthquake: See base scenario.

2.3.2 Radiation attenuation/heat generation

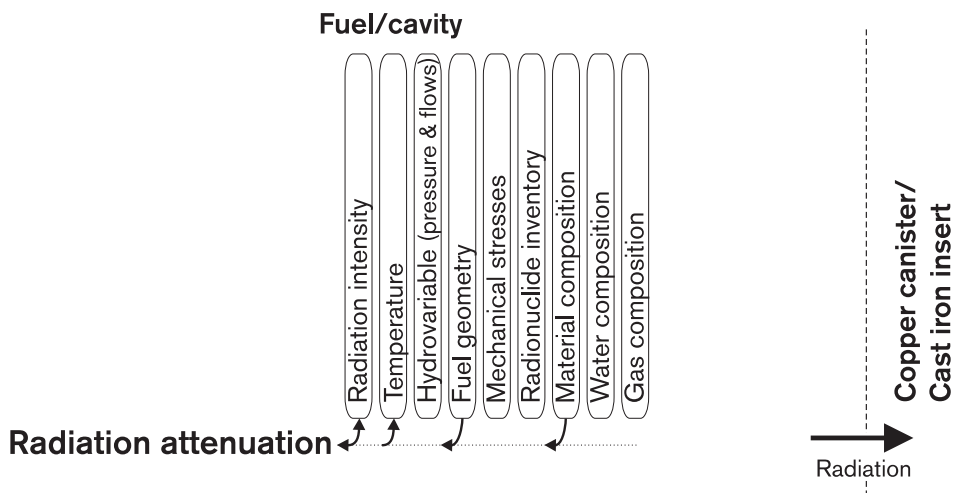


Figure 2-4. Radiation attenuation/heat generation.

Overview, general description

The radiation from radioactive decay interacts with the materials in the fuel and the canister cavity. Energy is thereby transferred to the materials and the radiation is attenuated. Most of the transferred energy is converted into thermal energy: heat generation. The thermal energy, or heat, that is generated in the fuel after it has been taken out of service is called residual or decay heat and is dependent on the fuel's radionuclide content. At first, the fuel's heat output is dominated by beta and gamma decay, but alpha disintegrations are also of some importance in the long term /Håkansson, 1996/. The isotopes which dominate during the first few centuries are Cs-137 (Ba-137m) and Sr-90 (Y-90), both with half-lives of around 30 years, which also results in a halving of the heat output in 30 years.

The process is of fundamental importance since it describes how heat is generated by the radiation. Furthermore, attenuation determines how much of the generated radiation reaches the canister.

Model studies/experimental studies

The fuel's heat output is directly dependent on the radioactive decay process, see section 2.3.1.

Time perspective

Heat generation in the fuel is only of importance for a few hundred years. After 1,000 years, heat generation is only about 5 percent compared with at the time of deposition.

Natural analogues

Not applicable.

Summary of uncertainties

Uncertainties in understanding: Heat output as a function of time can be calculated with great accuracy when the nuclide content is known. Our understanding of the process is good enough for the needs of the safety assessment.

Uncertainties in data: The uncertainties regarding heat output stem from uncertainties regarding the nuclide content of the fuel. These uncertainties are discussed in /Andersson, 1999/.

Handling in the safety assessment

Base scenario: The total power output of the fuel is calculated on the basis of its radionuclide content as well as decay energies and half-lives.

Canister defect scenario: See base scenario.

Climate change: See base scenario.

Earthquake: See base scenario.

2.3.3 Induced fission (criticality)

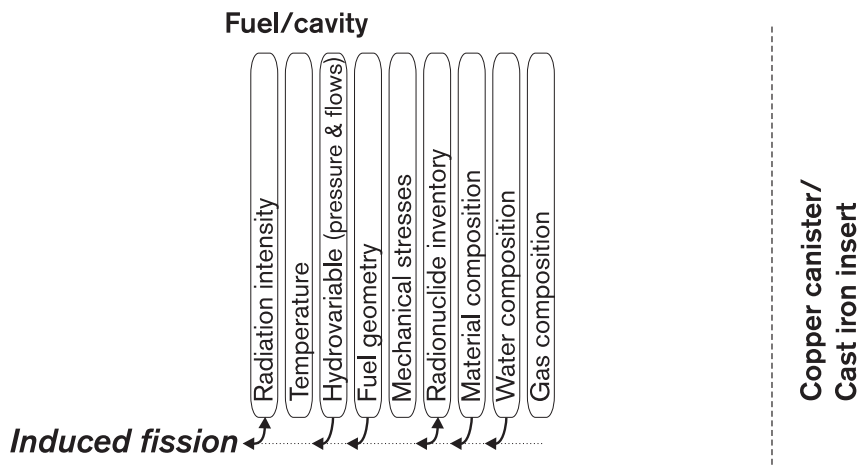


Figure 2-5. Induced fission (criticality). Only relevant when the copper canister is damaged.

Overview and general description

Neutrons from radioactive disintegrations can cause nuclear fission in certain isotopes in the fuel. As long as the copper canister is intact, the great majority of neutrons generated by these disintegrations will pass out of the fuel without causing fission and the process can be neglected.

In the case of U-235 and Pu-239 in particular, the efficiency of the process increases if the neutrons are moderated (slowed down) to lower energies by collisions with light atomic nuclei. The necessary conditions for this to happen would exist if water were to penetrate a broken canister. With its light hydrogen nuclei, the water could then act as a moderator. New neutrons are released by the fissions, and if more neutrons are formed than are consumed the process can become self-sustaining. The system is then said to be *critical* and large quantities of energy can then be liberated. It is this process that has been utilized under controlled forms in the nuclear reactor for energy production.

With the current design of the canister, criticality cannot arise if water enters the canister and the fuel assemblies are intact and not entirely unused /Efrainsson, 1996a; 1996b/.

If the fuel assemblies have been damaged and uranium and plutonium has been leached out, there are no probable courses of events that could lead to criticality /Oversby, 1996; 1998/.

Model studies/experimental studies

Nuclear fission has been thoroughly studied experimentally over a long period of time, and our theoretical understanding of the process is very good. The risks of criticality in the canister have been studied by /Efrainsson, 1996a; 1996b/.

Time perspective

The fraction of fissionable material in the spent fuel changes insignificantly with time, and the probability of criticality will remain unchanged for thousands of years.

Natural analogues

Criticality has been studied at the natural reactor in Oklo, see Oversby /1996; 1998/.

Summary of uncertainties

Fundamental understanding: The process has been thoroughly studied within reactor physics. Our understanding is sufficient for the needs of the safety assessment.

Data uncertainties: Data uncertainties exist for the situation with a failed canister in the deep repository. There are uncertainties relating to the situation for a failed canister in the deep repository. The conclusion that the risk of criticality can be neglected remains valid, however.

Handling in the safety assessment

Base scenario: Not applicable.

Canister defect scenario: Account of criticality studies for different types of fuel and burnup rates for a damaged canister directly in the main report.

Climate change: If the evolution leads to canister damage: See the canister defect scenario. Otherwise: See the base scenario.

Earthquake: If the evolution leads to canister damage: See the canister defect scenario. Otherwise: See the base scenario.

2.4 Thermal processes

2.4.1 Heat transport

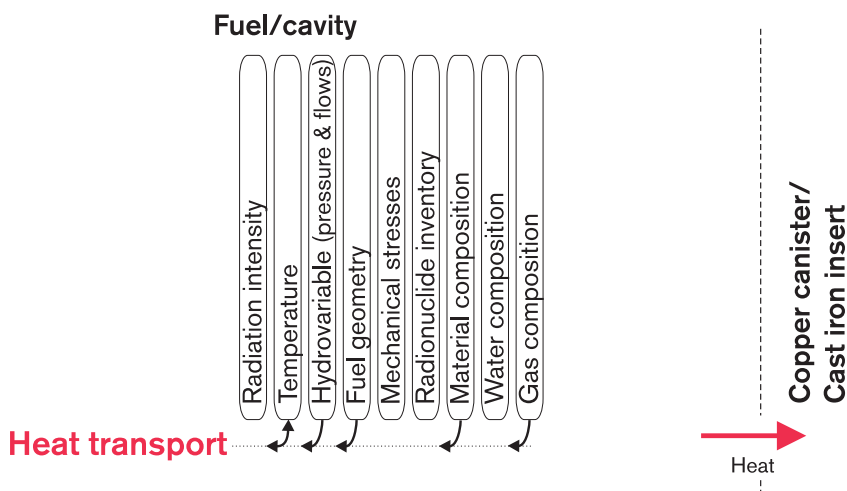


Figure 2-6. Heat transport.

Overview

Heat is transported in the fuel and cavity by conduction and radiation over to the canister insert and further to the near and far field. The process is dependent on the geometric configuration of the fuel and the thermal properties of the materials, which are given by the material compositions. The heat transfer to the canister insert sets the boundary conditions for the process. The result is a temperature change in the fuel/cavity.

The process constitutes a part of the thermal evolution of the repository.

General description

Depending on the residual gas composition in the cavity and depending on the radiation properties² of the metal surfaces on the fuel assemblies and the canister insert, heat conduction or radiation may come to dominate the heat transfer between fuel and canister. The temperature in the fuel and the cavity will be affected by the entire chain of heat transfers between the different components in the repository. In the longer perspective, the temperature evolution in the fuel and cavity will be controlled by the thermal power output of the fuel. In a shorter perspective, changes in the heat transfer properties of different components in the repository will have a great influence on the temperature of the fuel. The peak temperature in the fuel will be reached shortly after deposition.

Model studies/experimental studies

Temperature calculations have been carried out for the canister /Renström, 1997; Bjurström and Bruce 1997, 1998/. Uncertainties surrounding the heat transfer between the different components in the canister greatly influence the results. Experimental investigations will therefore be conducted.

Time perspective

The peak temperature of the fuel is reached shortly after deposition. It then takes several thousand years for the fuel to cool off to near-ambient temperature.

Natural analogues

Not applicable.

Summary of uncertainties

Understanding: Our fundamental understanding of the process is sufficient for the needs of the safety assessment.

Data uncertainties: Uncertainties surrounding the heat transfer between the cladding tubes and the cast iron insert lead to uncertainties in the assessment of the temperature of the fuel. Compared with the uncertainties surrounding the heat transfer between the cast iron insert and the copper canister and between the canister surface and the bentonite buffer before full water saturation has been achieved, the uncertainties surrounding the heat transfer from the fuel to the canister insert are small.

² Expressed as emissivity, i.e. capacity to emit electromagnetic radiation.

Handling in the safety assessment

Base scenario: An estimation of the maximum temperature reached by the fuel is carried out in the base scenario. This can be done with the aid of Renström /1997/ and Bjurström and Bruce /1997, 1998/.

Canister defect scenario: Intruding water modifies the heat conduction properties in the interior of the canister only marginally. The description of heat conduction in the canister defect scenario is therefore assumed to lie within the frame of the uncertainties for the equivalent description in the base scenario.

Climate change: If the evolution leads to canister damage: See the canister defect scenario. Otherwise: See the base scenario.

Earthquake: If the evolution leads to canister damage: See the canister defect scenario. Otherwise: See the base scenario.

2.5 Hydraulic processes

2.5.1 Water and gas transport in canister cavity, boiling/condensation

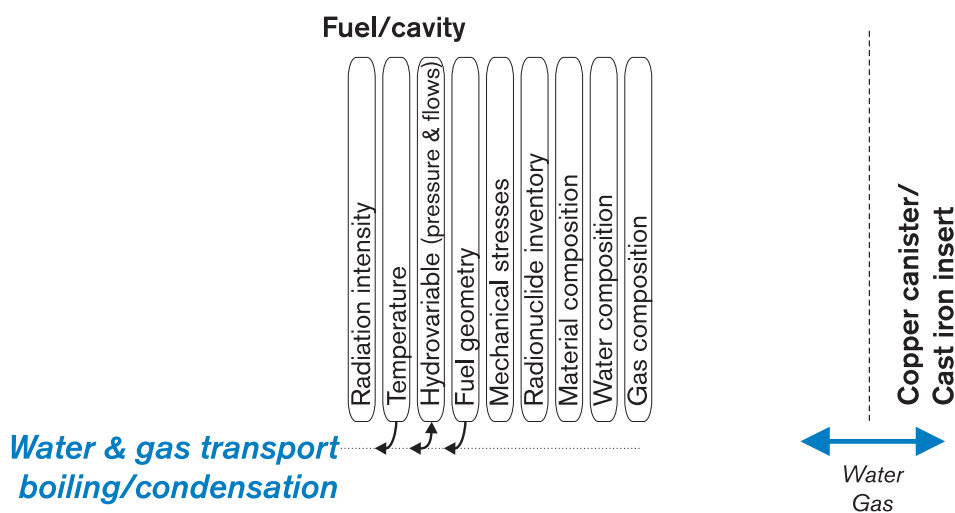


Figure 2-7. Water/gas transport, boiling/condensation. Only applicable when the copper canister is damaged.

Overview

If the copper canister is penetrated, water can enter the canister cavity as liquid or water vapour. Transport of water, water vapour and other gases in the canister is then determined by the detailed geometry of the canister cavities, the presence of water/vapour in the cavities, and temperature and pressure. Boiling/condensation comprises an integral part of water/gas transport. Pressures and flows of water and gas at the transition to the buffer set the boundary conditions for the process.

The process is strongly coupled to several other processes, for example corrosion of the canister insert, where water is consumed and hydrogen is formed.

Water/gas transport in the canister is of fundamental importance for a number of other processes that are dependent on the presence of water in the canister, such as fuel dissolution, radionuclide transport and corrosion of the copper insert.

General description and model studies/experimental studies

If the canister is penetrated, water will enter. The process is controlled by the pressure difference between buffer and canister cavity (initially 5–7 MPa) and the hydraulic conductivity in the bentonite. Water ingress can be expected to proceed very slowly. In the presence of water in the canister, gas will be generated both by radiolysis (see section 2.7.3) and by corrosion of the cast iron insert (section 3.7.1). The build-up of gas pressure in the canister will lead to a gradual decrease in the inflow of water and, when the pressure is sufficiently high, gas transport through the canister and the bentonite. The process has been investigated in several reports since 1990 for cracks in the canister /Wikramaratna et al, 1993/, and most recently in detail by /Bond et al, 1997/.

Qualitatively, the course of events can be described as follows: water enters through the hole in the copper canister and causes anaerobic corrosion of the iron surfaces. This leads to hydrogen gas formation, which gradually increases the pressure inside the cavity in the canister and thereby reduces the ingress of water. The corrosion leads to consumption of water. If the surface area available for corrosion is constant, the rate of water consumption will also be constant and the water level in the canister will reach a peak and then sink. Depending on the size of the hole in the canister and the corrosion rate, /Bond et al, 1997/ see three possibilities:

- 1) If the hole is so small that water is consumed by corrosion at the same rate as it enters, no water will collect inside the canister. The hydrogen gas pressure builds up gradually and approaches the external water pressure asymptotically. The corrosion rate will be governed by the inward diffusion of water vapour, which also declines asymptotically towards zero.

The hole sizes at which this applies depend on the corrosion rate. At a corrosion rate of 0.1 $\mu\text{m}/\text{y}$, the area of the hole must be less than 8.25 mm^2 . At a corrosion rate of 1 $\mu\text{m}/\text{y}$, the equivalent hole size is 825 mm^2 . When the inward transport of water due to the pressure difference between the inside and outside of the canister is lower than the inward transport by diffusion, canister corrosion will be diffusion-controlled (see below).

- 2) If the hole in the canister is larger than in case 1), but still sufficiently small, water will collect inside the canister. The water will be completely consumed before the pressure in the canister reaches the external pressure. Then the corrosion rate will be limited by the water supply rate and decrease with increasing hydrogen gas pressure as in case 1). The hydrogen gas pressure gradually builds up and approaches the external pressure asymptotically, while the corrosion rate declines asymptotically towards zero.

In the same way as in case 1), the hole size is dependent on the corrosion rate. The combination of corrosion rate 0.1 $\mu\text{m}/\text{y}$ and hole size 20 mm^2 belongs to this category, for example. When the inward transport of water due to the pressure difference between the inside and outside of the canister is lower than the inward transport by diffusion, canister corrosion will be diffusion-controlled (see below).

3) If the hole is sufficiently large in relation to the corrosion rate, the hydrogen gas pressure will reach the external pressure while there is still water in the canister. If the water level is then lower than the hole in the copper canister, hydrogen begins to leak out, but the internal pressure is still high and prevents new water from entering the canister. If the water level in the canister lies above the hole in the copper canister, water will first be pressed out until the water is on a level with the hole. Then hydrogen will leak out as long as the corrosion continues, i.e. until all water in the canister has been consumed.

In the same way as in case 1, the hole size is dependent on the corrosion rate and can be illustrated by the cases 0.01 $\mu\text{m}/\text{y}$ and hole size 5 mm^2 , and 1 $\mu\text{m}/\text{y}$ and hole size 0.18 m^2 , both of which belong to case 3). When the inward transport of water due to the pressure difference between the inside and outside of the canister is lower than the inward transport by diffusion, canister corrosion will be diffusion-controlled (see below).

Even after all liquid water has been consumed, iron corrosion will continue since water vapour can diffuse into the canister. This case has also been modelled by Bond et al, /1997/ for different corrosion rates, the hole in the canister and the area inside the hole that corrodes.

No experimental studies of the process of water ingress and water consumption by hydrogen-generating corrosion have been carried out.

Time perspective

After canister penetration, the time frame is a matter of hundreds to hundreds of thousands of years /Bond et al, 1997/.

Natural analogues

Not applicable.

Summary of uncertainties

Fundamental understanding: Sufficient for the needs of the safety assessment.

Data uncertainties: For generation of corrosion gases, the corrosion rates are well-determined empirically and can be modelled with a constant corrosion rate if the water supply is not limiting /Smart et al, 1997/. If the corrosion rate is greater than the supply of water, the corrosion process will be controlled by the transport of water into the canister /Bond et al, 1997/.

Handling in the safety assessment

Base scenario: Not applicable.

Canister defect scenario: The process is described as a part of an integral description of the evolution of the canister interior after damage.

Climate change: If the evolution leads to canister damage: See the canister defect scenario. Otherwise: See the base scenario.

Earthquake: If the evolution leads to canister damage: See the canister defect scenario. Otherwise: See the base scenario.

2.6 Mechanical processes

2.6.1 Thermal expansion/cladding failure

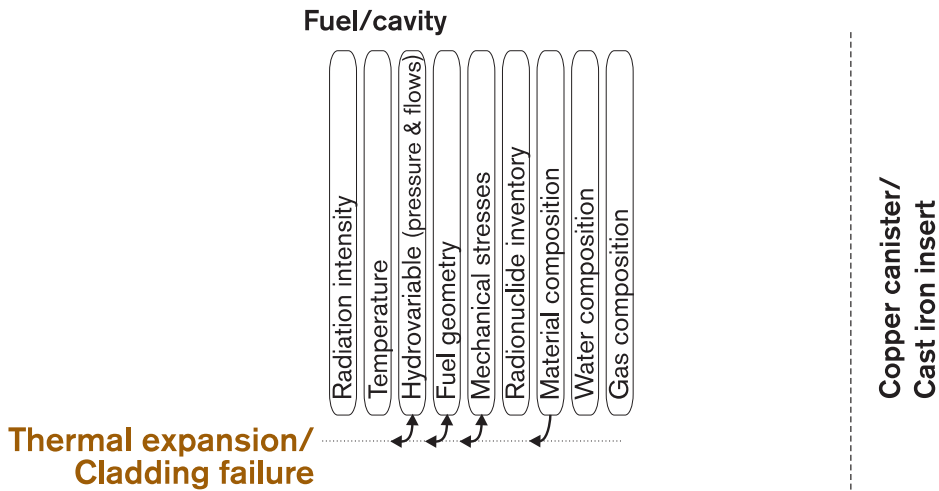


Figure 2-8. Thermal expansion/cladding failure.

Overview/General description

Temperature changes in the fuel and mechanical impact in conjunction with handling and transport will affect the cladding.

Temperature increases lead to increased gas pressure inside the cladding tubes and can cause failure. Uptake of hydrogen during reactor operation may have led to hydride formation with embrittlement, which can lead to failure of the cladding tubes. In most cases, the damage will be local and lead to a leaky cladding tube.

The process is of importance for the release of radionuclides from the fuel. This can only happen if the cladding tubes are damaged.

Model studies/experimental studies

Experimental studies and modelling have been carried out for dry storage purposes /BEFAST III, 1997/. Hydride formation and delayed failure have been studied for a long time /Northwood and Kosasih, 1983; Grigoriev, 1996/. Rothman /1984/ conducted a review of the state of knowledge based on requirements for direct disposal of spent fuel. The conclusion was that failure due to hydride formation, though unlikely, cannot be entirely ruled out.

Time perspective

A small portion of the fuel rods must be assumed to be damaged at the time of disposal. Even after disposal, hydride formation can lead to cracks in the cladding.

Natural analogues

Not applicable.

Summary of uncertainties

Our understanding of the process is not sufficient to permit reliable quantification. In cases where the process is of importance, i.e. when the copper canister is damaged, it can be handled pessimistically, see below.

Handling in the safety assessment

Base scenario: The process is of no importance for long-term safety as long as the copper canister is intact. To permit a discussion of retrieval, it can be pessimistically assumed that all cladding tubes may be damaged, but that they still provide physical protection for the fuel, and that the fuel assemblies retain their original geometry.

Canister defect scenario: In the modelling of radionuclide transport in the canister defect scenario, it is pessimistically assumed that all cladding tubes are damaged /Andersson 1999/.

Climate change: If the evolution leads to canister damage: See the canister defect scenario. Otherwise: See the base scenario.

Earthquake: If the evolution leads to canister damage: See the canister defect scenario. Otherwise: See the base scenario.

2.7 Chemical processes

2.7.1 Advection and diffusion

Solutes in the interior of the canister can be transported by advection and diffusion. These processes are not discussed explicitly, but dealt with (often with pessimistic simplifications) integrated with other processes. See also section 2.8.

2.7.2 Residual gas radiolysis/acid formation

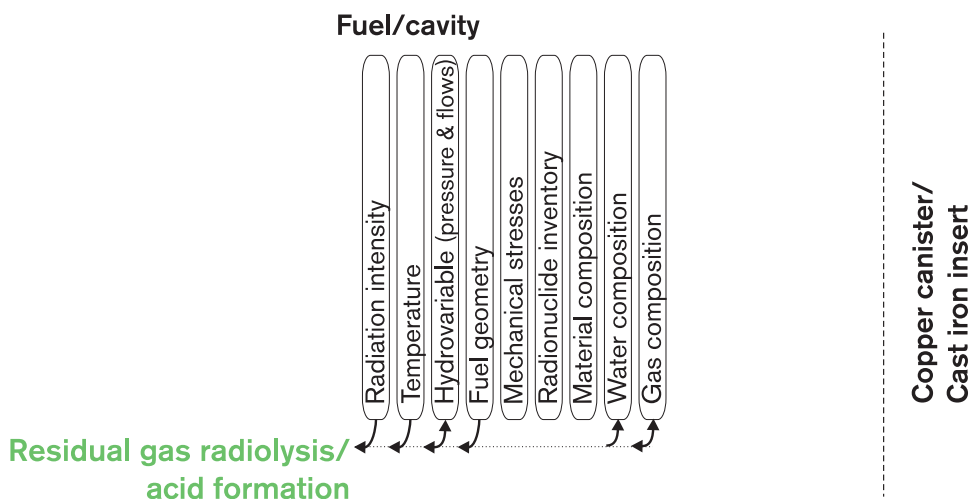


Figure 2-9. Residual gas radiolysis/acid formation.

Overview, general description

Air and water in an intact canister can be decomposed by means of radiolysis. The products can then be converted to corrosive gases such as nitric acid and nitrous acid. These gases can be of importance for stress corrosion on the canister insert, see section 3.7.3.

Model studies/experimental studies

The production of nitric acid has been calculated by Marsh /1990/, Henshaw et al, /1990/ and Henshaw /1994/ for two different dose rates and for different quantities of air and water in the canister. Not unexpectedly, the quantity of nitric acid formed is dependent on sufficient quantities of water and air. The rate at which nitric acid is formed is dependent on the dose rate. The calculations show that with 50 g of water, just under 160 g of nitric acid can be formed /Henshaw et al, 1990/. If the canister is evacuated and the air is replaced with an inert gas, the quantity of nitric acid is much lower. At 0.01 percent residual air, the quantity of nitric acid will be a few tenths of a milligram.

Time perspective

The transformation of residual air and water to nitric acid takes place over the course of years to tens of years, Henshaw et al /1990/, Henshaw /1994/.

Natural analogues

Not applicable.

Summary of uncertainties

The greatest uncertainty concerns the quantity of water that can inadvertently be introduced into the canister. The fuel bundles will be dried before they are transferred to the canister. The calculations that have been performed have assumed that 50 g of water can accompany the fuel into the canister despite drying. This quantity is equivalent to the empty volume in a punctured fuel pin. Since the great majority of fuel pins will be intact, this is a very pessimistic upper limit, and the quantity of water in the great majority of canisters will be considerably less.

Handling in the safety assessment

Base scenario: Residual air, water and radiolytically formed nitric acid will be consumed by corrosion reactions with the canister insert. The total scope of general corrosion is negligible. The process can therefore be neglected in the safety assessment. Consequences of stress corrosion cracking (SCC) are discussed in section 3.7.3.

Canister defect scenario: See the base scenario.

Climate change: See the base scenario.

Earthquake: See base scenario.

2.7.3 Water radiolysis

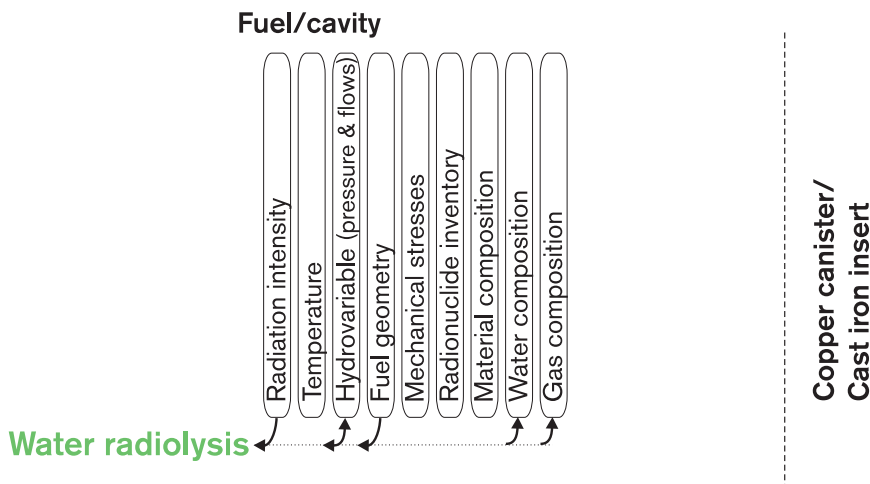


Figure 2-10. Water radiolysis. Only applicable when the copper canister is damaged.

Overview, general description

Any water that enters the canister and reaches the cavities between the fuel assemblies and the canister insert is split into reducing and oxidizing constituents by the gamma radiation in the canister's cavity. The oxidizing species that are formed will probably be consumed by corrosion of the canister insert in particular, but also to some extent of the fuel cladding. Radiolysis at fuel dissolution is dealt with section 2.7.5.

Production of reducing species results in a build-up of hydrogen gas in the void in the canister. After some time, the hydrogen gas pressure will reach a constant value and the result of continued gamma radiolysis will be reformation of water /Christensen and Bjergbakke, 1982; Christensen and Bjergbakke, 1984/. The quantity of hydrogen gas produced by radiolysis is dependent on the gamma dose rate. The contribution made by radiolysis to hydrogen gas formation is negligible compared with the contribution made by corrosion of the cast iron insert (see section 3.7.1).

Model studies/experimental studies

Radiolysis of water has been thoroughly studied by both experiments and modelling /Spinks and Woods, 1990/.

Time perspective

The process contributes to hydrogen gas formation during the first centuries after deposition. After that, gamma radiation declines to negligible levels.

Natural analogues

Not applicable.

Summary of uncertainties

Understanding: Our fundamental understanding of the process is sufficient for the needs of the safety assessment.

Data uncertainties: There are no data uncertainties of importance for the safety assessment.

Handling in the safety assessment

Base scenario: Not applicable.

Canister defect scenario: The contribution made by radiolysis to hydrogen gas production and other environmental impact is neglected. Radiolysis at fuel dissolution is dealt with in section 2.7.5.

Climate change: If the evolution leads to canister damage: See the canister defect scenario. Otherwise: See the base scenario.

Earthquake: If the evolution leads to canister damage: See the canister defect scenario. Otherwise: See the base scenario.

2.7.4 Metal corrosion

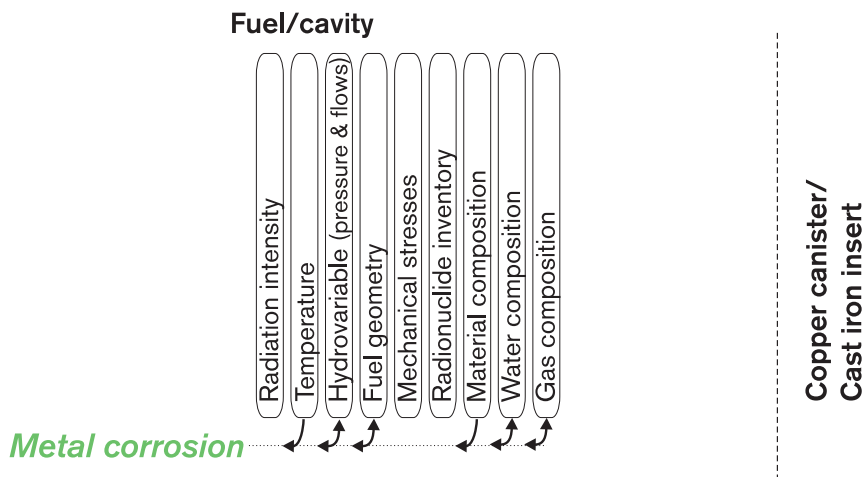


Figure 2-11. Metal corrosion. Only applicable when the copper canister is damaged.

Overview

Any water in the canister cavity can lead to corrosion of cladding tubes and other metal parts in the fuel. Besides by the composition of cladding tubes and metal parts, the process is controlled mainly by the chemical environment in the canister cavity and by the temperature.

The process affects the isolating function of cladding tubes and metal parts that enclose the fuel and is thereby of importance for the release of radionuclides from the fuel. The corrosion of metal parts also leads to release of the activation products that have formed in the metal parts.

General description

The cladding tubes for the fuel are made of Zircaloy. Other structural elements in the fuel are made of stainless steel, Inconel, Incoloy or Zircaloy. Some of the radioactivity in the fuel is present in the cladding tubes and other metal parts as activation products.

If water enters the canister, the metal parts will corrode. The corrosion rate and the release of activation products will be controlled by the dissolution rate of the surface film of zirconium dioxide which is tightly bound to the metal surface. The dissolution of the oxide film will be controlled by the solubility of ZrO_2 in the water in the immediate vicinity of the fuel and the removal of dissolved zirconium species. The solubility of ZrO_2 in water is very low, in the order of 10^{-9} M /Bruno et al, 1997/.

Considering the low corrosion rate of Zircaloy and in view of the low solubility of ZrO_2 in water, the rate of the release of activation products from the cladding tubes will be very low.

Model studies/experimental studies

No studies of the corrosion rate of Zircaloy have been conducted by SKB, but a thorough literature review was performed in 1984 by the Lawrence Livermore National Laboratory for a tuff repository /Rothman, 1984/. From Rothman's data, the corrosion rate can be estimated at approximately 2 nm/y, i.e. penetration of the cladding tubes is estimated to take place after 400,000 years at a tube thickness of 0.8 mm.

Although no detailed studies of corrosion of Zircaloy in the repository environment have been conducted, similar studies have been conducted for titanium /Mattsson and Olefjord, 1984; 1990; Mattsson et al, 1990/. The corrosion properties of titanium are very similar to those of zirconium; it is protected against general corrosion by a surface film of titanium oxide. The results of the investigations showed that the oxide film remained tightly bound to the underlying metal and that the corrosion rate was extremely low, approximately 2 nm/y, i.e. in agreement with the corrosion rate of Zircaloy based on Rothman's data.

The other engineering materials in the fuel are stainless steels or nickel-base alloys. SKB has not conducted any investigations of the corrosion resistance of these materials under repository conditions. Gdowski and Bullen /1988/ have conducted a literature review of the corrosion resistance of similar candidate materials for encapsulation of nuclear fuel for the American Nuclear Waste Management Program (NWMP). The corrosion rates for brief exposures in seawater, which is probably more aggressive than the groundwater in the deep repository, suggest values of tens of microns per year for stainless steels and microns per year for nickel-base alloys. The release of activation products will be controlled by these corrosion rates.

Time perspective

After water has come into contact with the cladding tubes, corrosion accompanied by release of activation products is expected to proceed at a constant rate for hundreds of thousands of years. The equivalent time frame for stainless steel components is hundreds of years, and for nickel-base alloys thousands of years.

Natural analogues

Not applicable.

Summary of uncertainties

Fundamental understanding: Our fundamental understanding of the process is sufficient for the needs of the safety assessment.

Data uncertainties: The uncertainties principally concern whether the corrosion rates that have been observed in short-duration experiments are valid for geological time spans.

The corrosion rate of Zircaloy (titanium) is measured during a short period compared with the expected life of the cladding tubes. The greatest uncertainty stems from the extrapolation of these short-term data. Mattsson and Olefjord /1990/ derive a logarithmic growth law for the oxide layer on titanium for measurement data of up to three years. It shows a rapid growth of an initial passivating film of about 7 nm, after which further growth takes place extremely slowly. An extrapolation to 10^6 years gives an oxide layer of 12 nm.

Mattsson and Olefjord's /1990/ data also show that for longer periods, 5 and 6 years, the growth rate deviates from the logarithmic law. After 6 years the film was 0.7 nm thicker than calculated, while the five-year samples showed considerable deviation – 4.9 and 15.5 nm, respectively – which speaks against an extrapolation according to the logarithmic law. At the shorter exposures, the oxide film was amorphous, but after longer periods it was partially crystallized. It is therefore possible that the higher growth rate is due to a more rapid transport through grain boundaries. This could be compared with active corrosion followed by a rapid repassivation. During the first year the film grows about 8 nm from the bare metal surface, which is passivated. This could be regarded as an upper limit for the corrosion rate and correspond to a life of 100,000 years for the Zircaloy cladding.

Since no relevant corrosion data have been gathered for other metal components in the fuel, the uncertainties are great. The corrosion rates are considerably greater than for the Zircaloy cladding, and a very pessimistic estimate would be to set the life of these components at 0 years.

Handling in the safety assessment

Base scenario: Not applicable.

Canister defect scenario: Available data suggest a life of the cladding tubes of at least 100,000 years. The tubes can pessimistically be assumed to be penetrated at deposition, but largely retain their mechanical integrity for a very long time and serve as a mechanical support for the column of fuel pellets. Release of activation products is assumed to occur immediately.

Other metal parts can be considered to be immediately dissolved as far as release and transport of radionuclides are concerned.

Climate change: If the evolution leads to canister damage: See the canister defect scenario. Otherwise: See the base scenario.

Earthquake: If the evolution leads to canister damage: See the canister defect scenario. Otherwise: See the base scenario.

2.7.5 Fuel dissolution

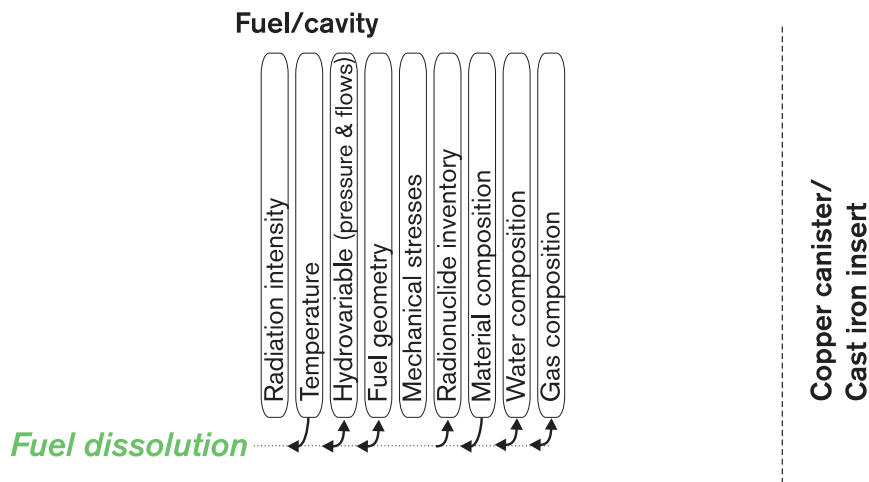


Figure 2-12. Fuel dissolution. Only applicable when the copper canister is damaged.

Overview

If water enters the canister cavity, the fuel may be dissolved/transformed, resulting in release of radionuclides. The process, which requires that the isolation of the cladding tubes has been broken, is controlled above all by the chemical environment in the fuel-clad gap, particularly the presence of oxidants, and by the fuel composition, where matrix structure and the presence of radionuclides in the fuel matrix are decisive.

The process is of fundamental importance, since it describes the release of radionuclides from the fuel.

General description

Non-matrix-bound activity

Radionuclides in materials that have been segregated to the fuel-clad gap will rapidly go into solution. The quantity of activity released is determined by the solubility and availability of segregated material. The release from the gap is independent of the dissolution or transformation of the uranium dioxide in the fuel. This is discussed in greater detail in section 2.7.6.

Matrix-bound activity

The majority of fission products and higher actinides in the fuel exist as a solid solution in the uranium dioxide matrix. Release of these radionuclides requires that the uranium dioxide be dissolved or otherwise altered, for example by oxidation. This can happen if water has entered the canister and the cladding tubes are damaged.

Fuel dissolution and release of radionuclides under anoxic conditions: Uranium dioxide is stable in oxygen-free water with low silicon activity and U(IV) has very low solubility in water. The scatter of experimental data spans several orders of magnitude /Fuger, 1993/ but seems to be relatively independent of the temperature.

Bruno et al /1997/ recommend a solubility of around $1.3 \cdot 10^{-7}$ for the safety assessment. This is roughly a factor of a hundred greater than the solubility of $UO_2(s)$ and may be regarded as a pessimistically chosen solubility.

The substances dissolved in the uranium dioxide matrix will be released as the chemical dissolution of the uranium dioxide proceeds. The total quantity that is released will be controlled by the quantity of dissolved uranium, which is in turn dependent on the interaction between the dissolution rate, the solubility of uranium and the water flux around the canister.

Fuel dissolution and release of radionuclides under oxidizing conditions: In the presence of oxygen, uranium will be oxidized to U(VI). The solubility of U(VI) species (uranyl) is considerably higher than that of U(IV) species. This solubility is also dependent on the presence of complexing agents, of which carbonate is the most important in natural Swedish groundwaters. Bruno and Sellin /1992/ recommend values of the solubility in the range $3 \cdot 10^{-4}$ to $3 \cdot 10^{-6}$ M, depending on the water's carbonate content.

In the presence of oxidants, the possibility that the oxidation rate of the uranium dioxide will be higher than its dissolution rate cannot be ruled out. This would lead to dissolution followed by precipitation of solid U(VI) phases on or near the fuel. The composition of these phases will depend on the water composition. In groundwater or bentonite pore water, uranyl oxides/hydroxides (schoepite) will probably dominate first, while in a longer time perspective more stable uranyl silicates (for example uranophane) will form.

As the uranium dioxide is converted, nuclides bound in the fuel will be mobilized and can, if they are readily soluble, be transported away from the fuel out into the near field. Less soluble nuclides can either be precipitated as separate phases or, by co-precipitation, be incorporated in the uranium phases or other phases that are formed on or near the fuel.

Redox conditions in connection with water ingress: When water comes into contact with the fuel, the uranium dioxide will begin to dissolve. This will occur by chemical dissolution or by oxidation/corrosion of the fuel, depending on the redox conditions immediately surrounding the fuel. Alpha and beta radiation will dominate in the fuel-clad gap. In the same way as gamma radiation splits water in the void in the canister (section 2.7.3), the alpha and beta radiation will split the water into oxidizing and reducing species, principally hydrogen, oxygen and hydrogen peroxide. Oxidizing and reducing species are produced in equivalent quantities and do not actually influence the redox conditions immediately surrounding the fuel.

Since hydrogen at the temperatures in question ($< 100^\circ\text{C}$) is considerably more slow-reacting than oxygen and hydrogen peroxide, the effect of the radiolysis will be an oxidation of the uranium dioxide in the fuel to U(VI) species. The oxidation rate is determined by the production rate of oxidizing radiolysis products, the rate of the oxidation reaction and the fuel area available for oxidation. The course of the reaction will be analogous to the oxidation of the uranium dioxide to schoepite in defective fuel rods in a reactor /Forsyth et al, 1990/. In a repository, where the dose rate is much lower than in the reactor, the oxidation process will be much slower. Since the Zircaloy cladding, even if it is perforated, is expected to remain around the fuel for a very long time after water ingress, the fuel will be oxidized by the water volume present between the fuel and the cladding tubes.

Model studies/experimental studies

Experimental studies of fuel dissolution have been conducted for more than 20 years, see for example Eklund and Forsyth /1978/ and Forsyth /1997/.

The radiolytic oxidation of fuel inside the Zircaloy cladding has been modelled by Eriksen /1997/. Eriksen's conclusions are that the oxidation process is dominated by the reaction between hydrogen peroxide and fuel. As the hydrogen gas pressure builds up, the consumption of oxidants will decrease, i.e. oxidation of the fuel will abate. The reason for this is the interaction between the alpha and beta radiolysis, where oxidizing radicals from the beta radiolysis are consumed by reactions with hydrogen.

Time perspective

After water has come into contact with the fuel, fuel transformation will proceed for hundreds of thousands of years.

Natural analogues

Naturally occurring uraninite can be of help in understanding the weathering sequence for uranium dioxide.

Summary of uncertainties

Fundamental understanding: There are no real uncertainties as far as our fundamental understanding of the process is concerned. The uncertainties primarily concern the size and importance of the different processes that control the fuel transformation.

Redox conditions in connection with fuel dissolution: Oxidation of iron will probably proceed much faster than oxidation of UO_2 inside a damaged canister. No direct comparison has been made, but an estimate of the time required to consume the oxygen in a copper canister shows that any residual oxygen will be consumed by oxidation of copper within a year or so /Johnson et al, 1996/. The consumption rate in an iron canister should be comparable, since the corrosion rates of iron and copper are comparable /Wersin et al, 1993/. There are therefore hardly any appreciable uncertainties surrounding the possibility that the water that will come into contact with the fuel may be oxygen-free. Fuel dissolution should therefore be modelled as oxidative dissolution where the radiolysis of water is the only source of oxidants. As has been evident from the earlier discussions of the durability of Zircaloy in the repository environment, the cladding tubes can be assumed to remain around the fuel for a very long time, and the environment in which fuel oxidation/dissolution takes place will be determined by groundwater equilibrated with bentonite and the alpha and beta radiation in the fuel-clad gap /Eriksen, 1997/. Even though the model is conceptually defensible, there are many uncertainties that can affect the result.

Handling in the safety assessment

Base scenario: Not applicable.

Canister defect scenario: Two models are used for the transformation of fuel in SR 97:

- In the model used in the main case, the transformation is assumed to be controlled by radiolytically produced oxidants. In the calculation model, the process is simplified by the use of a constant transformation rate.

- To illustrate the importance of the stability of the fuel matrix, a calculation will be carried out where the barrier function of the fuel is neglected. This is unreasonable, but gives an upper limit for the consequences of the process. This calculation case is warranted by the fact that uncertainties still exist in our understanding of the mechanisms of fuel dissolution.

Climate change: If the evolution leads to canister damage: See the canister defect scenario. Otherwise: See the base scenario.

Earthquake: If the evolution leads to canister damage: See the canister defect scenario. Otherwise: See the base scenario.

2.7.6 Dissolution of gap inventory

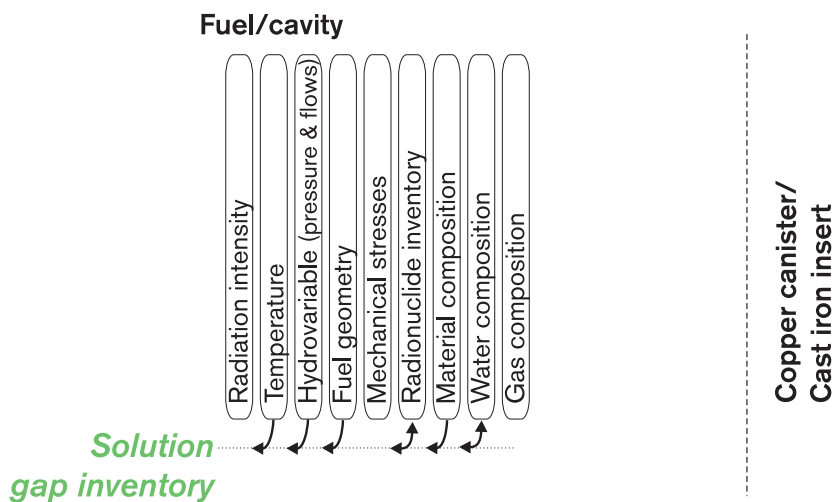


Figure 2-13. Dissolution of gap inventory. Only applicable when the copper canister is damaged.

Overview, general description

In the event of canister damage, water can enter the canister. If the fuel cladding is damaged, the water can also come into contact with the fuel. Most of the radionuclides in the fuel are evenly distributed in the UO_2 matrix and are released when the fuel dissolves (see section 2.7.5). A small fraction of the inventory of a few radionuclides has segregated to the fuel-clad gap and possibly also to grain boundaries in the fuel (see section 2.1.3).

On contact with water, these radionuclides can quickly go into solution. The quantity of activity released is determined by the solubility and the availability of segregated material. A study of the release of segregated nuclides in fuel has been performed by Johnson and Tait /1997/.

Model studies/experimental studies

An immediate release of caesium and iodine from the fuel on contact with water is experimentally verified, see e.g. Johnson and Tait /1997/.

Time perspective

The release can be regarded as immediate (in the order of days).

Natural analogues

Not applicable.

Summary of uncertainties

Uncertainties surrounding fundamental understanding: Our fundamental understanding of the process is sufficient for the needs of the safety assessment.

Data uncertainties: It has been experimentally shown that fractions of the content of fission gases, caesium and iodine can leave the fuel matrix during reactor operation. It is also known that Tc, Ru, Rh, Pd and Mo form metallic inclusions in the fuel. There are no major systematic studies of segregations in light water reactor fuel, with the exception of release of fission gases. Uncertainties surrounding the size of and, in some cases, the very existence of segregations of certain radionuclides are great. Uncertainties are discussed in greater detail by Johnson and Tait /1997/.

Handling in the safety assessment

Base scenario: Not applicable.

Canister defect scenario: Immediate release of radionuclides according to Andersson /1999/ based on Johnson and Tait /1997/.

Climate change: If the evolution leads to canister damage: See the canister defect scenario. Otherwise: See the base scenario.

Earthquake: If the evolution leads to canister damage: See the canister defect scenario. Otherwise: See the base scenario.

2.7.7 Speciation of iron corrosion products

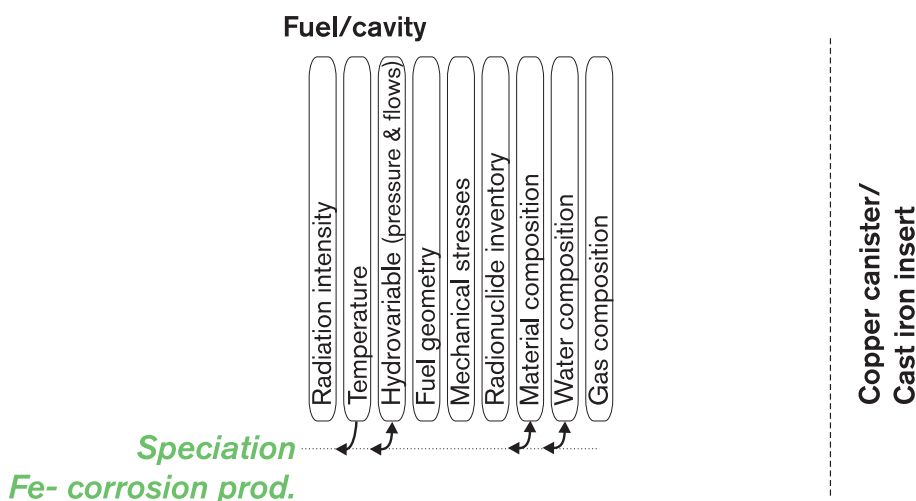


Figure 2-14. Speciation of iron corrosion products. Only applicable when the copper canister is damaged.

Overview, general description

If water enters the canister, the cast iron insert will corrode. The oxygen in the water has then in all probability already been consumed by reactions with minerals in the bentonite and by reacting with the copper canister. If the water should contain any residual oxygen, it will quickly be consumed by reacting with the cast iron (see section 3.7.1) and continued corrosion will take place by reaction with the water. The reaction between cast iron and water produces magnetite and hydrogen gas.

The process is of crucial importance for the hydrochemical environment in the canister cavity. As a result, reducing conditions will prevail in the cavity for a very long time.

Model studies/experimental studies

It is well known that magnetite and hydrogen are formed by anaerobic corrosion of iron. This has also been verified experimentally for the hydrochemistry that can be expected to prevail in the deep repository /Blackwood et al, 1995; Smart et al, 1997/.

Time perspective

The corrosion process will proceed for tens of thousands of years after water ingress.

Natural analogues

Not applicable.

Summary of uncertainties

There are no conceptual uncertainties. The uncertainties mainly relate to the quantity of dissolved Fe(II).

Handling in the safety assessment

Base scenario: Not applicable.

Canister defect scenario: A quantitative description of the chemical environment inside a defective canister is given.

Climate change: If the evolution leads to canister damage: See the canister defect scenario. Modified hydrogeochemical conditions may then need to be discussed. Otherwise: See the base scenario.

Earthquake: If the evolution leads to canister damage: See the canister defect scenario. Otherwise: See the base scenario.

2.7.8 Speciation of radionuclides, colloid formation

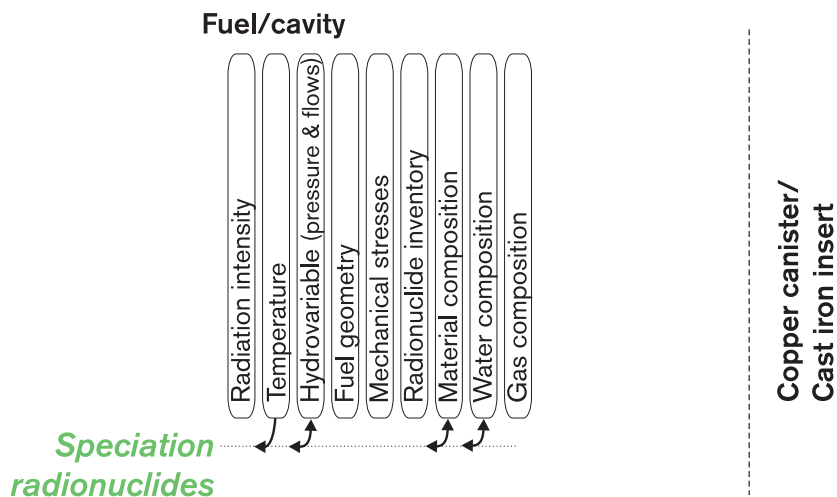


Figure 2-15. Speciation of radionuclides, colloid formation. Only applicable when the copper canister is damaged.

Overview, general description

Radionuclides that have been released from or exposed in the fuel matrix and other metal parts can dissolve in the water in the canister cavity and thereby become available for transport or precipitate as unavailable solid phases. The distribution between dissolved and solid phases is determined by the solubilities of the nuclides, which are in turn dependent above all on the chemical environment in the canister cavity and the temperature.

Alternatively, radionuclides can be released in the form of colloids or pseudocolloids. This is of no importance for radionuclide dispersal from the canister as long as the bentonite buffer, which acts as an efficient filter for colloids, remains in place.

Due to the ongoing corrosion of the canister insert, reducing conditions exist (see section 2.7.7). The solubilities and the speciation that are recommended in Bruno et al /1997/ pertain to reducing conditions and thereby also apply to the void in the canister. The process is of fundamental importance for the transport of radionuclides.

Model studies/experimental studies

Solubility calculations for SR 97: In solubility calculations for a safety assessment, a solubility-limiting phase is postulated for each radioelement. Phases are chosen which with great certainty can be formed under the conditions that prevail. Amorphous phases are, for example, chosen instead of crystalline ones, while stable sulphides and silicates that are not formed with certainty are often disregarded entirely in the modelling. The solubility calculations determine not only the solubility of the radioelement, but also the speciation of all radionuclides in the aqueous phase. Speciation is of importance for solubility, but also for the transport properties of the radionuclide in buffer and rock. Table 2-2 contains the solubility-limiting phases that are used in SR 97 as well as the dominant species /Bruno et al, 1997/.

Table 2-2. Solubility-limiting phases and speciation in SR 97

| Element | Solubility-limiting phase | Dominant species |
|---------|-------------------------------|---|
| Ag | Silver/AgCl | AgCl_x^- |
| Am | AmOHCO_3 | $\text{Am}(\text{OH})_2^+$, AmCO_2^+ , AmOH^{2+} |
| Cm | CmOHCO_3 | CmOH^{2+} |
| Ho | $\text{Ho}_2(\text{CO}_3)_2$ | HoCO_3^+ , $\text{Ho}(\text{CO}_3)_2^-$ |
| Nb | Nb_2O_5 | NbO_3^- |
| Ni | NiO | Ni^{2+} , NiCO_3 |
| Np | $\text{Np}(\text{OH})_4$ | $\text{Np}(\text{OH})_4$, $\text{Np}(\text{OH})_3\text{CO}_3^-$, $\text{Np}(\text{HPO}_4)_4^{6-}$ |
| Pa | Pa_2O_5 | PaO_2OH |
| Pd | PdO | $\text{Pd}(\text{OH})_2$ |
| Pu | $\text{Pu}(\text{OH})_4$ | $\text{Pu}(\text{OH})_4$, PuCO_3^+ , Pu^{3+} |
| Ra | RaSO_4 | Ra^{2+} , RaSO_4 |
| Se | $\text{FeSe}_{(2)}$ /Selenium | HSe^- |
| Sm | $\text{Sm}_2(\text{CO}_3)_2$ | SmCO_3^+ , $\text{Sm}(\text{CO}_3)_2^-$ |
| Sn | SnO_2 | $\text{Sn}(\text{OH})_4$, $\text{Sn}(\text{OH})_5^-$ |
| Sr | Celestite/Strontianite | Sr^{2+} |
| Tc | TcO_2 | $\text{TcO}(\text{OH})_2$ |
| Th | $\text{Th}(\text{OH})_4$ | $\text{Th}(\text{OH})_4$, $\text{Th}(\text{HPO}_4)_3^{2-}$ |
| U | UO_2 | $\text{U}(\text{OH})_4$ |
| Zr | ZrO_2 | $\text{Zr}(\text{OH})_4$ |

Available model studies/experimental studies for important elements in the safety assessment are discussed in the following.

Caesium and iodine: The elements that are segregated to the fuel-clad gap will immediately be released on contact with water. These elements are caesium and iodine, possibly also **chlorine** and **carbon**. There are no solubility limits for the three first elements, nor are they redox-sensitive. The most probable solution species are Cs^+ , I^- and Cl^- . Carbon could conceivably be released as carbonate, methane or other carbon compounds, depending on redox conditions and redox kinetics. The chemical formula of carbon in UO_2 is not known, but van Konynenburg /1994/ regards carbide, oxycarbide and elemental carbon as possible alternatives. Under oxidizing conditions, the release of carbon from the fuel appears to take place as carbon dioxide. If carbon is present as carbonate, it is conceivable that under certain conditions the release is solubility-limited by precipitation of solid carbonates.

After the gap inventory has been dissolved, further dissolution of these elements will be controlled by the fuel oxidation/transformation process.

Strontium: Strontium is present in solid solution in the fuel matrix and is not solubility-limited or redox-sensitive. It is released as the fuel oxidation/transformation proceeds. The cation Sr^{2+} will be the dominant solution species. Depending on the water chemistry, strontium sulphate or strontium carbonate will be solubility-limiting solid phases. Most likely, the strontium concentrations in the water will never reach the solubility limits. The strontium concentrations may possibly be reduced by co-precipitation with calcium carbonate.

Selenium: The fraction of ^{79}Se in the fuel is around 8 ppm according to Origen calculations (50 MWd/kg U, PWR) and approximately 1 ppm according to analyses /MCC, 1988/. The total amount of selenium in the fuel according to the Origen calculations is approximately 80 ppm. The radiometric analyses that were carried out for MCC assumed a half-life of 65,000 years. New determinations have given a half-life for ^{79}Se of $1.1 \cdot 10^6$ years /Songsheng et al, 1997/. With this value of the half-life, the concentration of ^{79}Se in the fuel is 15 ppb for the measured activity.

In the fuel corrosion experiments, no release of ^{79}Se has been observed within the experimental margins of error. In carbonate-containing water under oxidizing conditions, the uranium concentrations are in the order of 10^{-5} M. In the case of congruent dissolution, the selenium concentration would be $3 \cdot 10^{-9}$ and ^{79}Se would comprise one-tenth of this. Wilson /1990a/ reports attempts to radiometrically analyze ^{79}Se in experiments conducted under oxidizing conditions and stipulates a detection limit for ^{79}Se of 0.3 ng/ml. This corresponds to a selenium concentration of $4 \cdot 10^{-8}$ M. With a half-life of $1.1 \cdot 10^6$ years instead of 65,000 years, the actual detection limit is 5 ng/ml or $7 \cdot 10^{-7}$ M. Wilson also observes that the concentrations of ^{79}Se are below or around the detection limit, which is to be expected in view of the low selenium content of the fuel.

Bruno et al /1997/ give a solubility for selenium of less than 10^{-9} M for reducing conditions. The solution species for oxidizing conditions is selenate and for reducing conditions HSe^- . Solubility-limiting solid phases are the sequence from oxidizing conditions to reducing conditions: calcium selenate, elementary selenium, FeSe_2 and FeSe . The selenides have very low solubilities. If selenium has been released by oxidation, it may exist initially as selenate. The kinetics for reduction of selenate to selenide may be very slow. The analogous reduction of sulphate to sulphide takes place in natural waters only via sulphate-reducing bacteria.

Zirconium: Zirconium exists in solid solution in the fuel matrix and comprises approximately 0.5 percent of the irradiated fuel. It is released as the fuel oxidation/transformation proceeds. It is not redox-sensitive, but very poorly soluble. Bruno et al /1997/ recommend a solubility of approximately $2.5 \cdot 10^{-9}$ M. The contribution to zirconium in solution will in all probability be dominated by stable isotopes from the cladding tubes, and the concentrations of radioactive zirconium will be very small. In Studsvik's series 11 /Forsyth, 1997/, the concentrations are below the detection limit, which is around $1 \cdot 10^{-9}$ M. The solution species is $\text{Zr}(\text{OH})_4$ for all pH values of interest, and zirconium dioxide, probably amorphous, is the solubility-limiting solid phase.

Technetium: Most of the technetium in the fuel is located in metallic inclusions. The release of technetium is indirectly dependent on the dissolution of the fuel matrix in such a way that the inclusions are exposed to water as the surrounding fuel matrix is dissolved. When the inclusions are exposed to water, their dissolution is largely dependent on the dissolution of the fuel. Under reducing or anoxic conditions, technetium has very low solubility, in the order of 10^{-8} M /Bruno et al, 1997/. This value agrees fairly well with what has been observed in fuel corrosion experiments /Forsyth and Werme, 1992/. The dominant solution species are $\text{TcO}(\text{OH})_2$ with $\text{TcO}_2 \cdot x\text{H}_2\text{O}$ as the solubility-controlling solid phase.

Under oxidizing conditions, when pertechnetate, TcO_4^- , can be formed, solubility can be very high, and no solubility limitation has been observed for technetium in fuel corrosion experiments /Forsyth and Werme, 1992; Wilson 1990b/. In the presence of Fe(II)-containing minerals, pertechnetate will be reduced to Tc(IV) /Cui and Eriksen, 1996/. The corrosion products (magnetite) on the cast iron insert are therefore expected to efficiently reduce any Tc(VII).

Palladium: In the same way as in the case of technetium, most of the palladium in the fuel is located in metallic inclusions and is assumed to be released in an analogous fashion. Of the palladium isotopes that are formed by nuclear fission, only ^{107}Pd is radioactive. The ^{107}Pd fraction of the entire palladium inventory is about 15 percent. Palladium has very low solubility; Bruno et al /1997/ give a value in the range 10^{-8} to 10^{-9} M. In Studsvik's series 11 /Forsyth, 1997/, the concentrations are below the detection limit, which is around $2 \cdot 10^{-9}$ M. $\text{Pd}(\text{OH})_2$ is expected to be the dominant solution species, and PdO is the solubility-limiting solid phase /Bruno et al, 1997/.

Tin: The fraction of tin in the fuel is around 160 ppm (50 MWd/kg U, PWR), of which about 25 percent is ^{126}Sn . As in the case of ^{79}Se , calculated and measured ^{126}Sn values differ. The analyses give only 20 percent of the value calculated with Origen /MCC 1988/. The half-life of ^{126}Sn may also be underestimated, but unlike in the case of ^{79}Se the discrepancy is only a factor of 2 too low /Haas et al, 1996; Shengdong Zhang et al, 1996/. In the fuel corrosion experiments, no release of ^{126}Sn has been observed within the margins of error. Wilson's /1990a/ attempts to analyze ^{126}Sn gave values below or close to the detection limit for oxidizing conditions, as in the case of ^{79}Se . Wilson gives a detection limit of 0.02 ng/ml, equivalent to a tin concentration of $6 \cdot 10^{-10}$ M. This is of the same order of magnitude as the solubility of tin under reducing conditions /Bruno et al, 1997/. Expected tin concentrations in solution, based on the quantity of dissolved uranium, are in the order of 10^{-9} M.

The speciation of tin in solution depends primarily on the pH. $\text{Sn}(\text{OH})_4$ dominates at a pH of around 8, while $\text{Sn}(\text{OH})_5^-$ dominates at a pH of 9. The solubility-limiting phase is SnO_2 /Bruno et al, 1997/.

Neptunium: The concentration of neptunium (mainly ^{237}Np) increases with burnup and is around 0.08 percent for high-burnup fuel after several decades of decay, after which it increases to a few tenths of a percent. Neptunium in the form of neptunium dioxide is assumed to be in solid solution with the uranium dioxide and will be able to be dissolved as the uranium dioxide is dissolved or transformed. Data are available for neptunium from fuel corrosion experiments under both oxidizing and anoxic conditions. Wilson reports for series 2 /1990a/ $\log[M] = -8.6$ at 25°C and series 3 /1990b/ $\log[M] = -8.9$ at 25°C and $\log[M] = -9.1$ at 85°C . Studsvik has for series 11, an experimental series performed on a segment rod with a burnup varying from 21.2 to 49.0 MWd/kg U along the length of the rod, a mean value of the neptunium concentration of $\log[M] = -9.1$ for oxidizing conditions and $\log[M] = -10.4$ for anoxic conditions /Werme and Spahiu, 1998; Forsyth, 1997/. The concentrations show no correlation with the neptunium content of the fuel specimens, which could indicate some form of solubility control. The concentrations for oxidizing conditions agree fairly well with calculated values for reducing conditions /Bruno et al, 1997/, while for anoxic conditions the measured concentrations lie two orders of magnitude below calculated levels.

For the redox potentials and pHs that prevail in granitic groundwaters, $\text{Np}(\text{OH})_4$ is the dominant solution species. The solubility-limiting solid phase is $\text{Np}(\text{OH})_4(\text{am})$ /Bruno et al, 1997/. In a similar fashion as for technetium, oxidized Np will initially be reduced to Np(IV) on the cast iron insert's corrosion products /Cui and Eriksen, 1996/.

Plutonium: The fraction of plutonium in irradiated nuclear fuel lies just under one percent, relatively independent of burnup, since nuclear fissions of plutonium largely offset new production at even moderate burnups. Plutonium in the form of plutonium dioxide is assumed to be in solid solution with the uranium dioxide and will be able to be dissolved as the uranium dioxide is dissolved or transformed. Data are available for plutonium from fuel corrosion experiments under both oxidizing and anoxic conditions. Wilson reports for series 2 at 25 °C /1990a/ $\log[M] = -8.4$ for a PWR fuel with a burnup of 30 MWd/kg U and $\log[M] = -9.1$ for a PWR fuel with a burnup of 27 MWd/kg U. For series 3 /1990b/ the values are $\log[M] = -8.4$ at 25 °C and $\log[M] = -10.4$ at 85 °C. In Studsvik's series 11, a plutonium value of $\log[M] = -8.6$ was measured for oxidizing conditions and $\log[M] = -10.1$ for anoxic conditions /Werme and Spahiu, 1998; Forsyth, 1997/. The concentrations for anoxic conditions agree well with calculated levels / Bruno et al, 1997/. Bruno et al /1997/ give $\text{Pu}(\text{OH})_4$ as the dominant solution species for conditions prevailing in granitic groundwater with $\text{Pu}(\text{OH})_4(\text{am})$ as the solubility-limiting phase.

In earlier experimental series (series 3 and 7), the plutonium concentrations at the first contacts have been approximately one order of magnitude higher than has been measured for later exposures to water /Forsyth and Werme, 1992/. The same tendency exists for series 11, but less pronounced. For series 3 and 7 the plutonium concentrations, $\log[M] = -9.1$, were for water contacts after the first 200 days. This is slightly lower than in series 11, where the equivalent value is $\log[M] = -8.7$. For fuel with extremely low burnup, 0.5 MWd/kg U, where the plutonium content is only one percent of the content in normal fuel, ^{239}Pu concentrations of $\log[M] = -8.9$ were measured /Forsyth and Werme, 1992/. This value agrees well with plutonium concentrations measured in experiments with higher plutonium contents and would therefore indicate a solubility limitation for the plutonium release. The plutonium content of the low-burnup fuel is near the congruent quantity for the quantity of dissolved uranium. The possibility that the concentration is controlled by the uranium dissolution can therefore not be ruled out. In deionized water the plutonium concentrations for series 3 and 7 were $\log[M] = -7.9$ /Forsyth and Werme, 1992/ and for series 11 $\log[M] = -7.7$. For series 11, only 7 experiments have been carried out at neutral pH.

Americium and curium: The fractions in the fuel of the trivalent actinides americium and curium are burnup-dependent and are around 0.09 percent and 0.02 percent, respectively, for high-burnup fuel (50 MWd/kgU /MCC, 1988/).

Americium is difficult to analyze in solutions that have been in contact with fuel, both radiometrically and by mass spectroscopy, due to overlap between ^{241}Am and plutonium isotopes. Wilson /1990a, 1990b/ analyzes americium radiometrically after separation and notes the large scatter between data and the fact that filtration of the solution greatly affected the concentrations. Wilson's conclusion is that most of the americium is particles or colloids. This is not unreasonable, since it is known that americium sorbs strongly. Wilson reports concentrations of $\log[M] = -9.8$ for 25°C and $\log[M] = -12.3$ for 85°C in carbonate-containing water.

The quantity of americium congruent with uranium would have given concentrations of around $\log[M] = -8$. Bruno et al /1997/ calculate the solubility of americium to be 10^{-7} M. The much lower measured concentrations suggest that americium cannot be solubility-limited by a pure americium phase. The possibility that the measured concentrations are greatly influenced by sorption cannot be ruled out.

Bruno et al /1997/ name $\text{Am}(\text{OH})_2^+$ or AmCO_3^+ as the solution species, depending on the carbonate concentration in the groundwater. The solubility-limiting phase is AmOHCO_3 .

Wilson /1990a, 1990b/ has determined the curium concentrations by means of direct alpha spectrometry. Curium behaves in a manner similar to americium. Data are very scattered, and the concentrations are influenced strongly by filtrations. Wilson gives as approximate concentrations of curium $\log[M] = -11.3$ at 25°C and $\log[M] = -14.2$ at 85°C . Studsvik has routinely analyzed curium by alpha spectrometry, but the results are not normally evaluated. A preliminary reporting of curium concentrations was done by Forsyth et al /1988/. The concentrations were low, $\log [M] = -11.2$, which agrees well with Wilson's data.

Bruno et al /1997/ give $\text{Cm}(\text{OH})_2^+$ as the solution species and CmOHCO_3 as the solubility-limiting phase.

Colloid formation: In the experiments at Studsvik, a fraction of the leachate from each experiment was filtered through a membrane filter that only passes aggregates smaller than 15–20 Å. The purpose of the filtrations was to try to determine the fraction of colloids in the leachates. It is unclear whether the material on the filter represents colloids. The large scatter in data, from a few microns up to a hundred microns, may be an indication of the fact that the material on the filter is dominated by larger particles than colloids /Forsyth, 1997/. The median value for uranium can be estimated to be around 20 µg/200 ml (0.1 ppm), to be compared with a few ppm for the concentrations of uranium in solution under oxidizing conditions. For anoxic conditions, less data are available and the median value is also slightly lower. The quantities of uranium on the filters and in solution are comparable and in the order of tens of ppb.

Time perspective

Throughout the life of the repository.

Natural analogues

Not applicable.

Summary of uncertainties

Calculations of solubilities for application in safety assessment are always made with a certain measure of pessimism and are thus never an attempt to simulate real systems. The intention is instead to determine a defensible upper limit for the solubility of the element in question, based on known and well-defined solubility-limiting phases. The modellings that are done are, on the other hand, realistic simulations of the given sets of input data.

The uncertainties in the calculated solubilities with respect to input data are discussed in Bruno et al /1997/. It is above all redox conditions, pH, carbonate concentration and temperature that influence solubility. The solubility of some radioelements is not at all affected by reasonable variations of these parameters, but most are affected by at least one. Besides uncertainties in input data, uncertainties in the thermodynamic database used are also discussed, as well as the uncertainties in the calculation programs used for the calculations.

Handling in the safety assessment

Base scenario: Not applicable.

Canister defect scenario: Solubilities according to Anderson /1999/, are used. They are taken from Bruno et al /1997/.

Climate change: If the evolution leads to canister damage: See the canister defect scenario. The effects of modified hydrogeochemical conditions may need to be investigated. Otherwise: See the base scenario.

Earthquake: If the evolution leads to canister damage: See the canister defect scenario. Otherwise: See the base scenario.

2.7.9 Helium production

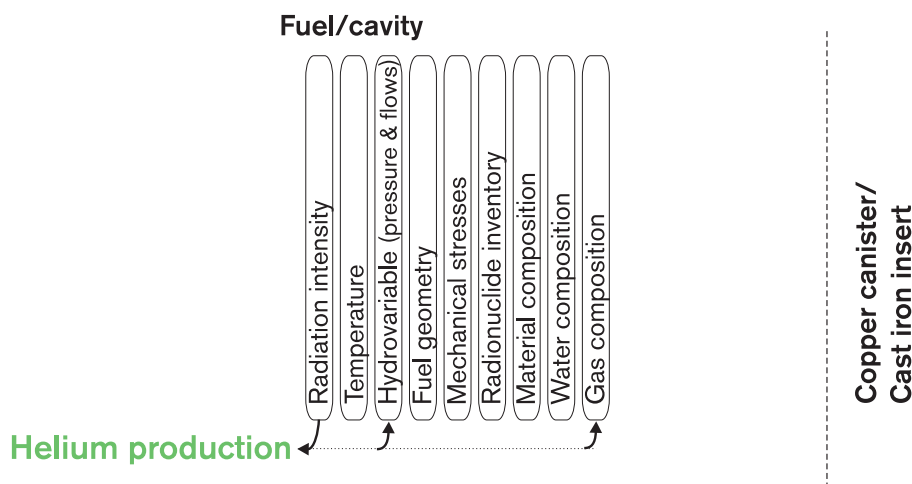


Figure 2-16. Helium production.

Overview, general description

α particles (helium nuclei) from α decay in the fuel form gaseous helium after they have been slowed down in the fuel matrix. Around a fuel rod with an intact cladding tube, this leads to a pressure build-up inside the tube, which can in turn lead to mechanical tube rupture, see section 2.6.1. If the cladding tubes are damaged, a negligible pressure increase arises in the canister cavity.

Model studies/experimental studies

The pressure increase lies in the range 10 to 20 MPa in 100,000 years, based on a void of 20 cm³. If this pressure should lead to rupture of the cladding tubes, the pressure increase in the void in the canister would be in the order of 0.1 MPa, which is completely negligible.

Time perspective

The helium build-up proceeds continuously as long as there is uranium left in the fuel.

Natural analogues

Not applicable.

Summary of uncertainties

No conceptual uncertainties.

The uncertainties concern when cladding tube rupture occurs due to the pressure build-up. The pressure build-up is slow at the same time as the Zircaloy cladding ages.

Handling in the safety assessment

Base scenario: A pessimistic assumption is that all fuel rods are so severely damaged that helium can leak out to the void in the canister insert.

Canister defect scenario: See base scenario.

Climate change: See base scenario.

Earthquake: See base scenario.

2.8 Radionuclide transport

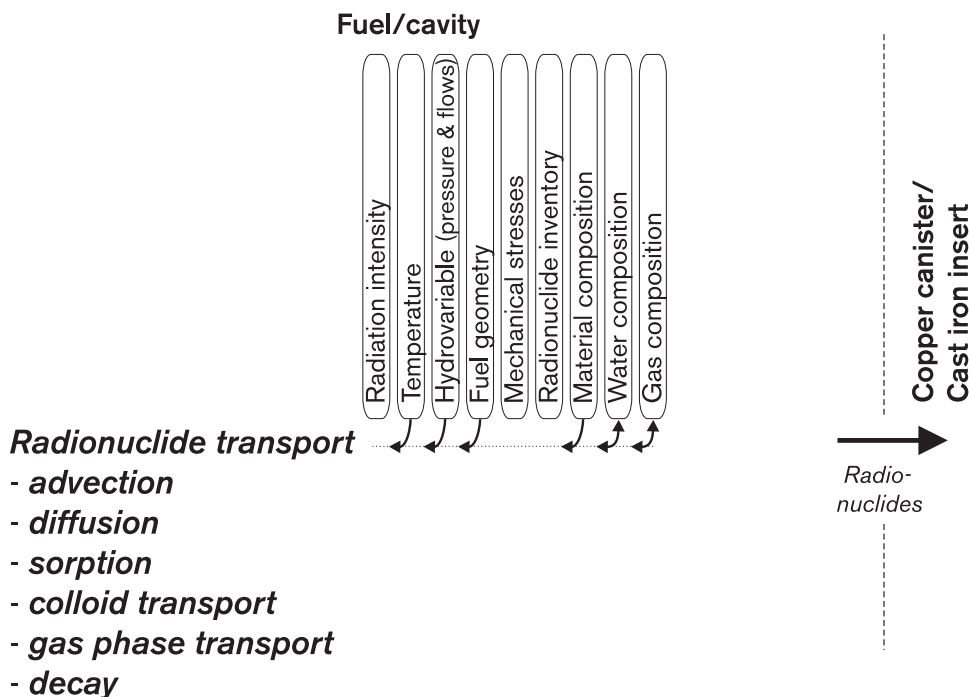


Figure 2-17. Radionuclide transport in fuel/canister.

Overview, general description

If water enters a damaged canister, corrosion of the cast iron insert and the fuel's metal parts begins, see section 3.7.1 and 2.7.4. With time, the evolution may allow water to come into contact with the fuel and thereby cause radionuclides to be released as water-soluble species or colloids, sections 2.7.5 and 2.7.8. Radionuclides are also present in the metal parts of the fuel and are released when they corrode.

Released radionuclides can be transported in the interior of the canister and exit through a damaged copper shell. Radionuclides dissolved in water inside the canister can be transported either by accompanying any movements of the water, *advection*, or by *diffusing* in the water. Transport in water is the predominant mode of transport of radionuclides. Some nuclides may occur in gaseous form in the canister and may then also be *transported in the gas phase*. This is particularly true of C-14, Rn-222 and Kr-85.

The geometry of the transport pathways in a damaged canister is determined by the original geometry of the canister and the fuel and by the changes to which the corrosion has led. In order for water to come into contact with fuel and permit release and transport of radionuclides, there must be penetrating breaches in both the cast iron insert and the Zircaloy cladding. Even if such breaches have occurred, the remaining structures can be expected to constitute considerable transport barriers, both to inflow of water (section 2.5.1) and to outward transport of water-dissolved nuclides. The structure of the four-metre-long cladding tubes, the other metal parts of the fuel, the cast iron insert and the copper canister prevent effective transport. Products from the corrosion of the cast iron insert in particular can also be expected to obstruct transport. The surfaces of all of these structures may also have good *sorption* properties for certain radionuclides.

Model studies/experimental studies

No direct studies of radionuclide transport are known for the conditions that are expected in a damaged canister. General knowledge concerning such processes as advection, diffusion and sorption is good, however, and the processes have been thoroughly studied.

Time perspective

After the copper shell has been breached, radionuclide transport in the interior of the canister is a relevant process in all of the safety assessment's time perspectives.

Uncertainties

The uncertainties surrounding water/gas flux in the interior of the canister (section 2.5.1), corrosion of the cast iron insert (section 3.7.1) and corrosion of the metal parts in the fuel (section 2.7.4) are particularly great. An assessment of the geometric conditions and thereby the geometry of the transport pathways is therefore also uncertain. The sorption properties of the materials in a damaged canister are also difficult to assess.

Radionuclide transport in the interior of the canister is therefore simplified pessimistically in the safety assessment, see below.

Handling in the safety assessment

Base scenario: Not applicable.

Canister defect scenario: Radionuclide transport in the interior of the canister is simplified for modelling purposes in the following way: After a given waiting period has passed since the breach of the canister's copper shell, the entire void in the canister on closure, about 1 m³, is assumed to be filled with water. The length of the waiting period is determined on the basis of the size of the breach in the copper shell and the subsequent water flux and corrosion.

After the waiting period, all water in the canister is assumed to be available for the fuel dissolution process, i.e. to be in direct contact with all fuel without being impaired by Zircaloy cladding or other structures. The water is assumed to be thoroughly mixed, i.e. there are no concentration differences between different parts of the interior of the canister. The fuel dissolution process then determines the rate of release of matrix-bound radionuclides. Segregated nuclides and radionuclides in the structural parts of the fuel are assumed to be available for dissolution in water immediately after the end of the waiting period. Sorption of radionuclides to the internal parts of the canister is neglected.

Transport of radionuclides through the breach in the copper shell is modelled as diffusion with an assumed geometry of the breach.

The modelling is carried out using the transport model COMP23 /Romero et al, 1999/, integrated with modelling of fuel dissolution, precipitation/dissolution of solubility-limited radionuclides and chain decay. Transport through the buffer/backfill and out to the surrounding geosphere is also handled in the same model.

The micropores in the buffer are expected to prevent all transport of colloids out of the canister. Colloid transport in the interior of the canister is therefore not dealt with, provided that the buffer completely envelops the canister.

Radionuclide transport in the gas phase is handled by approximate calculations.

Climate change: If the evolution leads to canister damage: See the canister defect scenario.

Earthquake: If the evolution leads to canister damage: See the canister defect scenario. If the effects of an earthquake also lead to a situation where the buffer no longer completely envelops a damaged canister, transport of fuel colloids must also be discussed.

2.9 References

- Andersson J, 1999.** SR 97 – Data and data uncertainties. Compilation of data and evaluation of data uncertainties for radionuclide transport calculations. SKB TR-99-09, Svensk Kärnbränslehantering AB.
- Barner J O, Cunningham M E, Freshley M D, Lanning D D, 1993.** Evaluation of fission gas release in high-burnup light water reactor fuel rods. Nucl. Techn. 102, 210–231.
- BEFAST III, 1997.** Further analysis of extended storage of spent fuel. Final report of a Co-ordinated Research Programme on the Behaviour of Spent Fuel Assemblies during Long-term Storage (BEFAST III) 1991–1996. IAEA TECDOC-944.
- Bjurström H, Bruce A, 1997.** Temperaturer i en kapsel enligt TR-95-02, en första uppskattning. SKB Inkapsling PPM 97-3420-28, Svensk Kärnbränslehantering AB.
- Bjurström H, Bruce A, 1998.** Temperaturer i en kapsel enligt TR-95-02, etapp 2. SKB Inkapsling PPM 98-3420-30, Svensk Kärnbränslehantering AB. (In Swedish).
- Blackwood D J, Naish C C, Platts N, Taylor K J, Thomas M I, 1995.** The anaerobic corrosion of carbon steel in granitic groundwaters. SKB Inkapsling PR 95-03, Svensk Kärnbränslehantering AB.
- Bond A E, Hoch A R, Jones G D, Tomczyk A J, Wiggin R W, Worraker W J, 1997.** Assessment of a spent fuel disposal canister. Assessment studies for a copper canister with cast steel inner component. SKB TR 97-19, Svensk Kärnbränslehantering AB.
- Bruno J, Sellin P, 1992.** Radionuclide solubilities to be used in SKB 91. SKB TR 92-13, Svensk Kärnbränslehantering AB.
- Bruno J, Cera E, de Pablo J, Duro L, Jordana S, Savage D, 1997.** Determination of radionuclide solubility limits to be used in SR 97. Uncertainties associated to calculated solubilities. SKB TR 97-33, Svensk Kärnbränslehantering AB.
- Börgesson L, 1990.** Some aspects of the water intrusion scenario for the Advanced Cold Process Canister. SKB AR 90-12, Svensk Kärnbränslehantering AB.
- Casas I, Gimenez J, Marti V, Torrero M E, de Pablo J, 1993.** Kinetically controlled dissolution of $UO_2(s)$ under oxidizing conditions. A combined dissolution-oxidation model. Mat. Res. Soc. Symp. Proc. 294, p 61–66.
- Christensen H, Bjergbakke E, 1982.** Radiolysis of groundwater from HLW stored in copper canisters. SKBF/KBS TR 82-02. Svensk Kärnbränslehantering AB.
- Christensen H, Bjergbakke E, 1984.** Radiolysis of concrete. SKBF/KBS TR 84-02. Svensk Kärnbränslehantering AB.
- Cui D, Eriksen T E, 1996.** Reduction of Tc(VII) and Np(V) in solution by ferrous iron. A laboratory study of homogeneous and heterogeneous redox processes. SKB TR-96-03, Svensk Kärnbränslehantering AB.

- Efraimsson H, 1996a.** Kriticitetsberäkningar för kapsel med gjutstålsinsats för slutförvaring av LWR-bränsle. SKB Inkapsling PPM 95-3430-04, Rev.1, Svensk Kärnbränslehantering AB. (In Swedish).
- Efraimsson H, 1996b.** Kriticitetsberäkningar och parameterstudier för slutförvaringskapsel med insats. SKB Inkapsling PPM 96-3430-06, Svensk Kärnbränslehantering AB. (In Swedish).
- Eklund U-B, Forsyth R, 1978.** Lakning av bestrålat UO₂-bränsle. KBS TR 70.
- Eriksen T, 1996.** Radiolysis of water within a ruptured fuel element. SKB PR U-96-29, Svensk Kärnbränslehantering AB.
- Forsberg K, He N, Masih A R, 1996.** Probabilistic analysis of nuclear fuel rod behavior using a quasi-Monte Carlo method. Nucl. Sci. and Eng. 122, 142–150.
- Forsström H, 1982.** Hantering och slutförvaring av plutoniumberikat bränsle (Mox-bränsle). SKBF/KBS AR 82-33. Svensk Kärnbränslehantering AB. (In Swedish).
- Forsyth R S, Mattsson O, Schrire D, 1988.** Fission product concentration profiles (Sr, Xe, Cs and Nd) at the individual grain level in power-ramped LWR fuel. SKB TR 88-24, Svensk Kärnbränslehantering AB.
- Forsyth R S, Werme L O, Bruno J, 1988.** Preliminary study of spent UO₂ fuel corrosion in the presence of bentonite. J. Nucl. Mater. 160, 218–223.
- Forsyth R S, Jonsson T, Mattsson O, 1990.** Examination of reaction products on the surface of UO₂ fuel exposed to reactor coolant water during power operation. SKB TR 90-07, Svensk Kärnbränslehantering AB.
- Forsyth R S, Werme L O, 1992.** Spent fuel corrosion and dissolution. J. Nucl. Mater. pp 190, 3–19.
- Forsyth R S, Eklund U-B, Werme L O, 1994.** A study of fission product migration and selective leaching by means of a power-bump test. Mat. Res. Soc. Symp. Proc. Vol. 333, 385–390.
- Forsyth R S, 1995.** Spent nuclear fuel. A review of properties of possible relevance to corrosion processes. SKB TR 95-23, Svensk Kärnbränslehantering AB.
- Forsyth R S, 1996.** Collected experimental data for the BTC/PTC experiments. Study of the Tc-99 source term for the BWR and PWR reference fuels. SKB AR 94-07, Svensk Kärnbränslehantering AB.
- Forsyth R, 1997.** The SKB Spent Fuel Corrosion Programme. An evaluation of results from the experimental programme performed in the Studsvik Hot Cell laboratory. SKB TR 97-25, Svensk Kärnbränslehantering AB.
- Fuger J, 1993.** Problems in the thermodynamics of the actinides in relation with the back-end of the nuclear fuel cycle. J. Nucl. Mater. 201 (1993) 3–14.
- Gdowski G E, Bullen D B, 1988.** Survey of degradation modes of candidate materials for high-level radioactive-waste disposal containers. Oxidation and corrosion. Report UCID-21362 Vol. 2. Lawrence Livermore National Laboratory, University of California, Livermore, California, USA.

- Gray W J, Strachan D M, Wilson C N, 1992.** Gap and grain boundary inventories of Cs, Tc, and Sr in spent LWR fuel. *Mat. Res. Soc. Symp.* Vol. 257, 353–360. Materials Research Society, Pittsburgh, USA.
- Gray W J, Thomas L E, Einziger R E, 1993.** Effects of air oxidation on the dissolution rate of LWR spent fuel. *Mat. Res. Soc. Symp.* Vol. 294, 47-54. Materials Research Society, Pittsburgh, USA.
- Gray W J, Steward S A, Shoesmith D W, Tait J C, 1994.** Interlaboratory comparison of UO_2 dissolution rates. *Proc. 5th Annual High-Level radioactive Waste management Conf. (Waste Management '94)* 4, 2597–2601.
- Gray W J, 1998.** Spent fuel dissolution rates as a function of burnup and water chemistry. Pacific Northwest Laboratory, Report PNNL-11895, UC-802.
- Grigoriev V, 1996.** Hydrogen embrittlement of zirconium alloys. *Studsvik Material, Report STUDEVIK/M-96/73.*
- Haas P, Gartenmann P, Golser R, Kutschera W, Suter M, Synal H-A, Wagner M J M, Wild E, Winkler G, 1996.** A new half-life measurement of the long-lived fission product ^{126}Sn . *Nucl. Instr. And Meth. B* 114, pp 131–137.
- Hallstadius L, Grapengiesser B, 1991.** Progress in understanding high burnup phenomena. In: IAEA Technical Committee Meeting on Fuel Performance at High Burnup for Water Reactors. Studsvik 1990. IAEA, IWGFPT-36, 52–57.
- Henshaw J, Hoch A, Sharland S M, 1990.** Further assessment studies of the Advanced Cold Process Canister. AEA Decommissioning & Radwaste, AEA D&R 0060.
- Henshaw J, 1994.** Modelling of nitric acid production in the Advanced Cold Process Canister due to irradiation of moist air. SKB TR 94-15, Svensk Kärnbränslehantering AB.
- Hocking W H, Duclos A M, Johnson L H, 1994.** Study of fission-product segregation in used CANDU fuel by X-ray photoelectron spectroscopy (XPS) II. *J. Nucl. Mater.* 209, 1–26.
- Håkansson R, 1996.** Beräkning av nuklidinnehåll, resteffekt, aktivitet samt doshastighet för utbränt kärnbränsle. Studsvik AR N(R)-96/079. (In Swedish).
- Johnson L H, 1982.** The dissolution of irradiated UO_2 fuel in groundwater. Atomic Energy of Canada Limited Report, AECL-6837.
- Johnson L H, Leneveu D M, King F, Shoesmith D W, Kolar M, Oscarson D W, Sunder S, Onofrei C, Crosthwaite J L, 1996.** The disposal of Canada's nuclear fuel waste: A study of post-closure safety of in-room emplacement of used CANDU fuel in copper containers in permeable plutonic rock. Volume 2: Vault model. Atomic Energy of Canada Limited Report, AECL-11494-2, COG-95-552-2.
- Johnson L H, Tait J C, 1997.** Release of segregated nuclides from spent fuel. SKB TR 97-18, Svensk Kärnbränslehantering AB.

Koizumi S, Umehara H, Wakashima Y, 1991. Study on fission gas release from high burnup fuel. In Fuel Performance at High Burnup for Water Reactors. Proceedings of an IAEA Technical Committee Meeting, Studsvik, June 1990. International Atomic Energy Agency, Vienna, IWGFPT/36, 102–109.

Marsh G P, 1990. A preliminary assessment of the advanced cold process canister. AEA Technology, Report AEA-InTec-0011.

Massih A R, 1997. Personal communication.

Mattsson H, Olefjord I, 1984. General corrosion of Ti in hot water and water saturated bentonite clay. SKB/KBS TR 84-19.

Mattsson H, Olefjord I, 1990. Analysis of oxide formed on titanium during exposure in bentonite clay. I. The oxide growth. *Werkstoffe und Korrosion* **41**, 383–390.

Mattsson H, Li C, Olefjord I, 1990. Analysis of oxide formed on titanium during exposure in bentonite clay. II. The structure of the oxide. *Werkstoffe und Korrosion* **41**, 578–584.

MCC (Materials Characterization Centre), 1988. Characterization of spent fuel approved testing material – ATM-106 – Pacific Northwest Laboratory, Report PNL-5109-106, UC-70.

Northwood D, Kosasih U, 1983. Hydrides and delayed hydrogen cracking in zirconium and its alloys. *Int. Metals Reviews* **28**, 92–121.

Oversby V M, 1996. Criticality in a high level waste repository. A review of some important factors and an assessment of the lessons that can be learned from the Oklo reactor. SKB TR 96-07, Svensk Kärnbränslehantering AB.

Oversby V M, 1998. Criticality in a repository for spent fuel: lessons from Oklo. *Mat. Res. Soc. Symp. Proc.* Vol. 506, p 781.

PLAN-Report 98, 1998. Svensk Kärnbränslehantering AB.

Renström P, 1997. Calculation of the fuel temperature in vacuous storage canisters made of copper with cast steel inserts. SKB Inkapsling PPM 97-3420-23, Svensk Kärnbränslehantering AB.

Romero L, Thompson A, Moreno L, Neretnieks I, Widén H, Boghammar A, Thompson A, 1999. Compartment model “NUCTRAN” (User’s Manual) SKB Report R-99-xx (In preparation)

Rothman A J, 1984. Potential corrosion and degradation mechanisms of Zircaloy cladding on spent fuel in a tuff repository. Lawrence Livermore National Laboratory report UCID-20172.

Schrire D, Matsson I, Grapengiesser B, 1997. Fission gas release in ABB SVEA 10x10 BWR fuel. *Proc. Int. Top. Meet. LWR Fuel Perform.* 104–117. American Nuclear Society, La Grange Park, IL.

Shengdong Z, Jingru G, Anzhi C, Daming L, Daming L, 1996. Measurement of the half life of ¹²⁶Sn using a radiochemical method. *J. Radioanal. Nucl. Chem., Letters* **212**(2), pp 93–99.

Smart N, Rance A, Blackwood D, 1997. Corrosion aspects of the copper-steel/iron process canister; consequences of changing the material for the inner container from steel to cast iron. SKB Inkapsling PR 97-04, Svensk Kärnbränslehantering AB.

Songsheng J, Jingru G, Shan J, Chungsheng L, Anzhi C, Ming H, Shaoyung W, Shilin L, 1997. Nucl. Instr. And Meth. B 123, pp 405–409.

Spinks J W T, Woods R J, 1990. An introduction to radiation chemistry. 3rd edition. New York, NY (USA). John Wiley and Sons Inc.

Stroes-Gascoyne S, Johnson L H, Sellinger D M, 1987. The relationship between gap inventories of stable Xenon, ^{137}Cs , and ^{129}I in used CANDU fuel. Nuclear Technology *77*, 320–330.

Stroes-Gascoyne S, 1996. Measurements of instant-release source terms for ^{137}Cs , ^{90}Sr , ^{99}Tc , ^{129}I and ^{14}C in used CANDU fuels. J. Nucl. Mater. *238*, 264–277.

Thomas L E, Charlot L A, Engelhard M H, 1988. Auger analysis of grain boundaries in LWR spent fuel. Pacific Northwest Laboratory, unpublished results.

Thomas L E, Guenther R J, 1989. Characterization of low-gas-release LWR fuels by transmission electron microscopy. Mat. Res. Symp. Proc. Vol. 127, 293–300. Materials Research Society, Pittsburgh, USA.

Torrero M E, 1995. Estudio de la disolución del UO_2 como análogo químico de la matriz del combustible nuclear gastado. Doctoral thesis, Universidad Politécnica de Cataluña, Barcelona.

van Konynenburg R A, 1994. Behavior of carbon-14 in waste packages for spent fuel in a tuff repository. Waste Management, v. 14, 363–383.

Werme L O, Forsyth R S, 1988. Spent UO_2 fuel corrosion in water; release mechanisms. Mat. Res. Soc. Symp. Proc. Vol. 112, 443–452.

Werme L O, Spahiu K, 1998. Direct disposal of spent nuclear fuel: Comparison between experimental and modelled actinide solubilities in natural waters. J. Alloys and Compounds *271–273*, 194–200.

Wersin P, Bruno J, Spahiu K, 1993. Kinetic modelling of bentonite-canister interaction. Implications for Cu, Fe and Pb corrosion in a repository for spent nuclear fuel. SKB TR 93-16, Svensk Kärnbränslehantering AB.

Wikramaratna R S, Goodfield M, Rodwell W R, Nash P J, Agg P J, 1993. A preliminary assessment of gas migration from the copper/steel canister. SKB TR 93-31, Svensk Kärnbränslehantering AB.

Wilson C N, 1990a. Results from NNWSI series bare fuel dissolution tests. Pacific Northwest Laboratory, Report PNL-7169, UC-802.

Wilson C N, 1990b. Results from NNWSI series 3 spent fuel dissolution tests. Pacific Northwest Laboratory, Report PNL-7170, UC-802.

3 Cast iron insert/copper canister

3.1 Description of cast iron insert and copper canister

3.1.1 General

The canister consists of an inner container of cast iron and a shell of copper, Figure 3-1. The cast iron insert provides mechanical stability and the copper shell protects against corrosion in the repository environment. The copper shell is 5 cm thick and the canister takes the form of an approximately 4.8 metre tall cylinder with a diameter of 1.05 metres.

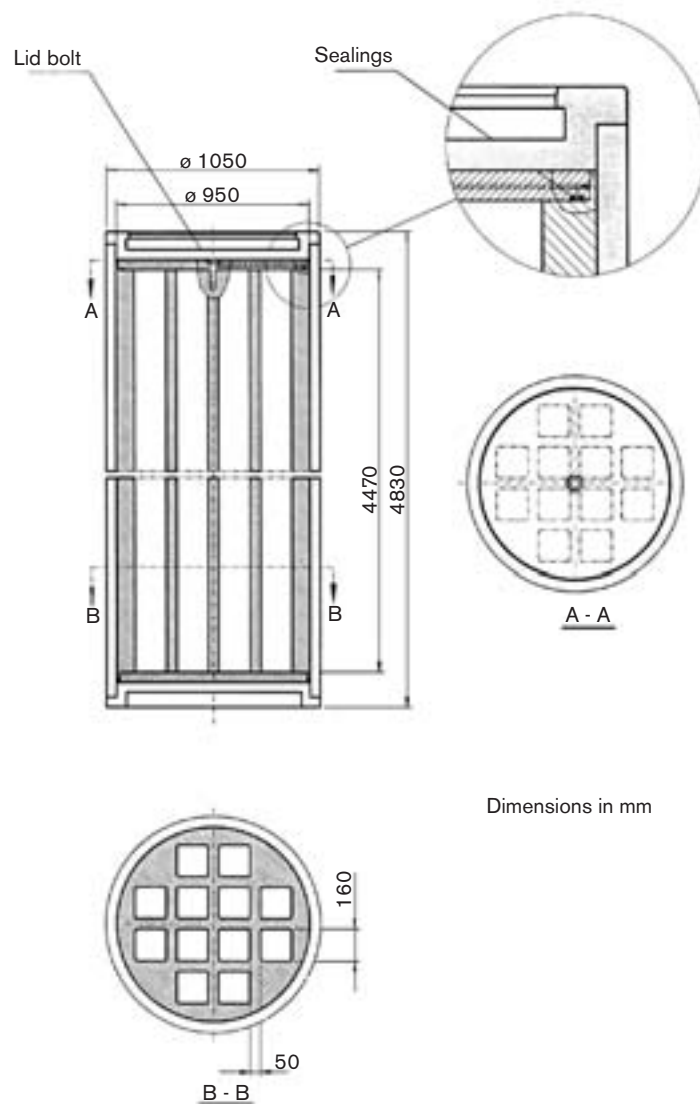


Figure 3-1. Copper canister with cast iron insert.

The insert has channels where the fuel assemblies are placed and is available in two versions: one for 12 BWR assemblies and one for 4 PWR assemblies. The fuel channels are fabricated in the form of an array of square tubes. The walls and bottom of the inner container are then fabricated by casting spheroidal graphite iron around the channel array.

The copper canister is fabricated either of drawn seamless tubes or by welding together two tube halves of rolled plate. A bottom is attached by an electron beam weld in such a way that the weld can be examined by ultrasonic and radiographic inspection.

After fuel has been placed in the canister, the insert is closed with an O-ring-sealed lid which is fastened with a bolt. The copper shell's lid is then attached by an electron beam weld, and leaktightness is tested by ultrasonic and radiographic inspection.

The canister weighs a total of about 25 tonnes when filled with 12 BWR assemblies. A canister holds about two tonnes of fuel. It is assumed in SR 97 that approximately 8,000 tonnes of fuel will be disposed of, equivalent to around 4,000 canisters.

3.1.2 Overview of variables

The subsystem cast iron insert/copper canister is described geometrically by the **canister geometry**.

The cast iron insert and copper canister are characterized radiation related by **radiation intensity** (mainly γ and neutron radiation) and thermally by **temperature**. **Mechanical stresses** and **material compositions** for insert and canister characterize the subsystem mechanically and chemically.

All variables are defined in Table 3-1.

Table 3-1. Variables in copper canister/cast iron insert.

| | |
|-----------------------------|--|
| Geometry | Geometric dimensions for the canister components. This also includes a description of any fabrication defects in welds etc. |
| Radiation intensity | Intensity of α -, β -, γ - and neutron radiation as a function of time and space in the canister components. |
| Temperature | Temperature as a function of time and space in the canister components. |
| Mechanical stresses | Mechanical stress as a function of time and space in the canister components. |
| Material composition | Material composition of the canister components. |

3.2 Overview of processes

Some of the radiation that reaches out into the canister is converted to thermal energy by *radiation attenuation*. *Heat transport* takes place by conduction inside the insert and the canister and to a large extent by radiation between these two parts.

Hydraulic processes can occur in the cavities that exist between canister and fuel and between cast iron insert and copper canister and are dealt with in the subsystem fuel/cavity.

Mechanically, the insert and the canister can be *deformed* by external loads. Furthermore, *thermal expansion* occurs, changing the cavity between insert and canister.

An important chemical process is external *copper corrosion*; *stress corrosion cracking* could also occur in both copper canister and cast iron insert. The materials could be changed by *radiation effects*. If water enters, *corrosion of the cast iron insert* (causing hydrogen formation) and *galvanic corrosion* will occur.

Radionuclide transport in the canister cavity is dealt with in the subsystem fuel/cavity.

The THMC diagram for cast iron insert/copper canister is given in Figure 3-2.

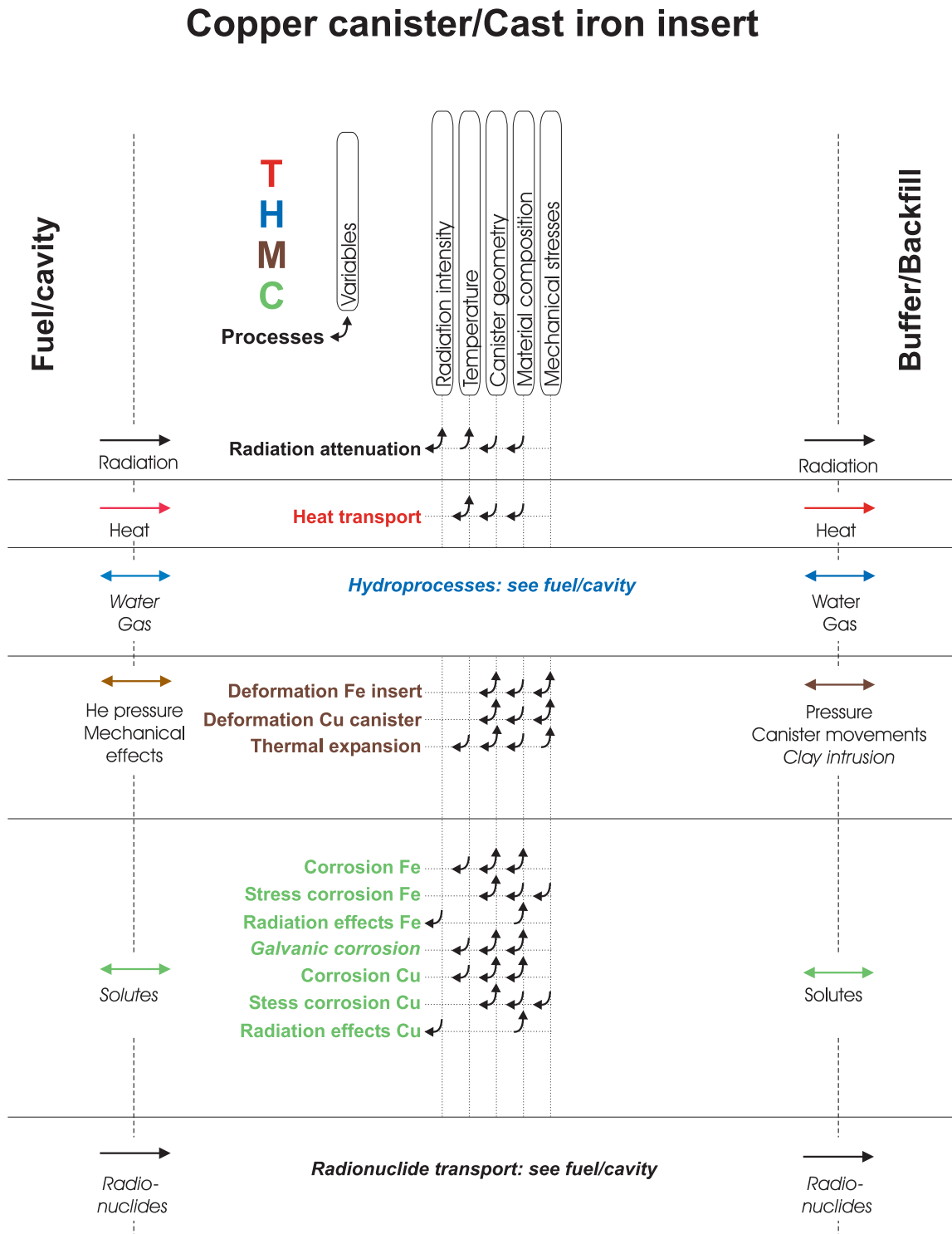


Figure 3-2. THMC diagram for cast iron insert/copper canister. Processes in italics only occur when the isolation of the copper canister is broken.

3.3 Radiation-related processes

3.3.1 Radiation attenuation/heat generation

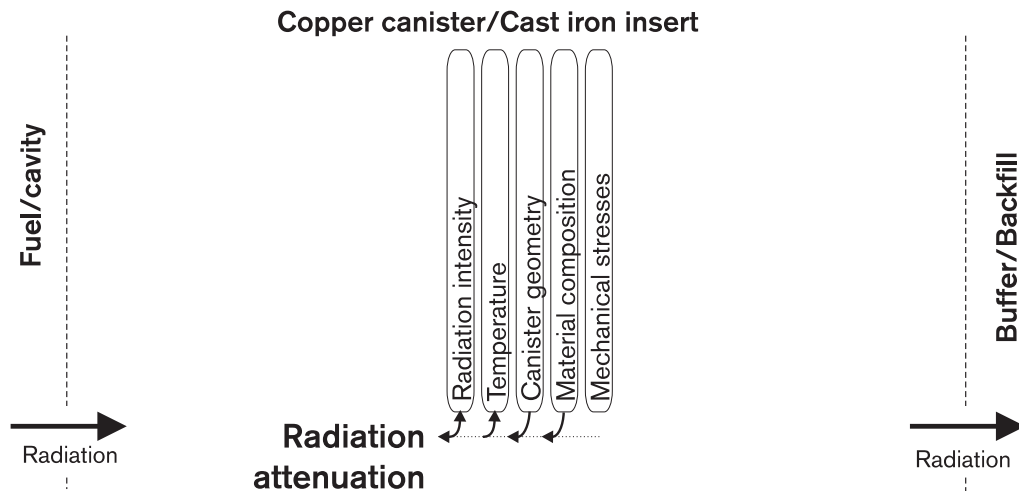


Figure 3-3. Radiation attenuation/Heat generation.

Overview, general description

The γ - and neutron radiation from the radioactive disintegrations in the fuel that reaches out into the canister interacts with the materials in the cast iron insert and the canister. Energy is thereby transferred to the materials and the radiation is attenuated. Most of the transferred energy is converted into thermal energy: heat generation.

In the case of α - and β - disintegrations, most of the radiation remains in the fuel due to the fact that the radiation is largely attenuated by the fuel itself. In the case of γ radiation, some of the surplus energy will leave the fuel and be attenuated by the canister materials, generating heat in the canister material. This fraction is estimated to comprise less than 10 percent of the total heat output.

Model studies/experimental studies

Calculations of the canister's radiation attenuation (dose rate calculations) have been performed by Håkansson /1995a; 1996/.

Time perspective

At first the γ -radiation is dominated by decay of ^{90}Sr and ^{137}Cs . These isotopes have a half-life of approximately 30 years, in other words the radiation intensity is halved every 30 years.

Natural analogues

Not applicable.

Summary of uncertainties

Both our fundamental understanding and the available data are sufficient for the needs of the safety assessment.

Handling in safety assessment

Base scenario: Calculations of radiation shielding in the canister. Heat generation in the canister materials is of no importance for the temperature distribution in the near field shortly after deposition and onward.

Canister defect scenario: See base scenario.

Climate change: See base scenario.

Earthquake: See base scenario.

3.4 Thermal processes

3.4.1 Heat transport

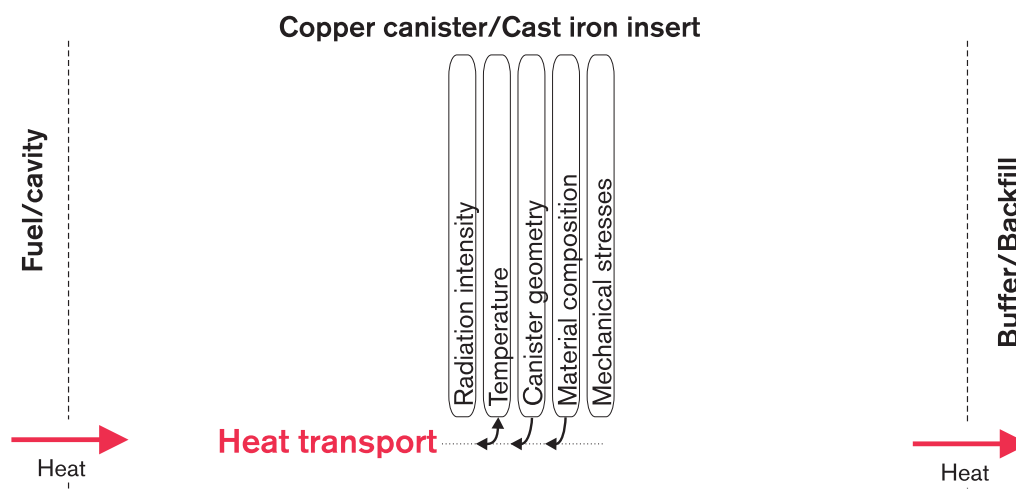


Figure 3-4. Heat transport.

Overview

Heat is transported in the metal in the cast iron insert and copper canister by conduction. The transfer from steel to copper takes place mainly by radiation. The process is controlled by and influences the temperature distribution in the materials. The heat flow towards adjacent subsystems (fuel and buffer) comprises boundary conditions. The process is a part of the repository's thermal evolution.

General description and model studies/experimental studies

It is assumed that the canister will be sealed either with the residual air in the canister or after evacuation of the residual air. This means that the heat transfer from the fuel bundles to the cast iron insert takes place by heat conduction and radiation or solely by radiation. The heat transfer between cast iron insert and copper canister takes place by radiation, since electron beam welding requires a vacuum in this space, and heat conduction through the bottom contact between insert and copper canister.

Temperature calculations have been carried out for the different situations to which the canister will be exposed during handling, from sealing of the lid to deposition /Renström, 1997; Bjurström and Bruce, 1997; 1998/. The thermal conductivity of iron and copper is so good that very small temperature differentials arise within the metal components.

The biggest temperature differential between the components in the canister is expected between the canister insert and the copper canister. Since heat transfer takes place by radiation, it is very dependent on the condition of the copper surface.

Calculations were carried out with the cautious assumption that the total amount of heat generated in the canister by radioactive decay was 2855 W, equivalent to a burnup of 55 MWd/kgU and a decay time of 30 years /Knopp, 1996/.

In calculations where only the radial heat flow was considered, the external temperature on the fuel rods was up to 405°C. The temperature on the canister insert was over 370°C if the surface temperature on the canister was set at 90°C and the emissivity of the copper surface was assumed to be 0.03. This emissivity corresponds to a smooth and clean copper surface. If the emissivity was assumed to be 0.10, the corresponding temperature was around 300°C on the fuel and around 265°C on the canister insert.

If the axial heat flow was also taken into account, in other words the cooling of the canister insert through the bottom contact between canister and insert, the corresponding temperatures on the fuel were about 350°C and 280°C, respectively, for emissivities of 0.03 and 0.10. The temperature in the canister insert will vary in the axial direction between just over 90°C in the bottom to 300°C in the top at an emissivity of 0.03.

Time perspective

Heat generation is halved every 30 years during the initial post-closure period. The highest temperatures and the greatest heat flows occur shortly after deposition and closure.

Natural analogues

Not applicable.

Summary of uncertainties

Assumptions regarding the emissivity of the copper surface (the material's capacity to emit electromagnetic radiation) are completely decisive for the calculation result. A smooth and clean copper surface has an emissivity of 0.03. A doubling of the emissivity would lead to a reduction of the temperature on the fuel cladding by 70°C. With the model that has been used, the result is completely controlled by the assumption regarding the copper's emissivity. Calculations taking into account the heat transfer through the bottom contact between insert and copper canister also show that the assumptions made regarding the emissivity of copper are decisive for the calculation result.

The great uncertainty when it comes to the temperature calculations lies in the assumptions regarding the heat transfer between the copper surface on the canister and the buffer in the deposition hole before water saturation. A reasonable estimate of the temperature distribution in fuel and canister requires better knowledge of the heat transfer between canister and buffer during the water saturation phase.

Handling in the safety assessment

Base scenario: Account of separate analyses as above. This process is not studied explicitly in the integrated model calculation.

Canister defect scenario: Since the heat transport described above applies to the period prior to water saturation of the buffer, no extra calculations need to be done for this scenario.

Climate change: See base scenario.

Earthquake: See base scenario.

3.5 Hydraulic processes

Water and gas flux in the interior of the canister is described in the chapter that deals with processes in the fuel/canister cavity. Therefore, no hydraulic processes are described here.

3.6 Mechanical processes

3.6.1 Introduction

Solid materials that are subjected to mechanical loads can behave in different ways. An *elastic* material deforms under load, only to resume its original shape when the load is removed. The deformation, for example a strain, is proportional to the applied stress (force per unit area).

Outside the elastic range, the material undergoes a permanent shape change, a *plastic* deformation, when the external forces are removed. The stress at which a significant plastic strain occurs is called the material's *yield stress or yield strength*.

Structural changes caused by the deformation cause a hardening of the material (strain hardening or work hardening), which means that progressively higher stresses must be used to further strain the material. These changes eventually lead to *failure*. If the strain at failure is great compared with the elastic strain, the material is said to be *ductile*. Otherwise the material is regarded as *brittle*. Failure strain (ultimate elongation) is used as a measure of ductility.

Creep is a continuous deformation with time. As a rule of thumb, metals begin to creep at temperatures between $0.3T_M$ and $0.4T_M$, where T_M is the melting temperature of the metal in Kelvin.

3.6.2 Deformation of cast iron insert

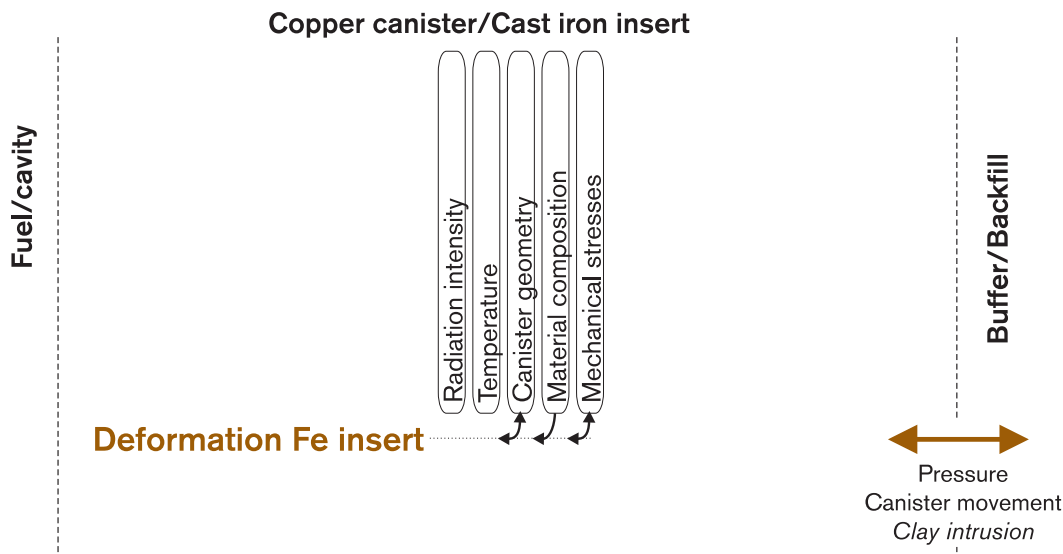


Figure 3-5. Deformation of cast iron insert.

Overview

When the canister is loaded mechanically, for example when the buffer swells, stresses will be built up in the canister material, which deforms elastically at first and, if the stresses are great, plastically as well. The size of the deformation at a given load is dependent on the strength of the cast iron insert, which is determined by its material properties and geometry. At extreme loads the cast iron insert will collapse.

The cast iron insert is the most important mechanical barrier in the repository. If it collapses, a number of safety functions are jeopardized. The process is therefore of central importance to the function of the repository.

General description

Under normal conditions in the deep repository, the cast iron insert will be subjected to an external load of 14 MPa, composed of a maximum swelling pressure from the bentonite of 7 MPa and a maximum water pressure of 7 MPa. The pressure can be regarded as isostatic, i.e. equally large over the entire surface. A canister can be subjected to increased load during an ice age. An ice cover about 3,000 m thick floating on the groundwater gives an increase of 27.5 MPa. The pressure can be regarded as isostatic in this case as well. These loads primarily give rise to compressive stresses in the canister.

As the bentonite becomes water-saturated, uneven pressure situations can arise. They may be associated with uneven water ingress or with oval or slightly curved deposition holes. In some cases an uneven stress could possibly persist for a long time. Such loads will, in addition to compressive stresses, also give rise to flexural stresses (tensile stresses).

Deviations from the normal load case can also arise due to flat (subhorizontal) rock displacements across the deposition hole. The results are flexural and tensile stresses in the canister insert. Extremely large displacements (several decimetres) lead to canister failure.

A mechanical load also results from internal pressure build-up due to internal gas formation caused by alpha decay. The large void in the canister will make the effects of gas build-up negligible for all reasonable time periods.

If the copper canister is damaged so that water comes into contact with the canister insert, this leads to corrosion, see section 3.7.1. The corrosion rate is low, but leads to a progressive reduction in the mechanical strength of the insert. This will eventually lead to failure. When and how this failure occurs depends on the extent of the breach, the geometry of the corrosion attack and the load situation for the canister in question.

Model studies/experimental studies

The canister's behaviour under isostatic load has been modelled. The results show that the greatest contribution to the stability of the insert comes from the partitions between the channels for the fuel assemblies.

In a uniaxial tensile test, the material will take maximum load at 16 percent logarithmic strain. The failure strain is 22 percent linear strain, which is 20 percent logarithmic strain. Nothing essential will happen with the behaviour of the canister until the canister's "spokes" are plasticized. This takes place after 16 percent strain has been reached in some part of the canister. A strain of 16 percent has therefore been chosen as the collapse criterion to provide a pessimistic assessment of the canister's resistance to external pressure.

The critical pressure for the PWR and BWR variants of the canister insert has then been calculated at 114 MPa and 80 MPa, respectively /Ekberg, 1995/. This should be compared with the greatest load to which the canister is assumed to be subjected in the repository in connection with an ice age: 41.5 MPa.

Uneven pressure build-up in the bentonite can occur both during and after water saturation. For the water saturation phase, three loads cases have been check-calculated by the handbook /Werme, 1998/.

- 1) The canister is rigidly fixed at its end surfaces and along one-tenth of the length of the cylindrical surface nearest the end surfaces. An evenly distributed horizontal load corresponding to fully developed bentonite swelling pressure acts along one side of the remaining canister surface.
- 2) The canister is supported at points situated one-tenth of the length of the cylindrical surface from the ends. An evenly distributed horizontal load corresponding to fully developed bentonite swelling pressure acts along one side of the remaining canister surface.
- 3) The canister is rigidly fixed at one end surface and along one-fifth of the length of the cylindrical surface nearest the end surfaces. An evenly distributed horizontal load corresponding to fully developed bentonite swelling pressure acts along one side of the remaining canister surface.

If the canister is tilted or inclined in the deposition hole, or if the rock is uneven, a permanent pressure disequilibrium can arise in the bentonite even after water saturation with full water pressure and ice load. The following two cases have therefore also been calculated /Werme, 1998/:

- 4a) The swelling pressure is fully developed on one side of the canister's cylindrical surface and on the end surfaces. On the other side of the cylindrical surface, the swelling pressure is 20 percent elevated along the central half and 20 percent reduced along the remaining quarters at the ends of the canister.
- 4b) Equivalent load cases, but where the swelling pressures are 50 percent higher and lower, respectively, are to be regarded as extreme cases for which no extra safety margins are required.

The results of the simple handbook calculations were that the yield strength of the cast iron insert (240 MPa) is not reached in cases 1, 2, 4a or 4b, while case 3 leads to collapse of the canister insert. FEM calculations have therefore been carried out for cases 2 and 3, where the material properties of the bentonite have also been taken into account to give a more realistic load on the canister /Börgesson and Hernelind, 1998/. The largest tensile stresses in the canister insert were then found to be lower than 55 MPa, which is below the yield strength of the cast iron insert.

Corroding canister insert: The consequences of a breach in the copper canister leading to corrosion of the copper insert have been investigated by Bond et al /1997/. In the analyzed case, the corrosion rate of the insert has been set to 0.1 μm per year and the original breach in the copper shell is so small that corrosion initially takes place on a limited area around the breach. After more than 200,000 years corrosion spreads to the entire surface of the insert after the copper shell has yielded to the pressure from the corrosion products. Up to that time the mechanical strength of the canister insert will not be appreciably reduced. Analyses have not been performed for longer periods.

Earthquake: Börgesson /1992/ has carried out calculations for a self-supporting steel canister with a cast iron insert with a diameter of 0.59 m and for rock movements of 0.1 m. The canister insert had a calculated collapse pressure of 60 MPa, i.e. slightly less than for the cast iron insert. The results showed that the shear movement did not lead to canister failure. The cast iron insert in its present design is deemed to have at least as good properties in this respect.

Time perspective

The pressure build-up to 14 MPa is expected to take from a few years to a few decades. The time perspective for climate-controlled changes is determined by the premises for the climate scenario.

Natural analogues

Not applicable.

Summary of uncertainties

The calculations are carried out for a canister insert of solid spheroidal graphite iron and must be considered reliable for the calculated situations. The principal uncertainties as regards canister strength stem from possible deviations from ideal conditions, undetected casting defects or deviations from the sought-after material properties for the spheroidal graphite iron.

Ekberg's /1995/ calculations show that significant casting defects can be tolerated without canister strength being degraded so that the critical load is lower than 45 MPa. Other variations and actual outcomes from fabrication cannot be determined until trial series of canister inserts have been evaluated.

Corroding canister: In the corrosion case there are uncertainties with regard to the mechanical properties of the corrosion products. There are also uncertainties with regard to the behaviour of the canister insert under loading caused by the growing corrosion products after corrosion has progressed from a local attack to corrosion over the entire surface of the insert. An experimental study of the corrosion products and of the forces which the corrosion products will exert on the copper canister and the canister insert is under way.

Earthquake: Even if the canister insert will remain intact in the face of the postulated shear movement in the rock, uncertainties remain concerning its behaviour over long periods of time if the copper shell has been deformed as a result of the shear movement.

Handling in the safety assessment

Base scenario: The above calculation cases are discussed in the account of the repository's mechanical evolution.

Canister defect scenario: The results from /Bond et al, 1997/ are discussed in the account of the mechanical evolution of a damaged canister and are used as a basis for modellings of canister damage in radionuclide transport calculations.

Climate change: The above calculation cases that concern glaciation are discussed in the account of the repository's mechanical evolution. The behaviour of an **initially damaged** canister during an ice age depends on the scope of the original breach and assumptions concerning corrosion attacks.

In the case of small initial breach which only leads to local corrosion attacks in the area around the breach, the strength of the canister will remain sufficient to withstand an ice load /Bond et al, 1997/.

Earthquake: In SR 97 it is pessimistically assumed that rock movements that lead to greater displacements in a deposition hole than 10 cm lead to canister penetration. The probability and consequences of this are dealt with in the earthquake scenario.

3.6.3 Deformation of copper canister from external pressure

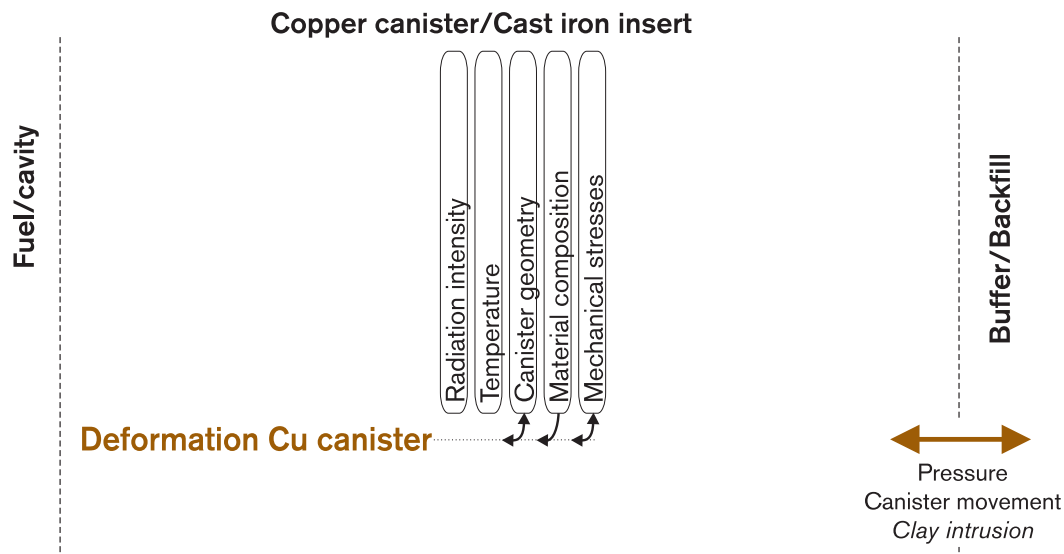


Figure 3-6. Deformation of copper canister from external pressure.

Overview, general description

The purpose of the copper canister is to be a corrosion barrier. The mechanical strength of the copper canister is of subordinate importance, but the canister must withstand the loads associated with handling, transport and deposition. The copper material must also possess sufficient ductility to allow the strains in the material that occur when the canister is deformed by the external load against the insert, either plastically or by creep.

Two consequences of this process need to be analyzed for the safety assessment: The mechanical stress on the copper canister, and changes in the size of the gap between the copper canister and the cast iron insert. The latter is of importance for the course of events if water should enter the canister.

Model studies/experimental studies

Calculations of stresses and strains in the copper canister after full pressure (14 MPa) has built up in the repository have been performed by Cakmak /1994/ and Børgesson /1992/.

Cakmak /1994/ presumed a rapid pressure build-up where full hydrostatic pressure had developed within an hour. The conclusions of the calculations were that:

- The copper shell is fully plasticized and contact occurs between the insert and the copper shell as a consequence of the external pressure. The lid is partially plasticized.
- The maximum strain, which is a few percent, occurs locally on the inside of the shell near the transition to the lid and is caused by plastic deformation. The strain due to creep in the copper is negligible.
- The axial and tangential tensile stress lies around the yield stress and occurs, among other places, on the outside of the shell opposite the inner corner in the shell/lid transition and in the centre of the lid.

Handbook calculations have also been carried out for two cases where the swelling pressure is fully developed around the lower half of the canister, while the swelling pressure is 20 percent and 50 percent, respectively, around the upper half. The resulting upward force, caused by the differences in pressure against the end surfaces of the canister, is balanced by a shear force along the lower half of the copper canister. Calculations show that these load cases give rise to axial stresses in the copper wall equal to 8.4 and 21 MPa, respectively /Werme, 1998/. These are low stresses compared with the yield stress of the copper material, which is 45 MPa.

Time perspective

The copper canister will be deformed inwards, and receive support from, the cast iron insert. The timescale is determined by the timescale for water uptake in the buffer and the time to develop full swelling pressure and full water pressure. In reality, this time is much longer than has been assumed in Cakmak's calculation, and the pressure build-up probably takes place over the course of years.

Natural analogues

Not applicable.

Summary of uncertainties

The principal uncertainties pertain to the loading of the canister from the swelling buffer. If the loading is very rapid (weeks to months), the copper canister will mainly be deformed plastically. Otherwise creep deformation may also be of importance, but is difficult to quantify. Furthermore, there are still uncertainties around the extrapolation and modelling of the creep deformation of the copper canister. At fully developed swelling pressure, the gap between canister and insert is expected to have been closed, except in areas near the bottom and lid.

The creep properties of the copper canister are also of importance for the deformation of the canister as a result of the build-up of corrosion products in the gap. This is dealt with in section 3.6.5.

Handling in the safety assessment

Base scenario: The copper canister is deformed according to Cakmak. The remaining gaps between canister and insert at the bottom and lid of the canister (2 mm over a distance of about 20 cm) are expected to be permanent. Contact between the insert and the shell is expected along the cylindrical surface.

Canister defect scenario: In the canister defect scenario, the size of the gap is of crucial importance for the course of events. The gap size is chosen to be 1 mm along the cylindrical surface.

Climate change: See base scenario.

Earthquake: See base scenario.

3.6.4 Thermal expansion (both cast iron insert and copper canister)

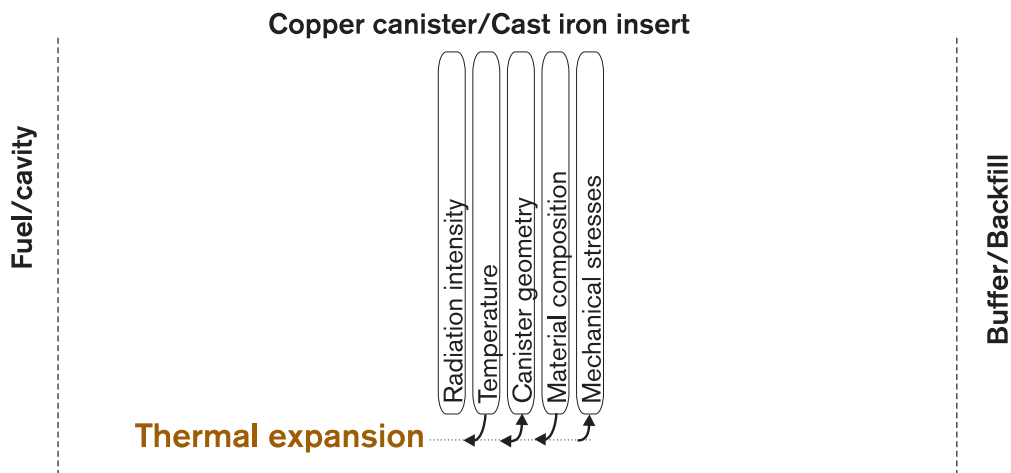


Figure 3-7. Thermal expansion.

Overview, general description, model studies/experimental studies

The gap between the cast iron insert and the copper shell may expand/close due to thermal expansion/contraction. If the gap is closed, further cooling gives rise to tensile stresses in the copper shell.

In the current design, the size of the gap between the cast iron insert and the copper canister is 2 mm. At the highest temperature calculated to arise in the canister and the insert, the linear expansion caused by the temperature difference between these two components can give rise to strains in the copper shell of 0.1%. Even if the strains are slightly greater locally, this is negligible from a strength viewpoint. It is moreover unlikely that the greatest temperature differences will be able to persist when the insert comes into contact with the copper shell.

Time perspective

Heating to the maximum temperature takes place very quickly after deposition. Cooling to the ambient temperature takes hundreds to thousands of years.

Natural analogues

Not applicable.

Summary of uncertainties

The uncertainties that exist concern the heat transfer between fuel, insert and copper canister and the temperature differences that arise between the different components before a steady state has been achieved. The size and importance of these temperature differences must be determined experimentally. At large temperature differences, axial tensile forces can arise in the copper shell.

Handling in the safety assessment

Base scenario: The process is discussed briefly in connection with the description of the repository's mechanical evolution.

Canister defect scenario: See base scenario.

Climate change: See base scenario.

Earthquake: See base scenario.

3.6.5 Deformation from internal corrosion products

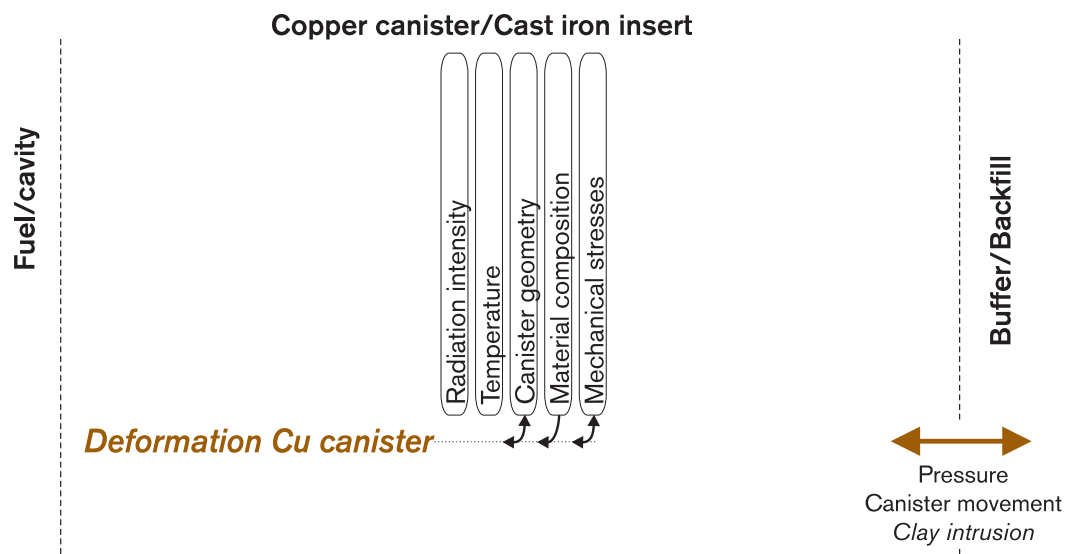


Figure 3-8. Deformation from internal corrosion products. Only applicable when the copper canister is damaged.

Overview

If the copper canister should be breached, water or water vapour will be able to enter into the gap between the canister insert and the copper shell and give rise to anaerobic corrosion of the insert, see section 3.7.1. If the water is also able to penetrate inside the lid on the insert, this will give rise to anaerobic corrosion of the inside of the channels for the fuel assemblies as well.

In both cases, this leads to a build-up of corrosion products, which in turn gives rise to mechanical stresses in the canister.

General description

The sequence of events in this process is expected to be roughly as follows:

Water runs into the gap between the canister insert and the copper shell and into the canister insert, with anaerobic corrosion as a result. This leads to hydrogen gas generation, which increases the pressure inside the canister, whereupon the inflow of water decreases. After some time, the transport of water or water vapour into the canister by diffusion will be greater than the leakage of water into the canister due to the pressure difference. The time required for this varies with the size of the penetration in the copper canister and the corrosion rate, and is for reasonable cases thousands of years. The inward diffusion of water vapour will prevent corrosion from ceasing entirely. The process leads to a slow build-up of corrosion products. These products occupy a larger volume than the equivalent quantity of cast iron, and with time an internal mechanical pressure is built up against the copper canister. This leads to local deformation and ultimately failure of the copper canister.

Model studies/experimental studies, time perspective

Different evolutions of an initial canister defect with subsequent corrosion of the canister insert have been modelled by Bond et al /1997/.

Regardless of the size of the canister penetration and the corrosion rate, a sufficiently large hydrogen gas pressure is expected to have built up after some time to prevent liquid water from entering the canister. After that, the corrosion will nevertheless be able to continue due to the fact that water vapour can diffuse into the canister.

Bond et al /1997/ developed a model for this diffusion-limited corrosion. The purpose was to predict how the solid corrosion products build up in the gap between insert and copper canister. The model took into account the change in the size of the gap during the corrosion process, possible change in the corrosion rate and the escape of corrosion-generated hydrogen gas from the canister.

The gap is expected to eventually fill with magnetite, Fe_3O_4 , and the calculations were used to analyze the consequences of this for the strength of the canister. Two situations were analyzed: one extreme case where the entire outside surface area of the insert corroded, and one case where the corrosion was limited to an area around the original defect. The latter case progresses into the former after the copper material around the original defect begins to give way. This is calculated in the model to take around 20,000 years. From the time of the initial penetration, it takes at least 100,000 years before more extensive damages arise on the copper canister, according to the calculations.

Natural analogues

Not applicable.

Summary of uncertainties

The modelling rests on assumptions regarding the properties of the corrosion products. These are not verified experimentally. There are also uncertainties surrounding the behaviour of the canister insert under loading caused by the growing corrosion products after the corrosion has progressed from being a local attack to corrosion over the entire surface area of the insert. An experimental study of the corrosion products and of the forces the growth of the corrosion products will exert on the copper canister and the canister insert is under way.

Handling in the safety assessment

Base scenario: Not applicable.

Canister defect scenario: The calculation cases described above are discussed in the account of the repository's mechanical evolution. To handle the uncertainties in the safety assessment, the process is illustrated with a pessimistically chosen case.

Climate change: If the evolution leads to canister damage: See the canister defect scenario. Changes in the composition of the groundwater may need to be discussed. Otherwise: See the base scenario.

Earthquake: If the evolution leads to canister damage: See the canister defect scenario. Changes in the inflow of water to the canister may need to be discussed if the buffer is damaged. Otherwise: See the base scenario.

3.7 Chemical processes

3.7.1 Corrosion of cast iron insert

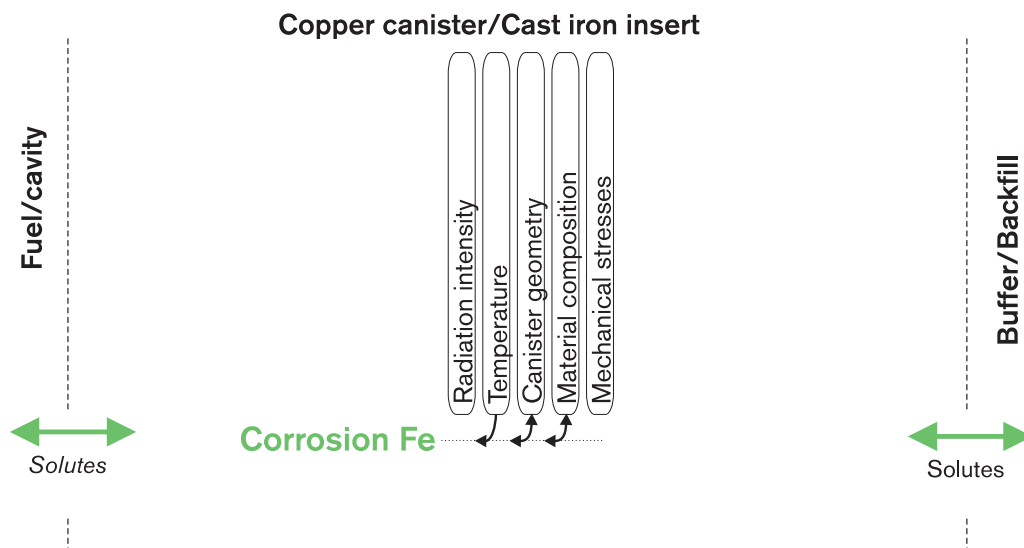


Figure 3-9. Corrosion of cast iron insert.

Overview, general description

Water in the canister cavity can corrode the cast iron insert. As a consequence of this process, the cast iron insert's integrity and mechanical strength may be jeopardized. Another result is formation of gaseous hydrogen and solid corrosion products, which can exert pressure against the copper canister.

The process is central to the canister's hydraulic, mechanical and chemical evolution if the copper shell should be damaged.

Corrosion caused by water inside an intact canister: The possibility cannot be ruled out that some water is brought into the canister enclosed in fuel pins. After the oxygen inside the canister has been consumed by corrosion, this water will give rise to anaerobic corrosion on the insides of the insert.

Corrosion caused by water that has entered a defective canister: Groundwater at repository depth is oxygen-free. The cast iron insert will therefore corrode anaerobically with hydrogen gas generation and formation of magnetite. The formed magnetite is expected to consist of a thin adherent layer and an outer, looser layer with poor adhesion. The transport resistance of the inner layer will determine the corrosion rate, which is therefore expected to remain constant over long periods, see below.

The scope of the corrosion will be determined by the quantity of available water. The corrosion rate of iron under anoxic conditions is dependent on the water composition and the temperature. The corrosion products and the corrosion process affect the chemical conditions inside the canister.

Model studies/experimental studies

Corrosion caused by water inside an intact canister: The fuel bundles will be dried before being transferred to the canister, but some water may nevertheless be transferred. A very pessimistic assumption would be that one fuel pin with maximum water fill is transferred to each canister.

The scope of the corrosion this could cause can be modelled using a simple mass balance approach:

The total quantity of water that can be accommodated in the void in a fuel pin is 50 g. If this water reacts solely with the iron in the canister and is pessimistically assumed to form FeO, a maximum of about 150 g of iron could corrode away. This is equivalent to a corrosion depth of less than 1 µm for the cast insert. This corrosion is assumed to take place when the temperature in the canister is sufficiently high for water to be in the gaseous phase. Pitting – i.e. local, deep corrosion attacks – can therefore not be ruled out.

Corrosion caused by water that has entered a defective canister: Anaerobic corrosion of cast iron has been studied experimentally by Smart et al /1997/, who found that the corrosion rate is very low and well below 1 µm/y after a few thousand hours, even in the most aggressive water tested (Äspö groundwater KAS-03), see Table 3-2.

Table 3-2. Composition (ppm) of synthetic Äspö groundwater KAS-03.

| Na ⁺ | K ⁺ | Ca ²⁺ | Mg ²⁺ | Cl ⁻ | HCO ₃ ⁻ | SO ₄ ²⁻ | pH |
|-----------------|----------------|------------------|------------------|-----------------|-------------------------------|-------------------------------|-----|
| 3000 | 7 | 4400 | 50 | 12,000 | 11 | 710 | 7-8 |

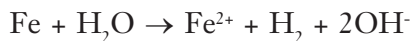
In the reaction between cast iron and water, magnetite and hydrogen are produced. The hydrogen production at the highest measured corrosion rate is 2 dm³/(m².y). The total internal surface area in the canister insert is approximately 33 m², which means the annual production of hydrogen would be 66 dm³ at the pressure at repository level (500 m).

The corrosion rate has proved to be independent of both the hydrogen gas pressure and the concentration of Fe²⁺ in the system. This suggests that the corrosion rate is most likely determined by the transport properties in the magnetite layer on the iron surface:

The magnetite consists of two layers: a thin, strongly adherent layer and an outer, looser layer with poor adhesion /Blackwood et al, 1994/. Blackwood et al /1994/ explain the formation of these two layers by saying that the adherent layer is formed directly on the metal surface by the reaction:



while the looser layer is probably formed by a precipitation process:



Due to the fact that magnetite forms these two layers, of which the adherent layer forms very quickly and then does not increase further in thickness, the corrosion rate is expected to be constant over long periods of time.

The corroding iron insert will influence the water chemistry in the void in the canister by generating high concentrations of dissolved hydrogen gas and small concentrations of dissolved Fe(II). Calculations with EQ3/6 show that the solubility of Fe(II) in the void in the canister is, as expected, dependent on the redox conditions, but can scarcely be higher than 10⁻⁷ mole/dm³. The hydrogen will be dissolved to a concentration equivalent to a hydrogen gas pressure of max. 14 MPa. The iron concentrations are too low to be of any crucial importance for the water chemistry. The hydrogen can be regarded as inert and, as mentioned above, has no influence on the corrosion process.

Time perspective

At a corrosion rate of 1 µm/y, metallic iron will be present for tens of thousands of years. The length of time iron is present is inversely proportional to the corrosion rate.

Natural analogues

Not applicable.

Summary of uncertainties

Corrosion caused by water inside an intact canister: There are great uncertainties surrounding the quantity of water that could conceivably be introduced into a canister by mistake. By far most canisters will probably not contain any water. The uncertainties here are of no importance, since the corrosion to which the water could at worst give rise would be negligible.

Corrosion caused by water that has entered a defective canister: The uncertainties regarding the corrosion rate are small, and the corrosion rate can be expected to be less than 1 µm/y, with 0.1 µm/y being a likely value. The experimental investigations show that if the protective magnetite layer is damaged, it will reform very quickly and the measured corrosion rates can be assumed to apply even for long periods of time.

Handling in the safety assessment

Base scenario: Even with a pessimistic assumption of 50 g water per canister, the effects of the process can be neglected.

Canister defect scenario: The above material is used in an integrated description of the evolution of a defective canister.

Climate change: If the evolution leads to canister damage: See the canister defect scenario. Changes in the composition of the groundwater may need to be discussed. Otherwise: See the base scenario.

Earthquake: If the evolution leads to canister damage: See the canister defect scenario. Otherwise: See the base scenario.

3.7.2 Galvanic corrosion

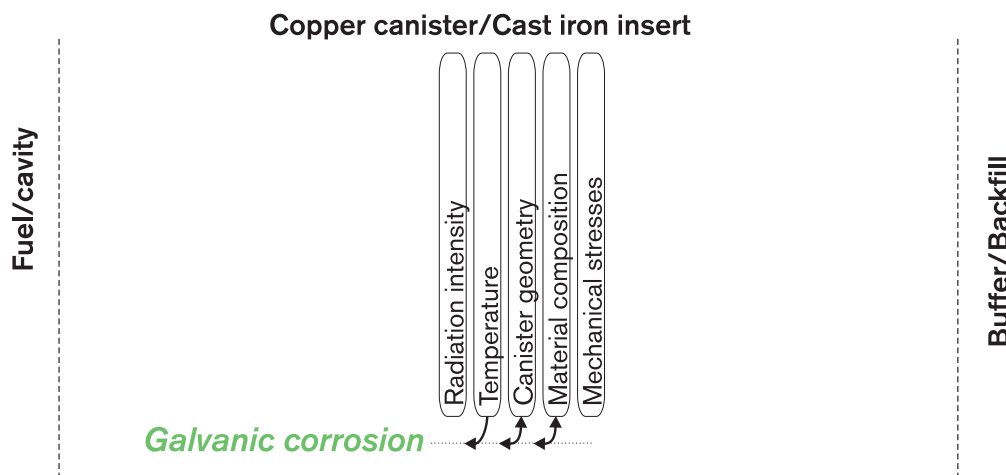


Figure 3-10. Galvanic corrosion. Only applicable when the copper canister is damaged.

Overview, general description

If the copper shell is damaged and groundwater comes into contact with the cast iron insert, electrochemical reactions on the copper surface will influence the corrosion of the insert. The consequences of galvanic corrosion have been investigated by Blackwood and Naish /1994/.

If the groundwater contains oxygen, the rate of steel corrosion may be up to three times higher than without the galvanic coupling. The supply of oxygen through the buffer is judged to be insufficient to permit any appreciable galvanic corrosion.

If the water is oxygen-free, the galvanic coupling will not be able to increase the corrosion rate by more than what corresponds to the increased area for reduction of water contributed by the copper canister. This results in a possible doubling of the corrosion rate. After a magnetite film has been formed on the iron insert, the galvanic coupling to the copper canister will be irrelevant, since transport through the magnetite layer will determine the corrosion rate.

Model studies/experimental studies

See above.

Time perspective

Takes place after canister penetration.

Natural analogues

Not applicable.

Summary of uncertainties

It is not likely that oxygen-containing water will enter into the canister.

In anoxic (oxygen-free) water, the effects will be small and the uncertainties surrounding the exact contribution made by galvanic corrosion are judged to be negligible compared with the uncertainties in assessments of the corrosion rate. A cautious hypothesis for the corrosion rate for anaerobic corrosion of the canister insert will cover any contributions from galvanic corrosion.

Handling in the safety assessment

Base scenario: Not applicable.

Canister defect scenario: The influence of galvanic corrosion lies within the margins of error for the corrosion rate of the iron and is therefore not dealt with, provided that entering water is anoxic. If oxygen should be initially present, the scope of the corrosion will be determined by the amount of available oxygen.

Climate change: If the evolution leads to canister damage: See the canister defect scenario. Changes in the composition of the groundwater may need to be discussed. Otherwise: See the base scenario.

Earthquake: If the evolution leads to canister damage: See the canister defect scenario. Otherwise: See the base scenario.

3.7.3 Stress corrosion cracking of cast iron insert

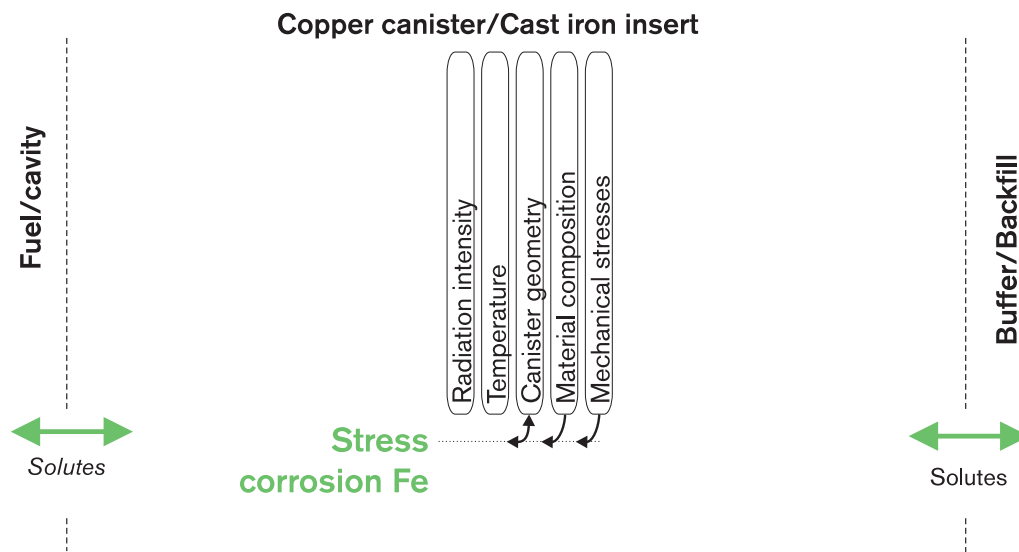


Figure 3-11. Stress corrosion cracking of cast iron insert.

Overview

Stress corrosion cracking (SCC) on metals can occur under a combination of static tensile stresses, special chemical environment and, in some cases, special metallurgical conditions. Unfavourable combinations of these conditions can lead to the formation and propagation of cracks. The propagation rate can vary over a wide range, from 10^{-9} mm/s to 10^{-1} mm/s.

In a canister with intact copper shell, nitric acid from radiolysis of residual quantities of air could conceivably cause SCC in areas with tensile stresses in the cast iron insert /Blackwood et al, 1995/.

General description, model studies/experimental studies

During the early phase after deposition and closure, the temperature of the insert nearest the fuel will be over 150°C . At that temperature there is no water in liquid form in the canister, and the relative humidity is too low for a water film to form on the metal surface, even if water should have been brought into the canister trapped in a fuel rod. (The largest quantity that could be brought into the canister in this manner is estimated to be 50 g, equivalent to the void in a fuel rod.) In order for a water film to form, a relative humidity of approximately 40 percent is required. Under these conditions, nitric acid is not stable but decomposes to NO_2 , which is the dominant radiolysis product in dry air /Reed and Van Konynenburg, 1991a; 1991b/. In order for the water and the oxygen in the canister not to be consumed during the time it takes for the temperature to drop so that water/nitric acid can condense, the corrosion rate must be extremely low.

In order for SCC to occur, not only a corrosive environment but also tensile stresses in the material are required. In the deep repository, the canister insert is under external pressure and tensile stresses occur on the cast insert only locally and in small areas, according to calculations /Ekberg, 1995/. It is therefore highly improbable that SCC could lead to penetrating cracks in the canister, and above all that this would jeopardize the integrity of the canister.

Time perspective

It is estimated that an equilibrium concentration of nitric acid will have been reached a few decades after closure of the canister. A similar timescale is judged to apply to the risks of stress corrosion cracking.

Natural analogues

Not applicable.

Summary of uncertainties

The risks of SCC are deemed to be small, since only local areas in the insert have tensile stresses. The greatest uncertainty concerns the quantity of water that may have been introduced into the canister.

Handling in the safety assessment

Base scenario: Stress corrosion cracking, if it occurs, is deemed to be of no importance for the life of the canister.

Canister defect scenario: See base scenario.

Climate change: See base scenario.

Earthquake: See base scenario.

3.7.4 Radiation effects

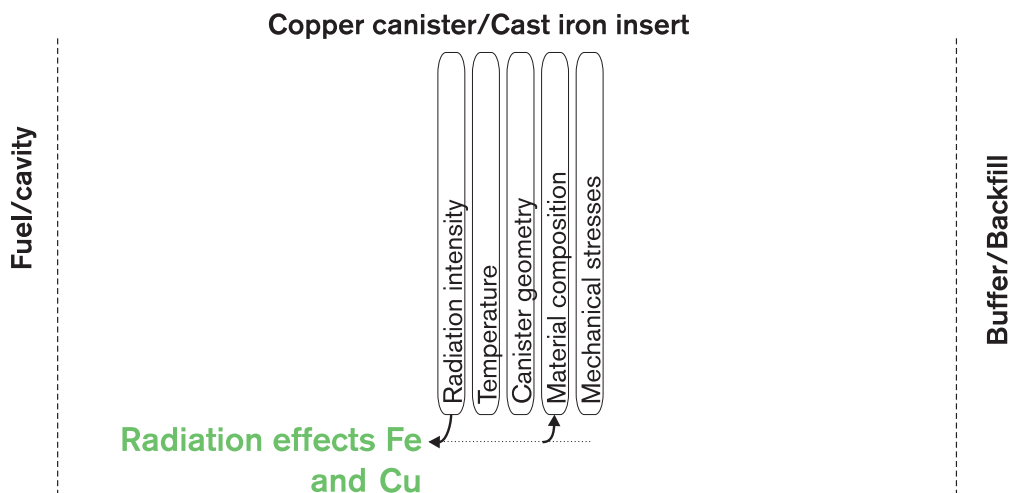


Figure 3-12. Radiation effects.

Overview, general description, model studies/experimental studies

Neutron radiation from the fuel can give rise to minor material changes in the cast iron insert and copper canister.

The effects of irradiation of the canister materials over a long period of time have been discussed by Werme /1997/. The spent fuel will emit α , β , γ and neutron radiation over a long period of time. Of these, only neutron radiation could possibly affect the material properties of the canister materials. The effects of neutron irradiation of solid materials have been known for a long time /see e.g. Billington and Crawford, 1961; Porter, 1960/.

Neutron irradiation alters the mechanical properties of the material, increasing its strength while reducing its ductility. An increase in strength is of no importance for the canister, but diminished ductility could shorten the life of the canister in the repository. A sensitive indicator of material changes is increase of yield stress during tensile testing. For iron and copper, the changes in mechanical properties are small for a neutron fluence of less than 10^{17} n/cm². At a neutron fluence of 10^{18} n/cm², the increase in yield strength for steel is up to 10 percent /Porter 1960/. Based on calculations by Håkansson /1995a and b/, the total (> 0.1 MeV) neutron fluence over 100,000 years can be pessimistically estimated at less than $5 \cdot 10^{14}$ n/cm². This is several orders of magnitude lower than is required for measurable changes in material properties ($> 10^{17}$ n/cm²).

Neutron irradiation might also lead to the formation of activation products in the canister insert. The activity quantities that could be formed are insignificant compared with other activation products in the fuel components. The neutron flux in the fuel during operation is approximately 10^{13} n/(cm²·s). The radiation dose to the canister material is thus several orders of magnitude lower.

Time perspective

The neutrons come from spontaneous fission and from (α , n) reactions in the fuel. Both phenomena diminish greatly with time, and 1,000 years after encapsulation the radiation dose has declined by a factor of thirty /Håkansson, 1996/.

Natural analogues

Not applicable.

Summary of uncertainties

There is no uncertainty about the fact that the effects of neutron irradiation are insignificant and can be completely neglected in an assessment of the performance of the canister in the deep repository.

Handling in the safety assessment

Base scenario: The process is neglected.

Canister defect scenario: See base scenario.

Climate change: See base scenario.

Earthquake: See base scenario.

3.7.5 Corrosion of copper canister

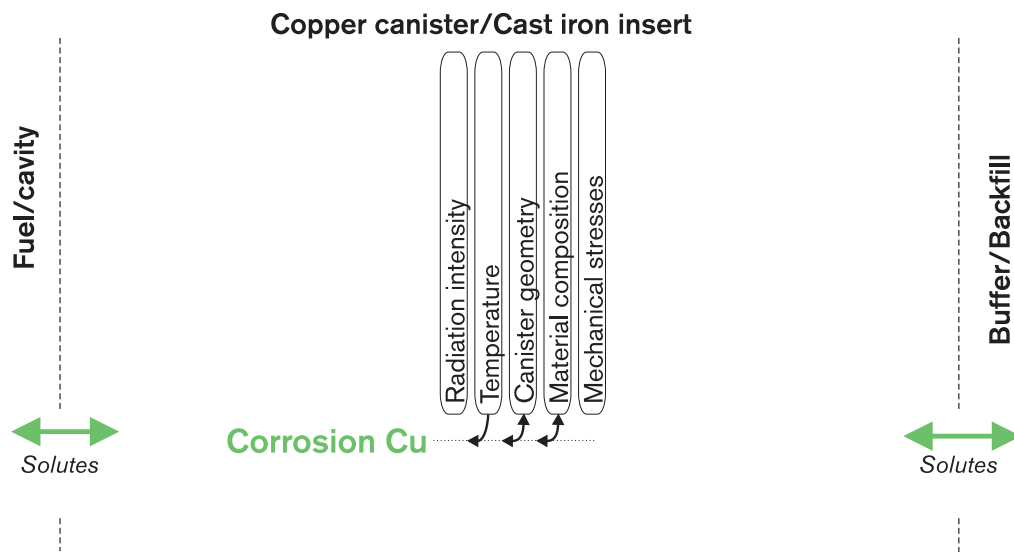


Figure 3-13. Corrosion of the copper canister.

Overview

The outside of the copper canister is judged to be able to be corroded in a deep repository by

- oxygen from the repository's operating period
- oxygen brought in from the buffer or from the groundwater via the buffer
- nitric acid formed by γ -radiolysis of nitrogen compounds in moist air in the gap between canister and buffer
- sulphide brought in from the buffer or from the groundwater via the buffer

The corrosion processes are marginally affected by the changes in temperature expected in the deep repository. The results of corrosion are corrosion products and a change in the thickness of the copper shell. After very long time spans the consequence is a breach of the shell's isolation.

General description, model studies/experimental studies

The copper shell is the canister's corrosion barrier. It is supposed to provide protection against corrosion in the repository for a long time after water saturation. It is also supposed to provide protection against atmospheric corrosion before deposition and after deposition before water saturation. No known forms of corrosion attack should be able to make the canister's life shorter than 100,000 years.

After water saturation, oxygen will still be present in the canister's surroundings. This oxygen is consumed by reactions with the copper canister and by reactions with minerals in the bentonite buffer. When the oxygen is consumed, the reducing conditions that prevailed before the repository was built are expected to be restored. The time this takes has been estimated at 10 to 300 years /Wersin et al, 1994a/. During this time, local corrosion in the form of pitting is also possible. These types of corrosion can lead to locally much deeper corrosion attacks than the average corrosion. The scope of pitting is often described by the pitting factor, which is the ratio between the greatest corrosion depth and the depth of the general corrosion.

When the water is reducing, copper is immune to corrosion. In order for further corrosion to take place, the water must contain solutes that can affect this immunity. Under deep repository conditions, dissolved sulphide or a combination of very high chloride concentrations and low pH are conceivable. Since deep groundwaters are neutral or slightly alkaline and the buffer counteracts acidification, dissolved sulphides are in practice the only corrosive substances that can react with the copper canister after the oxygen in the repository has been consumed. At repository depth the groundwaters have very low sulphide concentrations, much lower than $5 \cdot 10^{-5}$ mol/dm³, and the solubility of the sulphide minerals present in the bentonite is at most of the same magnitude. This means that the corrosion of the copper canister due to sulphides will be controlled by the availability and supply of sulphides from the groundwater and the buffer.

Corrosion in the presence of oxygen

In the presence of oxygen, copper will be oxidized to Cu₂O or CuO in pure water, depending on the redox potential. In the presence of ligands, hydroxysulphates, hydroxycarbonates or hydroxychlorides can form. These compounds can also form in conjunction with atmospheric corrosion.

Corrosion before deep disposal: External corrosion on the copper canister while awaiting disposal and during the initial phase of deep disposal has been assessed by Mattsson /1997/. During interim storage awaiting deposition, the canisters will be exposed to atmospheric corrosion. Storage is assumed to take place in a normal urban atmosphere, and if the surface temperature on the canisters is maintained at 20°C, the estimated corrosion rate will lie in the range 0.006 to 0.027 µm per annum. If the surface temperature of the canisters is the maximum permissible, 90°C, it is estimated that the corrosion rate will be 100 times higher. The estimate is based on an assumed doubling of the chemical reaction rate for every 10°C temperature increase. If corrosion takes place in dry air, a film of copper oxide will form on the canister surface. Corrosion of a micrometre or so prior to deposition will not affect the life of the canister in the repository.

Corrosion caused by water under aerobic conditions during the buffer saturation phase: After deposition and before water saturation, the canister is expected to stand in air with high humidity at a temperature of 90°C. Based on corrosion rates in connection with outdoor exposure of copper in urban atmosphere, Mattson makes the judgement that the corrosion rate may be as great as 100 to 300 µm per annum if the oxygen supply is not limited. The corrosion attack is expected to be uniformly distributed over the copper surface. The total corrosion attack can be modelled using a mass balance approach. A corrosion attack of 100 µm requires an oxygen quantity of 30 m³ if Cu₂O is formed as a corrosion product. The scope of the corrosion attack will be effectively limited by the availability of oxygen and will not affect the life of the canister in the repository.

Corrosion caused by nitric acid during the buffer saturation phase: Gamma irradiation of moist air in the canister-buffer gap leads to the formation of nitrogen oxides, which in contact with water form nitric acid. Marsh /1990/ shows a simple method to make a rough calculation of the quantity of nitric acid produced. The rate of formation of nitric acid is given by:

$$\frac{d[HNO_3]}{dt} = \frac{G \cdot V \cdot \rho \cdot D_0}{A_v} e^{-\frac{0.693t}{T}}$$

where G is the G value (in number of molecules/eV), V the irradiated air volume (dm³), ρ the density of the air (g/dm³), D₀ the initial dose rate (eV/g·y), A_v Avogadro's number, t the time (years) and T the half-life (years) of the radiation source. If it is assumed that the gamma radiation source has a half-life of 30 years, G = 0.02 molecules/eV and an air gap of 5 cm around the canister (V = 825 dm³), then a production rate for nitric acid of 0.002 mol/y is obtained. This is a small quantity, which does not appreciably affect the life of the canister.

Copper corrosion after water saturation; oxygen corrosion: Copper corrosion under the expected conditions in the deep repository after water saturation has been well studied /Swedish Corrosion Institute, 1978; 1983; Werme et al, 1992; Wersin et al, 1994b/. During a brief period of up to a few hundred years at most after deposition in the deep repository when oxygen will be present, the maximum corrosion depth is pessimistically estimated to be about 2 mm, but will probably be only a few microns /Wersin et al, 1994b/. The total corrosion attack will be determined by the quantity of available oxygen. It should be noted that it is the entrapped quantity of oxygen that causes the corrosion both before and after water saturation. The maximum corrosion attacks for these two cases should thus not be added.

Corrosion in the absence of oxygen

Copper corrosion after water saturation: In the absence of oxygen, copper is immune to corrosion in pure water. Corrosion with hydrogen gas generation can take place if the water contains dissolved sulphides. The corrosion products are then Cu₂S or CuS. High chloride concentrations in combination with low pH values can also cause corrosion on copper. In the former case, the corrosion rate will be controlled by the inward transport of sulphide ions, and in the latter case /Taxén, 1990/ by the outward transport of copper chloride complexes.

After the oxygen has been consumed and reducing conditions have been reinstated, copper corrosion under deep repository conditions will be controlled by the availability of dissolved sulphides. In the same way as for oxidizing conditions, Wersin et al, /1994b/ have estimated the extent of the corrosion with a very pessimistic assumption and a most likely case. In the pessimistic case, the corrosion depth is a few millimetres, but it will probably not exceed a few tenths of a millimetres in 100,000 years.

Copper corrosion after water saturation; bacterial corrosion: Normally, bacterial reduction of sulphate to sulphide does not pose any threat to the integrity of the canister, since this does not lead to elevated levels of dissolved sulphide in the groundwater. The concentrations of dissolved sulphide in the near field are controlled by the solubility of sulphide minerals in the bentonite, and in the rock the concentrations are generally well below 5·10⁻⁵ mol/dm³. At these low concentrations, the transport of sulphide from or through the buffer is very slow and will completely control the corrosion process.

A worst case would be if the bacteria formed a biofilm on the canister surface or were present in the buffer near the canister. The corrosion process would then be controlled by the transport of sulphate to the canister. This could lead to considerably accelerated corrosion, since the transport of sulphate is expected to be much faster than the transport of sulphide, due to the fact that the sulphate concentrations in the bentonite can be up to tens of mmol/dm³.

A study of the conditions for the growth of sulphate-reducing bacteria in compacted bentonite was conducted in 1995 by Pedersen et al /Motamedi et al, 1996). The results showed that the survival of sulphate-reducing bacteria in bentonite is dependent on the availability of water and the fact that if a bentonite of high quality is compacted to 2 g/cm³, equivalent to a water activity of 0.96, sulphate-reducing bacteria do not survive. There would thus not be any mechanism for bacterial corrosion inside the bentonite buffer if a water activity of 0.96 or lower can be maintained. Current knowledge suggests that bacterial sulphide corrosion can be ruled out in the repository environment.

Sulphate corrosion: Inorganic sulphate corrosion of copper has been deemed impossible under repository conditions, since the reaction is kinetically inhibited /Corrosion Institute, 1983; Grauer, 1991/.

Influence of temperature: The temperature in the repository will be elevated during the oxidizing phase, with a maximum temperature of 90°C on the copper surface. The temperature increase from 20°C to 90°C increases the copper corrosion rate by a factor of one hundred, based on the simple estimate that the reaction rate is doubled for every ten degrees of temperature increase. This is, however, of subordinate importance, since the diffusion of reactants is rate-controlling and the diffusivity is much less affected by the temperature. The influence of the temperature on the chemical equilibria for the corrosion reactions is completely negligible for the temperature range encountered in the repository.

Influence of chemical changes during glaciations: During a glaciation, the possibility cannot be completely ruled out that oxic (oxygen-containing) water will occasionally seep down into crushed zones and fractures of high conductivity. This has been discussed by Ahonen and Vieno /Ahonen and Vieno, 1994/.

During a deglaciation, oxic water could conceivably infiltrate down into the repository. The oxygen concentration in the water can be estimated at 10 mg/l. If it is assumed that a 100,000-year period includes a total of 5,000 years of deglaciation, when oxygenated water from the melting ice penetrates down into the repository (an equivalent flow of 1 litre per annum), then a total of approximately 400 g of copper will corrode. Assuming uniform corrosion, this is equivalent to 2.6 µm. With the pitting factor of 5 /Swedish Corrosion Institute, 1983/ that has been used in the KBS-3 study, the deepest pit would be 13 µm.

The attack will probably not be uniformly distributed, since oxygen could come through the tunnel and attack only the lid of the canister. The lid area constitutes approximately 5 percent of the whole surface area, and the deepest pit under these circumstances will be 260 µm.

Time perspective

Only the sulphide corrosion is of importance in a longer time perspective. Sulphide corrosion will proceed as long as sulphide is present and metallic copper is available.

Natural analogues

Corrosion of copper under oxidizing conditions can be studied on archaeological artefacts. Such studies have been conducted both to assess the risk of pitting /Bresle et al, 1983; Hallberg et al, 1984/ and to assess general corrosion over longer periods of time /Hallbert et al, 1988/. Bresle et al, studied the pitting factor on archaeological bronze objects buried in soil for long periods of time. The results indicated that the probable pitting factor lay in the range 2–5. Hallberg et al /1984/ performed a similar study of three lightning conductor plates that had been buried in the ground for 50 to 80 years and found a pitting factor of 5 in two of the cases and no pitting in the third case. Hallberg et al /1988/ examined a bronze cannon from the Swedish warship Kronan, which had lain buried with its muzzle downward in the mud on the bottom of the Baltic Sea since 1676. They estimated the corrosion rate to be $1.5 \cdot 10^{-5}$ mm/y. This is equivalent to 1.5 mm in 100,000 years, and with a pitting factor of 5 a maximum corrosion depth of 7.5 mm.

Summary of uncertainties

Copper corrosion after water saturation: Under the now known conditions at deep repository level, the canister is expected to remain intact for a very long time, much longer than the 100,000 years in the design requirements. The uncertainties in assessments of the repository's evolution over long periods of time are great, and the copper thickness has therefore been chosen with a large safety factor to ensure a canister life of 100,000 years.

Even though there are large uncertainties in the assessments over long time spans, it is very unlikely that general corrosion or pitting could lead to canister penetration during the 100,000 years the canister has been designed for. In other words, there are small uncertainties in the assessment that the canister life is at least 100,000 years as far as corrosion is concerned.

Handling in the safety assessment

Base scenario: Corrosion in accordance with the inward transport of corrodants that can be expected in the base scenario.

Canister defect scenario: See base scenario.

Climate change: Corrosion in accordance with the inward transport of corrodants that can be expected in the climate scenario.

Earthquake: See base scenario.

3.7.6 Stress corrosion cracking, copper canister

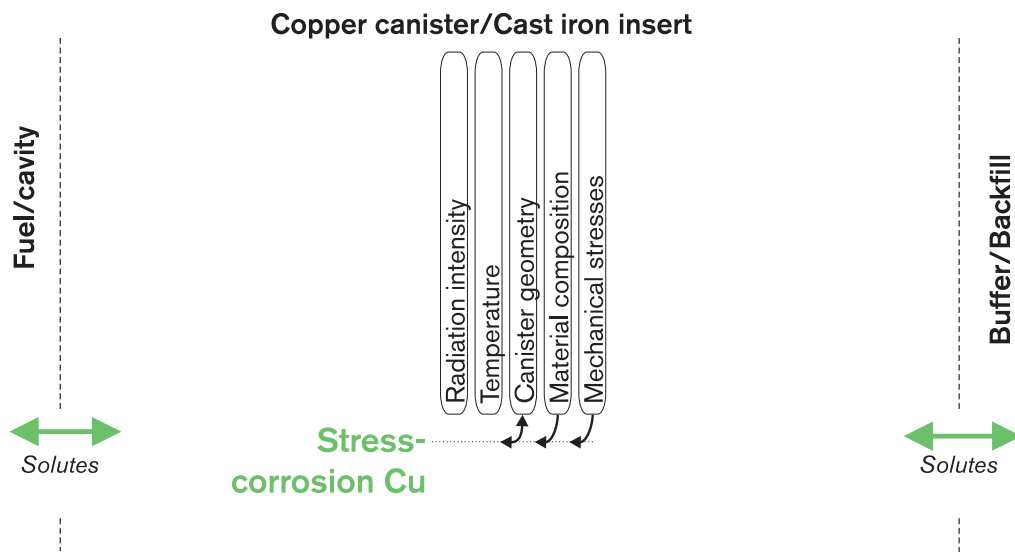


Figure 3-14. Stress corrosion cracking, copper canister.

Over view

Stress corrosion cracking (SCC) was described in general terms in section 3.7.3. Elevated concentrations of nitrites and ammonium can cause SCC of copper in the deep repository environment.

General description, model studies/experimental studies

In the KBS-2 study /Swedish Corrosion Institute, 1978/, the risk of SCC was considered to be non-existent for oxygen-free, pure copper. More recent investigations, discussed in the KBS-3 study /Swedish Corrosion Institute, 1983/ have shown that the risk cannot be ruled out entirely for the copper grades and the repository environment in question. Nitrogen compounds such as nitrite and ammonia can give rise to SCC in copper. Studies conducted by SKB have, however, shown that SCC must be deemed improbable under the expected repository conditions. These conclusions were based on results from SSRT (slow strain rate testing) /Benjamin et al, 1988/.

Time perspective

If SCC occurs, it will probably occur during an early phase in the repository when oxidizing conditions still prevail (< 300 years).

Natural analogues

Not applicable.

Summary of uncertainties

There is no evidence that SCC could occur in the repository environment, but the possibility cannot be entirely ruled out with present-day knowledge. There are no criteria for under what conditions SCC is possible or impossible.

Tensile stresses in the copper canister are a necessary prerequisite, and since the canister is under external pressure it is not likely that SCC could lead to canister penetration. This would require tensile stresses through the whole canister wall, and such a situation is not deemed to be possible under normal conditions in the repository.

Handling in the safety assessment

Base scenario: SCC cannot be modelled with present-day knowledge. The process can in all likelihood be neglected.

Canister defect scenario: See base scenario.

Climate change: See base scenario.

Earthquake: See base scenario.

3.8 Radionuclide transport

See section 2.8, "Radionuclide transport in fuel/canister cavity".

3.9 References

Ahonen L, Vieno T, 1994. Effects of glacial meltwater on corrosion of copper canisters. Report YJT-94-13. Nuclear Waste Commission of Finnish Power Companies.

Benjamin L A, Hardie D, Parkins R N, 1988. Stress corrosion resistance of pure coppers in ground waters and sodium nitrite solutions. *Br. Corros. J.* **88** (1988) 89–95.

Billington D S, Crawford J H, 1961. Radiation damage in solids. Princeton University Press, Princeton, New Jersey.

Bjurström H, Bruce A, 1997. Temperaturer i en kapsel enligt TR-95-02, en första uppskattning. SKB Inkapsling PPM 97-3420-28, Svensk Kärnbränslehantering AB. (In Swedish).

Bjurström H, Bruce A, 1998. Temperaturer i en kapsel enligt TR-95-02, etapp 2. SKB Inkapsling Projekt PPM 98-3420-30, Svensk Kärnbränslehantering AB. (In Swedish).

Blackwood D J, Naish C C, 1994. The effect of galvanic coupling between the copper outer canister and the carbon steel inner canister on the corrosion resistance of the Advanced Cold process canister. SKB Inkapsling PR 95-04, Svensk Kärnbränslehantering AB.

Blackwood D J, Naish C C, Rance A P, 1994. Further research on corrosion aspects of the Advanced Cold Process Canister. SKB Inkapsling PR 95-05, Svensk Kärnbränslehantering AB.

Blackwood D J, Henshaw J, Platts N, Hilditch J P, 1995. Stress corrosion cracking of the advanced cold process canister: Carbon steel in nitric acid vapour. SKB Inkapsling PR 96-05, Svensk Kärnbränslehantering AB.

- Bond A E, Hoch A R, Jones G D, Tomczyk A J, Wiggin R W, Worraker W J, 1997.** Assessment of a spent fuel disposal canister. Assessment studies for a copper canister with cast steel inner component. SKB TR 97-19, Svensk Kärnbränslehantering AB.
- Bresle Å, Saers J, Arrhenius B, 1983.** Studies on pitting corrosion on Archaeological bronzes. SKB TR 83-05, Svensk Kärnbränslehantering AB.
- Börgesson L, 1992.** Interaction between rock, bentonite, buffer and canister. FEM calculations of some mechanical effects on the canister in different disposal concepts. SKB TR 92-30, Svensk Kärnbränslehantering AB.
- Börgesson L, Hernelind J, 1998.** Kapselpåverkan vid inhomogena svälltryck från bufferten. FEM-beräkningar av effekten av ojämn vattentillgång i berget. SKB Inkapsling PPM 98-3420-33, Svensk Kärnbränslehantering AB. (In Swedish).
- Cakmak E, 1994.** Beräkningar av maximal töjning i kopparbehållare för slutförvaring av utbränt kärnbränsle. SKB Inkapsling PPM 95-3420-01, Svensk Kärnbränslehantering AB. (In Swedish).
- Ekberg M, 1995.** Lagringsbehållare för utbränt kärnbränsle, kollapstryck hos gjuten cylinder. SKB Inkapsling PPM 95-3420-11, Svensk Kärnbränslehantering AB. (In Swedish).
- Grauer R, 1991.** The reducibility of sulphuric acid and sulphate in aqueous solution (translated from German). SKB TR 91-39, Svensk Kärnbränslehantering AB.
- Hallberg R, Engvall A-G, Wadsten T, 1984.** Corrosion of copper lightning conductor plates. Br. Corros. J. Vol. 19:2, pp 85–88.
- Hallberg R O, Östlund P, Wadsten T, 1988.** Inferences from a corrosion study of a bronze cannon, applied to high level nuclear waste disposal. Applied Geochemistry, Vol. 3, pp 273–280.
- Håkansson R, 1995a.** Doserberäkningar för kapsel med använt kärnbränsle. Studsvik Nuclear AR N(R)-95/026. (In Swedish).
- Håkansson R, 1995b.** Beräkningar av doshastighet 1 m från kapsel med använt kärnbränsle samt 1 m från bårt använt bränsleelement. Studsvik Nuclear AR N(R)-95/050. (In Swedish).
- Håkansson R, 1996.** Beräkning av nuklidinnehåll, resteffekt, aktivitet samt doshastighet för utbränt kärnbränsle. Studsvik Nuclear AR N(R)-96/079. (In Swedish).
- Knopp U, 1996.** Feasibility Study of a Transport cask for the Transport of Canisters for Encapsulated Spent Fuel to Final Disposal. For canister with cast insert. SKB Inkapsling PR 96-07, Svensk Kärnbränslehantering AB.
- Marsh G P, 1990.** A preliminary assessment of the advanced cold process canister. Harwell Laboratory, AEA Industrial Technology, Report AEA-InTec-0011.
- Mattsson E, 1997.** Utvändig korrosion hos kopparkapslar i avvaktan på slutförvar och under slutförvarets inledningsskede. SKB Inkapsling PPM 97-3420-22, Svensk Kärnbränslehantering AB. (In Swedish).

- Motamedi M, Karnland O, Pedersen K, 1996.** Survival of sulfate reducing bacteria at different water activities in compacted bentonite. *FEMS Microbiology Letters* **141** (1996) 83–87.
- Pedersen K, Motamedi M, Karnland O, 1995.** Survival of bacteria in nuclear waste buffer materials. The influence of nutrients, temperature and water activity. SKB TR 95-27, Svensk Kärnbränslehantering AB.
- Porter L F, 1960.** Radiation effects in steel. In: *Nuclear Materials Applications*. ASTM Special Technical Publication No. 276, pp 147–196.
- Reed D T, van Konynenburg R A, 1991a.** Effect of ionizing radiation on the waste package environment. High Level Waste Management II, American Nuclear Society, La Grange Park, IL, 1396–1403.
- Reed D T, van Konynenburg R A, 1991b.** Progress in evaluating the corrosion of candidate HLW container metals in irradiated air-steam mixtures. *Proceedings Nuclear Waste Packaging, Focus '91*, American Nuclear Society, La Grange Park, IL, 185–192.
- Renström P, 1997.** Calculation of the fuel temperature in vacuous storage canisters made of copper with cast steel inserts. SKB Inkapsling PPM 97-3420-23, Svensk Kärnbränslehantering AB.
- Smart N, Rance A, Blackwood D, 1997.** Corrosion aspects of the copper-steel/iron process canister: Consequences of changing the material for the inner container from carbon steel to cast iron. SKB Inkapsling PR 97-04, Svensk Kärnbränslehantering AB.
- Swedish Corrosion Institute and its reference group, 1978.** Copper as canister material for unreprocessed nuclear waste – evaluation with respect to corrosion. KBS TR 90.
- Swedish Corrosion Institute and its reference group, 1983.** Corrosion resistance of a copper canister for nuclear fuel. SKBF/KBS TR 83-24. Svensk Kärnbränslehantering AB.
- Taxén C, 1990.** Corrosion on copper in chloride containing waters. A thermodynamic study. SKB Inkapsling PR 94-02, Svensk Kärnbränslehantering AB.
- Werme L, Sellin P, Kjellbert N, 1992.** Copper canisters for nuclear high level waste disposal. Corrosion aspects. SKB TR 92-26, Svensk Kärnbränslehantering AB.
- Werme L O, 1997.** Materialförändringar av betydelse för kapselns långtidsbeständighet. SKB Inkapsling PPM 97-3420-24, Svensk Kärnbränslehantering AB. (In Swedish).
- Werme L O, 1998.** Design premises for canister for spent nuclear fuel. SKB TR- 98-08, Svensk Kärnbränslehantering AB.
- Wersin P, Spahiu K, Bruno J, 1994a.** Time evolution of dissolved oxygen and redox conditions in a HLW repository for spent nuclear fuel. SKB TR 94-02, Svensk Kärnbränslehantering AB.
- Wersin P, Spahiu K, Bruno J, 1994b.** Kinetic modelling of bentonite-canister interaction. Long-term predictions of copper canister corrosion under oxic and anoxic conditions. SKB TR 94-25, Svensk Kärnbränslehantering AB.

4 Buffer/backfill

4.1 Description of buffer and backfill

4.1.1 General

In their deposition holes, the copper canisters will be surrounded by a buffer of bentonite clay, see Figure 4-1. On deposition, gaps are formed for technical reasons between canister and buffer and between buffer and rock. The inner gap is filled with water and the outer with bentonite pellets and water.

After deposition, the tunnel above the deposition hole will be backfilled with a material that is adapted to the chemical conditions on the repository site.

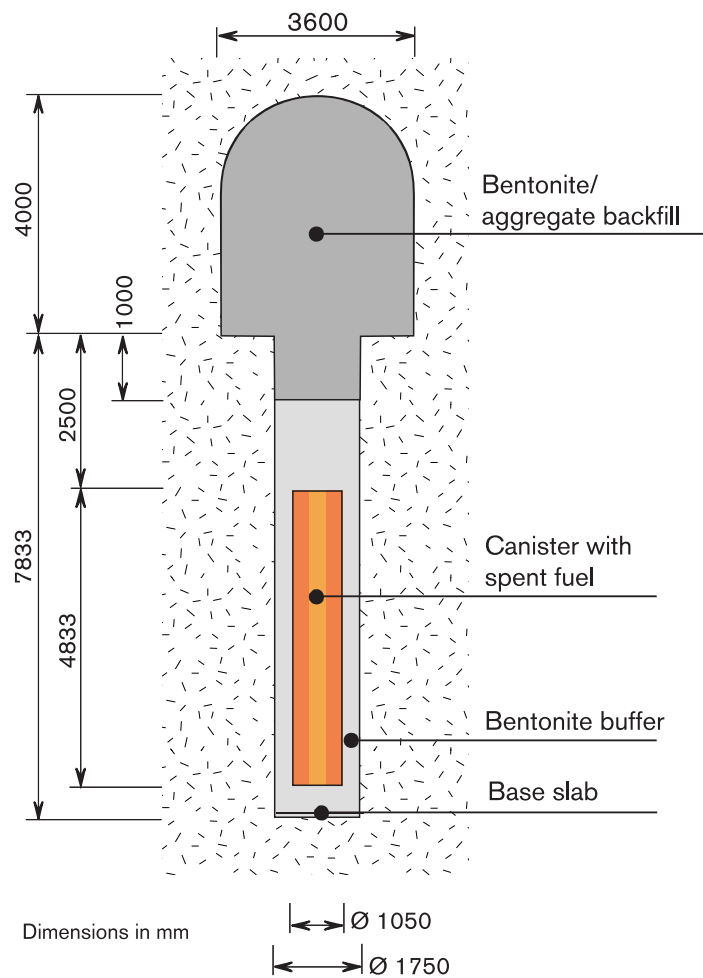


Figure 4-1. Deposition hole with bentonite buffer and canister. The figure also shows the backfilled tunnel above the deposition hole.

Buffer material

The buffer consists of MX 80 bentonite, a natural clay from Wyoming or South Dakota in the USA. The designation MX 80 is a trade name and specifies a certain grade and grain size of dried and ground bentonite.

MX 80 bentonite consists mainly of the smectite mineral montmorillonite (65–80 percent), where the clay particles are smaller than 2 μm . Chemically, montmorillonite is a polyelectrolyte, which means that a layer of exchangeable ions is associated with the surfaces of the clay particles. The clay swells in contact with water. The exchangeable ions in MX 80 consist predominantly of sodium, and the material is therefore called sodium bentonite. Water-saturated buffer contains about 25 weight-percent water. The water molecules are absorbed in the material, and water transport occurs mainly by diffusion.

MX 80 bentonite also contains the minerals quartz (about 15 percent) and feldspar (5–8 percent). Chemically important components in addition to the minerals are carbonates (e.g. calcite), sulphates, fluorides, sulphides (e.g. pyrite), iron(II) and organic matter.

When wetted with water, the bentonite contains a pore water of characteristic composition, which depends on the composition of the bentonite and the water used for wetting.

Backfill material

The backfill material consists of a mixture of bentonite clay and crushed rock. The proportions are adapted to the chemical conditions on the repository site so that the backfill will have the desired characteristics. Such site-specific adaptation has not been done in SR 97. Instead, a typical composition is used consisting of 15 weight-percent MX 80 bentonite clay and 85 weight-percent crushed rock.

4.1.2 Overview of variables

In the buffer/backfill subsystem, the buffer is bounded on the inside by the interface towards the canister, on the outside and bottom by the interfaces towards the deposition hole, and on the top by the interface towards the backfill. The backfill is constricted in space by backfilled tunnel systems and rock chambers. There are also plugs whose purpose is to seal the tunnel system hydraulically, but these have not been included in the description in SR 97.

The buffer as it is delimited by the variable **buffer geometry** is characterized thermally by its **temperature** and with respect to radiation by its **radiation intensity**, mainly γ - and neutron radiation. Hydraulically, the buffer is characterized by its **water content**, and sometimes by **gas concentrations** and by water pressure, water flow, gas pressure and gas flow. The last four, which are mainly of interest in the phase when the buffer is being saturated with water, have been combined in the variable **hydrovariables**. Mechanically, the buffer is characterized by a **swelling pressure**.

The chemical state of the buffer is defined by its **smectite content** and its **smectite composition**, which is the composition of the actual clay mineral, including the ionic species associated to the surface, different **impurity contents** and a **pore water composition**.

The same set of variables is used for the backfill as for the buffer. The crushed rock, which comprises 85 percent of the backfill, is included in the variable **impurity contents**.

All variables are defined in Table 4-1.

Table 4-1. Variables in buffer/backfill.

| | |
|-------------------------------|---|
| Geometry | Geometric dimensions for buffer/backfill. A description of e.g. interfaces on the inside towards the canister and on the outside towards the geosphere. |
| Pore geometry | Pore geometry as a function of time and space in buffer and backfill. The porosity, i.e. the fraction of the volume that is not occupied by solid material is often given. |
| Radiation intensity | Intensity of (α -, β -), γ - and neutron radiation as a function of time and space in buffer (and backfill). |
| Temperature | Temperature as a function of time and space in buffer and backfill. |
| Smectite content | Smectite content as a function of time and space in buffer and backfill. |
| Water content | Water content as a function of time and space in buffer and backfill. |
| Gas contents | Gas contents (including any radionuclides) as a function of time and space in buffer and backfill. |
| Hydrovariables | Flows and pressures of water and gas as a function of time and space in buffer and backfill. |
| Swelling pressure | Swelling pressure as a function of time and space in buffer and backfill. |
| Smectite composition | Chemical composition of the smectite (including any radionuclides) in time and space in buffer and backfill. This variable also includes material sorbed to the smectite surface. |
| Pore water composition | Composition of the pore water (including any radionuclides and dissolved gases) in time and space in buffer and backfill. |
| Impurity levels | Levels of impurities in time and space in buffer and backfill. Impurities also include minerals, other than smectite. In backfill, crushed rock is an impurity. |

4.2 Overview of processes

On emplacement, the buffer comes into contact with the hot canister surface, the thermal energy is spread through the buffer by *heat transport* and the temperature increases. The γ and neutron radiation emitted by the canister decreases in intensity by *radiation attenuation* in the buffer.

A negative capillary pressure exists originally in the pores in the buffer, causing *water to be transported* in from the surrounding rock. After the buffer has been saturated with water, this water transport is very slow. *Gas transport* can occur during the saturation process, when water vapour can flow from the hotter parts of the buffer to condense in the outer, colder parts. Originally there is also air in the buffer, which can leave the buffer by dissolving in the pore water; *gas dissolution*. After water saturation, gas transport can occur if a canister is damaged, leading to hydrogen formation in the canister.

On absorbing water, the buffer and backfill *swell* and a swelling pressure is built up. The swelling pressure is different in the buffer and backfill, which therefore *interact mechanically*. The swelling pressure is decisive for the mechanical interaction between canister and buffer, which can cause the canister to move in the buffer. On heating, the pore water may expand due to *thermal expansion*.

The chemical evolution in buffer and backfill is determined by a number of transport and reaction processes. Solutes in the water may be transported by *advection* and *diffusion*. In the buffer, advection occurs almost exclusively during the water saturation process, subsequently diffusion. By means of *ion exchange/sorption*, the original ions on the surfaces of the clay particles in the buffer may be replaced by other ionic species. Chemical smectite degradation may occur, for example in the form of illitization. Impurities undergo various *dissolution/precipitation* reactions in the buffer. On swelling, the buffer penetrates out into the fractures in the surrounding rock, where it may form colloids which may be carried away by the groundwater, leading to gradual erosion of the buffer. The clay may be transformed by *radiation effects* and the pore water may be decomposed by *radiolysis*. Finally, *microbial processes* may occur in buffer/backfill.

After water saturation, *radionuclide* transport is expected to take place in the buffer exclusively by *diffusion* in the pores of the buffer, possibly also on the surfaces of the clay particles. Neither *advection* nor *colloid transport* is expected in a saturated buffer. Radionuclides may be sorbed to the surfaces of the clay particles. A crucial factor for this is the chemical form of the radionuclide, which is determined by the chemical environment in the buffer via the process of *speciation*. Together with the transport conditions, the rate of *radioactive decay* determines to what extent radionuclides from a broken canister will decay before reaching the outer boundary of the buffer.

Virtually the same processes occur in the backfill as in the buffer, but sometimes to a different extent. Furthermore, the crushed rock (defined as an impurity in the backfill) plays a slightly different role than the impurities in the buffer, for example by contributing to sorption.

The THMC diagram for buffer/backfill is given in figure 4-2.

Buffer/Backfill

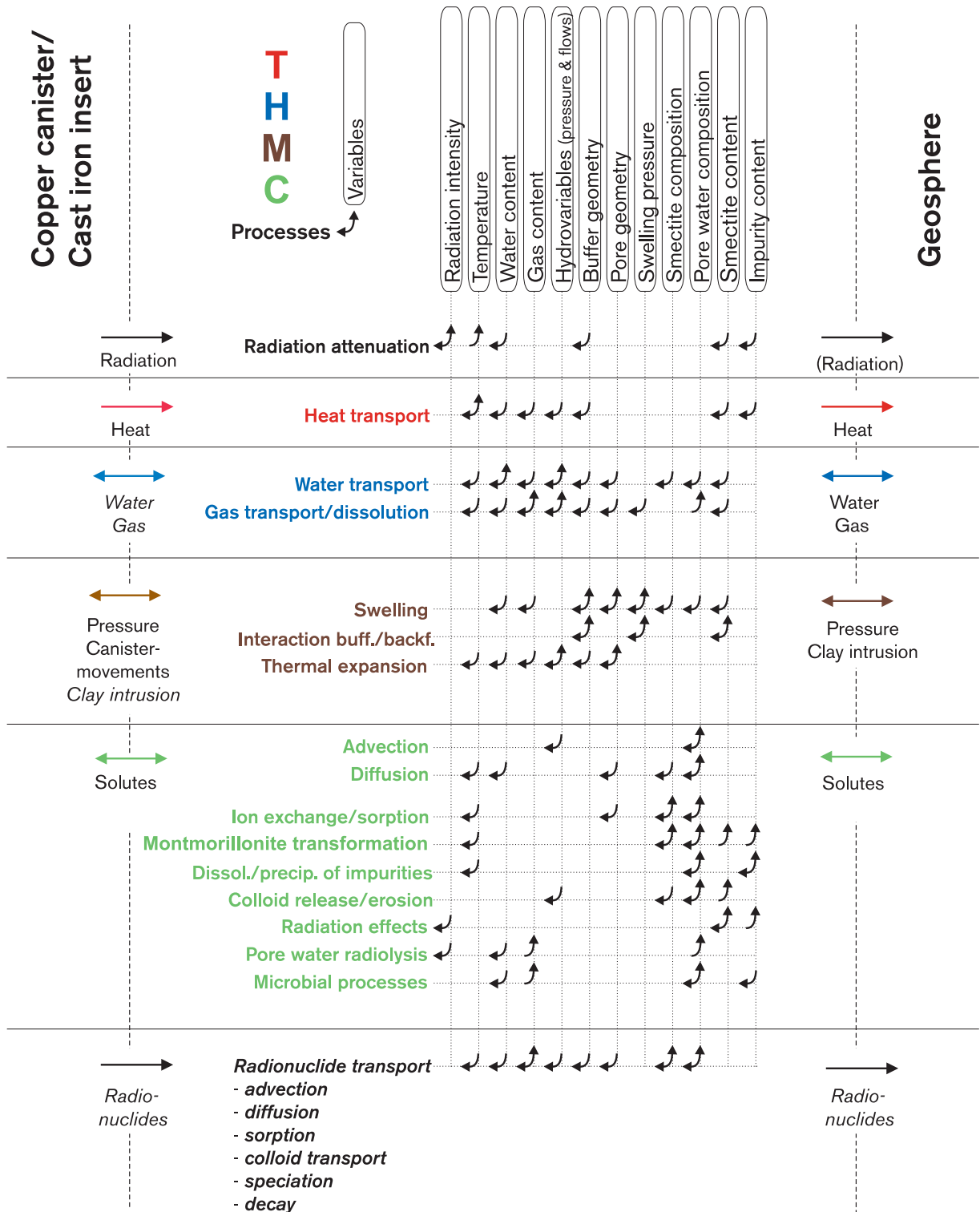


Figure 4-2. THMC diagram for buffer/backfill. Processes and interactions in italics only occur when the isolation of the copper canister is broken.

4.3 Radiation-related processes

Besides radiation attenuation (see below), any radionuclides in the buffer undergo radioactive decay. Radioactive decay is described in the chapter that deals with fuel/cavity.

4.3.1 Radiation attenuation/heat generation

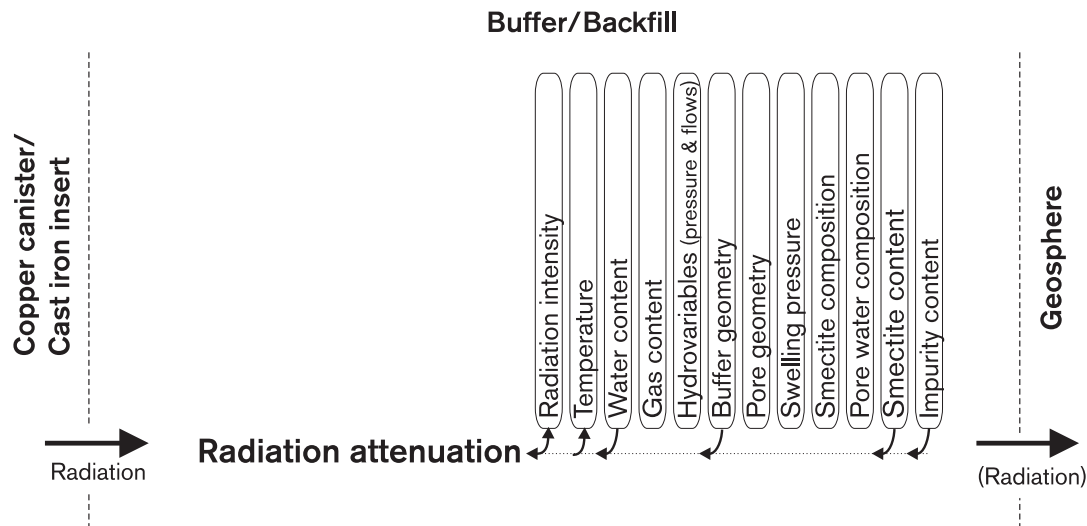


Figure 4-3. Radiation attenuation/heat generation.

Overview, general description

γ and neutron radiation from the canister are attenuated in the buffer. The magnitude of the attenuation is dependent above all on the density and water content of the buffer. The result is a radiation field in the buffer that can lead to radiolysis and have a marginal impact on the montmorillonite. The radiation that is not attenuated in the buffer reaches out into the near-field rock.

Attenuation of γ - and neutron radiation will raise the temperature of the buffer, but the effect is negligible compared with other temperature-raising processes. The radiation is of importance for the chemical processes *radiation-induced montmorillonite decomposition and γ -radiolysis of pore water*.

Model studies/experimental studies

Attenuation of γ - and neutron radiation can be calculated theoretically for an arbitrary material if geometry and composition are known, see e.g. the model studies mentioned for the equivalent process in the canister. Experimental studies of radiation attenuation in bentonite are reported in section 4.7.8.

Time perspective

See equivalent process for the canister.

Natural analogues

Not applicable.

Summary of causes

Understanding: Our understanding of the process is good enough for the needs of the safety assessment.

Data: Data for a quantitative description of the process are known with sufficient accuracy for the needs of the safety assessment.

Handling in the safety assessment

Base scenario: A simple calculation of dose rate on the inside and outside of the buffer is carried out. Heat generation is neglected.

Canister defect scenario: See base scenario.

Climate change: See base scenario.

Earthquake: See base scenario.

4.4 Thermal processes

4.4.1 Heat transport

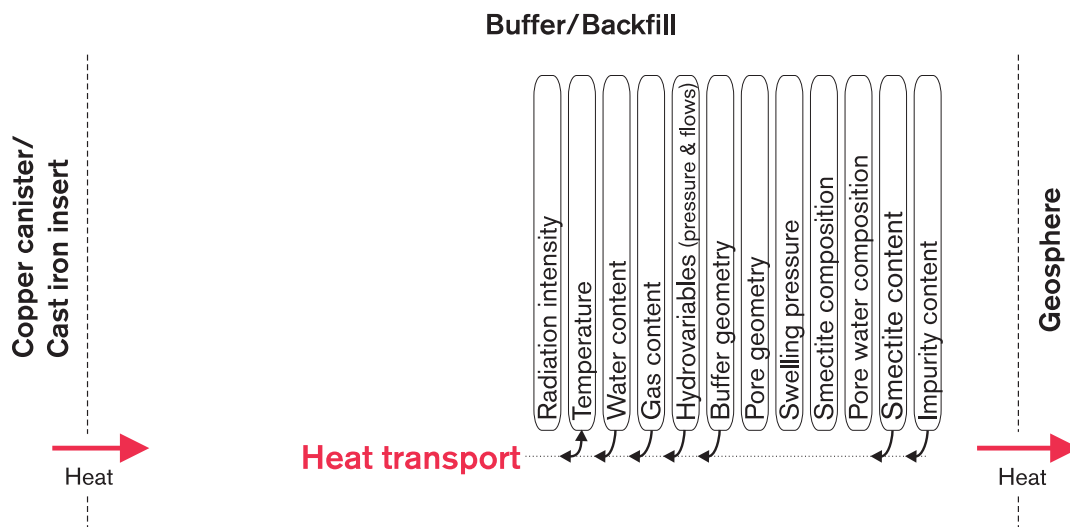


Figure 4-4. Heat transport.

Overview

Heat is transported in buffer and backfill mainly by conduction. Before full water saturation has been achieved, vapour flow in the buffer can also contribute to heat transport.

Thermal conductivity is mainly dependent on the composition and water content of the bentonite.

General description

Heat is transported from the canister surface to the buffer, through the buffer and finally from the buffer to the rock both directly and via the tunnel backfill. Transport may possibly take place during some time period via gaps between canister and buffer and between buffer and rock. The efficiency of the heat transport through the buffer region is important for the performance of the system, since it affects two important temperatures: that on the canister surface, and that in the buffer itself. The importance of the heat transport capacity of the tunnel backfill in these respects is, however, small and is therefore dealt with only briefly in the following.

When the buffer has been water-saturated and has swelled out so that all gaps and joints are filled, all heat transport takes place by conduction. Before full water saturation, a small portion of the heat transport in the buffer material takes place by vaporization, vapour flow and condensation. At an early stage there may also be gaps filled with air or water vapour. In water-filled gaps, heat transport across the gap takes place by flow and conduction, in gaps filled with air and water vapour also in part by radiation. After a week or so, heat transport through the buffer is largely independent of the heat capacity of the buffer, and heat conduction in the buffer can be approximately described by the time-independent heat conduction equation:

$$\nabla \cdot (\lambda \nabla T) = 0$$

The most important parameter is thus the thermal conductivity, λ , of different parts of the system. The thermal conductivity of bentonite is primarily dependent on density, water saturation and mineral composition. The thermal conductivity of water-saturated MX-80 bentonite that has swelled out to its intended density, 2,000 kg/m³, is about 1.2 W/(m·K). At application, the water saturation of the blocks is lower, but their dry density is higher, which gives approximately the same thermal conductivity. The water conductivity of gaps filled with water and air is 0.60 W/(m·K), while that of gaps filled with water vapour is about 0.025 W/(m·K) (West, 1973).

Influence of water content: The water conductivity of bentonite with a high montmorillonite content can be estimated with the aid of the expressions in (1-2 to 1-4), which give the thermal conductivity as a function of the degree of saturation S_r and the porosity n , which, together with the mineral density, determine the density of the buffer (Knutsson, 1983).

$$\lambda = \lambda_0 + K_e (\lambda_1 - \lambda_0) \quad (1-2)$$

where

λ_0 = thermal conductivity at $S_r = 0$ (dryness)

λ_1 = thermal conductivity at $S_r = 100$ percent (water saturation)

$K_e = 1 + \log S_r$

λ_0 and λ_1 are determined according to (1-3) and (1-4):

$$(1-3)$$

$$\lambda_1 = 0.56^n \cdot 2^{(1-n)}$$

$$(1-4)$$

Equation (1-2) gives values with an estimated accuracy of 20 percent.

The influence of the density is expressed implicitly in the form of the porosity n . The porosity n of water-saturated highly-compacted MX-80 bentonite with a density of $2,000 \text{ kg/m}^3$ at water saturation is 0.44, and the thermal conductivity according to Equ. (1-4) is $1.14 \text{ W/(m}\cdot\text{K)}$. If the degree of saturation is reduced to 50 percent, the thermal conductivity is $0.85 \text{ W/(m}\cdot\text{K)}$.

Influence of temperature and pressure: Different models have been proposed for estimating the influence of increasing pressure and temperature on the thermal conductivity of bentonite /Knutsson, 1983/. They show a slight increase of the thermal conductivity, but the effect is not sufficiently verified to be able to be credited /Börgesson et al, 1994/. The thermal conductivity of water and air/water vapour also increases slightly with the temperature, but the effect is small and can be neglected.

Influence of montmorillonite content: The montmorillonite content *per se* is not decisive for the buffer's thermal conductivity, since the most common accessory minerals have a similar thermal conductivity. An exception is quartz, which has a higher thermal conductivity.

Influence of convective vapour transport on heat transport: The contribution made by convective vapour transport to heat conduction can be estimated to increase the thermal conductivity by a few tenths of a $\text{W/(m}\cdot\text{K)}$ /Börgesson et al, 1994/. However, due to the difficulty of studying the process experimentally, this contribution should be pessimistically neglected.

Heat conduction in transition canister/buffer: If the gap between the buffer and the surface of the canister is water-filled, transport across the gap takes place by conduction with a thermal conductivity of about $0.6 \text{ W/(m}\cdot\text{K)}$, which differs insignificantly from the thermal conductivity of partially unsaturated bentonite. If the gap is gas-filled, the thermal conductivity is approximately $0.025 \text{ W/(m}\cdot\text{K)}$ and a considerable temperature differential can arise between canister surface and buffer. The size of the differential depends on how efficiently heat can be transferred by radiation, i.e. on the emissivity of the canister surface, and on how well the canister is cooled via other surfaces where there is no gas-filled gap. The size of the temperature differential can be up to 30°C /Bjurström, 1997/. In the case of a gas-filled annular gap around the canister surface, a disproportionately large portion of the canister's heat output may be transferred to the buffer via the canister's base surfaces.

Influence of geometry on heat transport: The resistance to heat transport in the buffer is dependent on the distance between the canister and the canister hole boundary, which entails changes in the temperature of the buffer if the dimensions of the canister hole or the location of the canister in the hole should be altered. After water saturation, however, the variations in geometry that could occur due to block breakout or a poorly centred canister have negligible effects. This is also true of effects of instantaneous or time-dependent deformations that can alter the geometry of the canister hole. Before water saturation, a poorly centred canister can be of importance for the distribution of gas-filled volumes and therefore for the temperature level and temperature distribution in the buffer.

Influence of heat transport on buffer temperature: The temperature at the boundary of the canister hole is as good as independent of the heat transport capacity of the buffer. The temperature difference between the outer and inner buffer boundary, on the other hand, is determined at a given canister power (heat output) by the heat transport capacity of the buffer so that the temperature in the inner parts is high if the thermal conductivity is low, for example due to drying-out.

Influence of heat transport on backfill temperature: The temperature of the backfill is determined by the surrounding rock, which has a higher thermal conductivity. The only influence of the heat transport capacity of the backfill itself is that the average effective heat transport resistance of the near field is slightly greater if the transport capacity is low. However, the volume of the tunnels in relation to the total volume of the near field is so small that changes in the backfill's contribution to the heat transport resistance have small effects on the temperature, both in the backfill and in the buffer.

Model studies/experimental studies

Model studies. Prediction of the temperature evolution in the near field has been done analytically /Claesson and Probert, 1996/ and numerically /Thunvik and Braester, 1991; Hökmark, 1996/.

The temperature at the buffer/canister transition reaches a peak after about 10 years. A peak is reached at the buffer/rock transition after about 50 years.

The temperature levels that will apply at the canister hole boundary are dependent on the thermal diffusivity of the rock, the canister power, the tunnel spacing and the canister spacing. By means of analytical solutions it is possible to estimate the temperature in the rock in different positions in relation to a canister for arbitrary repository geometries and canister powers /Claesson and Probert, 1996/. For example, a maximum temperature increase of about 56°C at the canister hole boundary is obtained for an initial canister power of 1,680 W if the tunnel spacing is 40 m and the canister spacing is 6 m. If the canister power is reduced to 1,050 W and the tunnel spacing is reduced proportionally, i.e. to 25 m, the temperature increase is instead about 47°C /Hökmark, 1996/.

The temperature levels that will apply in different parts of the buffer and in the canister/buffer transition are further dependent on the heat conduction properties of the buffer and on the possible presence of gaps and drying cracks. If it is assumed that the effective thermal conductivity between canister and rock is 0.7 W/(m·K), the temperature difference between them will be 20°C to 25°C at an initial canister power of about 1,050 W /Thunvik and Braester, 1991/. The difference decreases after about 10 years and is about 10°C after 100 years and only a degree or so after 1,000 years.

The temperature evolution in the backfill can be determined using analytical methods [8]. The temperature increase in the tunnel floor is approximately 45°C at a canister power of 1,680 if the tunnel spacing is 40 m and the canister spacing is 6 m. If the output is reduced to 1,050 W and the tunnel spacing is reduced proportionally, i.e. to 25 m, the temperature increase is instead about 40°C /Hökmark, 1996/.

The duration of the temperature pulse is a few thousand years. After 2,000 years the excess temperature in the repository is about 20°C and after 5,000 years about 15°C /Hökmark, 1996/. No gradients exist in the near field after about 2,000 years.

Experimental studies: Field tests involving simulation of the conditions in half-scale KBS-3-type deposition holes in Stripa showed, on sampling after 10 to 15 months, that steeply dipping cracks had emanated from the electric heaters to about half the buffer thickness in holes with little water inflow /Pusch and Börgesson, 1983/. The cracks emanated radially from the hot surface and deviated at a 45° angle in towards the water-saturated surface zone as a consequence of stresses generated by swelling pressure. The temperature gradient over the nearest 3 cm was about 5°C/cm, which shows that heat transfer was poor nearest the heaters. This was due to the fact that the original gap of less than 1 millimetre had been increased to several millimetres, plus the creation of

fine drying cracks and a decline in the degree of saturation. No verified quantitative relationships have been found between effective thermal conductivity and degree or type of cracking.

An important lesson learned from laboratory experiments and from the field tests in Stripa is that water saturation of bentonite blocks in contact with each other leads to healing of joints and drying cracks /Pusch, 1980; Pusch et al, 1985a/. It is thus only during the water saturation period that bentonite blocks can be separated by open joints.

Time perspective

There are two time perspectives: the water saturation perspective and the heat production perspective. The time it takes to achieve full water saturation is dependent on, *inter alia*, the pressure conditions in the groundwater in the near field. The process is estimated to take a number of years, see section 4.5.1. After that, all heat transport takes place by conduction and under well-defined conditions with known thermal conductivities. Before then, heat transport can be influenced by the presence of gaps and joints. After a few thousand years, heat production and thereby heat transport through the buffer will have been reduced to a few percent of their original values.

Natural analogues

Not applicable.

Summary of uncertainties

Understanding: Heat transfer from the hot canisters via the buffer to the near-field rock and backfill is in principle a simple process that can be described with reference to the basic laws of physics. The character of the subprocesses that participate in the heat transport is also known and the theoretical modelling of their function is based on well-known physical principles.

Data: The numerical values of individual thermal quantities cannot be determined theoretically due to the complex structure of the materials and the transient events that take place both in laboratory experiments and in a final repository, which gives rise to uncertainties. The most important quantity is the thermal conductivity λ , which varies throughout the buffer, both in the initial phase with incomplete water saturation and at full water saturation.

The temperature distribution in the rock, including the temperature at the canister hole boundary, is independent of the buffer properties and can be calculated for given values of tunnel spacing, canister spacing, initial canister power and thermal diffusivity of the rock, which has been demonstrated by comparison between numerical and analytical calculations /Claesson and Probert, 1996; Hökmark, 1996/, see further section 5.4.1.

Handling in the safety assessment

Base scenario: In SR 97, temperature calculations are carried out for the base scenario for all sites with site-specific repository layouts. The temperature is calculated as a function of time for different places in the repository. A dominant uncertainty in the temperature calculations is the possible propagation of a gas-filled gap between the canister and the buffer. Variation calculations will therefore be carried out to illustrate the importance of such a gap.

Canister defect scenario: See base scenario.

Climate change: Temperature changes in the buffer as a consequence of climate changes are discussed qualitatively where necessary.

Earthquake: See base scenario.

4.5 Hydraulic processes

4.5.1 Water transport under unsaturated conditions

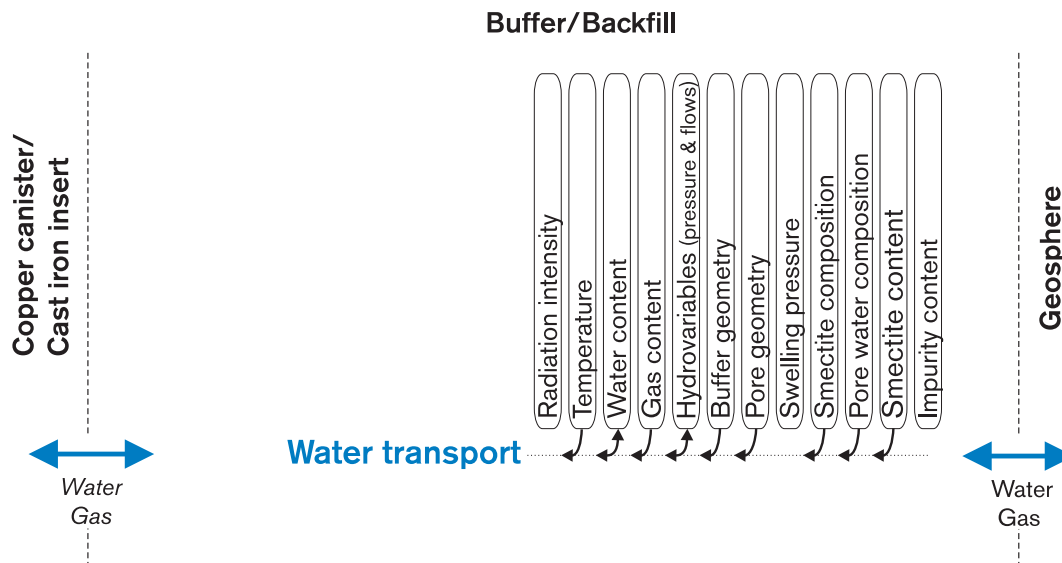


Figure 4-5. Water transport.

Overview

Water transport in the buffer under unsaturated conditions is a complex process that is dependent on, *inter alia*, temperature, smectite content and water content in the different parts of the buffer. The most important driving force for water saturation under deep repository conditions is a negative capillary pressure in the pores of the buffer that leads to water uptake from the surrounding rock. The supply of water in the rock is also a decisive factor for the temporal evolution of the process.

The detailed description of the process is complicated, but can be modelled with sufficient accuracy for the needs of the safety assessment. It is not important to know all the details of the saturation process for the safety assessment. However, it is important to show that full water saturation is reached in order to provide a reliable description of the long-term evolution following saturation.

General description

Following is a detailed description of the process. The degree of detail is appropriate to indicate a general understanding, but is not necessary for the needs of the safety assessment to, for example, model the main features of the hydraulic evolution of the buffer.

The following hydraulic sub-processes can be distinguished:

- Transport of water in liquid phase, which is controlled and driven by
 - A1) a pressure gradient in the water
 - A3) an osmotic gradient
 - A4) gravity (coupled to A1)
 - A5) a density gradient (coupled to A1)
- Transport of water in vapour form, where transport is controlled and driven by
 - B1) a pressure gradient in the water
 - B2) a temperature gradient
 - B3) an osmotic gradient
 - B4) gravity
 - B5) a density gradient
- Phase transitions between water and vapour by:
 - C1) evaporation
 - C2) condensation
- Thermal expansion of
 - D1) water
 - D2) air
- Compression of
 - E1) water
 - E2) air
- Transport in water of
 - F1) dissolved air

These processes are coupled, and are in some cases different sides of the same process. They can be described and modelled in different ways. An important variable is the pore water pressure u_w . It is normally described in relation to the pore gas pressure u_a as $u_w - u_a$. $u_w - u_a$ is always negative in an unsaturated soil and is called, with the opposite sign, the suction potential. The suction potential can be described from a geotechnical view-point as the sum of the matrix suction potential, which can be said in simplified terms to stem from capillary effects, and the osmosis suction potential, which is dependent on differences in ionic concentration.

Our understanding of the processes that drive water transport in unsaturated buffer and backfill materials and our knowledge of how the processes are influenced by different factors is not comprehensive. The following description pertains chiefly to the models that are used for non-swelling soil materials /Fredlund and Rahardjo, 1993/. It has not yet been fully clarified whether the approach is sufficiently all-inclusive to fully describe the processes in swelling clay minerals. However, our understanding is sufficiently good to carry out reliable model calculations in the safety assessment.

A1. Transport of water in liquid phase which is driven by a water pressure gradient can be described by a refined version of Darcy's law. The parameters that control the process are the material's hydraulic conductivity K and the difference between the pore water pressure and the pore gas pressure $u_w - u_a$. Both of these can be described as functions of the void ratio e , the degree of saturation S_r , the ion concentration in the pore water i_c and the temperature T . The pore water pressure for unsaturated clays is also a function of the wetting history, i.e. whether the material undergoes wetting or drying.

The driving force for the liquid-phase water flow is the pore water pressure gradient, which is caused by differences in matrix suction potential. The hydraulic conductivity varies strongly with the degree of saturation.

- A3. Transport of water in liquid phase which is driven by an ion concentration gradient, osmosis. Significant osmotic effects can arise at high salinities in the groundwater and in conjunction with salt enrichment in the buffer.
- A4. Transport of water in liquid phase which is driven by gravity. Gravimetrically generated flow is probably negligible in buffer material due to the low hydraulic conductivity. It can, however, influence the flow in the backfill, cf. process A1.
- A5. Transport of water in liquid phase which is driven by a density gradient in the water. Differences in the density of the water can be caused by e.g. differences in temperature or salinity. Density-generated flow is probably negligible in buffer material, cf. process A1.
- B1. Transport of water in vapour phase which is driven by a vapour pressure gradient. The vapour pressure u_v in the fraction of the pores that are air-filled or the relative humidity ($RH = u_v / u_{v0}$ where u_{v0} is the saturation pressure in the air) is in equilibrium with the suction potential in the liquid phase. If the RH is higher than the equilibrium relationship, water vapour condenses and increases the quantity of liquid, which in turn reduces the suction potential until equilibrium arises. If the suction potential differs in different parts of a soil, for example due to different water ratios, this leads to different vapour pressures, and transport of water vapour in the unfilled portion of the pores takes place with the vapour pressure difference as a driving force. In this way, water is transported in vapour phase from one place with a lower suction potential to another place with a higher negative pore pressure. However, this transport is parallel to process A1, which takes place in liquid phase. The relationship between these transport mechanisms has not been fully investigated.
- B2. Transport of water in vapour phase which is driven by a temperature gradient appears to be the most important process for vapour transport. This process can also be regarded as a part of process B1. A temperature difference brings about a vapour pressure difference which transports vapour from a warmer part to a colder part. It can also be modelled as a diffusion process driven by a temperature difference /Philip and de Vries, 1957/.

The vapour transport causes a water ratio difference and thereby a difference in suction potential, which in turn leads to a liquid-phase transport in the opposite direction. In a closed system, with constant water content, an equilibrium situation arises after a time where the vapour transport is equal to the liquid transport in all parts. A steady state arises with water ratio differences that reflect the temperature differences in the system.

- B3. Transport of water in vapour phase which is driven by an osmotic gradient.
- B4 and B5. Transport of water in vapour phase which is driven by gravity or a density gradient. These processes are presumably insignificant in the buffer's pore system, but may be of great importance in gaps, particularly in the vertical gap between canister and bentonite.

- C1 and C2. Phase transitions via evaporation and condensation are constantly occurring in a temperature gradient where evaporation in the warmer part is accompanied by condensation in the colder part. Aside from the fact that it can lead to heat transport, it is only significant as evaporation if the buffer is not isolated from the atmosphere. It can occur if a very dry deposition hole is allowed to stand open towards the tunnel for a very long time or if the backfill is dry.
- D1 and D2. Thermal expansion of water in liquid and vapour phase can indirectly affect the flow by changing either the water pressure or the density (convection). Other consequences are dealt with under mechanical processes.
- E1. Compression of water in liquid phase is of little importance for the liquid transport processes other than for a water-saturated system, where the size of the pressure build-up associated with a temperature increase is dependent on the compressibility of the water.
- E2. Compression of air can be an important factor in the water saturation process (Boyle's law). If the air is trapped, it must be compressed and go into solution in the water in order for water saturation to be achieved. In highly-compacted bentonite, the suction potential appears to be sufficiently high for this to occur and full water saturation is achieved without any external water pressure. Highly-compacted pure bentonite is thus able to achieve water saturation by itself. The backfill, however, has such low suction that a pressurized air volume will remain if the air cannot seep out. It disappears for the most part when full water pressure has developed.
- F1. Transport of dissolved air in water. When trapped air is compressed during the water saturation phase, a portion of the volume is dissolved in the water. This solubility (Henry's law) is approximately 2 percent at air temperature but decreases rapidly at increasing temperature. In order for additional air to be dissolved, the dissolved air must be transported away, which takes place by diffusion.

Influence of salinity on wetting rate: High salinity in the groundwater that is absorbed from the near-field rock limits the swelling of the bentonite grains and initially leaves relatively wide passages for penetration of water. An advantage is that saturation of the buffer can take place faster than if low-salinity water is absorbed.

The salinity of the groundwater influences the vapour pressure relation and thereby the water saturation process. For typical Swedish groundwater conditions, the effect in the buffer is small, but the influence of saline groundwater is of decisive importance for water uptake in the backfill.

Model studies/experimental studies

A preliminary material model containing unsaturated water flow has been devised /Börgesson and Johannesson, 1995/ and is being developed. The calculations are performed using the finite element method with the program ABAQUS. Certain general parts of the model are described in the manual /Hibbit et al/, while other parts are tailor-made for SKB /Börgesson and Johannesson, 1995/. The model includes the processes A1, A4, A5, B2, D1 and E1, which are the most important ones for the buffer. It does not, however, include the processes that handle air (except for B2), which can be important for the saturation process in the backfill.

The models have been both calibrated and partially verified by laboratory experiments. Models for unsaturated buffer are being evaluated within three international projects (DECOVALEX, CATSIUS CLAY and VALUCLAY). These projects include calculation examples and comparisons with measurement results for both laboratory experiments and field tests. See e.g. Börgesson and Hernelind /1995/; Alonso and Alcoverro /1997/; Börgesson and Hernelind /1997/.

The big field test BMT (Buffer Mass Test) was performed some years ago in Stripa, Sweden, to study the wetting process, among other things. In this test, highly-compacted bentonite and heaters were installed in six simulated deposition holes on a scale of 1:2. The tunnel above two of these holes was backfilled with sand-bentonite mixtures containing 10 and 20 percent bentonite. The tests were interrupted after a few years, whereupon buffer and backfill were excavated with detailed sampling and water ratio determination. The results showed that the wetting had gone to near water saturation in three of the holes, while the others had not increased their water content more than marginally. The water inflow in the three first-mentioned holes was greater than in the others. On the other hand, the gap towards the rock was left open in these three holes, while the gap in the three "dry" holes was filled with bentonite powder. There was no tendency towards uneven water uptake from the rock. The three wet holes with empty gaps had a high, uniform water ratio with a degree of saturation higher than about 80 percent. The three dry holes with powder-filled gaps were dry nearest the heater and wet nearest the rock, in a way that could be expected to result from the redistribution process that occurs in the presence of a temperature gradient.

Interaction with rock: A key issue for the saturation process is the interaction between rock and buffer. If water is only conducted to the buffer in the water-bearing fractures and the rest of the water has to go through the rock matrix, water saturation can be both uneven and take a long time. If there is a permeable excavation-disturbed zone (EDZ) that distributes water from the fractures along the rock wall, the wetting will be faster and more even.

The interaction between rock and buffer is influenced to a high degree by the permeability of the rock matrix. Studies of deposition hole walls in Finnish test holes suggest that there is an EDZ nearest the hole with a hydraulic conductivity that is one to two orders of magnitude greater than in the undisturbed rock matrix. If the distance between the water-bearing fractures is sufficiently small and the water pressure in the fractures sufficiently great, the water may be distributed along the hole wall at the rate at which the buffer is able to take up water. The water uptake will thereby be as even and fast as if free water were available in a filter against the rock wall. If, on the other hand, the distance between the water-bearing fractures is great and the water pressure is low, only areas around the fractures will be supplied with water. The water uptake will thereby be uneven and delayed. In the extreme case where there are no water-bearing fractures, all water must be transported through the rock matrix, and the uptake rate will then be so slow that the situation in the buffer is characterized by a redistribution of the existing water. The rock/buffer interaction needs to be verified by further tests and calculations.

When excavated, the backfill in BMT was highly water-saturated in the outer 1–1.5 m zone, while the inner portion was relatively unaffected. The uniform wetting indicates that the EDZ was sufficiently permeable to distribute the water evenly over the rock surface, but may also be due to the fact that the water has been able to flow in the backfill or in the backfill/rock interface.

Time perspective

The above analysis shows that the time to full water saturation of the buffer can vary a great deal, depending above all on the interaction with surrounding rock. If conditions are optimal so the rock distributes the water as needed by the buffer, saturation may be reached within 10–15 years. If there are no fractures so all water has to go via the rock matrix, it may take more than 100 years.

Summary of uncertainties

Understanding: Our understanding of the process is good enough for the needs of the safety assessment.

Data: The greatest uncertainty/variability concerns the hydraulic conditions in the near-field rock.

Handling in the safety assessment

Base scenario: Models are available to describe the saturation process in the buffer (see section on model studies). The boundary condition, i.e. the supply of water at the outer buffer boundary, is decisive for the wetting rate. Calculations are therefore carried out for several situations, for example:

- Free supply of water at the boundary
- Impervious rock – water is taken through the rock matrix
- Water uptake from deposition tunnel

Canister defect scenario: See base scenario.

Climate change: See base scenario.

Earthquake: See base scenario.

4.5.2 Water transport under saturated conditions

Overview

Water transport in saturated buffer is a complex interplay between a number of sub-processes on a microscopic scale. On a macroscopic level, the result is that the permeability of a saturated buffer is very low, and this is also the essential result for the safety assessment. The above also applies to the backfill, but permeability is higher here.

General description

Water flow in saturated buffer and backfill is a special case of unsaturated flow. The processes involved are the same as for unsaturated conditions, but can vary widely in importance compared with unsaturated conditions.

The most important mechanism under unsaturated conditions is transport of water in liquid phase, which is driven by a water pressure gradient. The process can be described by Darcy's law. Any deviations from Darcy's law, which can occur at low gradients, are favourable in that they lead to a reduced throughflow rate. The hydraulic conductivity K is a function of the composition of the buffer and the backfill, the void ratio e , the ion concentration in the pore water i_c and the temperature T .

Influence of density, temperature and salinity for the buffer: In the buffer, $K = 5 \cdot 10^{-14} - 5 \cdot 10^{-13}$ m/s at the densities in question. Transformations to other minerals with reduced montmorillonite content as a result generally leads to a higher hydraulic conductivity. Permissible limits for density deviations /Bäckblom, 1996/ give an approximate difference in hydraulic conductivity by a factor of 10. The temperature influences the conductivity by changing the viscosity of the water, whereby a temperature increase from 20°C to 90°C entails an approximate increase in conductivity by a factor of 3 at. An increase in salinity to 6.1 M NaCl (saturated solution) entails an approximate increase in conductivity by a factor of 10.

Influence of density and salinity for the backfill: The dependency on density and ion concentration is greater for the backfill, due to the fact that the bentonite density in the pore system of the aggregate is low. For backfill with 15 percent bentonite, $K = 10^{-10} - 10^{-9}$ m/s for fresh groundwater at the densities expected to be achieved after saturation. The influence of the ion concentration is great. An increase in salinity to 1.2 percent (Äspö conditions) leads to an increase in K by a factor of 10–100. To achieve the same hydraulic conductivity, the bentonite content must then be increased to 30 percent. Other factors of importance are the compaction and mixing methods used. These affect microstructural homogeneity via the density distribution of the bentonite phase in the aggregate pores, and macrostructural homogeneity via lower density in the roof due to compaction problems. In summary, the necessary hydraulic conductivity (at most that of the surrounding rock) is achieved by means of suitable technology and suitable material choice.

In summary, the following can be said about water flow in saturated buffer and backfill:

Buffer: The permeability of the buffer to low-salinity water after complete saturation is approximately 10^{-13} m/s. The condition that must be met for transport by flow to be more important than diffusive transport is given by: $D_e / \Delta L < Ki$, where D_e = the effective diffusivity, ΔL = the transport length (one-dimensional), K = the hydraulic conductivity and i = the hydraulic gradient. For the stage after restoration of the hydraulic situation in the repository, i can be set equal to 10^{-2} and, for anions $D_e = 10^{-12}$ m²/s, which for the buffer thickness $\Delta L = 0.35$ m requires that K exceed $3 \cdot 10^{-10}$. This is at least two orders of magnitude higher than the real conductivity of the buffer. The margin for cations is considerably greater. The conclusion is thus that the only important transport mechanism for both water and dissolved species through the buffer is diffusion. Diffusive transport is dealt with in section 4.7.3.

Backfill: The permeability of the backfill to water after saturation is determined by the montmorillonite content, the pore water chemistry and the density. Unlike the buffer, the backfill cannot become highly homogeneous, in part because the mixing procedure does not give a uniform distribution of the bentonite and crushed rock, and in part because deposition and compaction cannot be done as efficiently over the entire cross-section and length of the backfill /Gunnarsson et al, 1996; Pusch, 1985b/.

Model studies/experimental studies

Flow in water-saturated buffer and backfill has only been studied on a laboratory scale in the form of permeability tests and swelling/compression tests in oedometers /Börgesson, et al, 1995; Johannesson et al, 1998/.

Time perspective

The hydraulic gradient that exists after water saturation and pore pressure equilibrium have been reached around a repository is expected to be low. A simple estimate can be made of the time required for all the water in the buffer to be exchanged. If the gradient is set equal to 0.01, the hydraulic conductivity $K = 10^{-13}$ m/s and the cross-sectional area to 10 m^2 , according to Darcy's law it takes 15 million years for the approximately 5 m^3 of water present in the buffer to be exchanged.

Summary of uncertainties

An uncertainty exists as to whether Darcy's law applies at the low gradients that are expected to arise, since all laboratory tests are done at very high gradients. All measured deviations show, however, that the flow is lower than is expected by Darcy's law.

Another uncertainty is the effect of transformations, which are expected to give higher hydraulic conductivity. The effects of very high salinities are also inadequately understood.

A number of uncertainties exist for bentonite-containing backfill. The properties of the backfill are measured directly after mixing. The risk and effect of possible homogenization of the bentonite density in the aggregate pores is not known. The measured hydraulic conductivities assume that there are no channels or gaps.

Handling in the safety assessment

Base scenario: The base scenario should show that the processes that can influence the diffusivity and conductivity of the bentonite always remain within the limits where diffusion will dominate over advection in the saturated buffer.

Canister defect scenario: It is assumed in the canister defect scenario that no advection occurs in the saturated buffer. In the backfill, however, it is possible that transport by means of advection and diffusion may be of similar magnitudes and the effect will be investigated.

Climate change: See base scenario.

Earthquake: See base scenario.

4.5.3 Gas transport/dissolution

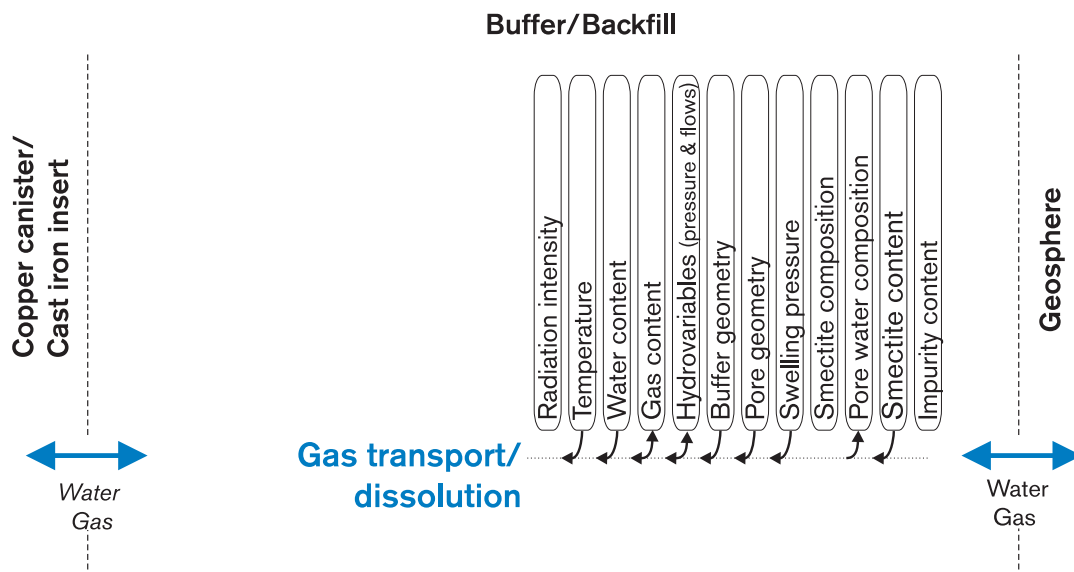


Figure 4-6. Gas transport/dissolution.

Overview

Transport of gas in the buffer can occur in two phases of the repository's evolution:

- When the repository is sealed, air will be trapped in the buffer. When the buffer becomes saturated with water, the air must escape.
- If a canister should have a through-wall defect and water should penetrate through the copper shell, the cast iron insert is expected to corrode and release hydrogen. If more hydrogen is produced than can be dissolved in the water in the canister, a gas phase will form.

Gas which is trapped in or by the buffer and backfill can escape in two ways:

- If the production rate is low or the gas quantity is small, the gas can be dissolved in the pore water and be removed by diffusion.
- If the production rate is high or the gas quantity is large, a gas phase will form, the pressure will rise, and a flow path will be formed through the buffer at a critical pressure.

General description

Water saturation phase: Gas flux in conjunction with wetting of the buffer and backfill is described in section 4.5.1. Under these conditions, all gas is expected to be dissolved in the buffer's pore water and transported by diffusion.

Gas transport from broken canister before saturation: Before the buffer is saturated, water is only expected to be able to get into the canister via vapour-phase diffusion. Hydrogen production from corrosion will therefore be limited and the gas that is formed is expected to be able to leave the buffer. The gas transport resistance in an unsaturated buffer is also considerably lower than in a saturated one.

Gas from broken canister after saturation:

Diffusion: Hydrogen gas formed by corrosion of the cast iron insert can dissolve in the pore water and migrate from the canister by diffusion. The maximum transport capacity has been calculated by Wikramaratna et al /1993/.

The results of the calculations show that the diffusive transport capacity is considerably lower than the hydrogen gas production from corrosion, if it is assumed that the entire surface of the cast iron insert is accessible for corrosion and the water supply does not limit corrosion, see also section 3.7.1. Under such conditions it is probable that a gas phase will be formed inside the canister and that the gas must escape by gas-phase flow.

Gas flow: Figure 4-7 shows gas pressure build-up in and gas flow through a saturated buffer. In an initial phase after canister breakthrough, water is expected to enter the canister, resulting in corrosion and hydrogen gas generation. The gas pressure in the canister will thereby rise.

The following picture of the subsequent course of events is an interpretation of the results of theoretical and experimental studies: At a critical pressure (opening pressure), the buffer is expected to allow the gas to pass through. A large number of experiments have shown that bentonite /Pusch et al, 1985b; Horseman and Harrington, 1997; Tanai et al, 1997/ does not allow gas to pass until the pressure exceeds the sum of the swelling pressure and the water pressure. When the pressure reaches this value, a transport pathway is formed through the buffer and gas is released. The pressure falls, and if the gas production is low enough, the transport pathway is expected to close. This takes place at a so-called “shut-in pressure”, which is dependent on the swelling pressure. At pressures lower than the shut-in pressure, gas migrates solely by diffusion, see Figure 4-7. The laboratory experiments have shown that the shut-in pressure is also dependent on the swelling and water pressures, but is much less than the sum of these – for a total swelling and water pressure of 12 MPa, the shut-in pressure is 9 MPa. Due to this difference, the gas is expected to migrate out with a continuous flow until the pressure inside the canister falls to the shut-in pressure. When the gas flows out of the canister, it will be very difficult for water to come in. Corrosion and gas production therefore decline so that the pressure eventually reaches the shut-in pressure. The pressure inside the canister is then expected to increase again, and after some time the transport pathway opens again.

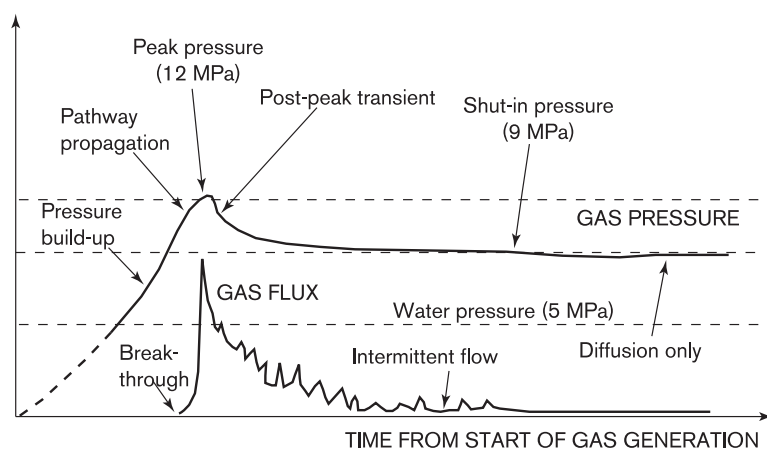


Figure 4-7. Temporal course of gas transport through bentonite /SKB, FUD-Programmet 98, 1998/.

If the gas that is left trapped in the buffer after the first gas transport has dissolved in the pore water and been carried away, the opening pressure in the second gas cycle is expected to be identical to that in the first. If, on the other hand, gas remains in the buffer, the second opening is expected to occur at a lower pressure. It has not been fully clarified what the transport pathway will look like, but it is probable that the gas forms a system of small flow channels /Nash et al, 1998/. The buffer will therefore not be dried out, and it is quite clear that the quantity of water which the gas can displace from the buffer is very small. When the gas has reached the excavation-disturbed zone (EDZ) in the near-field rock, the pressure required to get it to migrate further is much lower than in the buffer. It must exceed the sum of the water pressure and the capillary tensions in the fine fractures in the EDZ or in channels in fractures that intersect the deposition holes, which together gives a pressure of 5–10 MPa.

The energy that drives the gas transport comes from compression of the gas inside the canister and is proportional to the available gas volume. If it is assumed that the volume is half a cubic metre and the gas pressure drops from 12 to 9 MPa, 15 MJ will be released when the transport pathway is formed. In a system with confined clay (deposition holes), the gas will presumably be released in a controlled fashion, i.e. it will not entrain the buffer material along with it, but experiments under open conditions, i.e. without surrounding counter-pressure, show that gas breakthrough can be a violent process /Donohew et al, 1998/.

Available experimental results show that gas can migrate through a highly-compacted buffer without jeopardizing the continued function of the engineered barriers. However, no experiment has been conducted with a gas volume equivalent to the volume in the canister cavity (approx. 1 m³), and it is therefore not completely clear what the effect the release of large quantities of gas will have on the performance of the repository.

Model studies/experimental studies

Gas dissolution: No specific studies have been conducted for the purpose of studying how gas dissolves in the pore water in the bentonite. However, experience from water saturation tests shows that highly-compacted bentonite is normally completely water-saturated and that no trapped gas remains. The mechanical interpretation is that the swelling pressure of the bentonite compresses trapped gas, which is dissolved in the pore water and transported out by diffusion.

Gas transport: The gas transport process has been studied in controlled flow experiments in Boomclay and MX-80 bentonite /Harrington and Horseman, 1997/. The gas pressure as a function of time from these experiments is very similar to those from the response of hydraulically induced fractures in the clay /Murdoch 1993/. Details in the results suggest channelling and propagation, which indicates that the gas moves in a network of microchannels created by tensile fractures in the clay under the high gas pressure. If channels were not formed, the clay would probably be impermeable to gas /Harrington and Horseman 1997/. When the gas injections were stopped in the tests, the pressure fell spontaneously and after a while assumed a minimum value, the shut-in pressure. This pressure is dependent on the swelling pressure of the clay and was around 4 MPa above the water pressure for MX-80 with a dry density of 1.55 t/m³. Shut-in pressure can be interpreted as the lowest gas pressure capable of sustaining a continuous gas network through the bentonite.

On repeated gas injection cycles in laboratory tests, the breakthrough pressure decreases compared with the first breakthrough, which shows that the transport pathways do not disappear entirely during experimental timescales. Gas-filled cavities remain in the transport pathways. However, an experiment with Boomlera has shown that the original breakthrough pressure can be reinstated by flushing the pores in the clay with water /Harrington and Horseman, 1997a/, suggesting that the transport pathways close when the gas in the cavities disappears. Under repository conditions, dissolution and diffusion will be the dominant transport mechanisms for the residual gas in the cavities.

Time perspective

Gas transport can occur when water is in contact with the cast iron insert in a damaged canister.

Natural analogues

Tissot and Pelet /1971/ write about oil and gas movements in clay shale: “The extraction of oil or gas from a finely structured clay matrix runs contrary to the capillary laws and is in principle impossible. However, the barrier can be broken in one way. The pressure in the fluids that is formed in the pores in the clay increases when kerogen is formed. When this pressure exceeds the mechanical strength of the clay, microchannels will form which are orders of magnitude larger than the natural pores and will thereby allow an oil or gas phase to pass, until the pressure falls below a threshold value and the channels fill again and a new cycle begins.” These observations recall the conclusions from the gas transport experiments in bentonite.

Summary of uncertainties

Gas dissolution: The effect of reduced gas solubility in the buffer’s pore water as a consequence of raised temperature is calculable, but experimental studies have not been carried out. At atmospheric pressure the solubility of the gas is very low at the peak temperature of the bentonite. For the backfill, the groundwater pressure plays a crucial role for the solubility of trapped gas, since only small swelling pressures develop. The water saturation process in the backfill material is thus coupled to the restoration of the hydrostatic pressure and is thereby difficult to predict with our present state of knowledge.

Gas transport: A remaining uncertainty in our understanding of gas transport in the buffer material concerns the number, size and spatial arrangement of the gas-bearing fractures and the volume behaviour of the clay during gas injection. The experiments that have been performed to date indicate that the clay must expand (grow in volume) during gas transport and that changes in gas content must be balanced by an increased total volume /Harrington and Horseman, 1999/.

This is interpreted as meaning that the gas forms a fracture network through the clay and traditional two-phase flow models for porous media, where gas displaces the pore water, are not applicable. Since the clay expands when the gas forms a network, the boundary conditions in the experiments are very important. It is not certain that the behaviour will be the same in an experiment where the bentonite specimen is subjected to a constant external pressure (corresponding to the hydrostatic pressure plus the swelling pressure in the repository) as in an experiment where the specimen is confined in a constant volume (corresponding to the walls of the deposition hole). Preliminary results from experiments conducted during the production of this report have confirmed that the breakthrough pressure is higher for a specimen with constant volume than for one under constant external pressure. This is consistent with the model of the build-up of a fracture network. These experimental observations cannot be directly extrapolated to a real repository. For while the deposition hole does have a constant volume, the quantity of buffer in the hole is such that a compression of the buffer could go more easily than in a laboratory experiment on a 5 centimetre scale, since the cross-sectional area of the gas channel does not have to be bigger in a real case than in the experiment.

Another uncertainty is the shut-in pressure. There is no model today for how the shut-in pressure is dependent on the swelling pressure; all knowledge of the shut-in pressure is based on a few experimental observations. Extrapolation of experimental observations to a full-scale repository has not been tested, since no full-scale experiments have ever been performed.

Handling in the safety assessment

Base scenario: See “Water transport under unsaturated conditions”. The gas quantity in a deposition hole is approximately 6 volume-percent at atmospheric pressure. When the hydrostatic pressure has been built up, the gas volume will have declined by a factor of 50. This small quantity will rapidly dissolve in the pore water and can be neglected in the water saturation calculations.

Canister defect scenario: Account of model and experimental studies of gas build-up and transport in conjunction with the modelling of the corrosion of the cast iron insert and water transport in the canister.

Climate change: If the evolution leads to canister damage: See the canister defect scenario. Otherwise: See the base scenario.

Earthquake: If the evolution leads to canister damage: See the canister defect scenario. Otherwise: See the base scenario.

4.6 Mechanical processes

4.6.1 Swelling

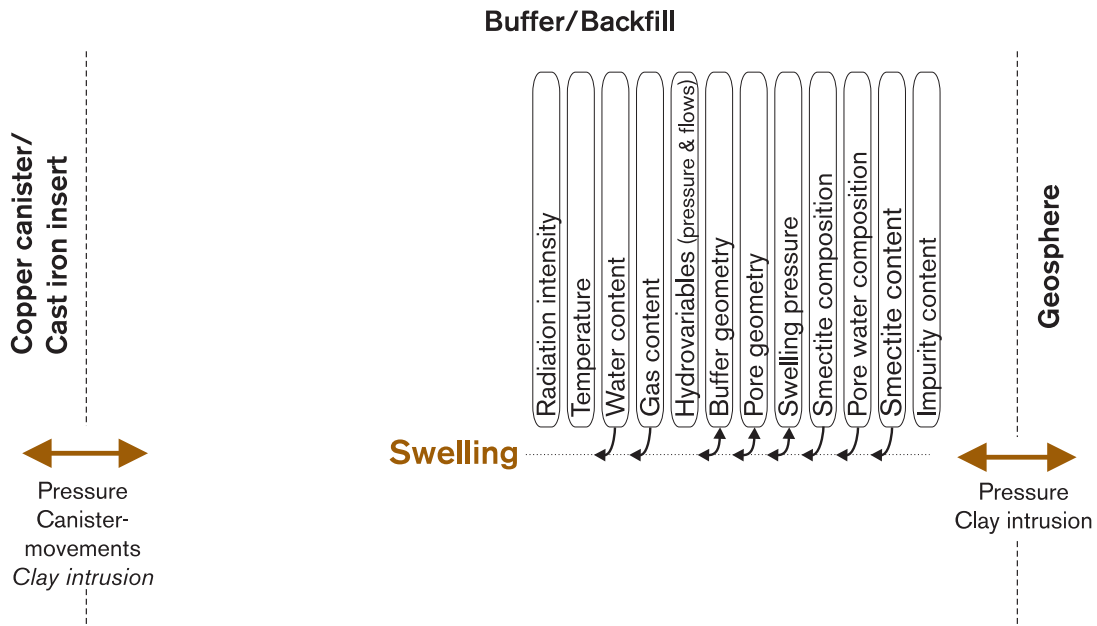


Figure 4-8. Swelling.

Overview

Water is absorbed by unsaturated bentonite and causes swelling. If the bentonite is unable to expand freely, a swelling pressure develops which reaches its peak at full water saturation.

The swelling leads to compression of the backfill above the deposition holes, a mechanical pressure on the canister and the edges of the deposition hole, and clay intrusion in fractures around the deposition hole. Depending on the conditions in the near-field rock, the clay in the fractures could be carried away by the groundwater, allowing new clay to penetrate, which could lead to gradual erosion of the buffer, see section 4.7.7. Aside from these mechanical effects, the buffer's hydraulic conductivity and diffusion properties are altered by the swelling.

General description

The buffer has the form of a cylindrical stack of blocks of highly-compacted bentonite powder surrounded by an annual gap filled with bentonite pellets. In the wetting phase, interlamellar hydrate layers are built up by inflowing water. The stacks of montmorillonite layers swell, and resistance to swelling due to limitation of the swelling volume is manifested by the evolution of a swelling pressure.

The following description illustrates the principles for modelling of swelling from a geotechnical perspective and does not concern the underlying mechanisms.

The swelling can be conceived of as being caused by a force of repulsion between the montmorillonite layers. If there is a limited supply of water in a free specimen, the swelling is counteracted by a negative pressure in the pore water. If a specimen is water-saturated, i.e. all pores are filled with water, the swelling is counteracted by the formation of a negative pressure in the pore water in the water menisci on the surface of the specimen. The negative pore pressure is equal to the internal swelling pressure if no external pressure is applied. If the specimen is unsaturated, the water menisci develop inside the specimen as well. The negative pressure in the pore water is chiefly a function of the water ratio in the specimen, i.e. the quantity of water per unit weight of dry material. This negative pressure is called suction potential. When water is added to a free specimen, the water ratio increases, and the repulsion forces and the suction potential decrease, which causes the specimen to swell until a new equilibrium is established with a lower internal swelling pressure. If the volume is kept constant, a portion of the internal swelling pressure is instead transferred to an external swelling pressure, which can be measured. When a specimen with constant volume is completely water-saturated and the pore water pressure is kept positive, the entire swelling pressure becomes an external pressure. At water saturation, the swelling pressure and the pore water pressure are independent quantities and give a total pressure that is the sum of the pressures. In principle, this applies even before full water saturation is reached, but since not all pores are filled with water, the forces do not act on the whole specimen and the pressures are not simply addable.

The swelling pressure's dependence on the variables listed below can be explained by a change in the resulting repulsion forces between the montmorillonite layers.

The variables that influence swelling or shrinking and the generated swelling pressure in the bentonite are:

1. density,
2. montmorillonite content,
3. adsorbed cation species (montmorillonite composition),
4. degree of cementation,
5. pore water composition,
6. degree of saturation.

The influence of these factors on the swelling capacity is dealt with briefly in this chapter. Factors 2–5 are further dealt with under section 4.7, “Chemical processes”.

Influence of density: The density at water saturation is decisive for the water ratio and thereby for the number of interlamellar water molecule layers, which in turn determines the swelling potential and the swelling pressure. Figure 4-9 illustrates the difference in swelling pressure at different densities.

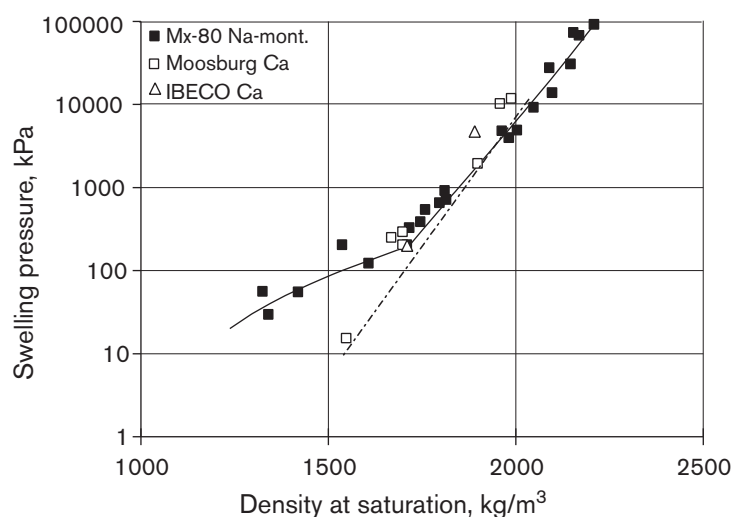


Figure 4-9. Dependence of swelling pressure on density and adsorbed ion species (revised based on Børgesson et al /1995/).

Influence of montmorillonite content and type of smectite plus species of adsorbed cation: According to Figure 4-9, the swelling pressure is relatively independent of the adsorbed ion species if the density exceeds approx. 1,800 kg/m³ in the saturated state and the montmorillonite content is the same. At lower densities the swelling pressure is lower if the adsorbed ion species is Ca or some other polyvalent cation (e.g. Cu and Fe). Table 4-2 gives a picture of the dependency of the swelling pressure on smectite content and smectite type. Data is given for a number of commercial bentonites with different smectite contents and for mixtures of Na-bentonite and sand aggregate. These values can be considered to represent expected effects of transformations of sodium bentonite. A reduced smectite content can be conceived of as being equivalent to the addition of an inactive aggregate. A transformation of Na-bentonite to Ca-bentonite, which takes place by ion exchange, is expected to give a swelling pressure equivalent to those given for Ca-bentonite. Distilled water was used for saturation of the investigated clay materials.

Table 4-2 Examples of swelling pressure in MPa as a function of smectite content and density /Pusch, 1995a/.

| Bentonite | Smectite content (percent) | Density at saturation, kg/m ³ | |
|------------------|----------------------------|--|------|
| | | 1800 | 2000 |
| MX-80 | 75 | 1.2 | 8.7 |
| IBECO Na | 70 | 0.6 | 7.3 |
| IBECO Ca | 80 | 0.2 | 4.7 |
| Kunigel | 40 | 0.2 | 1.0 |
| Beidellite | 35 | 1.5 | 4.2 |
| Saponite | 70 | 2.5 | 8.8 |
| 30/70 MX-80/sand | 20 | 0 | 0.5 |
| 50/50 MX-80/sand | 40 | 0.2 | 2.0 |

Influence of degree of cementation: Natural bentonites, which have undergone cementation by precipitation of silicon and aluminium compounds in conjunction with heating, exhibit low swelling pressures and poor swellability despite a considerable content of montmorillonite/beidellite /Müller-Vonmoos et al, 1990; Pusch, 1983b/.

Influence of chemical composition of pore water: If the pore water in the bentonite contains salt, which can be the consequence of either water saturation of the bentonite with saline groundwater or diffusion of salt into the pore water after water saturation, swelling pressure and swelling capacity are affected /Kornland, 1997a/. Swelling pressure decreases with increasing salinity. The decrease is relatively greatest at low densities.

Influence of degree of saturation: In an unsaturated state, the bentonite/water system shrinks on drying and expands on wetting. The volume change on water uptake in e.g. a block is less in the unsaturated state, since the swelling takes place partially in previously unfilled pores. Shrinking due to drying is expected to take place near the canister, which can lead to cracking of the buffer.

Importance of swelling/shrinking for the general performance of the buffer:

Swelling or shrinking of the buffer alters its density, which is of importance for its performance in terms of water, ion, colloid and gas transport, as well as mechanical effects:

1. Influence on hydraulic conductivity. A decrease in density due to swelling in deposition holes increases hydraulic conductivity. The effect can be assumed to be small under normal conditions, however.
2. Influence on diffusive ion transport. See 1.
3. Influence on the swelling pressure exerted on the canister, backfill and near-field rock. The swelling pressure decreases when the density decreases, which could lead to uneven swelling pressure on the canister. The effect can be assumed to be small under normal conditions, however.
4. Influence on its capacity to bear the canister. Bearing capacity declines with declining density. The effect can be assumed to be small under normal conditions, however.

Model studies/experimental studies

Saturated bentonite: Bentonite's swelling capacity and swelling pressure under water-saturated conditions has been studied in detail by means of laboratory experiments /Börgesson et al, 1995/. The results have been used to devise a material model that can be used for FEM calculations. It is based on the effective stress theory and coincides by and large with models for other soils, although the magnitude of the swelling and pressure are considerably greater for bentonite. Experiments are currently being conducted with volume creep to model the changes in volume and swelling pressure that can occur over a long period of time.

The material models have been used to calculate different evolutions that are associated with volume changes in a repository. Examples of modellings are the following:

- Swelling of buffer against the backfill in deposition holes /Pusch and Börgesson, 1992/.
- Settlement experiment in Stripa /Börgesson, 1993a/. Comparisons of calculated and measured movements and densities when canisters are loaded in deposition holes.

- Modelling of canister movements for design with two canisters in a deposition hole /Börgesson, 1993b/.

Unsaturated bentonite: A few experiments have been conducted to study the volume change as a function of degree of saturation and pore ratio. These experiments have been used to calibrate the material model for unsaturated clay. Additional experiments need to be done to improve our understanding and the model.

Time perspective

The water saturation phase is expected to take between 10 and 100 years, depending on the properties of the rock. During this timespan, the portion of the expansion that is limited by the consolidation rate (which is controlled by the hydraulic conductivity) will probably also take place. Volume creep can proceed for thousands of years, but is not judged to be of a such a magnitude that it appreciably influences buffer performance.

Summary of uncertainties

In a water-saturated state, the swelling process is deemed to be sufficiently well-known that density changes in the buffer can be calculated with sufficient accuracy. The greatest uncertainty arises in calculating the size of the swelling pressure after swelling, where the possible deviation is judged to be ± 30 percent, depending on the scatter in swelling pressure measurements and the uncertainty in certain material parameters. Some validation has been done by means of laboratory /Pusch and Adey, 1986/ and field tests /Börgesson, 1993a/, and continued validation is taking place via the field tests in the Äspö HRL.

In the long term, swelling properties can change due to transformations and cementation (see section 4.7.5, “Montmorillonite transformation”). The mechanical consequences of transformations can be assumed to lead to properties that are equivalent to the properties of corresponding “natural minerals”. Our knowledge of the properties of these minerals and what causes the differences is limited.

Cementation effects cause significant changes in the physical properties of the buffer, since they can produce a material that is brittle and without swelling capacity and thus can crack and open channels and gaps in the buffer. They have not yet been thoroughly studied.

The mechanical function of water-unsaturated bentonite is complicated to model, and the models that exist today are incomplete, especially for modelling of volume change and swelling pressure.

Handling in the safety assessment

Base scenario: Handled together with water saturation. Long-term changes also need to be dealt with.

Canister defect scenario: See base scenario.

Climate change: Influence of altered ionic strength in the water.

Earthquake: The importance of the swelling pressure for the buffer’s ability to cushion mechanical stresses on the canister arising from rock movements is dealt with in this scenario.

4.6.2 Mechanical interaction buffer/backfill

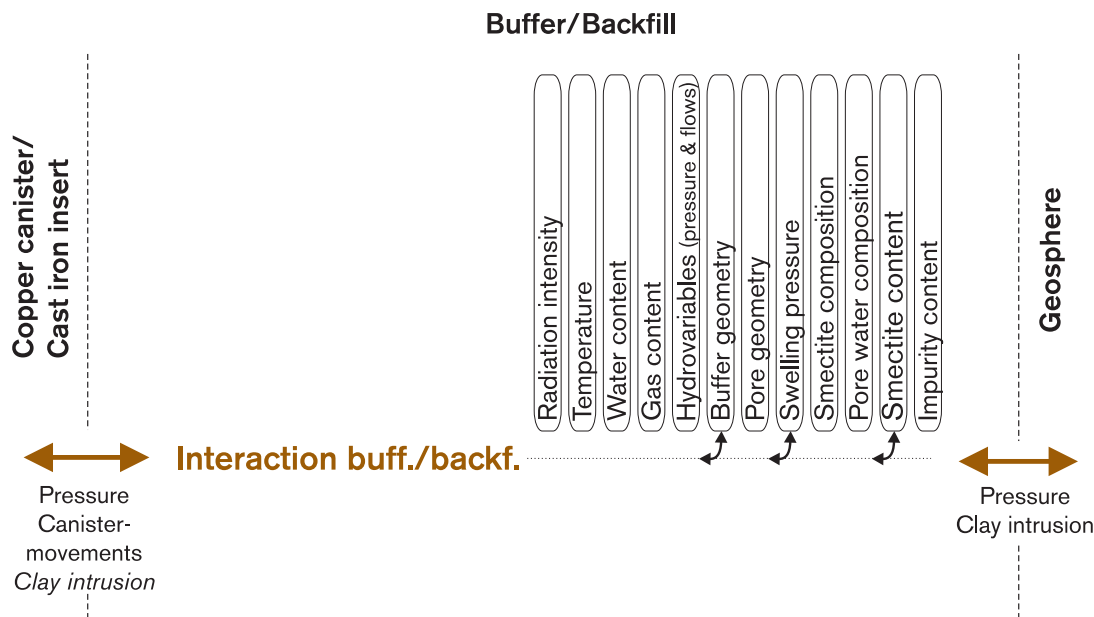


Figure 4-10. Mechanical interaction buffer/backfill.

Overview and general description

In the interface between the buffer and the backfill, the buffer exerts a swelling pressure against the backfill and *vice versa*. Since the difference in swelling pressure is great, a net pressure arises against the backfill whereby the buffer swells and the backfill is compressed. In this process, the swelling pressure from the buffer decreases as the density decreases. At the same time, the counter-pressure from the backfill increases as it is compressed and its density increases. The swelling of the buffer and compression of the backfill are counteracted to some extent by friction against the rock. When the force of the swelling pressure in the buffer is equal to the sum of the force of the counter-pressure in the backfill and the friction against the rock, the process ceases since equilibrium has been established.

The size of the swelling depends on the original densities of the buffer and the backfill and associated expansion and compression properties.

Due to the friction against the rock and friction in the buffer, the homogenization of the buffer is not complete. The density reduction due to the swelling therefore decreases with increasing distance from the interface. At the normal expected density in the backfill, the density reduction probably does not reach down to the canister, which lies 1.5 m below the interface.

Figure 4-11 illustrates the result of a simplified equilibrium calculation of the upward swelling of the buffer in the deposition holes in conjunction with compression of the backfill in the deposition tunnels /Pusch et, al 1985a/.

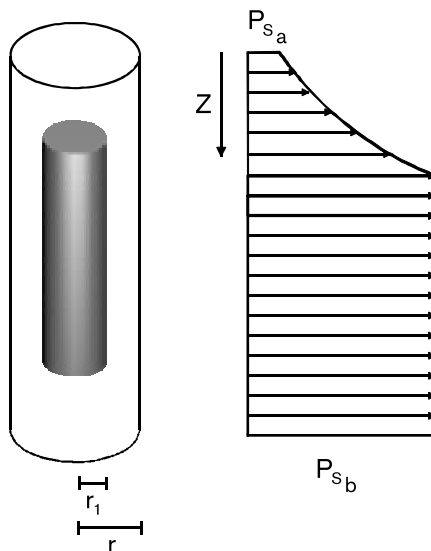


Figure 4-11. Schematic illustration of the reduced swelling pressure in the uppermost portion of the buffer as a consequence of the upward expansion.

Model studies/experimental studies

Several model studies have been carried out with FEM calculations using ABAQUS:

A calculation of an extreme case was performed for PASS /Pusch and Börgesson, 1992/ where the buffer was assumed to have a density of 2.1 t/m^3 after water saturation and the density of the backfill was assumed to be 1.9 t/m^3 after water saturation, which corresponds to higher density in the buffer and lower in the backfill than is stipulated in the reference case /Bäckbom, 1996/. This gave an upward displacement of about 30 cm.

In conjunction with studies of the function of deposition holes with two canisters, a calculation was made of the movements of the canisters which included upswelling towards the backfill /Börgesson, 1993b/. In this calculation the backfill was assumed to be considerably stiffer, with a density after water saturation of 2.2 t/m^3 . The calculated upswelling was about 7 cm.

Experience is available from field tests in Stripa. In BMT (Buffer Mass Test). 6 deposition holes were simulated on half scale. The movement of the interface was measured with a coin that was placed in the interface and levelled before and after the tests. The measured outswelling varied between 4 and 7 cm, depending on test time and degree of saturation in the buffer.

Time perspective

The time to equilibrium is controlled by the wetting rate, the permeability of the buffer and the size of the swelling. It takes an estimated 10 to 100 years if creep effects are neglected.

Summary of uncertainties

Understanding: The mechanisms for this interaction are well-known and partially confirmed in BMT.

Data: The uncertainty consists in the choice of parameter values, which is in turn dependent on the density reached in the backfill.

Handling in the safety assessment

Base scenario: The process is modelled in the base scenario as a part of the hydraulic/mechanical evolution in the buffer/backfill.

Canister defect scenario: See base scenario.

Climate change: See base scenario.

Earthquake: See base scenario.

4.6.3 Mechanical interaction buffer/canister

Overview

Mechanical interaction buffer/canister arises from the buffer through the clay matrix, which generates both compressive stresses and shear stresses, through the pore water, which generates only compressive stresses, and through gas in the buffer, which also generates only compressive stresses. Changes in these three factors take place during the water saturation process and can also occur in response to external forces. The weight of the canister influences the buffer, while the influence of the weight of the buffer on the canister is negligible.

General description

The mechanical interaction between buffer and canister is of the following nature:

- Swelling pressure and water pressure are exerted on the canister.
- Thermally induced pore water pressure is exerted on the canister.
- Trapped gas in the buffer exerts pressure on the canister.
- Canister corrosion products exert pressure on the canister.
- Vertical movement of canister in buffer.
- Transfer of shear stresses from rock via buffer to canister, especially during an earthquake.
- Intrusion of buffer in a damaged canister.

Swelling pressure and water pressure are exerted on the canister

Swelling pressure develops as the buffer undergoes wetting. If the wetting is even, the swelling pressure increases equally on the canister's periphery, except on the end surfaces where wetting of the buffer takes the longest time because the buffer is thicker there. If the wetting is uneven, the build-up of swelling pressure on the canister will be uneven. In the event of unfortunate combinations of wetting areas, the canister may be subjected to substantial stresses, similar to those exerted on a beam which is freely supported or rigidly fixed.

Water pressure on the canister does not arise until the bentonite is water-saturated. Theoretically, this pressure can also be uneven if certain parts of the buffer are saturated up to the canister and certain parts are not.

After full water saturation and full water pressure, the total swelling and water pressure will be the sum of these pressures.

Thermally induced pore water pressure is exerted on the canister

If the buffer is water-saturated before the maximum temperature has been reached, the temperature increase will cause the water to tend to expand, but because of the confined volume it cannot expand. Instead a pressure increase occurs which can theoretically be very great. However, such a pore pressure increase causes the water to drain out through the rock at the same time, compensating for the pressure increase. Preliminary calculations show that no big pressure ever has time to build up /Pusch and Börgesson 1992/.

Trapped gas in the buffer exerts pressure on the canister

Gas generated or shut in at the canister surface exerts a pressure on the canister. This gas pressure is, however, limited to the bentonite's opening pressure (see section 4.5.3). The gas is released through the bentonite either through a temporary channel that forms, or by dissolving in the water and diffusing out.

Canister corrosion products exert pressure on the buffer

External corrosion of the copper canister, which can be both local and global, increases the volume, since the corrosion products have a lower density. The increase in the volume of the canister causes consolidation of the buffer and an increase in the pressure between buffer and canister. In the event of a defect in the copper shell, a similar effect may occur in the cast iron.

Vertical movement of canister in buffer

The fact that the canister has a higher density than the buffer means in principle that it will sink in the same way as a house foundation settles, i.e. by consolidation and creep. The movements of the canister are complex in practice, since the upward swelling of the buffer in the holes dominates at first, causing heave of the canister due to a decrease in the density and swelling pressure above the canister. The settlement, or subsidence, occurs after the buffer becomes water-saturated and expands and consists mainly of very slow creep.

Transfer of shear stresses from rock via buffer to canister

Rock movements in the form of shear along a fracture plane affect the canister via the buffer. The buffer thereby acts to cushion the sharp and hard rock wedge. Since the movement does not change the total volume of the buffer, the effect is essentially a shear deformation, whereby the shear strength of the buffer regulates the impact. The shear strength is fairly low, since the friction angle at the density of the buffer is only about 10 degrees /Börgesson, 1986/. The shear strength increases rapidly with increasing density, however, and doubles at a density increase of about 5 percent.

Intrusion of buffer in a damaged canister

Bentonit can intrude into a defect in the canister. The influence on the buffer is, however, negligible compared with intrusion into fractures in the rock (se section 4.7.7).

Model studies/experimental studies

Swelling pressure and water pressure are exerted on the canister

Swelling pressure exerted by the buffer on the canister has been measured in BMT in Stripa /Pusch et al, 1985/ and on a laboratory scale in canister shear tests /Börgesson, 1986/. The evolution of swelling pressure in the six deposition holes in BMT differed markedly between the three “wet” holes and the three “dry” holes, due to the fact that the wetting was completely different. The measured swelling pressures were similar within the same holes, however. In the canister shear test, the swelling pressure increased evenly because water was supplied evenly via a filter which simulated the entire surrounding rock surface.

Thermally induced pore water pressure is exerted on the canister

See section 4.6.6.

Canister corrosion products exert pressure on the buffer

Preliminary modelling /Band et al, 1997/ showed that the influence was not significant. The buffer was not modelled in detail in this calculation, however.

Vertical movement of canister in buffer

A field trial was conducted in Stripa /Börgesson, 1989; Börgesson, 1993a/. A 100 cm long canister with a diameter of 20 cm with surrounding bentonite blocks was installed in a 3 m deep borehole with a diameter of 40 cm. The canister's movement was measured over 5 years via a pipe attached to the top of the canister. An incrementally increasing load was applied to this pipe that ultimately amounted to 12 tonnes. The resulting movement was a heave of the canister despite the high load. Numerical simulation of this test with ABAQUS showed that the heave is caused by swelling and decreased density in the overlying bentonite.

The movements of the canister have been calculated for the concept with 2 canisters in a deposition hole /Börgesson, 1993b/. This calculation shows that the resulting movement will be a heave that occurs early, and that the subsequent subsidence due to creep movements is small. A preliminary estimate for the buffer density in the KBS-3 concept is that the subsidence will be negligible or possibly negative, i.e. take the form of an insignificant heave. A calculation based on creep data derived from model experiments in the laboratory arrives at a final settlement of less than 10 mm in 10^6 years for the KBS-3 canister /Pusch and Adey, 1986/.

Transfer of shear stresses from rock via buffer to canister

Thorough studies have been made of the effects of rock shear on canister and buffer. In model tests on a scale of 1:10, rock shear movements equivalent to approximately 20 cm shear in a deposition hole have been simulated /Börgesson, 1986/. Numerical modelling of the process has also been done /Börgesson, 1992/.

The conclusions of these studies are that this mechanical process is understood and can be modelled. The studies also show that the effect on the canister depends on the rate of the shear movement and the density of the buffer. The copper shell plasticizes and bends at a shear of 10 cm and expected shear rates if the density after water saturation is higher than about 2 t/m^3 . At lower densities the canister tips without plasticizing.

Time perspective

The influence on the canister of uneven swelling pressures during the water saturation phase occurs within about 100 years, after which the swelling and water pressures are not expected to change in the base scenario. Possible heave of the canister due to upward swelling of the buffer takes place during the water saturation and homogenization phase, i.e. within about 100 years after deposition. The downward creep caused by the weight of the canister declines logarithmically with time.

Summary of uncertainties

The processes involved in the mechanical interaction between buffer and canister after water saturation are fairly well understood. The uncertainty primarily consists in the evenness of the wetting and the pressure build-up caused by possible gas formation. The greatest uncertainty stems from the fact that the properties of the buffer are changed in the event of cementation or transformation.

Handling in the safety assessment

Base scenario: Calculations will be carried out for the most important processes, including vertical movement of the canister. How the swelling pressure affects the canister is described in section 3.6.2.

Canister defect scenario: See base scenario. Further pressure is exerted by corrosion products from the cast iron insert.

Climate change: See base scenario.

Earthquake: The effects of shear movements in the geosphere are analyzed.

4.6.4 Mechanical interaction buffer/near-field rock

Overview, general description

The mechanical interaction between buffer and near-field rock can be divided into

1. swelling pressure from the buffer,
2. pressure from the canister via the buffer,
3. forces of friction from the buffer due to upward swelling against the backfill,
4. thermal expansion of the buffer,
5. convergence of the deposition hole,
6. shear movements due to sliding along fracture.

Swelling pressure from the buffer is transferred to the rock but is not expected to lead to significant rock movements. The elastic deformation of the rock at the expected swelling pressures is small due to the rock's high modulus of elasticity. Plastic deformations caused by movements along the fracture plane can occur along rock wedges that go up to the tunnel floor.

Pressure from the canister can be propagated via the buffer. Such pressures can arise from canister corrosion products and gas pressure build-up.

Forces of friction arise against the rock walls in the deposition hole due to swelling of the buffer against the backfill. The process is described in section 4.6.2.

Thermal expansion of the buffer can be serious for the rock if the buffer is water-saturated when the temperature increase occurs. This process is described in section 4.6.6.

Convergence of the deposition hole occurs when the rock creeps due to the high rock stresses after rock excavation. Assuming an anisotropic primary state of stress with reasonable components, calculations have shown that the diameter can decrease by a centimetre or so after 10,000 years /Pusch, 1995b/. The resulting density increase in the buffer leads to an increase in the swelling pressure by an MPa or so. The effect can be even greater at higher rock stresses, caused by e.g. glaciation.

Shear movements due to sliding along a fracture in the rock is a process that can be serious for the canister if the displacement is rapid and great. The process is partially dealt with in section 4.6.3 and can be modelled uncoupled to the rock. Rock movements are dealt with in the process descriptions for the geosphere, see sections 5.6.4 and 5.6.5.

Model studies/experimental studies

The influence of the buffer on the rock is difficult to investigate experimentally in any other way than by measuring the swelling pressure on the rock. This has been done in BMT in Stripa /Pusch et al, 1985a/. Calculations of the effect on the rock of corrosion of the cast iron insert show that the influence is little Bond et al, 1997/. The effect on the rock of the buffer's upward swelling in the deposition hole has been modelled /Pusch and Börgesson, 1992/. These studies show that a rock wedge can, if the backfill is poorly compacted, move upward 0.2–0.3 m and reduce the density of the buffer in the upper part of the deposition hole. Thermal expansion of the buffer causes similar pressure increases on the rock as on the canister. Theoretically, the pressure could become very high. This is dealt with in section 4.6.6.

The influence of the rock on the buffer in connection with shear movements along fracture planes has, as reported in section 4.6.3, been studied in both experimental and model studies. This process is not harmful for the buffer (if its rheological properties have not been changed) but only for the canister.

Time perspective

Processes 1, 3 and 4 occur during the first 100 years after closure of the repository. The other processes occur or can occur throughout the lifetime of the repository.

Summary of uncertainties

The uncertainties concerning processes 1–4 stem mainly from uncertainties in other processes and are dealt with elsewhere (canister corrosion, gas formation, etc.).

Convergence of the deposition holes is normally negligible.

Handling in the safety assessment

Base scenario: Included in an integrated description of the evolution of the near field.

Canister defect scenario: See base scenario. The effect of iron corrosion products also needs to be discussed.

Climate change: Discussion of the effect of convergence of deposition holes under ice loading.

Earthquake: Discussion of the effect of deformation of deposition holes.

4.6.5 Mechanical interaction backfill/near-field rock

Overview and general description

In a KBS-3 repository, the backfill should have a hydraulic conductivity that does not appreciably exceed that of the surrounding rock. In the preliminary design of the near field /Bäckblom, 1996/, a composition of 15 percent bentonite and 85 percent crushed rock is stipulated. The properties of the backfill are determined not only by its composition, but also by the salinity of the groundwater. Groundwater salinity is of great importance for the properties due to the fact that both swelling pressure and hydraulic conductivity are determined by the properties of the bentonite in the aggregate's pore system. Since the bentonite density is low, the properties are very sensitive to salinity. This means that the mixture 15/85 may be suitable for a site with a non-saline groundwater, while a site with more saline water may require a higher bentonite content. The exact composition of the backfill will be chosen when all data are available on the relevant site.

The following factors are of importance for the interaction backfill/near-field rock:

1. Swelling pressure and weight of the backfill
2. Indirect effects of upswelling of the buffer
3. Creep movements in the rock around the tunnel
4. Block breakout in the roof and walls of the tunnel

The swelling pressure and weight of the backfill act as a support against rock breakout but otherwise exert too little pressure to affect the rock. The pressure is greatest in the floor, if the same material is used in the whole tunnel, since compaction is expected to be best and the weight of the backfill will be greatest near the floor. The swelling pressure is dependent partly on what backfill composition is chosen and partly on the salinity of the groundwater. An aim is to achieve at least 100 kPa of swelling pressure against the roof in order to resist some block breakout and to obtain a residual swelling capacity which can seal the possible effects of piping and creep movements in the backfill. 30 percent bentonite appears to be needed for saline water of the Äspö type, while 10–20 percent appears to be sufficient for non-saline water according to ongoing laboratory tests in conjunction with backfill trials in Äspö.

Indirect effects of upswelling of the buffer mainly relate to the friction between the backfill and the rock wall in the upper part of the deposition hole and the propagation of the buffer's swelling pressure through the backfill against the roof. The pressure against the roof is expected to increase by about 400 kPa due to the latter effect, since the pressure spreads through the backfill with a factor of about 2:1.

Creep movements in the rock around the tunnel arise because the pressure from the backfill is not sufficient to prevent or significantly counteract rock movements in walls and floor. This means that creep-induced deformations in the near field around the tunnels and the upper part of the deposition holes will develop regardless of the backfill until the deformations have become so large that the backfill has been compressed enough to mobilize significant counter-pressure. The effect is further discussed in section 5.6.6.

Block breakout in the roof and walls of the tunnel is prevented partly by the pressure of the backfill against the rock wall, since 100 kPa corresponds to the pressure in the roof from the weight of a 5 m high rock block. (If the backfill should lack swelling pressure, progressive loosening of blocks can take place as a result of creep deformations /Pusch, 1994; Pusch, 1995b/. A stable arch shape is formed after a period of time estimated at a few hundred to a thousand or so years. This means that the rock mass situated between the backfill and an imaginary arched plane at a distance of 1–2 m from the original tunnel roof becomes riddled with fractures and highly permeable. If the tunnels are oriented in such a way that wedge-shaped blocks become unstable, they will detach from the rock and sink down onto the fill, which will consolidate under the load and widen the gap that can form between the blocks and the remaining rock /Pusch, 1994/.)

Model studies/experimental studies

The effect of the friction from the pushing-up of the backfill due to the swelling of the buffer has, as mentioned in 4.6.2, been modelled /Pusch and Börgesson, 1992/. Otherwise, no studies have been made of the rock/backfill interaction, with the exception of BMT in Stripa, where the pressure exerted by the backfill against the rock was measured.

Time perspective

Processes 1 and 2 occur during the water saturation phase, i.e. within about 100 years of closure. Creep movements in rock proceed for a long time.

Summary of uncertainties

The swelling pressure on the roof is dependent on the density achieved in compaction. The difficulties of compacting against the roof make it difficult to guarantee a given swelling pressure.

The swelling pressure is created by the bentonite in the pores of the aggregate and is dependent not only on the average density of the bentonite, but also on its homogeneity. An inhomogeneous mixture can give a high swelling pressure in the beginning, but it is not known whether the swelling pressure decreases due to homogenization, owing to the fact that the bentonite swells out from pores with high bentonite density.

The uncertainties regarding rock creep are dealt with in the chapter on the geosphere.

Handling in the safety assessment

Base scenario: The process is included in the integrated description of the evolution of the near field.

Canister defect scenario: See base scenario.

Climate change: See section 5.6.6.

Earthquake: See base scenario.

4.6.6 Thermal expansion

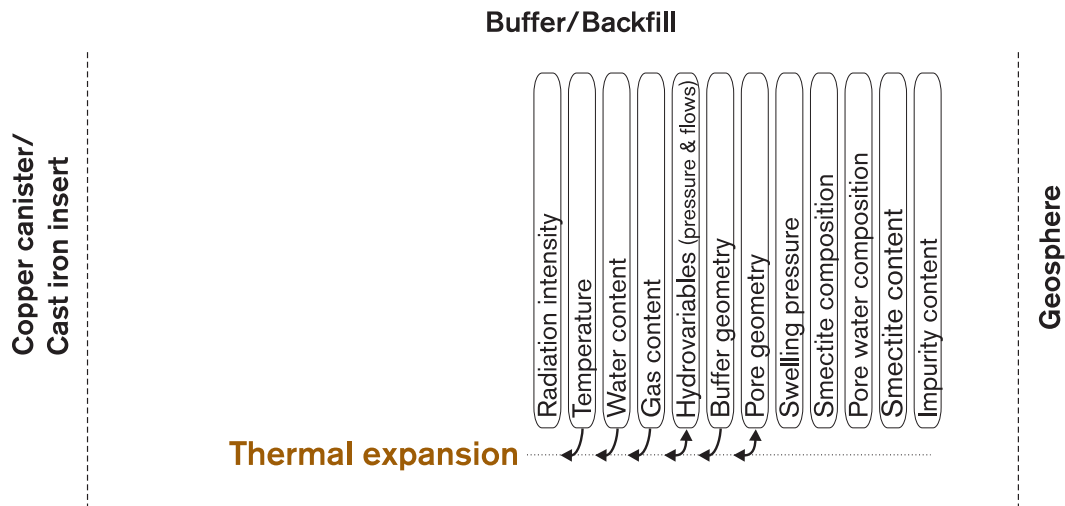


Figure 4-12. Thermal expansion/contraction.

Overview

When the temperature changes in the buffer, the volume of the pore water will change more than the volume of the mineral phase. The pore water pressure rises when the temperature increases, and temperature differences between different parts of the buffer thereby lead to pressure differences, which in turn cause movement of the pore water to equalize the differences. In the interface against the backfill, the process can lead to upward expansion of the buffer.

General description

A change in the temperature of the buffer has the following mechanical consequences:

1. The mechanical properties of the buffer can change
2. Water, particles and pore gas in the buffer expand

The influence on the mechanical properties of the buffer in the water-saturated state is small /Börjesson et al, 1995/. In the unsaturated state, this influence is presumably small but is not sufficiently well-known.

The expansion of the particles and the pore gas is relatively small. The expansion of the water, which is about 100 times greater than the expansion of the particles, completely dominates this process.

The influence of the water's expansion is completely dependent on whether the buffer is water-saturated or not. **Before water saturation** the volume of the water can expand with virtually no other resistance than that offered by the compression properties of the pore gas. At constant volume this leads (to simplify slightly) to an increase in the degree of saturation when the temperature increases. The consequences of this are that the negative pressure in the pore water (suction potential) decreases and that the total pressure and the pore gas pressure increase. This causes the swelling pressure against an external restraint to increase slightly. At constant pressure, a slight increase of the volume is obtained in the same way. However, these changes are small and apparently without practical significance. The increase in degree of saturation is about 2 percent at a temperature increase of 50 degrees.

The consequences can be more serious in **water-saturated** buffer, since there are no gas-filled pores to swallow the volume increase. At constant volume the pore pressure increase is great, since the water must be compressed. Theoretically, the resultant pressure increase against the surroundings can amount to several tens of MPa at the temperature changes in question. However, the pressure increase is counteracted by drainage of the water through the rock and backfill. This causes a decrease in pore pressure which occurs in parallel with the temperature increase. This process is relatively fast and can greatly reduce the pore pressure increase if the temperature increase is slow.

Model studies/experimental studies

The process has been simulated under water-saturated conditions in laboratory tests, which show that expected stress increases occur, followed by falling stresses due to drainage of water. A numerical modelling of this process /Börgesson, 1992/ shows that the maximum pore pressure increase amounts to 8 MPa due to the fact that the rock drains the buffer. However, this calculation assumes that the rock acts as a filter for the pore water.

Time perspective

Temperature calculations /Thunvik and Braester, 1991/ show that the maximum temperature in the bentonite at the canister wall is reached after about 10 years, at the rock wall after about 30 years and furthest away from the canister after another ten years or so. In the most favourable case, water saturation can arise in the whole buffer after 10–15 years. In other words, there is a risk that a pressure increase will arise in the interval between 10 and 50 years after deposition. However, the temperature increase is very moderate and slow during this time interval. Furthermore, a temperature decrease takes place simultaneously nearest the canister after about 10 years, which counteracts the effect.

The corresponding process takes place in the backfill as long as 500 years after deposition, due to the distance to the nearest canister. In the backfill, however, the hydraulic conductivity is so high that drainage ought to be complete.

Summary of uncertainties

The process is well understood for water-saturated bentonite. For water-unsaturated bentonite the thermo-mechanical theory formation is not complete, but the consequences of this process are deemed in this case to be unimportant for safety.

Handling in the safety assessment

Base scenario: The process is included in the integrated modelling of water saturation

Canister defect scenario: See base scenario.

Climate change: See base scenario.

Earthquake: See base scenario.

4.7 Chemical processes

4.7.1 Introduction, cementation

The term “cementation” has often been used in a broad sense to describe effects of chemical and mineralogical processes which can lead to various changes in the rheological properties of the buffer material, for example increased mechanical strength, brittleness or reduced swelling capacity. A number of completely different processes could conceivably cause similar effects, and the underlying reactions can occur directly in the montmorillonite mineral, in the interlamellar space between montmorillonite layers, or in accessory minerals. The resultant cementation does not necessarily have to appear in the same area as the underlying process, since released species can be transported in the buffer by various prevailing gradients (thermal, concentration, etc.) and be precipitated in various locations and in various forms. The processes discussed in the following include those reactions that have been offered as possible causes of cementation of the buffer. On the other hand, it is not correct to discuss cementation as a process in its own right in this context.

4.7.2 Advection

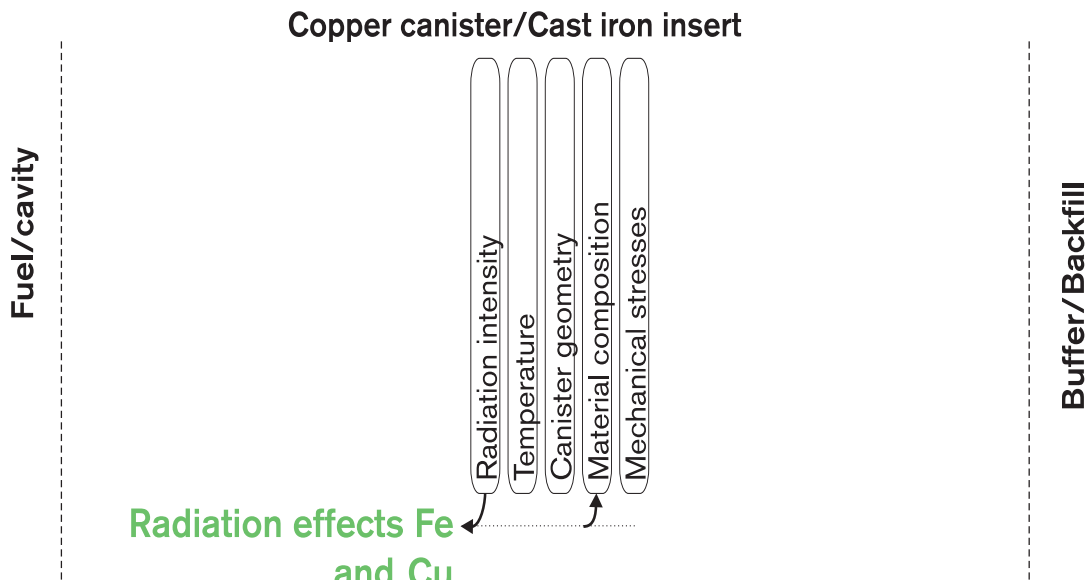


Figure 4-13. Advection.

Overview, general description

Solutes (dissolved substances) can be transported with pore water by pressure-induced flow: advection. In this way, solutes move from areas of higher water pressure to areas of lower pressure. The process leads to redistribution of solutes in the pore water and thus affects the pore water composition.

The process is of importance in the buffer during the unsaturated period when a net flow of water takes place in to the buffer. The principal flow during this phase takes place in the direction towards the canister, provided that the rock supplies the buffer with groundwater. Under saturated conditions, the transport of solutes in the pore water is dominated completely by diffusion, see section 4.5.2, possibly with the exception of sudden events such as gas pulses or earthquakes, which can cause pressure changes in the buffer. Water flow in the buffer under unsaturated conditions is dealt with in detail in section 4.5.1.

Model studies/experimental studies

Several SKB projects have studied flow of water in bentonite material, both during water uptake and after complete water saturation. Large quantities of quantitative data are available on different physico-chemical conditions, e.g. densities, temperatures, salt solutions.

Influx of solutes as a consequence of water flow has also been investigated. Due to these investigations, our knowledge of flow through water-saturated bentonite is good.

Time perspective

Flow transport in conjunction with water saturation takes place on a timescale of up to hundreds of years. Flow transport after water saturation is expected to be negligible in relation to diffusive transport.

Natural analogues

Summary of uncertainties

Handling in the safety assessment

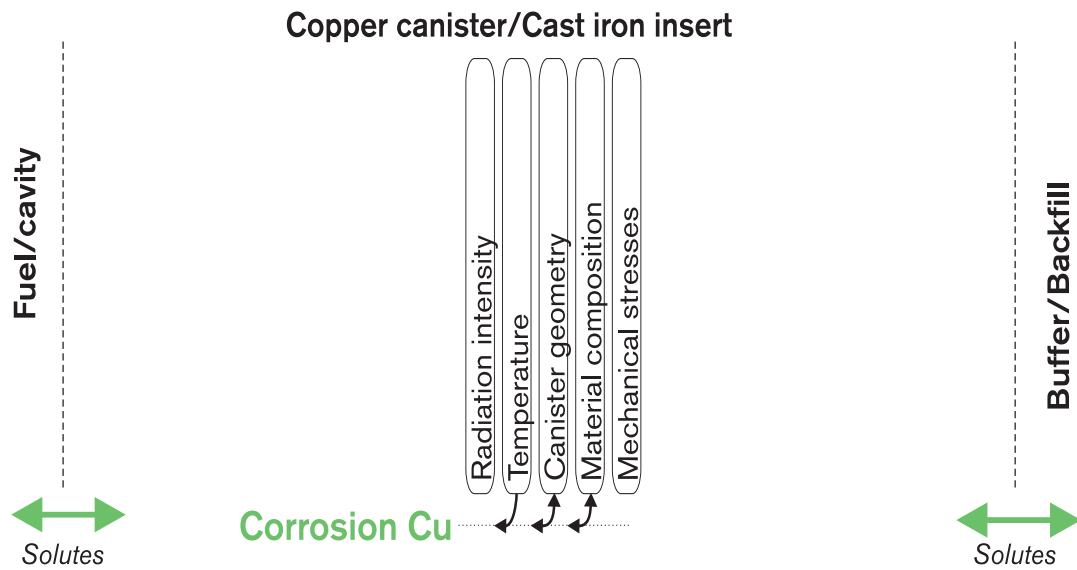
Base scenario: The process is handled in simplified terms in an integrated modelling of the chemical evolution in the near field.

Canister defect scenario: See base scenario.

Climate change: See base scenario.

Earthquake: See base scenario.

4.7.3 Diffusion



Figur 4-14. Diffusion.

Overview

Solutes can be transported in stagnant pore water by diffusion. Solutes thereby move from areas of higher concentration to areas of lower concentration. The process leads to redistribution of solutes in the pore water and thus affects the pore water composition.

The diffusion process is strongly coupled to nearly all chemical processes in the buffer, since it accounts for transport of reactants to and reaction products from the processes. Diffusion of Na^+ and Ca^{2+} ions is, for example, of crucial importance to the ion exchange process, diffusion of K^+ is an important limiting factor for the illitization process, and so on. Diffusion is thereby a central process for the entire chemical evolution in the buffer.

General description

Diffusion in bentonite has been thoroughly studied in conjunction with radionuclide transport. This is described in section 4.8.6. The description is applicable to diffusion in general.

Model studies/experimental studies

Time perspective

Natural analogues

Summary of uncertainties

Handling in the safety assessment

Base scenario: The process is handled in simplified terms in an integrated modelling of the chemical evolution in the near field.

Canister defect scenario: See base scenario. Diffusion of radionuclides is also dealt with.

Climate change: If the evolution leads to canister damage: See the canister defect scenario. Otherwise: See the base scenario, possibly with changed groundwater composition.

Earthquake: If the evolution leads to canister damage: See the canister defect scenario. Otherwise: See the base scenario. Effects of modified buffer thickness resulting from rock movements may need to be discussed.

4.7.4 Ion exchange/sorption

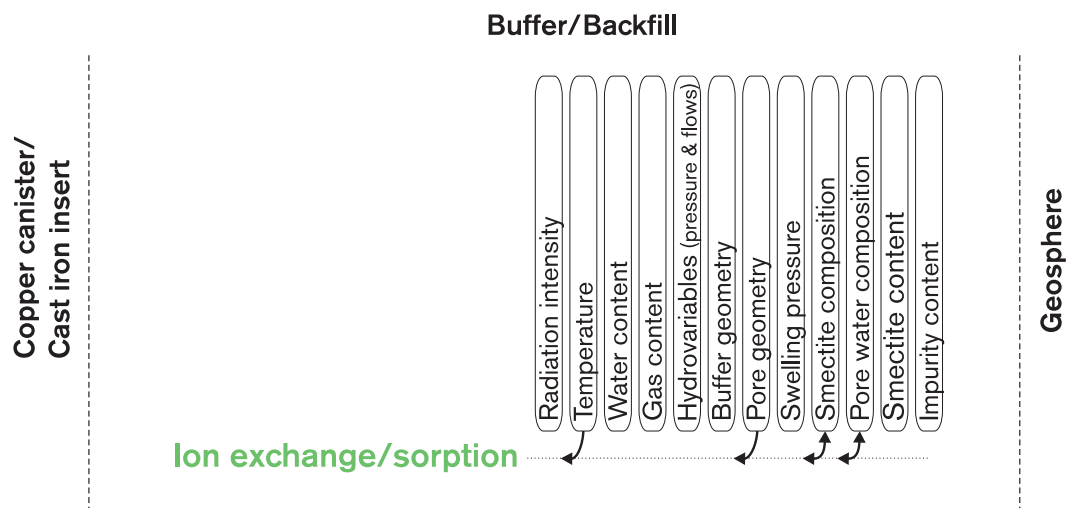


Figure 4-15. Ion exchange/sorption.

Overview

When the bentonite material in buffer and backfill swells, water is taken up between the individual particles in the principal mineral montmorillonite. The structure of the bentonite material is thereby altered drastically, providing the desirable physical properties. The capacity to bind water between the individual montmorillonite particles (inter-lamellar hydration) is influenced by the ion content of the bentonite's pore water. The physical properties of the bentonite can thereby be greatly affected by the ion content of the pore water.

Under the chemical conditions that are expected to prevail in a deep repository, it is above all the total salinity and exchange from Na^+ to Ca^{2+} that can influence the properties of the bentonite to an appreciable extent. Both increase of ionic strength and ion exchange to calcium affect the bentonite's swelling capacity, principally by limiting its maximum water binding capacity. Material with a low montmorillonite density, e.g. the backfill, is thereby affected more than material with a high montmorillonite density, e.g. the buffer.

Ions in the buffer's pore water can be bound to the surfaces of the bentonite material. This phenomenon is usually described as sorption and is of essential importance for the function of the buffer, since it can affect the mobility of the ions. Two main types of sorption can be distinguished. The one is characterized by physically dominant bonding forces (van der Waals or electrostatic bonding) and bonding of the ions is relatively weak. In the other type, the bonding is of a chemical character (covalent bonding) and thereby considerably stronger. Essential differences between the two types are that physical bonding is controlled to a high degree by the concentration of the ions in the system, while the chemical bonding is normally strongly pH-dependent and takes place to specific reactive positions and thereby has a pronounced limitation in scope. Differences in the bonding character between e.g. sodium (physical bonding, ion exchange character) and cobalt ions (chemical bonding, surface complex character) that have been adsorbed on montmorillonite are well-documented experimentally /Jansson and Eriksen, 1998/.

General description

Surface chemical processes affect the microstructure and thereby the physical properties of the buffer and backfill materials. The processes can be roughly divided into ion exchange and alteration of the total quantity of cations. The most important factor for both processes is the ion content of the pore water, which is principally determined by the original cations in the montmorillonite's exchange positions, readily soluble minerals in the original bentonite material, and by the surrounding groundwater.

At relatively low salinities, the potential swelling is determined by which cations occur in exchange positions in the montmorillonite. Large differences between different cations are well documented for different types of smectite minerals /Schultz, 1969/. In the case of MX-80 bentonite, most univalent ions in exchange positions entail a large potential swelling, while larger univalent cations (from Cs⁺) and polyvalent cations entail a much smaller potential swelling. Potassium, for example, does not entail any special problem from the viewpoint of surface chemistry.

Different cations are bound more or less tightly to the montmorillonite surface depending on how polarizing the ion is. In general, divalent ions are bound more tightly than univalent ones and therefore tend to replace univalent ions in exchange positions. An ion exchange from Na⁺ to Ca²⁺ can be expected to take place in the bentonite in a deep repository. H⁺ ions can also be bound to ion exchange positions, which means that pH changes can occur due to ion exchange and change of the total cation content. At high concentrations of cations or with divalent ions in ion exchange positions, H⁺ ions are forced out into the pore solution and the pH falls. Due to its ampholytic properties, i.e. ability to both receive and donate hydrogen ions, the montmorillonite can counteract external changes in pH. Certain organic compounds can also be bound to ion exchange positions.

Increased ion concentration generally leads to a reduced potential swelling, and thereby to effects on the pore geometry that are similar to those of an ion exchange to divalent ions /Norrish, 1954/. Increased ion concentration further leads to a reduction of the swelling pressure due to osmotic effects, and to changes in the pore geometry that affect the hydraulic conductivity of the material /Karnland, 1997a/.

Influence on pore geometry, hydraulic conductivity and swelling pressure in buffer: The volume of the buffer is so limited that a maximum swelling of the bentonite cannot be achieved even after complete ion exchange to Ca^{2+} . The pore geometry, and thereby also the hydraulic conductivity, are therefore not expected to be significantly altered after such an ion exchange. Very high ion concentration in the pore water leads to a significant reduction in the swelling pressure due to osmotic effects, and to an increase in the hydraulic conductivity. A maximum content of sodium chloride (36 percent, equivalent to saturated solution) leads to a reduction in the swelling pressure by approximately 50 percent, and an increase in the hydraulic conductivity by approximately a factor of 10.

Influence on pore geometry, hydraulic conductivity and swelling pressure in backfill: Due to limitations in present-day compaction technology, in combination with the quantity of bentonite mixed into the backfill material, the density of the montmorillonite phase is much lower than in the buffer. In the basic state, the montmorillonite is therefore swollen to a volume that exceeds the maximum swelling for the material after ion exchange with Ca^{2+} . The pore geometry in the backfill material will therefore be significantly changed by such an ion exchange. An increase in the total quantity of cations in the pore water leads to a corresponding effect even at low salinities in the groundwater (a few percent NaCl). The changes lead to a sharp increase in hydraulic conductivity, lost contact with the rock and an increased risk of piping (channel formation at high water flow). See further section 4.5.2.

Model studies/experimental studies

Ion exchange is a relatively well-investigated process and quantitative models exist for calculation of equilibrium states. In principle, for pore water with equivalent concentrations of univalent and divalent ions, low ion concentrations lead to a heavy preponderance of polyvalent ions in ion exchange positions.

Ion exchange from sodium to calcium states has been modelled for deep repository conditions. Calculations have been carried out for expected repository conditions with respect to calcium mineral (calcite) and groundwater flows /Wanner 1992/.

Laboratory studies have been performed with MX-80 bentonite that has been completely ion-exchanged to calcium form. The material was investigated with respect to hydraulic conductivity and swelling pressure. Salinities of up to 3.5 percent in NaCl and CaCl_2 solutions were investigated at temperatures of up to 130°C. No significant differences between ion-exchanged and original MX-80 bentonite could be detected for densities equivalent to that of the buffer /Karnland et al, 1992/.

The effect of high ion concentration on swelling pressure can be calculated with thermodynamic models. In maximally pessimistic models, the swelling pressure declines with rising salinity, ceasing entirely in the buffer at an NaCl content of about 7 percent /Low, 1987/. Calculations based on less pessimistic assumptions and preliminary experimental studies show that swelling pressure can be expected even in saturated salt solutions /Karnland, 1997a/. Laboratory studies of Canadian bentonite provide support for the latter calculation method /Dixon, 1996/. Temperature effects on swelling pressure and hydraulic conductivity are not experimentally documented for very high salinities.

Time perspective

Influx of groundwater can take place during the water saturation process.

Diffusion of above all Na⁺ and Ca²⁺ into the bentonite can take place relatively rapidly after water saturation if high ion concentrations occur in the groundwater.

The ion exchange process is fast in itself, so the dissolution rate of other minerals and the transport rate in groundwater and bentonite will control the ion exchange from Na⁺ to Ca²⁺. Relevant changes are expected to occur on the hundred-thousand-year scale according to Wanner's model. Pessimistic assumptions regarding buffer permeability in the model ($k = 10^{-11}$ m/s) entail that the backfill will not deviate dramatically from calculated buffer values at low salinities. At higher salinities (>1 percent), the elevated conductivity entails that the transformation can be expected to take place on a 100-year timescale.

Natural analogues

Many bentonite deposits contain pore water with high salinities. Investigations of effects of high salinity in natural smectites exist but have not been utilized specifically for repository-related questions.

Summary of uncertainties

A conceptual description of the swelling pressure in the montmorillonite-saltwater system exists in report form and shows that the buffer retains a considerable swelling pressure even in saturated salt solutions /Karnland, 1997a/. A marked uncertainty exists as regards quantification of hydraulic conductivity at very high salinities (brines, containing over 10 percent salinity). Temperature effects on equilibrium constants for ion exchange are not well-documented. Temperature effects on swelling pressure and hydraulic conductivity at very high salinities have not been investigated. Both conceptual understanding and a large quantity of measurement data exist for systems with relatively low salinities (below 3.5 percent).

Handling in the safety assessment

Base scenario: The process is included in an integrated modelling of the chemical evolution in the buffer.

Canister defect scenario: See base scenario. The evolution described in the base scenario forms a basis for solubility and sorption calculations in the canister defect scenario.

Climate change: Effects of altered groundwater composition are discussed.

Earthquake: See base scenario.

4.7.5 Montmorillonite transformation

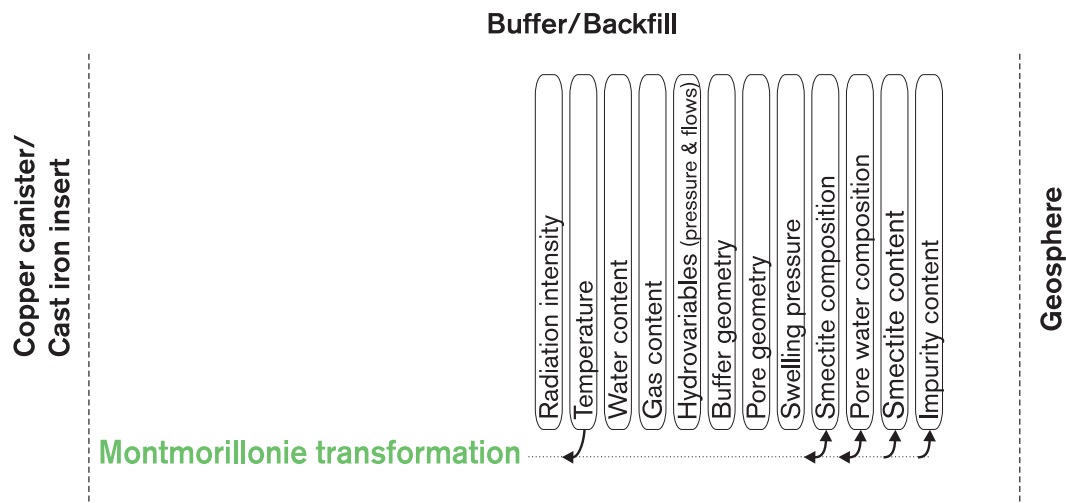


Figure 4-16. Montmorillonite transformation.

Overview

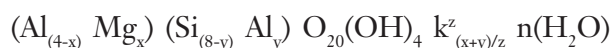
The advantageous physical properties of the buffer, e.g. swelling pressure and low hydraulic conductivity, are determined by the interaction between water and the montmorillonite mineral in the bentonite. This interaction can be influenced by changes in the pore water (see section 4.7.4) and by changes in the mineral structure of the montmorillonite. The mineralogical stability of the montmorillonite is therefore decisive for the function of the buffer in a deep repository. The mineral is very stable in its natural environment, but transformations can be expected under very special geochemical circumstances.

The processes can lead to a reduction of the montmorillonite content, and it is therefore important to evaluate the extent to which this occurs in a long time perspective.

One type of transformation that occurs in natural sediments gives illite clay. The transformation rate for this reaction is determined above all by the availability of potassium and by the temperature in the buffer.

General description

The principal mineral in MX-80 bentonite is montmorillonite, which normally comprises more than 75 percent of the mass of the bentonite. The structural formula for ideal montmorillonite can be written



where the sum of x and y can vary by definition between 0.4 and 1.2 units (charge per $\text{O}_{20}(\text{OH})_4$), and $x > y$. A certain quantity of aluminium (Al) can thus be regarded as exchanged for magnesium (Mg), and a smaller fraction of silicon (Si) is exchanged for aluminium (Al). k designates exchangeable cations, e.g. Na^+ or Ca^{2+} , which are needed to balance all exchanges. The exchange of trivalent aluminium for divalent magnesium thus leads to a negative net charge in the mineral structure (layer charge), which is balanced by the cations.

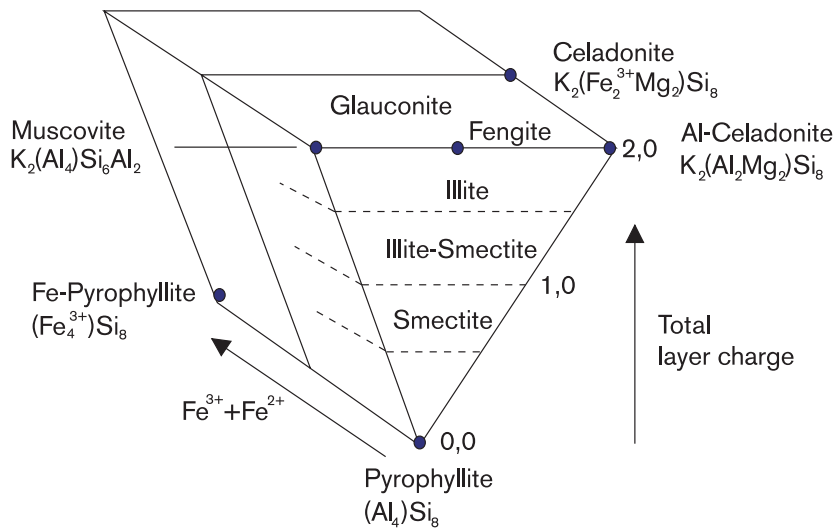


Figure 4-17. Composition of a number of dioctahedral end minerals based on the formula unit $O_{20}(OH)_4$ and structure ranges for mica, illite and smectite (montmorillonite). Modified from Newman and Brown, 1987/.

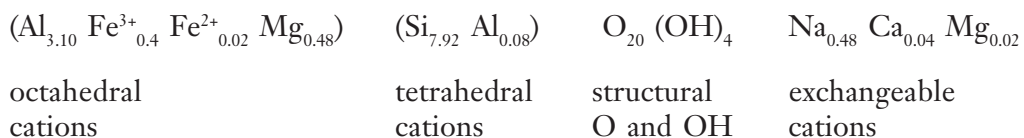
Minerals with wide variation in layer charge occur in nature, see Figure 4-17. If the charge $(x+y)$ per $O_{20}(OH)_4$ is near zero (pyrophyllite), there is virtually no interaction with water, which results in radically different properties than in montmorillonite. Increasing layer charge and thereby more balancing cations naturally leads to greater interaction with water. In materials with a sufficiently high layer charge, however, the cation can be bound to the mineral surfaces and the interaction with water once again ceases. The end mineral for this series has a charge of 2 per $O_{20}(OH)_4$ (mica mineral). The typical properties of montmorillonite consequently require a mineral with medium-high layer charge.

The fixation of charge-balanced cations is dependent to a high degree on the properties of the ion. K^+ ions are, for example, bound at a lower layer charge than Na^+ ions, which are in turn bound at a lower layer charge than Ca^{2+} ions. Illite designates material with a layer charge between that of the montmorillonite and the mica mineral. K^+ ions are therefore bound in illite material, but not Na^+ and Ca^{2+} ions.

The illitization process: In natural systems, elevated temperature leads to transformation of montmorillonite in the direction towards illite. The process can be described in simplified terms as follows:



The average mineralogical composition of the montmorillonite in MX-80 is



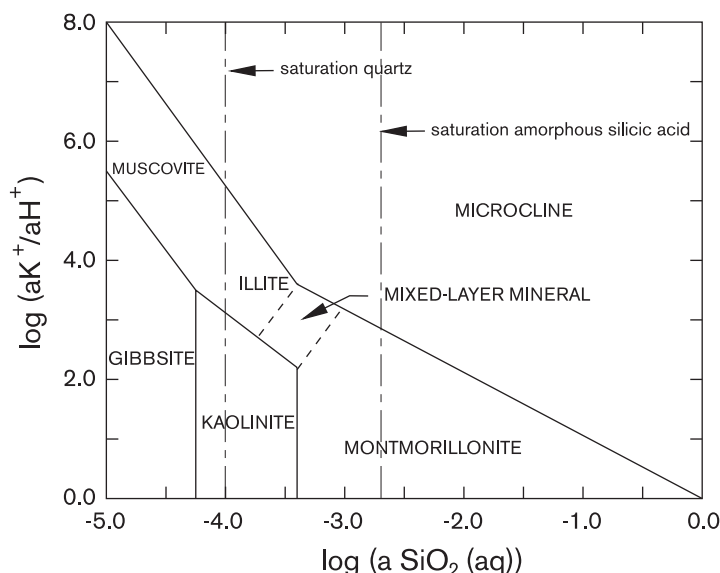
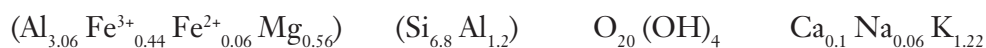


Figure 4-18. Stability ranges for montmorillonite/illite with respect to pH, potassium and silicon content at 25°C. Simplified after /Aagard and Helgeson, 1983/.

which can be compared with an average composition for 24 illite materials /Weaver, 1973/:



The transformation thus includes a marked increase in the layer charge, which is balanced by uptake and fixing of potassium ions from surrounding pore water. The charge increase normally takes place through a reduction of the silicon content.

Transformation can take place as a partial change in the original mineral structure, i.e. silicon leaves and illite is formed directly via uptake of potassium. Alternatively, montmorillonite can go into solution and illite and quartz can be formed locally or after transport.

No general consensus exists today on the underlying causes of the transformation. One possible driving mechanism is the fact that the montmorillonite's pore water generally contains a higher concentration of dissolved silicon than the saturation value for quartz, see Figure 4-18. At elevated temperature, quartz is more likely to precipitate and more silicon can thereby be dissolved from the montmorillonite, leading to increasing layer charge /Abercrombie, 1994/.

Effects of transformation: Change in the layer charge of the montmorillonite leads to change in the interaction with water and thereby to effects on the swelling pressure. On illitization, the interaction virtually ceases and the water previously bound between the individual layers is released. The pore geometry is thereby changed towards fewer and bigger pores. Swelling between remaining montmorillonite layers will partially balance the negative effects. The quantity of remaining montmorillonite will thereby determine the system's swelling pressure and hydraulic conductivity. A high degree of transformation leads to a system similar to that in the backfill. Consequently, sensitivity to the ion content of the pore water increases with the degree of transformation. Released silicon is expected to lead to a deterioration of the buffer's rheological properties, see section 4.7.6.

Model studies/experimental studies

The illitization process is of great importance from several viewpoints in connection with prospecting and extraction of oil deposits. The great commercial interest, in combination with the mineralogically interesting process, has led to very extensive research since the 1960s. A large number of publications therefore exist as a basis for the assumption that the illitization process is not expected to be important in a deep repository.

The argumentation can be summarized in three points:

- The bentonite material is close to mineralogical equilibrium to start with.

In its original environment, the bentonite normally comprises a system that is close to mineralogical equilibrium, i.e. only insignificant mineralogical changes take place. In a deep repository, the exchange between buffer and surrounding environment is strongly limited, and the mass of the buffer is relatively great. The bentonite in the buffer will therefore create its own chemical environment to start with/see e.g. Fritz et al, 1984/. Two early changes in the chemical environment are obvious, however:

- Increase in the ion content of the pore water as a result of inward transport of solutes during water saturation. For ordinary groundwater, the increase is small in relation to the naturally high cation concentration that exists in the montmorillonite in the buffer.
- Temperature increase as a result of fuel decay. The period with significantly elevated temperature is, however, relatively short (<5,000 years) /Thunvik and Braester, 1991/.

The system can thus be expected to be close to mineralogical equilibrium during most of the repository period.

- Temperature-induced transformation is limited by a shortage of K⁺.

In order for a transformation to illite to take place, the charge increase must be balanced by potassium ions. Since the natural fraction of potassium in the buffer may be kept low, potassium must be transported in from the surroundings. The potassium requirement to completely convert the montmorillonite in the buffer is about five weight-percent, which is equivalent to nearly a tonne of potassium for a deposition hole. Calculations and modellings show that the inward transport is expected to take place very slowly and that this in itself constitutes an effective obstacle to a substantial transformation /Hökmark, 1995/.

- The transformation rate at the repository's maximum temperature is very low.

Kinetic models have been developed for calculation of degree of transformation in smectite-to-illite transformation. Relationships and constants have been established by means of laboratory experiments and comparisons with natural systems /e.g. Eberl 1976; Pytte, 1982; Huang 1993/. Model calculations show that the transformation rate in the buffer can be expected to be very low at the temperatures that will prevail in a deep repository even at relatively high potassium concentrations /Karnland et al, 1995/.

Time perspective

Relevant changes in the montmorillonite content of the buffer are expected to occur on a million-year timescale. According to e.g. Huang's model, 50 percent of the bentonite is expected to be unaffected after one million years, at a potassium concentration in the pore water equivalent to that of seawater (0.01 M) and a constant temperature of 90°C, i.e. the maximum temperature in the deep repository. At temperatures and potassium concentrations that are expected in the deep repository, the transformation is calculated to amount to a few percent after a million years.

Natural analogues

Besides in SKB-related investigations, the transformation of smectite to illite is well-documented for a large number of geological formations. Natural sediments have been studied by, among others, Burst /1959/; Perry /1970/; Hower /1976/; Colten-Bradley /1987/; Lynch /1997/. The studies show that increased sediment depth (increasing temperature) leads to increased illite content, and that low availability of potassium can be linked to reduced transformation. Special formations where temperature effects have been obtained from e.g. volcanic activity have revealed a similar transformation /e.g. Pytte, 1982; Lynch, 1985; Brusewitz, 1986/. Cementation effects as a consequence of transformation have been studied specifically by, among others, Hower /1976/ and Boles /1979/.

Summary of uncertainties

The detailed mechanism of the illitization process has not been clarified, so conceptual uncertainties remain.

The development of a temperature gradient can lead to transport of dissolved silicon, which could possibly influence not only the transformation rate but also the character of the transformation process. Transformation of montmorillonite could therefore proceed along a continuous scale, and in both directions.

If temperature-controlled precipitation of silicon is the controlling kinetic process, layer charges similar to those in illite can be expected. If the temperature gradient in the buffer leads to transport of silicon, the increase in the layer charge could conceivably be higher and mica mineral could be formed even in the absence of potassium. The process probably does not pose any threat to the buffer, since the temperature gradient is maintained during a relatively short period.

Conditions in the buffer that depart significantly from the expected have been found in laboratory experiments to be able to lead to faster transformation under the following conditions:

- vapour influence, repeated drying-out /Cotour, 1985; Karnland et al, 1994/
- pH effects /high pH: Velde and Vasseur, 1992; 1992, Karnland, 1997b; low pH: Zyseth 1992/

Velde reports significant effects even at relatively low temperature (35°C). Karnland reports small effects even after extensive percolation with KOH, pH 13.8, for 16 months. The percolation was equivalent to 10 pore water changes in the buffer.

The high Fe content of the montmorillonite may influence the properties of the buffer via:

- redox reactions in the octahedral position,
- cementation with iron compounds in connection with dissolution of the montmorillonite,
- chloritization, i.e. binding of e.g. Al, Fe or Mg hydroxide between remaining montmorillonite layers in connection with dissolution of montmorillonite. The process leads to a loss of swellability, but with greater layer spacing than in the case of illitization. A greater degree of transformation is therefore required in order to alter the properties of the material compared with illitization.

Experimental verifications: Since the processes are very slow, laboratory experiments must be conducted under accelerated conditions, i.e. at high temperatures and potassium concentrations, in order to obtain measurable results /Karnland et al, 1995/. Comparisons with natural transformations provide an opportunity to verify laboratory results /Elliot, 1996/.

In transport calculations, the diffusion constants in rock, bentonite and transformed bentonite constitute an uncertainty. Impurities of potassium-rich minerals can occur in the bentonite. Release of potassium from these impurities can be calculated. Even for reasonably pessimistic assumptions for all conditions, calculated transformations do not pose a threat to the function of the buffer.

Handling in the safety assessment

Base scenario: An upper limit for the ultimate scope of the process is obtained by estimating the initial quantity of potassium and the influx of potassium from groundwater and backfill. One weight unit of potassium is equivalent to 20 weight units of montmorillonite in the transformation. Estimates are made for both buffer and backfill.

Canister defect scenario: See base scenario.

Climate change: Like the base scenario but with modified flows and potassium concentrations. The flow can be expected to increase as a result of infiltration of glacial water, while the potassium content should decrease.

Earthquake: Like the base scenario but possibly with modified flows. Flows around deposition holes can be affected. This may necessitate different handling compared with the base scenario.

4.7.6 Dissolution/precipitation of impurities

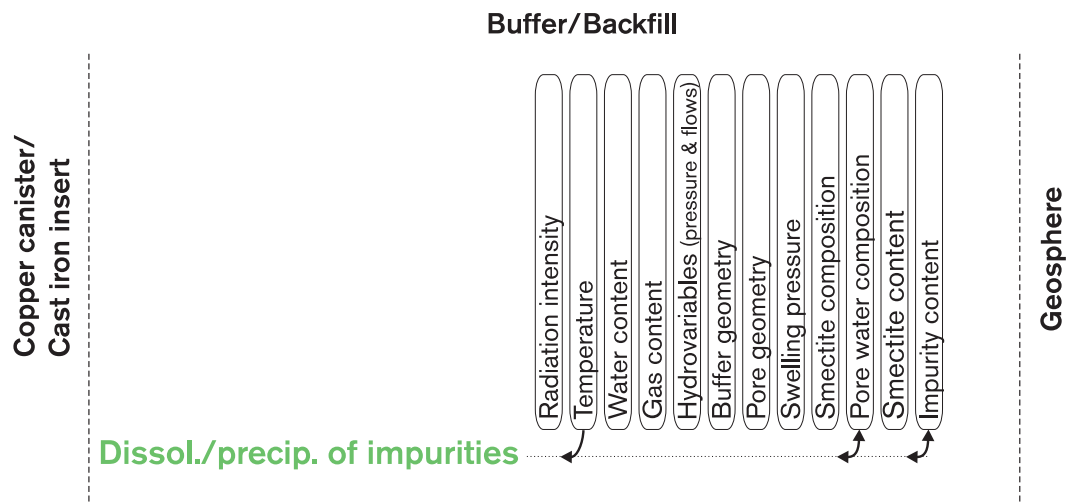


Figure 4-19. Dissolution/precipitation of impurities.

Overview

The buffer material, bentonite MX-80, consists not only of montmorillonite, but also other accessory minerals as well as impurities. In the repository environment, these can be dissolved and sometimes re-precipitated depending on the prevailing conditions.

Precipitation of carbonates and sulphates nearest the canisters may lead to the formation of a porous contact zone between the buffer and the canister surface and an increase in the strength of the buffer. When the heat period is over and temperature gradients no longer exist in the buffer, it is likely that the precipitations will be dissolved to some degree and diffuse in ionic form out through the buffer. Precipitation of silicon may reduce the swelling potential, among other things.

General description

MX-80 bentonite contains approximately 75 percent Na-montmorillonite and 25 percent other minerals. The other minerals are mainly quartz, plagioclase and low concentrations of calcite (CaCO_3), siderite (FeCO_3), pyrite (FeS_2) and other clay minerals, Table 4-3.

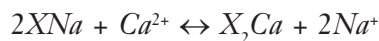
Table 4-3. Impurities and accessory minerals in MX-80 bentonite /Müller-Vonmoos et al, 1983/.

| Component | Concentration (wt-%) |
|----------------------------|----------------------|
| Carbonate (calcite) | 1.4 |
| Quartz | 15 |
| Pyrite | 0.3 |
| Non-swelling clay minerals | 1.4 |
| Kaolin | <1 |
| Feldspar | 5–8 |
| Humic substances | 0.04–0.4 |
| Other | 2 |

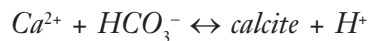
The calcite and pyrite contents are of decisive importance for pH, Eh and alkalinity in the repository's near field. The bentonite also contains small quantities of gypsum (CaSO_4), which may be of importance in an early phase with high temperatures.

The accessory minerals in the bentonite are stable in the environment where they were originally mined. In the repository, however, they will be exposed to a water which differs in some respects from that on the original site, in terms of both composition and temperature. Most accessory minerals in the bentonite are nevertheless stable in normal Swedish groundwaters. There are, however, some dissolution processes that are important:

Calcite dissolution: Calcite is stable in groundwater. In the bentonite, however, the ion exchange process (4.7.1) will compete for the free calcium ions. The reaction

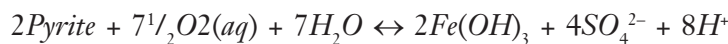


competes with



The carbonate contents of the groundwaters that may be encountered are sufficiently low for the ion exchange process to dominate and calcite will be dissolved. This will entail a consumption of hydrogen ions, i.e. an increase in pH. The water flux in the buffer is very low, and the reactions are close to equilibrium.

Pyrite oxidation: Pyrite is also stable in groundwater. However, penetrating oxygenated water can oxidize the pyrite in accordance with



Pyrite oxidation releases protons and can thereby lower the pH, but this is buffered by the aforementioned calcite dissolution. There is enough pyrite in the buffer (the MX-80 material) to consume all initial oxygen left after closure of the repository. The quantity is also sufficient to prevent any penetrating oxygenated water from coming into contact with the canister for hundreds of thousands of years.

Dissolution of calcium sulphates: Calcium sulphates (gypsum and anhydrite) and calcite have lower solubility at high temperatures than at low ones. At an early stage, when the canister temperature is high, it is possible that they will be dissolved in the colder portion of the buffer and precipitate on the canister surface.

Precipitation/dissolution of silicon: The largest portion of the impurities in the bentonite consists of quartz and feldspars. These are normally stable in the natural repository environment, but their solubilities increase with increasing temperature. Silicon will dissolve due to high temperature close the canister and will be transported by diffusion outwards into the colder parts where silicon precipitation may take place. In the Buffer Mass Test in Stripa, the buffer was analyzed with respect to the distribution of silicon, but no definite conclusion could be drawn regarding possible enrichment in the coldest part /Pusch, 1985b/.

Model studies/experimental studies

Hydrothermal tests with purified standard bentonite (SWY-1) heated to 150–200°C have shown that cooling leads to precipitation of silicon compounds in various forms. The precipitation is assumed to cause cementation effects, including a strength increase, which has been demonstrated in several laboratory investigations /Pusch and Karnland, 1988; Pusch and Karnland, 1991/. According to these investigations, the scope of the precipitations is dependent on the temperature. At the highest temperature in the buffer (90°C), the cementation was not of such a great extent that it can be regarded as problematical. The tests were carried out without a temperature gradient, which cannot be regarded as pessimistic conditions.

Precipitation of sulphate and carbonate could be observed in one-year tests with hydrothermal treatment of MX-80. XRD analyses indicated that sulphates and calcite had gone into solution and been transported to the hot iron surface, where they had been precipitated. It is also probable that feldspars went into solution. Quartz was enriched at the colder boundary /Pusch et al, 1993/.

Several laboratory investigations have been carried out for the purpose of studying the distribution of readily soluble ions in the buffer's pore space after water uptake against a temperature gradient. Effects of the clay's density, degree of saturation, testing time, open or closed conditions, and ion content and pressure in the ambient water solution have been investigated. The experimental results show that the enrichment of solutes is insignificant in specimens with high clay density, and that a high original water content and high ambient water pressure reduce the enrichment in specimen with lower density /Karnland, 1995/. Similar studies are currently being conducted in field tests in Äspö (the LOT project), and in laboratory experiments under the auspices of ENRESA.

Time perspective

The chemical precipitation/dissolution processes are most important at an early stage when the temperature is high and oxygen remains in the repository tunnels. At later stages, most of the processes go towards equilibrium. The accessory minerals in the bentonite are, however, very important if the chemistry in the repository should be disturbed for some reason; both pH and Eh are buffered very effectively by the minerals that are common in different bentonite materials.

Natural analogues

Development of salt crusts in arid regions resembles in principle certain conditions during the water saturation phase. Direct SKB-related studies have not been conducted, but a large body of literature exists on the subject.

Silicon precipitation occurs at a large number of places where hydrothermal transformation of bentonite has taken place. Numerous scientific articles have been published, some directly linked to repository questions, see for example Pusch et al, 1998.

Summary of uncertainties

Most of the conceivable processes are in themselves well known and can be modelled for less complex systems. However, conditions in the buffer as far as transport and reaction kinetics are concerned are not fully understood for all processes. Transport of solutes can take place in different forms and cannot be fully described at present. In particular, modelling problems remain during the water saturation phase, when water is transported both in vapour and liquid form. Modelling of the system must therefore be coupled to the THM processes that proceed in parallel with transport and reaction kinetics.

Silicon is the most common element in the buffer and occurs in a number of different minerals and phases. The following processes are not fully understood:

- release of silicon from the different minerals,
- transport of dissolved silicon driven by the prevailing temperature gradient,
- precipitation of silicon minerals.

Precipitation of silicon is particularly complex, since it is dependent on several interacting factors and since several conceivable forms occur, both crystalline and amorphous.

The greatest uncertainty concerns the scope of cementation processes as a consequence of dissolution, transport and precipitation of silicon or Si/Al/Ca compounds. The scope and consequences of cementation cannot be predicted with reasonable certainty today.

Handling in the safety assessment

Base scenario: The processes are included in the modelling of the chemical evolution in the buffer.

Canister defect scenario: See base scenario. The evolution described in the base scenario serves as a basis for solubility and sorption calculations in the canister defect scenario.

Climate change: Effects of changes in the groundwater composition are discussed.

Earthquake: See base scenario.

4.7.7 Colloid release/erosion

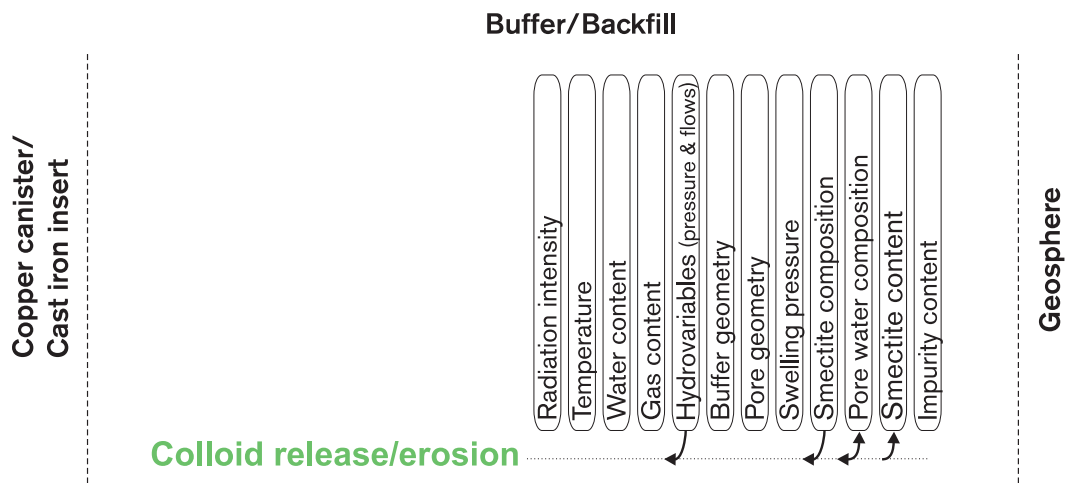


Figure 4-20. Colloid release/erosion.

Overview

Montmorillonite from the expanding buffer can intrude into fractures around the deposition hole. The groundwater in the fractures can erode the buffer. There are two basic types of erosion:

- Mechanical erosion where particles are torn loose by the flowing water
- Chemical erosion where low salinity disperses the clay gel

The processes are influenced by the groundwater flow, the compositions of the groundwater and the clay, and the fracture geometry. The result of the process may be a reduction in the density of the buffer, which can be of importance for a number of other processes in the buffer, and that the buffer supplies the groundwater with clay colloids, which could potentially transport radionuclides.

General description

The sensitivity of the buffer to erosion is dependent on its density, which is in turn dependent on the external pressure that resists swelling. If the bentonite is allowed to expand freely, it swells out to a gel with very low density. Since the gel is made up of thin montmorillonite layers, the bentonite's erosion tendency is related to the magnitude of the cohesion between the expanding layers.

Expansion does not take place completely freely in a fracture due to friction between the bentonite and the fracture wall. The friction gives rise to a residual pressure in the bentonite that decreases with the depth of penetration. After finished swelling, an equilibrium situation arises where further expansion is prevented by forces of friction. However, furthest in at the surface of the gel against the water in the fracture the pressure is close to zero, since there are no forces of friction in the centre of the surface. The innermost gel layer is thus expanded and sensitive to erosion.

If *sufficient water velocity* arises against the surface layer of the gel, the outermost layer will be eroded away. Under this layer the density is higher and the gel is more resistant. A new equilibrium is established and the gel has the same density as before the erosion, and the process is repeated. The erosion rate is limited only by the rate of swelling and the transport capacity of the flowing water.

The buffer consists mainly of a very large number of montmorillonite particles in the form of very thin mineral layers with a thickness of 10 Å and a length/width ratio of up to 1 µm. The binding of these particles to one another in the buffer is dependent on the prevailing physico-chemical conditions, for example temperature and ion concentration.

The mineral layers can be released from each other principally by swelling, i.e. uptake of water between the layers. In the deposition holes, swelling is prevented by the limited volume, and individual colloidal particles can therefore in principle not be formed.

Free swelling leading to the separation of individual mineral layers, or small groups of mineral layers (dispersion), could take place in fractures in the walls of the deposition holes.

Influence of groundwater composition: Theoretically, the clay could form particles that are small enough to diffuse away in the groundwater (colloids). In order for the clay gel to be stable and not be dispersed to a colloidal suspension, the water must contain sufficiently high concentrations of positive ions. Highly charged ions (highly polarizing) are the most effective. Concentrations of divalent ions, especially Ca²⁺, in deep Swedish groundwaters are generally fully adequate. If the concentration is over 0.1 mM (4 ppm), a stable clay gel is obtained. Univalent ions such as Na⁺ can fill the same function, but then a much higher concentration is required.

Influence of groundwater flow: Calculation of the critically high water velocity needed to erode clay gels in fractures shows that it exceeds the mean water velocity in the water-saturated repository by a factor of at least 1,000. This means that the water velocity in channels into which bentonite has penetrated cannot erode away smectite aggregates under normal hydraulic gradients /Le Bell, 1978/.

In the backfill, the risk of erosion is greatest if there is a gap against the roof where the density of the backfill is lowest. This can occur if a gap exists from the start due to inadequate compaction or the occurrence of piping during compaction.

When the backfill has become thoroughly wetted, it strives to expand and consolidate the boundary zone, and the risk of further erosion is eliminated. At the low density which the backfill will probably have at the tunnel roof, however, the expansion capacity of the backfill in accordance with the repository's specification does not suffice to maintain contact with the roof and upper walls of the tunnels, and the risk of washing-away and considerable heterogeneity in the backfill persists. This can be avoided by backfilling with blocks with a higher bentonite content near the tunnel roof.

In SR 97, it is assumed that the backfill has a higher conductivity, of the same order of magnitude as in the surrounding rock. To achieve this, site-specific adaptation of the backfill may be required.

Model studies/experimental studies

Several laboratory studies have provided a basis for estimation of the penetration rate, and models have been derived that have been checked against field data /Le Bell, 1978/.

The calculated penetration of the bentonite gel according to the models is about 0.15 mm after 2 years at a fracture width of 0.1 mm, and 15 mm at 1 mm width. After 10 years the equivalent values are 0.52 and 52 mm, respectively, and after 1,000 years 1.5 and 150 mm. After 100,000 years, the penetration depth may be 2.5 and 250 mm, respectively, with a mean density of the clay gel of 1,500 kg/m³. The results of excavation of the simulated deposition holes in the Stripa BMT showed that the penetration depth of buffer of such density in water-bearing fractures with an aperture of approx. 0.5 mm was 5–10 mm after 2–3 years, which is in good agreement with the predictions.

The conclusion of the modellings, laboratory tests and field results is that the loss of buffer out in fractures that have channel widths that can be accepted with regard to water inflow during buffer application, i.e. about 0.1–0.5 mm, will be negligible.

The concentration of colloids formed from bentonite in granitic groundwater has been tested in laboratory experiments /Missana et al/. With a saturated buffer, the leached-out concentration of colloids was below 1 ppm.

Time perspective

Erosion and colloid formation, to the extent that the processes occur, must be considered on all timescales.

Summary of uncertainties

The estimates made indicate that the risk of chemical and mechanical erosion of large quantities of bentonite is small. The process should, however, be further studied.

Handling in the safety assessment

Base scenario: The above discussion suggests that erosion of the buffer is not of significance for the long-term performance of the repository. The process is neglected in SR 97 but should be further studied.

Canister defect scenario: See base scenario. See also radionuclide transport with colloids in geosphere processes.

Climate change: See base scenario. The effect of changes in groundwater composition may need to be discussed.

Earthquake: See base scenario.

4.7.8 Radiation-induced montmorillonite transformation

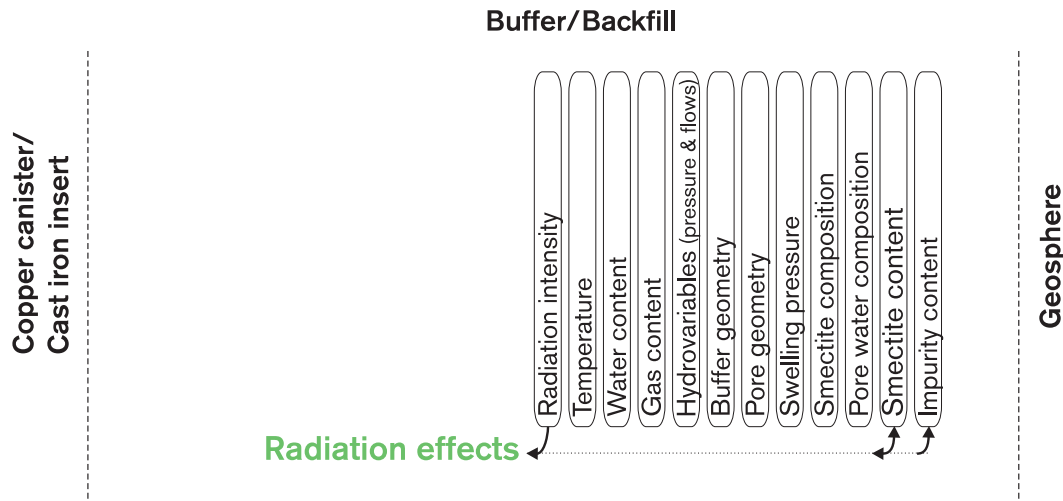


Figure 4-21. Radiation-induced montmorillonite transformation.

Overview, general description

Montmorillonite in the buffer can be broken down by γ radiation. The result is a decrease in the montmorillonite concentration.

Model studies/experimental studies

Experimental studies have shown that the accumulated radiation doses to which the bentonite will be exposed in a deep repository do not cause any measurable changes in the montmorillonite concentration. MX-80 bentonite saturated with weakly brackish water to a density of $2,050 \text{ kg/m}^3$ was irradiated for one year with a total radiation dose of $3 \cdot 10^7 \text{ Gy}$. The specimen was confined in a cylinder whose one closed end consisted of iron and irradiated with a ^{60}Co source, while the other end consisted of a porous steel filter through which a water pressure of 1.5 MPa acted /Pusch et al, 1993/. The irradiated end, which had an adsorbed dose rate of $3,972 \text{ Gy/h}$, was kept at 130°C , and the opposite end, which had a dose rate of 456 Gy/h , at 90°C .

Mineral assays (XRD, IR, CEC) of this specimen and of a parallel specimen not exposed to radiation but to the same hydrothermal environment as the irradiated specimen, showed no significant change in the montmorillonite quantity in either of the specimens.

Time perspective

Natural analogues

Summary of uncertainties

Only one experiment has been conducted and it only involved γ -radiation. The effect of α radiation in connection with a canister failure has thus not been taken into consideration.

Handling in the safety assessment

Base scenario: The process is neglected.

Canister defect scenario: See base scenario.

Climate change: See base scenario.

Earthquake: See base scenario.

4.7.9 Radiolysis of pore water

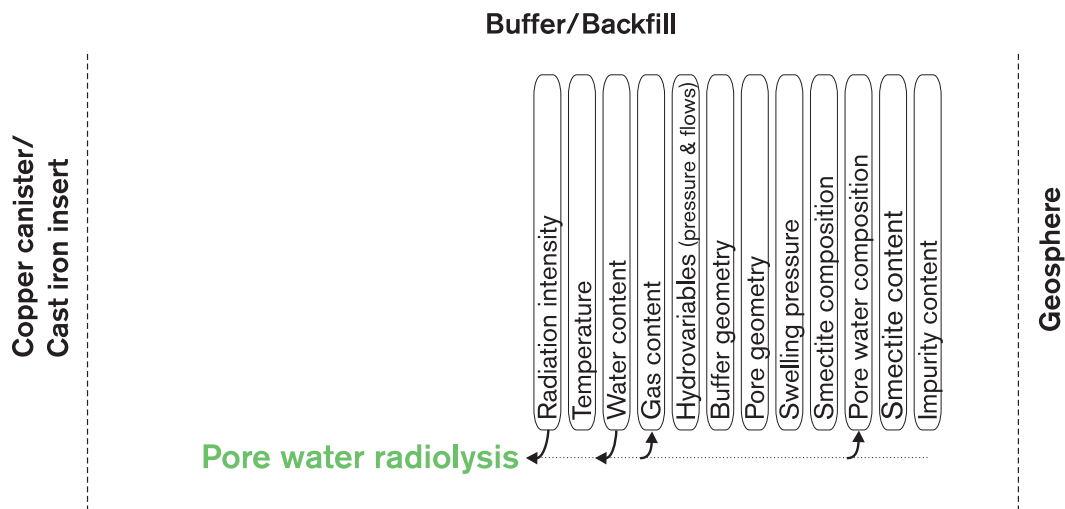


Figure 4-22. γ -radiolysis of pore water.

Overview, general description

Gamma radiation from the fuel that penetrates through the canister can decompose pore water by radiolysis, forming OH radicals, H_2 , O_2 and several other components. The oxygen is consumed rapidly by oxidation processes which affect the redox potential, while the hydrogen is transported away. The canister's wall thickness is, however, sufficient so that the effect of γ -radiolysis on the outside is negligible /Werme, 1998/.

Model studies/experimental studies

Time perspective

Natural analogues

Summary of uncertainties

Handling in the safety assessment

Base scenario: The process is neglected.

Canister defect scenario: The process is neglected.

Climate change: The process is neglected.

Earthquake: The process is neglected.

4.7.10 Microbial processes

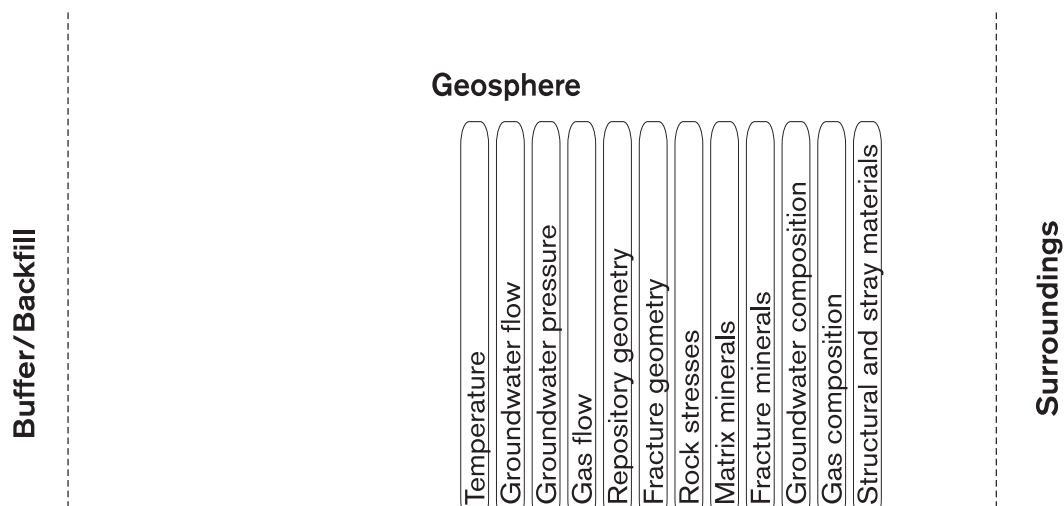


Figure 4-23. Microbial processes.

Overview, general description

Microbial processes can under certain conditions result in the formation of gas and sulphide. Gas formation can give rise to disrupting mechanical effects on the buffer, and sulphide can corrode the copper canister. Sulphide formation must take place in the buffer, near the canister, and be of considerable scope for corrosion to be possible, mainly due to the fact that the solubility of sulphide, and thereby its diffusive transport capacity, is very low. It is also known that bacteria can bind and transport metals in ionic form /Pedersen and Albinsson, 1991/. In order for the above-described processes to take place, the bacteria must be active and have access to water, nutrients and space /Pedersen and Karlsson, 1995/.

Many bacteria are very radiation-resistant, and the radiation intensity in the buffer does not constitute an obstacle to bacterial life there.

In a full-scale experiment with buffer material consisting of 50/50 percent sand/bentonite, live bacteria could, with few exceptions, only be detected at moisture ratios in excess of 15 percent /Stroes-Gascoyne et al, 1997/. This is equivalent to a moisture ratio of about 30 percent in a pure bentonite buffer as regards availability of water for bacteria. The reason for the poor survival rate is that when the bentonite material in the buffer swells, water is absorbed between the layers in the montmorillonite from the

surroundings. Bacteria must then compete for available water with the montmorillonite, which means that the bacteria must compensate for drying-out by pumping in ions from the outside so that the osmotic pressure is equal inside and outside the cell membrane. Another strategy is for the bacteria to manufacture polyalcohols, or other osmotically active organic molecules. This requires a supply of energy and salts, but the supply of energy, e.g. degradable organic matter, is limited in bentonite. This may mean that even if a bacterium should be able to actively compensate for a falling water activity, this is not possible in a compacted buffer. A high buffer density can thus prevent bacterial growth and result in a kill-off of certain microbe groups. Drying-resistant bacteria can survive in inactive form. Ongoing laboratory experiments indicate that sulphate-reducing bacteria can only survive in swelling bentonite if they exist in the form of endospores. A bacterial endospore is a drying-resistant inactive form in which the bacterium can survive, but does not then form sulphide or gas. In summary, bacteria are not expected to survive in a water-saturated buffer with a density above 1,800 kg/m³ /Pedersen et al, 1995/.

Bacteria vary in size from 0.2 to 600 µm and are unable to move in a buffer, since the space between the clay layers is of the order of 0.002 µm. Bacterial radionuclide transport should therefore be able to be ruled out in a functioning buffer.

The possibilities of bacterial activity in the backfill material increase with decreasing density and increasing water supply. Many bacteria consume oxygen in their respiration of organic matter, methane, iron(II) and sulphur. Bacterial activity in the backfill can therefore be advantageous, since it will make a considerable contribution to desirable oxygen reduction there.

Model studies/experimental studies

A full-scale experiment with a heated canister and 50/50 percent bentonite/sand was carried out in AECL's underground research laboratory in Canada. With few exceptions, live bacteria were only found in bentonite with a moisture content in excess of 15 percent, which is roughly equivalent to the availability of water in a Swedish buffer with a density of 2,000 kg/m³ /Pedersen and Karlsson, 1995/. Elevated temperature had no influence on the occurrence of bacteria. The conclusion was that the bacteria in the parts of the buffer with a moisture ratio of less than 15 percent died of drying-out

The Canadian experiment was followed up by laboratory experiments. Two species of sulphate-reducing bacteria (sulphide formers) were exposed to MX-80 bentonite of varying density. Surviving bacteria could be detected at up to 1,800 kg/m³, but no life was found at 2,000 kg/m³ /Motamedi et al, 1996/.

Additional experiments are under way or planned to investigate the probability that bacteria will survive and be active in compacted bentonite. The working hypothesis at present is that this probability is very low.

Time perspective

Any bacterial processes in buffer and backfill ought to start more or less immediately, after groundwater reaches the buffer and backfill. Bacterial activity in the backfill at least may possibly be greatest immediately after backfilling, only to decline as organic matter and oxygen in the backfill are consumed.

Natural analogues

There is a natural analogue in Dunarobba, Italy, where a bentonite slide buried a forest approximately one and a half million years ago. Trees that have not been decomposed by microorganisms can still be found. This indicates that conditions for microbial activity in bentonite clay are unfavourable.

Summary of uncertainties

There are many millions of different species of bacteria and at least a hundred different sulphate-reducing bacteria. It is not possible to test the working hypothesis (that the bacterium cannot exist and be active in highly-compacted bentonite) on all of these species. Instead, the work is focused on investigating representatives of different groups with different requirements on water, temperature and nutrients. The working hypothesis was recently tested with 10 different species during the LOT test on Äspö, and laboratory experiments have been initiated where survival and activity of these 10 bacteria will be studied. Finally, tests will be performed to investigate bacteria and their activity during the field experiments with backfilling and a prototype repository on Äspö.

Handling in the safety assessment

Base scenario: Bacterial processes are neglected, provided that the density of the buffer/backfill material is not less than 1,800 kg/m³.

Canister defect scenario: See base scenario.

Climate change: See base scenario.

Earthquake: See base scenario.

4.8 Radionuclide transport

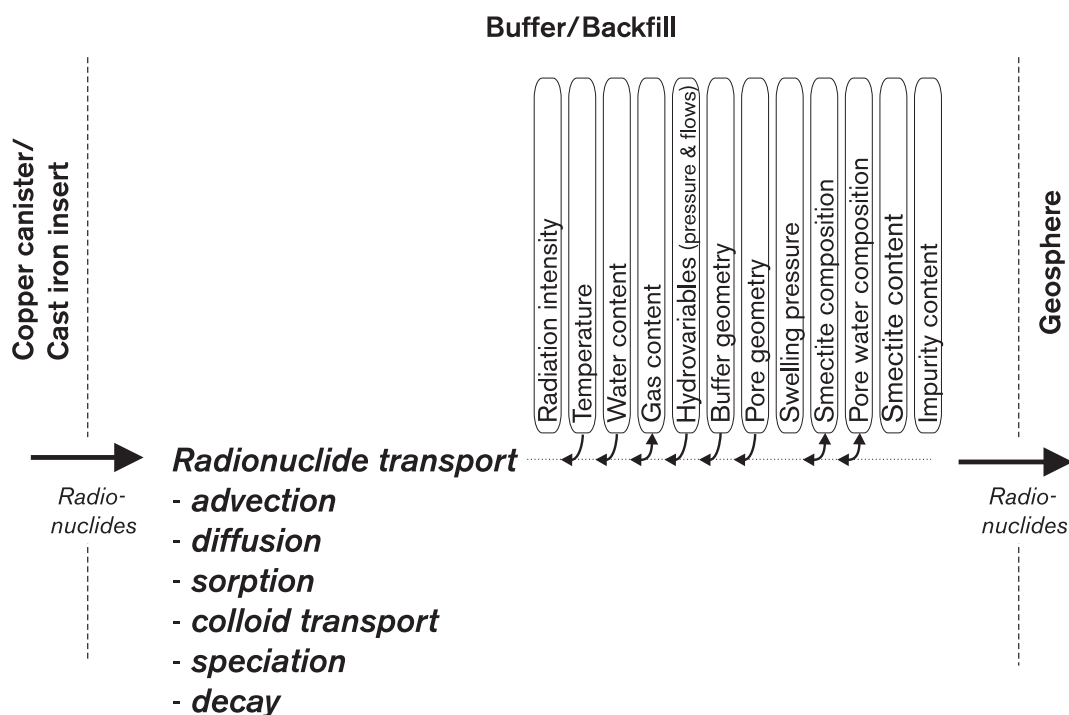


Figure 4-22. Radionuclide transport in buffer/backfill.

4.8.1 Overview

After water saturation, *radionuclide* transport in the buffer is expected to take place exclusively by *diffusion* in the pores of the buffer, possibly also on the surfaces of the clay particles. Neither *advection* nor *colloid transport* occurs, due to the properties of the buffer. Radionuclides can be sorbed to the surfaces of the montmorillonite. Of crucial importance for this process is the chemical form of the radionuclide, which is determined by the chemical environment in the buffer via the process of *speciation*. Along with transport conditions, *radioactive decay* determines to what extent radionuclides from a broken canister will decay before reaching the outer boundary of the buffer.

4.8.2 Advection

Owing to the low hydraulic conductivity of the buffer material, all transport of solutes in the buffer after water saturation is expected to take place by diffusion, see section 4.5.2.

The backfill has a hydraulic conductivity and a diffusivity that lie in a range where both diffusion and advection can be important transport mechanisms. However, calculations show that even with a very high flow through the backfill, the outward transport of radionuclides will be no more than twice as much as in the case with diffusion alone /Moreno, 1999/.

4.8.3 Colloid transport

General description

Particles with sizes in the order of 10^{-9} - 10^{-6} m (colloids) could form on dissolution of the fuel. The diffusive transport of radionuclides with colloids through highly-compacted bentonite is, however, assumed to be negligible, due to the tortuosity and small size of the bentonite pores. Experiments with 15 nm gold colloids show that the microstructure of a bentonite with a dry density of $1,000 \text{ kg/m}^3$ effectively filters colloids /Kurosawa et al, 1997/.

Model studies/experimental studies

In diffusion tests with large organic molecules in bentonite, no transport could be detected. No direct measurements of the bentonite's ability to filter colloids have been performed, however.

Time perspective

Natural analogues

Summary of uncertainties

Handling in the safety assessment

Base scenario: Not applicable.

Canister defect scenario: Does not occur, provided the buffer completely envelops the canister and has a density of at least 1,000 kg/m³.

Climate change: If the evolution leads to canister damage: See the canister defect scenario. Otherwise: See the base scenario.

Earthquake: If the evolution leads to canister damage: See the canister defect scenario. Otherwise: See the base scenario.

4.8.4 Speciation of radionuclides

General description

Speciation of radionuclides is of importance for sorption and diffusion in the buffer. It is influenced by what speciation the nuclide had at the boundary to the buffer, i.e. inside the canister (see section on fuel/cavity), but also by the chemical conditions in the buffer.

Model studies/experimental studies

If the water chemistry in the buffer is known, the speciation of radionuclides can be calculated with a thermodynamic equilibrium model, e.g. EQ3/6.

Time perspective

All.

Natural analogues

Not applicable.

Summary of uncertainties

The same applies as for speciation in fuel/cavity, see section 2.7.8.

Handling in the safety assessment

Base scenario: Not applicable.

Canister defect scenario: The data that are used for diffusion and sorption are based on one (or more) assumed speciation(s) calculated for the water compositions that can occur in the buffer.

Climate change: If the evolution leads to canister damage: See the canister defect scenario. Otherwise: See the base scenario. Any changes in pore water composition influence the speciation, which in turn influences diffusion and sorption.

Earthquake: If the evolution leads to canister damage: See the canister defect scenario. Otherwise: See the base scenario.

4.8.5 Sorption

General description

The following discussion is based on /Yu and Neretnieks, 1997/.

The surface of smectitic clays has a permanent negative charge, see section 4.7.4. The charge imbalance between the layers is neutralized by exchangeable cations. When the clay is thoroughly saturated, the exchangeable cations are hydrated and an electrical double layer is formed in the water/clay interface.

The charge-balancing cations are readily exchangeable and can be replaced by other cations in the solution that is in contact with the clay surface. The sorption of cations in smectite minerals takes the form of ion exchange reactions and can be modelled with thermodynamic equilibrium constants or selectivity coefficients. Ion exchange is the typical sorption mechanism for alkali, alkaline-earth and many transition metals.

Radionuclides can also be sorbed via reactions with the functional groups on the surface. The functional groups on the surface are chemically reactive molecular units located so that they can be reached by molecules in solution. Since the functional groups are locked in the solid material, their reactivity is dependent on the reaction stage of the nearest groups. When a functional group reacts with a molecule from the solution to form a stable unit, a so-called surface complex has been formed and the sorption mechanism is called surface complexation. Most actinides and lanthanoids form surface complexes. Nuclides sorbed as surface complexes cannot be transported by surface diffusion, see section 4.8.6.

Influence of pore water composition: The sorption of cations by ion exchange is affected by the concentration of competing ions in solution – the sorption of strontium, for example, is highly dependent on the calcium concentration, since the selectivity for calcium is higher. The dissolution of accessory minerals in the bentonite can raise the ionic strength and thereby reduce the sorption of radionuclides in cationic form.

Influence of density: Sorption is also influenced by density, for example the K_d for caesium is halved when the density of the water-saturated system changes from 1,300 to 1,950 kg/m³.

Influence of temperature: Most experiments have been carried out at room temperature. An increase or decrease of the temperature is of importance for sorption, but the effect in the temperature range expected in the repository is deemed to be covered with good margin by other uncertainties.

Model studies/experimental studies

In studies of radionuclide transport from a repository, the sorption equilibrium is normally described as a linear relationship between the sorbed concentration and the concentration in solution, characterized by a distribution coefficient K_d , which is defined

$$K_d = \frac{q}{C_w}$$

where q is the sorbed concentration as mass per weight unit of solid phase and C_w the concentration in solution. When the concentration of the species in solution is low, which is normally the case for radionuclides, the linear approximation gives a satisfactory result. There are, however, other relationships that can be applied at higher concentrations, e.g. the Freundlich and Langmuir isotherms or ion exchange models.

Surface complexation models with parameters from well-controlled experiments should be able to be used to better describe the sorption's dependence on external parameters such as pH, etc.

Time perspective

Sorption in the buffer is an important process for many radionuclides. The timescales that are of interest are dependent on the half-life of the individual nuclide. If the travel time through the buffer is of the same order of magnitude or longer, sorption is of great importance for the amount released. Otherwise its importance is secondary.

Natural analogues

Not applicable.

Summary of uncertainties

The distribution coefficient K_d is a measured value which only applies for the conditions under which the value was measured, and cannot really be extrapolated to other conditions. The case with sorption in highly-compacted bentonite is particularly complicated, since virtually all water is interlamellar and it can be difficult to define the chemistry. This makes it impossible to apply the results of sorption measurements in batch tests.

In /Yu and Neretnieks, 1997/, values are given for the apparent diffusivity, D_a , which is the parameter that is really of importance for the retardation of radionuclides, and the effective diffusivity, D_e , which controls the transport capacity through the buffer, see section 4.8.6.

Handling in the safety assessment

Base scenario: Ion exchange models can be used for calculation of the transformation from Na-smectite to Ca-smectite, see section 4.7.4.

Canister defect scenario: The sorption is calculated with the model COMP23 and data are taken from /Yu and Neretnieks, 1997/. The report contains both realistic and pessimistic data sets for both saline and non-saline water.

In the case of the backfill, the sorption coefficients for the radionuclides are calculated for a 15/85 mixture for all sites, see Andersson /1999/. SR 97 does not take into account the fact that the backfill may have to be made site-specific to meet the stipulated requirements.

Climate change: If the evolution leads to canister damage: See the canister defect scenario. Otherwise: See the base scenario. Any changes in pore water composition influence speciation, which in turn influences diffusion and sorption.

Earthquake: If the evolution leads to canister damage: See the canister defect scenario. Otherwise: See the base scenario.

4.8.6 Diffusion

General description

The entire discussion of this process applies not only to radionuclides, but also to other solutes transported in the buffer (canister corrodants, potassium and calcium which can affect the bentonite, etc.).

Owing to the low hydraulic conductivity of the bentonite, solute transport will be dominated by diffusion, see section 4.5.2. Diffusion mechanisms for radionuclides, together with selected diffusion data, are described in detail in /Yu and Neretnieks, 1997/. The following text is based on that presentation.

Diffusion in a porous medium takes place according to Fick's first law:

$$J = -D_p \varepsilon \frac{dC_p}{dx},$$

where J is the diffusive flux, D_p the diffusion coefficient in the pore solution, ε is the porosity and C_p the concentration of the diffusing species.

The pore diffusion coefficient in the pore solution is lower than the diffusion coefficient in a free volume of the same solution D_w . This is due to the tortuosity of the pores, which increases the length of the diffusion path, and the fact that there may be "cul-de-sacs" in some pores. The relationship between D_p and D_w is:

$$D_p = D_w \frac{\delta}{\tau^2}$$

where δ is the constrictivity (the cul-de-sacs) and τ the tortuosity of the pores.

For sorbing species there are experimental indications of yet another diffusion mechanism, which is usually called surface diffusion. The reason for surface diffusion may be that cations, sorbed in ion exchange positions, are hydrated in the water-saturated clay and can change place by diffusion. They are, however, bound to nearness to the montmorillonite surface and in that way sorbed with ion exchange.

Fick's second law, the diffusion equation, describes changes in concentration of a diffusing species in time and space. For diffusion of a sorbing species in a porous material, it can be formulated as follows:

$$\varepsilon \frac{\partial C_p}{\partial t} + \frac{\partial q}{\partial t} = \varepsilon D_p \frac{\partial^2 C_p}{\partial x^2} + \rho D_s \frac{\partial^2 q}{\partial x^2}$$

where ρ is the material's bulk density and D_s the surface diffusion coefficient. If linear sorption is assumed, the equation can be written:

$$\frac{\partial C_p}{\partial t} = \frac{D_e}{\varepsilon + K_d \rho} \frac{\partial^2 C_p}{\partial x^2} = D_a \frac{\partial^2 C_p}{\partial x^2}$$

where K_d is the distribution coefficient, D_e is the effective and D_a the apparent diffusion constant, which are defined as follows:

$$D_e = \varepsilon D_p + K_d \rho D_s$$

$$D_a = \frac{D_e}{\varepsilon + K_d \rho}$$

With the assumption of a linear sorption isotherm, C_p can be replaced by the total concentration in the porous material by multiplying by $\varepsilon + K_d \rho$ in the previous equation, which gives:

$$\frac{\partial C}{\partial t} = D_a \frac{\partial^2 C}{\partial x^2}$$

where C is the total concentration. This is the equation that is normally used for diffusion studies of radionuclides in bentonite. For diffusion of non-sorbing species, D_a is equal to D/ε .

Surface diffusion: It has been observed in several experiments that the apparent diffusion coefficient (D_a) for cations and their respective distribution coefficient (K_d) have not agreed. D_a has been higher than expected from K_d and traditional diffusion-sorption theory. Two explanations of the phenomenon have been proposed: surface diffusion or reduction of K_d in highly-compacted bentonite compared with batch experiments (loose gels or suspensions).

Surface diffusion can be explained by cation diffusion in the electrical double layer, see section 4.8.5. The absence of anions in the double layer makes it possible for cations to move relatively freely. The sorbed species thus have an alternative transport pathway with very high gradients, even though the diffusion coefficient may be lower than in the pores.

Several studies support the theory of surface diffusion, but the phenomenon is still in question. It is, however, clear that certain cations may have high diffusivities (be transported effectively), which must be taken into consideration in safety assessments. This is particularly true of the elements Cs, Sr and Ra.

Influence of sorption: Alternative explanations of the unexpectedly high diffusion coefficients for certain cations may be that all surfaces in highly-compacted bentonite are not available for sorption, which means that K_d decreases, or that the actual ionic strength of the compacted bentonite is higher than in experiments with loose bentonite gels, which also influences sorption.

Influence of density: The transport of radionuclides in bentonite is influenced by the density of the material (the degree of compaction). It is not clear whether this is due to variation in porosity or altered sorption. In most experiments, however, the apparent diffusivity decreases with increasing density.

Anion exclusion: When bentonite has such high density that the electrical double layers between two planes are superimposed, a phenomenon known as anion exclusion occurs. Anions cannot penetrate into the interlamellar pores due to the electrostatic forces between the negatively charged surfaces and the anion. Anion exclusion significantly reduces the porosity available for diffusion. The effect of anion exclusion becomes less at high salinities, and in sand-bentonite mixtures it is negligible. The safety-related importance of anion exclusion is very great – it is one of the few processes that limits the transport of anions from a damaged canister.

The importance of montmorillonite composition: The interlamellar space is dependent on which ion is in the ion exchange positions. Calcium will eventually replace the sodium that was originally present in the ion exchange positions. This will cause the space and the diffusivity to increase.

Importance of speciation: Different species of the same element can have radically different diffusivities. As mentioned previously, anionic species have lower diffusivity than cations, but there are other examples as well: strontium has lower diffusivity at high pHs than at neutral ones, which can be explained by the formation of the neutral complex SrCO_3 .

Model studies/experimental studies

A large number of investigations are described in the literature concerning diffusion experiments in bentonite and similar clays. It is important to observe which technique has been used and how the diffusivities have been determined. If, for example, metal filters have been used, they can greatly influence the results. There is a detailed discussion in /Yu and Neretnieks, 1997/ of different experimental methods and how the results can be interpreted.

Time perspective

Diffusion processes in the buffer material are of the greatest importance on all timescales. If the canister is intact, the process is of importance for the stability of the canister and the buffer. In the event of a defective canister, diffusion is very important in delaying, reducing and in many cases completely preventing releases of radionuclides.

Natural analogues

The usefulness of natural analogues for determining diffusion constants is limited due to the difficulty of determining what conditions existed in the past.

Summary of uncertainties

There are shortcomings in our understanding of diffusion processes in compacted bentonite. The data used in the safety assessment are normally taken directly from experimental observations. In this way the experiments in the modelling are plagiarized without full awareness of all underlying details. /Ochs 1997/ contains a review and summary of the uncertainties surrounding diffusion and sorption in bentonite.

Handling in the safety assessment

Base scenario: Diffusion models are used to calculate canister corrosion and the evolution of the chemical environment in the near field, mainly the influence on/of the buffer material.

Canister defect scenario: Diffusion is one of the most important processes when it comes to determining the release of radionuclides from a damaged canister. Diffusive transport is calculated using the model COMP23 and data is taken from /Yu and Neretnieks, 1997/. The report contains both realistic and pessimistic data sets for both saline and non-saline water.

Climate change: If the evolution leads to canister damage: See the canister defect scenario. Otherwise: See the base scenario. Any changes in pore water composition can influence sorption and anion exclusion and thereby diffusion.

Earthquake: If the evolution leads to canister damage: See the canister defect scenario. Otherwise: See the base scenario.

4.8.7 Decay

See decay in fuel/canister, section 2.3.1. Decay of radionuclides in the buffer is handled in the safety assessment with the models used to calculate radionuclide transport in the near field.

4.9 References

- Aagard P, Helgeson H C, 1983.** Activity/composition relations among silicates in aqueous solution II. *Clay and Clay Minerals* 31, 207.
- Abercrombie H J, Hutcheon I E, Bloch J D, de Caritat P, 1994.** Silica activity and the smectite-to-illite reaction. *Geology*, v. 22, p. 539–542.
- Alonso E, Alcoverro J, 1997.** CATSIUS CLAY – Calculation and testing of behaviour of unsaturated clay as barrier in radioactive waste repositories (Stage 1: Verification exercises). EC Internal Report.
- Bjurström H, 1997.** Värmeöverföring i en spalt. SKB AR D-97-07, Svensk Kärnbränslehantering AB (in Swedish).
- Boles J R, Franks S G, 1979.** Clay diagenesis in wilcox sandstones of southwest Texas: Implication of smectite diagenesis on sandstone cementation. *J. Sediment Petrol* 49:55–70.
- Bond A, Hoch A, Jones G, Tomczyk A, Wiggin R, Worraker W, 1997.** Assessment of a spent fuel disposal canister. Assessment studies for a copper canister with cast steel inner component. SKB TR 97-19, Svensk Kärnbränslehantering AB.
- Brusewitz A-M, 1986.** Chemical and physical properties of paleozoic bentonites from Kinnekulle, Sweden. *Clays and Clay Mineralogy* 34:442–454.
- Burst J F Jr., 1959.** Diagenesis of Gulf Coast clayey sediments and its possible reaction to petroleum migration. *AAPG Bull.* 68:73–93.
- Bäckblom G, 1996.** Preliminär utformning av djupförvarets närområde. Djupförvar, SKB AR D-96-011, Svensk Kärnbränslehantering AB (in Swedish).
- Börgesson L, 1986.** Model shear tests of canisters with smectite clay envelopes in deposition holes. SKB TR 86-26, Svensk Kärnbränslehantering AB.
- Börgesson L, 1989.** Interim report on the settlement test in Stripa. SKB TR 89-29, Svensk Kärnbränslehantering AB.
- Börgesson L, 1992.** Interaction between rock, bentonite buffer and canister. FEM calculations of some mechanical effects on the canister in different disposal concepts. SKB TR 92-30, Swedish Nuclear Fuel and Waste Management Co.
- Börgesson L, 1993a.** Interim report II on the pilot settlement test in Stripa. SKB TR 93-09, Svensk Kärnbränslehantering AB.
- Börgesson L, 1993b.** Study of the mechanical function of the buffer in the concept with two canisters in a KBS3 deposition hole. SKB AR 93-13, Svensk Kärnbränslehantering AB.

- Börgesson L, Fredrikson A, Johannesson L-E, 1994.** Heat conductivity of buffer materials, SKB TR 94-29, Svensk Kärnbränslehantering AB.
- Börgesson L, Hernelind J, 1995.** DECOVALEX 1 – Test Case 3: Calculation of the Big Ben Experiment – Coupled modelling of the thermal, mechanical and hydraulic behaviour of water-unsaturated buffer material in a simulated deposition hole. SKB TR 95-29, Svensk Kärnbränslehantering AB.
- Börgesson L, Johannesson L-E, 1995.** Thermo-Hydro-Mechanical modelling of water unsaturated buffer material. Status 1995. SKB AR 95-32, Svensk Kärnbränslehantering AB.
- Börgesson L, Johannesson L-E, Sandén T, Hernelind J, 1995.** Modelling of the physical behaviour of water-saturated clay barriers. Laboratory tests, material models and finite element application. SKB TR 95-20, Svensk Kärnbränslehantering AB.
- Börgesson L, Hernelind J, 1997.** THM-modelling of a small scale wetting-heating test on compacted bentonite. CATSIUS CLAY PROJECT. Benchmark 2.2. SKB PR U-97-16, Svensk Kärnbränslehantering AB.
- Claesson J, Probert T, 1996.** Temperature field due to time dependent heat sources in a large rectangular grid. 1- Derivation of analytical solution. SKB TR 96-12, Svensk Kärnbränslehantering AB.
- Colten-Bradley V A, 1987.** Role of pressure in smectite dehydration – Effects on geopressure and smectite-to-illite transformation. AAPG Bull. 71:1414–1427.
- Couture R A, 1985.** Steam rapidly reduces the swelling capacity of bentonite. Nature, Vol. 318 (p. 50).
- Dixon D A, Gray M N, Graham J, 1996.** Swelling and hydraulic properties of bentonites from Japan, Canada and the USA. Environmental Geotechnics, Kamon (ed.), Balkema, Rotterdam.
- Donohew A, Horseman S T, Harrington J F, 1998.** Gas entry into unconfined and initially water-saturated clay pastes between the plastic and liquid limits. Technical Report WE/98/-, Fluid Processes Group, British Geological Survey (in prep).
- Eberl D D, Hower J, 1976.** Kinetics of illite formation: Geol. Soc. Amer. Bull. 87, 1326–1330.
- Elliott W C, Matisoff G, 1996.** Evaluation of kinetic models for the smectite to illite transformation. Clays and Clay Minerals 44: 77–87.
- Fredlund D G, Rahardjo H, 1993.** Soil mechanics for unsaturated soils. John Wiley & Sons, Inc., New York.
- Fritz B, Kam M, Tardy Y, 1984.** Geochemical simulation of the evolution of granitic rocks and clay minerals submitted to a temperature increase in the vicinity of a repository for spent nuclear fuel. KBS TR 84-10. Svensk Kärnbränslehantering AB.
- Gunnarsson D, Johannesson L-E, Sandén T, Börgesson L, 1996.** Field test of tunnel backfilling. PR HRL 96-28, Svensk Kärnbränslehantering AB.

- Harrington J F, Horseman S T, 1997.** Gas transport properties of clays and mudrocks. In: *Mudrocks at the Basin Scale*, Special Publication, ed. A. J. Fleet, Geological Society of London (in press).
- Harrington J F, Horseman S T, 1999.** Gas transport properties of clays and mudrocks. In: Aplin, A C, Fleet, A J and Macquaker, J H S (eds.) *Muds and Mudstones: Physical and Fluid Flow Properties*, Geological Society, London, Special Publications 158, 107–124
- Hibbitt, Karlsson and Sorensson.** ABAQUS manuals.
- Horseman S T, Harrington J F, 1997.** Study of gas migration in Mx80 buffer bentonite. Technical Report WE/97/7, Fluid Processes Group, British Geological Survey.
- Hower J, Elsingher E, Hower M E, Perry E A, 1976.** Mechanism of burial metamorphism of argillaceous sediment: 1. Mineralogical and chemical evidence. *Geol. Soc. Am. Bull.* 87:725–737.
- Huang W-L, Longo J M, Pevear D R, 1993.** An experimentally derived kinetic model for smectite-to-illite conversion and its use as a geothermometer. *Clays and Clay Minerals* 41, 162–177.
- Hökmark H, 1995.** Smectite-to-illite conversion in bentonite buffers; application of a technique for modeling degradation processes. SKB AR 95-07, Svensk Kärnbränslehantering AB.
- Hökmark H, 1996.** Canister positioning. SKB AR D-96-014, Svensk Kärnbränslehantering AB.
- Jansson M, Eriksen T, 1998.** CHEMLAB – in situ diffusion experiment using radioactive tracers. *Radiochim Acta* 82, p. 153–156.
- Johannesson L-E, Börgesson L, Sandén T, 1998.** Backfill materials based on crushed rock (part 2). Geochemical properties determined in the laboratory. SKB IPRL-99-23, Svensk Kärnbränslehantering AB (in press).
- Karnland O, Pusch R, Sandén T, 1992.** Electrolytens betydelse för de fysikaliska egenskaperna hos MX-80 bentonit. SKB AR 92-35, Svensk Kärnbränslehantering AB.
- Karnland O, Pusch R, Sandén T, 1994.** Effects of cyclic hydration/dehydration on Na- and K-bentonites. SKB AR 94-40, Svensk Kärnbränslehantering AB.
- Karnland O, 1995.** Salt redistribution and enrichment in compacted bentonite exposed to a thermal gradient – results from laboratory tests. SKB AR 95-31. Svensk Kärnbränslehantering AB.
- Karnland O, Pusch R, Warfvinge P, 1995.** Smectite-to-illite conversion models. Factors of importance for KBS3 conditions. SKB AR 95-27, Svensk Kärnbränslehantering AB.
- Karnland O, 1997a.** Bentonite swelling pressure in strong NaCl solutions. Correlation between model calculation and experimentally determined data. SKB TR 97-31, Svensk Kärnbränslehantering AB.

- Karnland O, 1997b.** Cement/bentonite interaction. Results from 16 month laboratory tests. SKB TR 97-32, Svensk Kärnbränslehantering AB.
- Knutsson S, 1983.** On the thermal conductivity and thermal diffusivity of highly compacted bentonite. SKB TR 83-27, Svensk Kärnbränslehantering AB.
- Kurosawa S, Yui M Yoshikawa H, 1997.** Experimental study of colloid filtration by compacted bentonite. In: Scientific Basis for Nuclear Waste Management XX edited by Gray W and Triay I (MRS symp. proc. 465) pp. 963–970.
- Le Bell J C, 1978.** Colloid chemical aspects of the “confined bentonite concept”. KBS Technical Report 97.
- Low P F, 1987.** Structural component of the swelling pressure of clays. *Langmuir*, 3, 18.
- Lynch F L, 1985.** The stoichiometry of the smectite-to-illite reaction in a contact metamorphic environment. M.S. Thesis, Hanover, N.H. Dartmouth College. 93 p.
- Lynch F L, 1997.** Frio shale mineralogy and the stoichiometry of the smectite-to-illite reaction: the most important reaction in clastic sedimentary diagenesis. *Clays and Clay Minerals*, vol. 45, No. 5:618–631.
- Missana T, Turrero M J, Melón A, Adell A, Yllera A, Gutiérrez M G.** Laboratory Experiments: colloid characterisation, colloid generation batch and column experiments in Project Caress 2nd Annual Progress Report
- Moreno L, 1999.** Impact of the water flow rate in the tunnel on the release of radionuclides. SKB R-xx-xx, Svensk Kärnbränslehantering AB (in preparation).
- Motamedi M, Karland O, Pedersen K, 1996.** Survival of sulfate reducing bacteria at different water activities in compacted bentonite. *FEMS Microbiol. Lett.* 141:83–87.
- Müller-Vonmoos M, Kahr G, 1983.** Mineralogische Untersuchungen von Wyoming Bentonit MX-80 und Montigel, Nagra Technischer Bericht 83–12.
- Müller-Vonmoos M, Kahr G, Madsen F T, 1990.** Investigation of Kinnekulle K-bentonite aimed at assessing the long-term stability of bentonites under repository conditions. *Eng. Geol.*, Vol. 28 (pp. 269–280).
- Murdoch L C, 1993.** Hydraulic fracturing of soil during laboratory experiments. Part 2. Propagation. *Geotechnique*. 43(2), 267–276.
- Nash P J, Swift B T, Goodfield M, Rodwell W R, 1998.** Modelling gas migration in compacted bentonite. POSIVA 98-08. Posiva Oy, Finland.
- Newman A C D (ed.), Brown G, 1987.** The chemical constitution of clays, mineralogical society monograph No.6.
- Norrish K, Quirk J P, 1954.** Crystalline swelling of montmorillonite. *Nature* 173: 255–256.
- Ochs M, 1997.** Review of a report on diffusion and sorption properties of radionuclides in compacted bentonite. SKB R-97-15, Svensk Kärnbränslehantering AB.

- Pedersen K, Albinsson Y, 1991.** Effect of cell number, pH and lanthanide concentration on the sorption of promethium by *Shewanella putrefaciens*. *Radiochim. Acta* 54:91–95.
- Pedersen K, Karlsson F, 1995.** Investigations of subterranean microorganisms – Their importance for performance assessment of radioactive waste disposal. SKB TR 95–10, Svensk Kärnbränslehantering AB.
- Pedersen K, Motamedi M, Karnland O, 1995.** Survival of bacteria in nuclear waste buffer materials. The influence of nutrients, temperature and water activity. SKB TR 95-27, Svensk Kärnbränslehantering AB.
- Perry E A Jr, Hower J, 1970.** Burial diagenesis in Gulf Coast pelitic sediments. *Clays and Clay Minerals*. 18:165–177.
- Philip J R, de Vries D A, 1957.** Moisture movement in porous materials under temperature gradients. *Trans. Amer. Geophys. Union*, vol. 38, no. 2, pp. 222–232.
- Pusch R, 1980.** Water uptake, migration and swelling characteristics of unsaturated and saturated highly compacted bentonite. SKBF/KBS TR 80-11. Svensk Kärnbränsleförsörjning AB.
- Pusch R, 1983a.** Stability of bentonite gels in crystalline rock – Physical aspects. SKBF/KBS TR 83-04. Svensk Kärnbränsleförsörjning AB.
- Pusch R, 1983b.** Stability of deep-sited minerals in crystalline rock – chemical aspects. SKBF/KBS TR 83-16. Svensk Kärnbränsleförsörjning AB.
- Pusch R, Börgesson L, 1983.** Buffer Mass Test – Improved models for water uptake and redistribution in the heater holes. Stripa Project Int. Rep. 83-05, Svensk Kärnbränslehantering AB.
- Pusch R, 1985a.** Buffertar av bentonitbaserade material i siloförvaret. SKB AR SFR 85-08, Svensk Kärnbränslehantering AB.
- Pusch R, Börgesson L, Ramqvist G, 1985a.** Final Report of the Buffert Mass Test – Volume II: Test results. Stripa Project TR 85-12, Svensk Kärnbränslehantering AB.
- Pusch R, 1985b.** Final Report of the Buffer Mass Test – Volume III: Chemical and physical stability of the buffer materials. Stripa Project TR 85-14, Svensk Kärnbränslehantering AB.
- Pusch R, Ranhagen L, Nilden K, 1985b.** Gas migration through Mx80 bentonite. Nagra Technical Report NTB-85-36. Nagra Switzerland.
- Pusch R, Adey R, 1986.** Settlement of clay-enveloped radioactive canisters. *Applied Clay Science*, Vol. 1 (pp. 353–365).
- Pusch R, Karnland O, 1988.** Hydrothermal effects on montmorillonite. A preliminary study. SKB TR 88-15, Svensk Kärnbränslehantering AB.
- Pusch R, Karnland O, 1991.** Final Report of the Rock Sealing Project. – Sealing properties of smectitic clay grouts. Stripa Project TR 91-30, Svensk Kärnbränslehantering AB.

- Pusch R, Börjesson L, 1992.** PASS – Project on alternative systems study. Performance assessment of bentonite clay barrier in three repository concepts: VDH, KBS-3 and VLH. SKB TR 92-40, Svensk Kärnbränslehantering AB.
- Pusch R, Karnland O, Lajudie A, Decarreau A, 1993.** MX-80 clay exposed to high temperatures and gamma radiation. SKB TR 93-03, Svensk Kärnbränslehantering AB.
- Pusch R, 1994.** Waste disposal in rock. Developments in geotechnical engineering, 76. Elsevier Publ. Co.
- Pusch R, 1995a.** Selection of buffer materials with special respect to their performance in a long-term perspective. SKB AR 95-21, Svensk Kärnbränslehantering AB.
- Pusch R, 1995b.** Rock mechanics on a geological base. Developments in geotechnical engineering, 77. Elsevier Publishing Co.
- Pusch R, Takase H, Benbow S, 1998.** Chemical processes causing cementation in heat-affected smectite – the Kinnekulle bentonite. SKB TR-98-25, Svensk Kärnbränslehantering AB.
- Pytte A, 1982.** The kinetics of smectite to illite reaction in contact metamorphic shales. M.A. Thesis. Dartmouth College: Hanover, N. H. 78 p.
- Schultz L G, 1969.** Lithium and potassium absorption; Dehydroxylation and structural water content of aluminous smectites. *Clays and Clay Minerals* 17, 115–149.
- Stroes-Gascoyne S, Pedersen K, Haveman S A, Dekeyser K, Arlinger J, Daumas S, Ekendahl S, Hallbeck L, Hamon C J, Jahromi N, Delaney T-L, 1997.** Occurrence and identification of microorganisms in compacted clay-based buffer material designed for use in a nuclear fuel waste disposal vault. *Can. J. Microbiol.* 43:1133–1146.
- Tanai K, Kanno T, Gallé C, 1997.** Experimental study of gas permeabilities and breakthrough pressures in clays. Symposium on the Scientific Basis for Nuclear Waste Management, XX, Boston, Materials Research Society, 1003–1010.
- Thunvik R, Braester C, 1991.** Heat propagation from a radioactive waste repository. SKB 91 reference canister. SKB TR 91-61, Svensk Kärnbränslehantering AB.
- Tissot B, Pelet R, 1971.** Nouvelles donnees sur les mecanismes de genese et de migration du petrole simulation mathematique et application a la prospection. In: 8th World Petroleum Congress, Moscow, Russia. 35–46.
- Velde B, Vasseur G, 1992.** Estimation of the diagenetic smectite illite transformation in time-temperature space. *Amer. Mineral.* 77, 967–976.
- Wanner H, Wersin P, Sierro N, 1992.** Thermodynamic modelling of bentonite-groundwater interaction and implications for near field chemistry in a repository for spent fuel. SKB TR 92-37, Svensk Kärnbränslehantering AB.
- Weast R (ed.), 1973.** Handbook of Chemistry and Physics. CRC Co, Cleveland, Ohio.
- Weaver C E, Pollard L D, 1973.** The chemistry of clay minerals. Elsevier, New York.
- Werme L, 1998.** Design premises for canister for spent nuclear fuel. SKB TR-98-08, Svensk Kärnbränslehantering AB.

Wikramaratna R S, Goodfield M, Rodwell W R, Nash P J, Agg P J, 1993. A preliminary assessment of gas migration from the copper/steel canister. SKB TR 93-31, Svensk Kärnbränslehantering AB.

Yu J-W, Neretnieks I, 1997. Diffusion and sorption properties of radionuclides in compacted bentonite. SKB TR 97-12, Svensk Kärnbränslehantering AB.

Zysset M, 1992. Die protoneninduzierte Auflösung von K-Montmorillonit. M. A. Thesis. Universität Bern.

5 Geosphere

5.1 Description of the geosphere

5.1.1 General

The deep repository will be situated in crystalline rock of granitic composition. Granitic bedrock consists for the most part of quartz, feldspars (potassium feldspar and plagioclase), mica minerals (biotite and muscovite) and amphiboles (hornblende). In addition there are small quantities of accessory minerals, which may be of geochemical importance. Examples of such minerals are pyrite, chlorite, magnetite, calcite, dolomite, fluorite, apatite, anhydrite and different clay minerals.

The crystalline rock is also characterized by a system of fractures. The frequency, spatial distribution, size distribution, shape and orientation of the fractures are crucial in determining both hydraulic and mechanical properties in the rock. Fractures occur on all scales from microscopic fractures in the rock matrix to fracture zones, i.e. large zones of significantly elevated fracture frequency in relation to the surrounding rock. Fracture zones often constitute dominant flow paths for the groundwater, and their size also determines the the size of rock movements that can occur in a the zone.

5.1.2 Overview of variables

The subsystem geosphere is bounded inwardly by the repository geometry, i.e. the interface between geosphere and buffer/backfill. The geosphere is bounded upwardly by the biosphere. In other directions, no clear boundary has been defined for that part of the geosphere that is included in the repository system and is thus described in detail. As a rule of thumb, detailed local analyses of e.g. groundwater flow and heat transport are carried out in a volume that extends from the repository to the surface and equally far, i.e. around 500 metres, in other directions as well. Those parts of the geosphere that lie outside this volume are called “distant geosphere” and are included in the surrounding environment. Where the boundary goes is allowed to vary as needed in different analyses.

The geosphere as it is delimited by the variable **repository geometry/boundary** is characterized by the mineralogical composition of the rock matrix, **matrix minerals**, the **temperature** of the rock and its mechanical **rock stresses**. The structure of the fracture system is expressed by the **fracture geometry**, and the mineralogical composition of the fracture surfaces and fracture infillings by the variable **fracture minerals**. Hydraulically, the geosphere is characterized by **groundwater flows** and **gas flows** in the fracture system. **Groundwater composition** is decisive for the chemical evolution of the geosphere, which is also influenced by **gas composition** and the presence of **engineering and stray materials** in the repository.

All variables are dependent on both time and space. A characteristic of the geosphere is that the majority of variables change very slowly in time, whereas the geosphere's spatial variation or heterogeneity is great.

All variables are defined in Table 5-1.

Table 5-1. Variables in geosphere.

| | |
|--|---|
| Repository geometry | Geometric description of deposition holes, tunnels, ramps, plugs, rock supports etc. |
| Temperature | Temperature as a function of time and space in the geosphere. |
| Groundwater flow | Groundwater flow as a function of time and space in the geosphere's fracture system. |
| Groundwater pressure | Groundwater pressure as a function of time and space in the geosphere's fracture system. |
| Gas flow | Gas flow as a function of time and space in the geosphere's fracture system. |
| Fracture geometry | Geosphere's cavities after construction of the repository. All cavities are included, from fracture zones to micropores in the matrix. Also included here is the excavation-disturbed zone (EDZ) and any other geometric changes in the fracture structure induced by construction. |
| Rock stresses | Rock stresses as a function of time and space in the geosphere. |
| Matrix minerals | Chemical composition of the rock matrix as a function of (time and) space, i.e. a description of the various minerals that occur and their extent. |
| Fracture-filling minerals | Chemical composition of the fracture minerals as a function of (time and) space, i.e. a description of the various fracture-filling minerals that occur. Also the amount and composition of fracture-filling minerals in existing fractures. |
| Groundwater composition | Chemical composition of the groundwater as a function of time and space in the geosphere, i.e. concentrations of relevant components in the groundwater. This variable also includes quantities such as Eh and pH, as well as any radionuclids and dissolved gases. |
| Gas composition | Chemical description of gases in geosphere cavities including any radionuclides. |
| Engineering and stray materials | Chemical composition and quantities of grouts, rock supports, plugs, etc. |

5.2 Overview of processes

The geosphere will be heated up by *heat transport* from the fuel via the canister and the buffer.

The groundwater will be redistributed in the geosphere's fracture system by *groundwater flow*. Gas flow may also occur.

A mechanical state exists initially in the geosphere determined by the natural rock stresses and fracture systems on the repository site plus the changes to which construction of the repository has given rise.

The mechanical evolution is determined by how the geosphere responds to the different mechanical loads to which it is subjected. The loads may consist of the *thermal expansion* to which the heating of the repository leads, the pressure from swelling buffer/backfill, effects of earthquakes and the large-scale tectonic evolution. Changes in the geosphere may include *fracturing*, *reactivation* (sudden movements in existing fractures) or *rock creep* (slow redistributions in the rock). *Movements in intact rock*, i.e. compression/expansion of otherwise intact rock blocks, also occur.

Geosphere

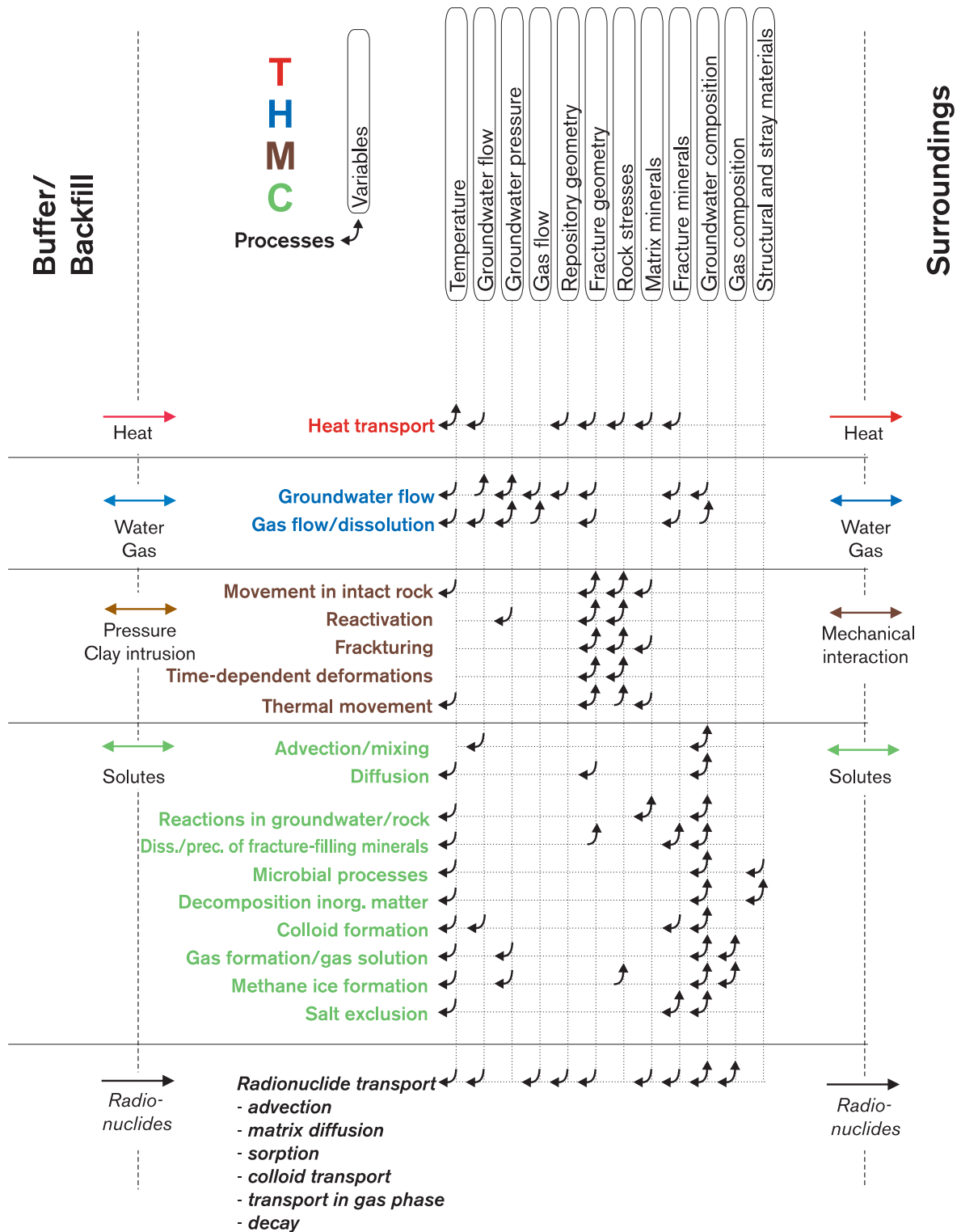


Figure 5-1. THMC diagram for the geosphere. Processes and interactions in italics only occur when the isolation of the cooper canister is broken.

The post-closure chemical evolution is determined by a number of transport and reaction processes. The predominant transport process is *advection* over long distances, but *diffusion* also plays an important role over shorter distances and in stagnant water. In advection, solutes accompany the flowing water. The process leads to mixing of different types of water from different parts of the geosphere. Reactions occur between the groundwater and fracture surfaces in the form of *dissolution/precipitation of fracture-filling minerals*. In addition very slow *reactions occur between the groundwater and the minerals in the rock matrix*. In the groundwater, *microbial processes, decomposition of inorganic materials* from repository construction, *colloid formation* and *gas formation* take place. During a glaciation, *methane ice formation* and *salt exclusion* can also occur.

If radionuclides are released, they can be transported with the flowing groundwater, *advection*. *Diffusion* can also be important under stagnant conditions. An important aspect of this is *matrix diffusion*, i.e. radionuclides diffuse in the stagnant water in the micropores of the rock and are thereby retained and transported more slowly than the flowing water. *Sorption*, where radionuclides adhere (sorb) to the surfaces of the fracture system and the rock matrix, is also crucial for radionuclide transport. Matrix diffusion and sorption are the two most important retention processes for radionuclides in the geosphere. Another factor that can be of importance for retention is sorption on *colloidal particles* and transport with them. The chemical environment in the water determines what *speciation* (chemical form) the radionuclides will have, which is crucial particularly for the sorption phenomena. Some nuclides can be transported in the *gas phase*. *Radioactive decay* influences the groundwater's content of radionuclides and must therefore be included in the description of transport phenomena.

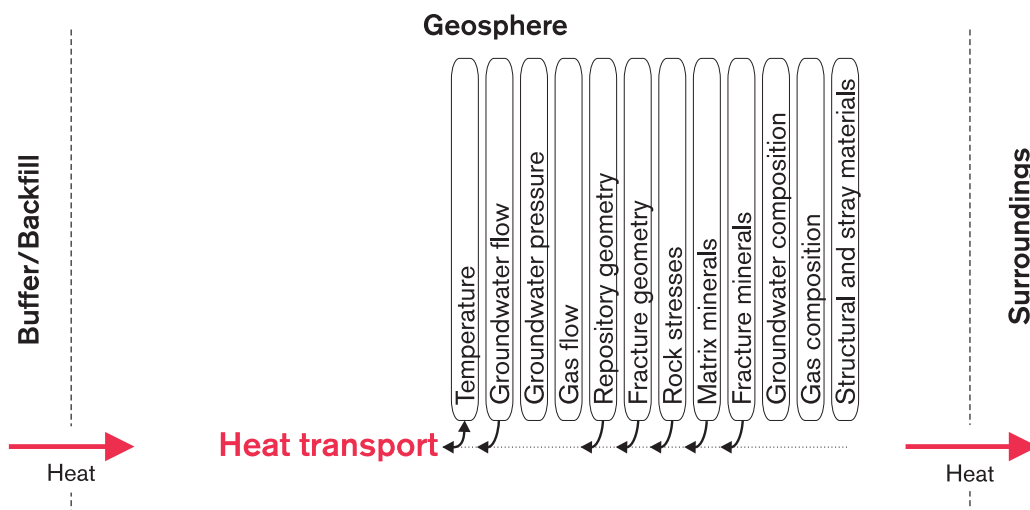
The complete THMC diagram for the geosphere is shown in Figure 5-1.

5.3 Radiation-related processes

No radiation-related processes of importance for the safety of the repository have been identified in the geosphere. Radioactive decay is discussed in the section about radionuclide transport (5.8).

5.4 Thermal processes

5.4.1 Heat transport



Figur 5-2. Heat transport.

Overview

Heat is transported in the bedrock principally by heat conduction in the intact rock. The thermal conductivity and heat storage properties of the rocks, which are both a function of mineral composition, are decisive for the process. To some extent, heat can also be transported by flow with the groundwater. Heat transfer from buffer/backfill to the surroundings comprises the boundary condition of the process.

General description

By heat transport is meant the transport of thermal energy that takes place between two points of differing temperature. Heat transport can take place by conduction, flow (convection) or radiation. Heat can also be transmitted between different phases in conjunction with condensation and evaporation. Under steady-state (time-independent) conditions, the heat transport in solid phases is determined solely by the thermal conductivity λ of the medium. Under transient (time-dependent) conditions, the heat storage capacity of the medium is also a factor, given by the specific heat capacity c and density ρ . In general, temperature propagation can be designated as a diffusion process with the diffusion constant (thermal diffusivity) $\alpha = \lambda/(c \cdot \rho)$.

A natural heat transport takes place in the earth's crust from deeper, hotter parts to the earth's surface, where a cooling takes place by heat transfer to the atmosphere and by radiation. Depending on the rock type, heat can also be generated in superficial layers by radioactive decay in the rock material. The geothermal heat flow is steady-state and is therefore determined by the rock's thermal conductivity and by the geothermal gradient. The latter provides a measure of the variation of the temperature with depth. At a depth of 500 m, the geothermal temperature is between 7°C and 20°C in Swedish bedrock /Sundberg, 1995/.

The natural temperature conditions in the bedrock are to be regarded as very stable in a long time perspective as well, especially at great depths. Near the ground surface there is some climatic impact, but large and persistent climatic variations are required in order for this impact to have effect at depths of the order of several hundred metres. Examples of such climatic variations are glacial cycles with periods of permafrost and glaciation.

Heat transport in the geosphere can be equated with heat transport in rock. The volumes of other material present in soil strata at the ground surface or in altered fracture zones, where the principle of heat transport differs somewhat from that in the rock, are far too limited to be of importance for the thermal evolution in the host rock.

Crystalline rock generally has a low porosity, which means that heat transport takes place principally by conduction. Convection occurs, but it can easily be shown that the low mean porosity and the low flow rates in the rock together make the contribution of convection to heat transport from the repository negligible, see e.g. Thunvik and Braester /1980/. Furthermore, it is pessimistic to disregard this contribution.

Heat production in the deep repository will give rise to a heat wave that propagates in all directions from the repository. Heat conduction in rock is roughly linear, so the heat flow from the repository is independent of the geothermal heat flow and will be superimposed on it. The process is transient and determined by the total thermal power output in the repository, by the power distribution and by the thermal diffusivity of the rock. Heat propagation in the repository declines with time in accordance with known power-time relationships /Thunvik and Braester, 1991; Hökmark, 1996/. After 100 years, decay power will have been reduced by about 70 percent. At a repository depth of about 500 m, the heat wave will reach the ground surface a couple of hundred years after deposition.

Influence of repository geometry: The repository geometry is of great importance. The temperature at the boundary of the deposition hole is influenced by two factors at a given canister power and given heat transport properties: the initial power density and the balance between tunnel and canister spacing. Most important is the power density, which will be 7 W/m^2 at a tunnel spacing of 40 m, a canister spacing of 6 m and a canister power on deposition of 1,680 W. If the power density is halved, for example by doubling the canister spacing, the maximum temperature increase at the deposition hole boundary will be more or less halved. The balance between tunnel and canister spacing is of less importance, which can be shown by analytical solution, as described below under "Model studies". If the canisters, with an unchanged power density of 7 W/m^2 , are instead arranged in the square array $15.5 \text{ m} \times 15.5 \text{ m}$, for example, the peak temperature is reduced by around 5°C compared with deposition in the rectangular array $6 \text{ m} \times 40 \text{ m}$. At some distance from the canisters, the balance between tunnel and canister spacing is without importance.

Influence of the boundaries: The ground surface acts as a cooled boundary, contributing towards reducing the temperatures in the repository. However, the boundary does not start to have an influence until the heat pulse reaches the ground surface, which occurs long after the temperature in the vicinity of the canisters has begun to drop. The maximum temperature in the near field is therefore not affected by conditions at the ground surface.

The bentonite buffer transfers the canister power to the rock, and thereby acts as a boundary for the geosphere. A few weeks after deposition, the heat pulse has reached and passed the deposition hole boundary. After that the heat flow through the buffer is quasi-steady-state, i.e. heat is transferred to the rock at the same rate as it is generated in the canister. After a few weeks, the heat transport properties of the buffer and the canister are therefore without importance for the temperatures in the rock.

The tunnel backfill has a thermal conductivity of $1.5 \text{ W/(m}\cdot\text{K)}$ – $2.5 \text{ W/(m}\cdot\text{K)}$ in water-saturated conditions and therefore slightly reduces the average thermal conductivity in the near field. The volume of the tunnels in relation to that of the near field is so small, however, that the effect can be neglected. The small importance of the tunnel backfill for heat transport is illustrated by the FEM calculations done for the Prototype Repository in the Äspö HRL /Ageskog and Jansson, 1998/.

Influence of matrix properties: The matrix composition is decisive for the thermal conductivity and heat storage capacity of the rock. The thermal conductivity of ordinary Swedish rock types varies in the range 2.7–3.6 W/(m·K) /Sundberg, 1995/. The conductivity of quartzite is 6.6 W/(m·K). The effective thermal conductivity of the host rock is determined by the proportions of the constituent rock types, and by their stochastic distribution. The effective thermal conductivity of the rock mass for three Finnish siting alternatives has been determined to be 3.1, 2.7 and 2.7 W/(m·K), respectively /Kukkonen and Lindberg, 1995/. Specific heat capacity and density also vary with rock type. In the near field of the canisters, the heat flow will become quasi-steady-state after a short time, which means that the thermal conductivity is more important than the heat storage capacity, i.e. than the density and the specific heat capacity, for the temperature nearest the deposition holes. In heat transport calculations, the standard value 800 J/(kg·K) is usually used for the specific heat capacity. The density normally varies between 2,600 and 2,800 kg/m³. The thermal conductivity of the dominant rock type at Äspö, Äspö diorite, has been determined to be 2.8 W/(m·K) by direct measurement of thermal diffusivity, density and specific heat capacity /Sundberg and Gabrielsson, 1998/.

Influence of temperature: The temperature in itself has a fundamental influence on the process, since temperature differences between different points in space comprise the very driving force for heat conduction. Furthermore, thermal conductivity is weakly temperature-dependent. At low temperatures, between 20°C and 100°C, the thermal conductivity typically declines by about 10–15 percent /Kukkonen and Lindberg, 1995/. In the area nearest a canister, the maximum temperature increase can amount to 50–60°C, which means that the thermal conductivity is reduced at most by about 10 percent. At a distance of a few metres from the deposition holes, the reduction is much less. The approximation that is generally made in temperature calculations, namely that the heat transport properties of the rock are temperature-independent, is therefore warranted.

Influence of fracture geometry: The presence of fractures reduces the thermal conductivity, particularly if the fractures are filled with air ($\lambda \approx 0.025$ W/(m·K)). Air-filled fractures represent such a small fraction of the total volume that the effect can be neglected, however. For water-filled fractures, $\lambda = 0.6$ W/(m·K), which means that this influence can also be neglected.

Influence of rock stresses: As the stresses increase, fractures are compressed, which can marginally increase the thermal conductivity. The effect is small and can be neglected.

Influence on the surface: Heat transport has a marginal influence on the thermal conditions on the ground surface. The time integral of the thermal power expression gives the thermal energy that is generated during a given period of time. If it is assumed that 4,000 canisters are deposited with an initial power output of 1,680 W each, it is found that a thermal energy of approximately 12 TWh is evolved during the first 1,500 years after deposition. If all of this energy reaches the ground surface and is transferred to the atmosphere during the period 500–1,500 years after deposition, the annual energy contribution is the same as that from 600 detached homes, each with an annual gross energy consumption of 20,000 kWh.

Importance for thermal evolution in fuel, buffer and canister: At a given canister power and deposition geometry, the heat transport in the rock is decisive for the temperature at the deposition hole boundary and thereby for the temperature in the buffer and in the canister. This is the most important safety-related aspect of the process heat transport in the geosphere.

The temperature at the boundary of the deposition hole will act as a boundary condition for the heat flow in the buffer and thereby be decisive – together with the heat transport properties of the buffer, the canister power and any gas-filled gaps – for the temperature on the canister surface and in the buffer. Design criteria have been set up for these temperatures that make it possible – with knowledge of the heat transport conditions in the canister/buffer system – to specify a maximum permissible temperature at the deposition hole boundary. With the analytical calculation method described below under “Model studies”, the temperature in the near field, for example at the deposition hole boundary, can be calculated for different assumptions regarding the heat conduction properties in the rock, the deposition geometry and the deposition sequence, which will also make it possible to determine for which assumptions the design criteria will be satisfied.

Model studies

Numerical temperature calculations with an FEM code have been done by Thunvik and Braester /1991/. Furthermore, several numerical temperature calculations have been done in conjunction with thermomechanical analyses /see e.g. Hakami et al, 1998; Hökmark, 1996/.

Claesson and Probert /1996/ developed a system for analytically calculating the temperature at an arbitrary point in the host rock as a function of time after deposition. The repository is assumed to be designed as one or more rectangular areas. Both the temperature at large distances from the repository and the temperature in the area between tunnels and deposition holes can be calculated. Input data to the calculation are the heat transport properties of the rock, the power output of the canisters at the time of deposition, the height of the canister, the power decay, the depth below the ground surface and the deposition geometry, i.e. tunnel spacing and canister spacing. It is assumed in the analytical solution that the rock is homogeneous and isotropic and that its heat transport properties are independent of the temperature. The analytical solution has been verified by comparison with results from numerical calculation of the rock temperature in the near field in a KBS-3 repository /Hökmark, 1996/. The solution has also been verified by comparison with numerical calculations of the temperature in the far field /Israelsson, 1995/. Figure 5-3 shows analytically calculated temperatures at three points in the near field.

The analytical solution, which is based on the superposition principle, can also be used to analyze effects of dividing the repository up into smaller, separate units and effects of performing deposition on several occasions spread out in time.

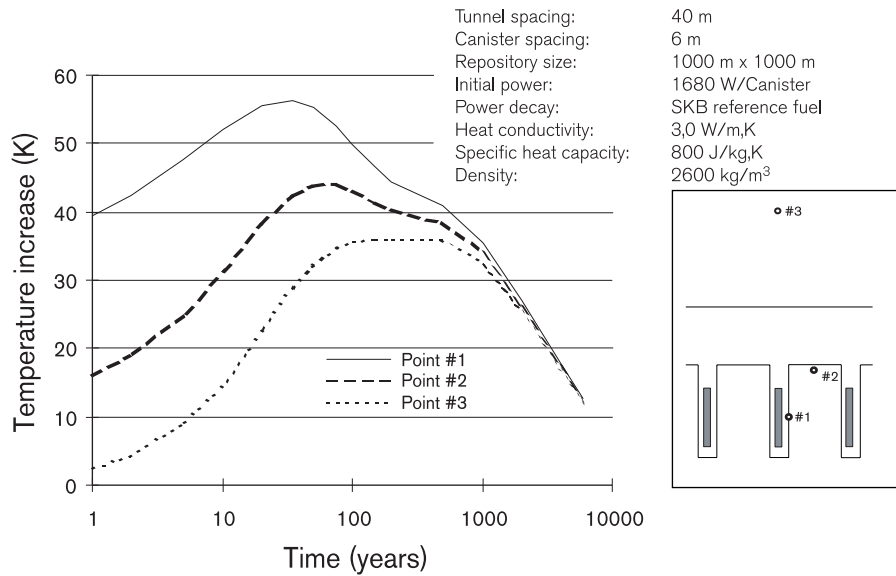


Figure 5-3. Temperature increase at three points in the near field. The temperatures are calculated using an analytical solution derived from Claesson and Probert /1996/. Absolute temperatures are obtained by adding the geothermal temperature.

Summary of uncertainties

Uncertainties in understanding: There are no conceptual uncertainties regarding the process.

Uncertainties in data: Some data uncertainty exists when it comes to effective thermal conductivity and specific heat capacity at the different repository sites. The maximum temperature increase at the canister hole boundary varies between 60 and 50°C if the effective thermal conductivity varies in the range 2.7–3.5 W/(m·K). There is also an uncertainty regarding how the deposition sequence in time and space influences the temperatures at the beginning of the thermal evolution, i.e. during the first decades after deposition.

Handling in the safety assessment

Base scenario: Temperature calculations for all candidate sites are performed in SR 97 with site-specific repository layouts and thermal data.

Canister defect scenario: See base scenario.

Climate scenario: Effects of modified boundary conditions are discussed.

Earthquake scenario: See base scenario.

5.5 Hydraulic processes

5.5.1 Groundwater flow

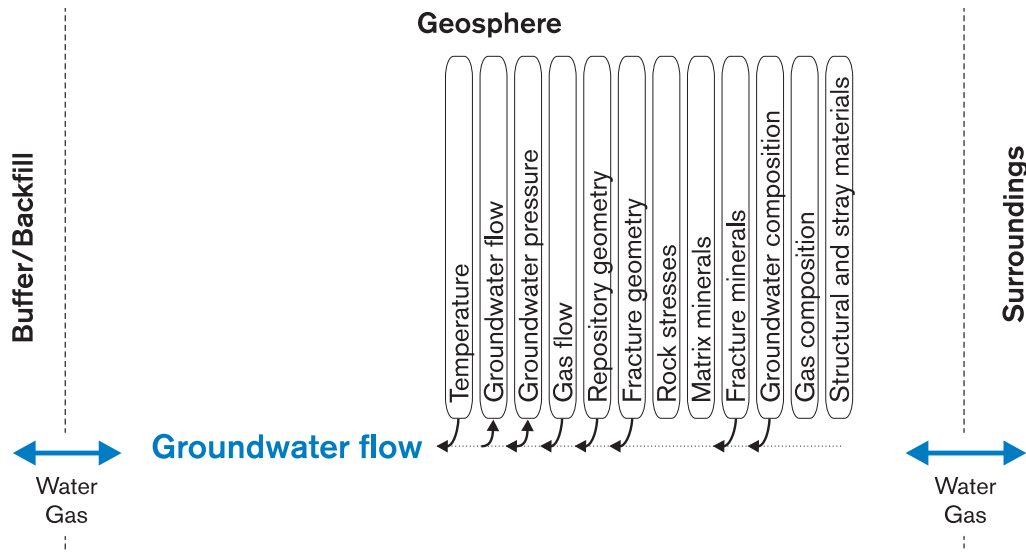


Figure 5-4. Groundwater flow.

Overview

The driving force for the water flow in the geosphere consists of differences in potential energy within the geosphere, where the potential energy of a point is determined by the pressure and density of the water and the vertical position of the point.

The density of the water is chiefly dependent on the temperature and composition of the water, above all its salinity.

If the groundwater has constant density, the driving force can be expressed as a gradient of a flow potential.

The size of the water flow is dependent on the size of the driving force and the water-conducting capacity of the geosphere. This water-conducting capacity is dependent on the flow properties of the pore structure and the flow properties of the water in the geosphere. In loose deposits, the flow properties of the flow structure are determined by the particle size distribution and the shape and compaction of the particles. In crystalline rock, the flow properties of the pore structure are determined by the fracture structure.

The flow properties are dependent on both the flow properties of each fracture and how the fractures are interconnected. The flow properties of the fractures are influenced by the prevailing effective stress in the geosphere and any gas presence in the fracture system. The flow properties of the water are controlled by the viscosity, which is affected above all by temperature and by the chemical composition of the water. The flow properties of the water vary within a relatively narrow range, while the flow properties of the pore structure exhibit a very wide range of variation.

The groundwater flow is of central importance in the safety assessment. It influences the chemical composition of the flowing groundwater and thereby the chemical environment of the repository. In the event of radionuclide release from the repository, the flowing groundwater comprises a necessary prerequisite for the transport of radionuclides from the repository to the biosphere.

General description

The hydrologic cycle

The natural cycle of water in nature is usually termed the hydrologic cycle /e.g. Knutsson and Morfeldt, 1995; de Marsily, 1986/. It is normally divided into the following components:

- Water enters the atmosphere via evaporation from lakes, seas, land and vegetation and transpiration from plants.
- The water is carried by winds and falls as precipitation over land and sea.
- The precipitation infiltrates through the soil or runs on the ground surface to nearby streams, lakes or sea.
- The portion of the infiltrating water that is not taken up by plants or transported up by capillary forces percolates down towards the groundwater table and recharges the groundwater reservoir.
- The groundwater moves below the ground surface under the control of prevailing hydraulic driving forces and eventually discharges into springs or directly into streams, lakes or seas.

Precipitation is what ultimately drives the groundwater flow, while the topography and the flow properties of the geosphere control the flow pattern.

Calculation of groundwater flow

The most common approach for calculating groundwater flows in the geosphere is based on Darcy's law, which says that the size of the flow per unit area (q) is proportional to the gradient multiplied by the water-conducting capacity of the geosphere. The general form of Darcy's law is as follows:

$$q = -\frac{k}{\mu} \cdot (\text{grad}(p) + \rho \cdot g \cdot \text{grad}(z)) \quad (5-1)$$

The mass flow is given by

$$\text{div}(\rho \cdot q) + \frac{d(\rho \cdot n)}{dt} = 0 \quad (5-2)$$

The equations of state are:

$$\rho = f(T, C, p) \quad (5-3)$$

$$\mu = f(T, C, p) \quad (5-4)$$

These equations form the basis for calculating a water flow taking into account pressure, temperature and density conditions. The permeability (k) is given by the properties of the pore system and the dynamic viscosity (μ) determines the properties of the fluid. The flow vector is composed of a pressure gradient ($grad(p)$) and a gradient dependent on the forces of gravity ($\rho \cdot g \cdot grad(z)$). Density and viscosity are functions of temperature (T), solute concentration (C) and water pressure (p). Other parts of the equations are the acceleration of gravity (g), porosity (n) and time (t). If the water has constant density, then:

$$q = -\frac{k \cdot \rho \cdot g}{\mu} \cdot grad\left(\frac{p}{\rho \cdot g} + z\right) = -K \cdot grad\left(\frac{p}{\rho \cdot g} + z\right) = -K \cdot grad(h) = K \cdot i \quad (5-5)$$

The water-conducting capacity is expressed in equation 5-5 as hydraulic conductivity (K); the hydraulic head (h) and the hydraulic gradient (i) are in this case dimensionless. The flow cannot always be calculated with Darcy's law. In compact clays at low gradients, the flow is less than given by Darcy's law if K is determined at high gradients /de Marsily, 1986/. The flow is also less than given by Darcy's law at high gradients, since friction losses arise due to turbulence /de Marsily, 1986/. In practice, turbulent losses only arise near pumped wells or near boreholes where water is allowed to flow freely into a tunnel.

The driving forces and the water-conducting capacity of the geosphere are influenced by a number of factors, which are described in brief below.

Driving forces

In Sweden, the level of the groundwater table is closely linked to the topography. The reason is the relatively heavy precipitation and the relatively low permeability of the bedrock. Local flow systems controlled by the topography usually form near the ground surface, see Figure 5-5. In groundwater contexts, the hydraulic gradient is sometimes expressed in percent. The hydraulic head is then expressed as metres water, and the gradient becomes dimensionless, see equation 5-5. Under natural conditions the gradient is usually one or two tenths of a percent near the ground surface and usually decreases and levels out towards the regional topographical gradient.

Flow systems that described associated recharge and discharge areas exist on various scales. These scales can, for Swedish conditions, be from hundreds of metres to hundreds of kilometres. The length and appearance of the flow path of a water particle is determined by the topography, the water's density distribution, and the water-conducting properties of the rock's fracture system and of the loose soil strata. Recharge and discharge in a deep repository area are also dependent on the large-scale groundwater flow pattern.

Saline groundwaters are often encountered in near-coast areas and at deeper levels in the interior, with increasing salinity towards greater depth. As salinity increases the density of the water increases, which in turn influences the pressure conditions. Increasing salinity with depth causes the flow to decrease with depth, and the groundwater can, under certain conditions, be more or less immobile /Claesson, 1992; de Marsily, 1986/. If the boundary conditions at the ground surface change, for example due to postglacial land uplift in the coastal areas, a considerable flow can, however, also arise in the deep saline groundwater /Voss and Andersson, 1993/.

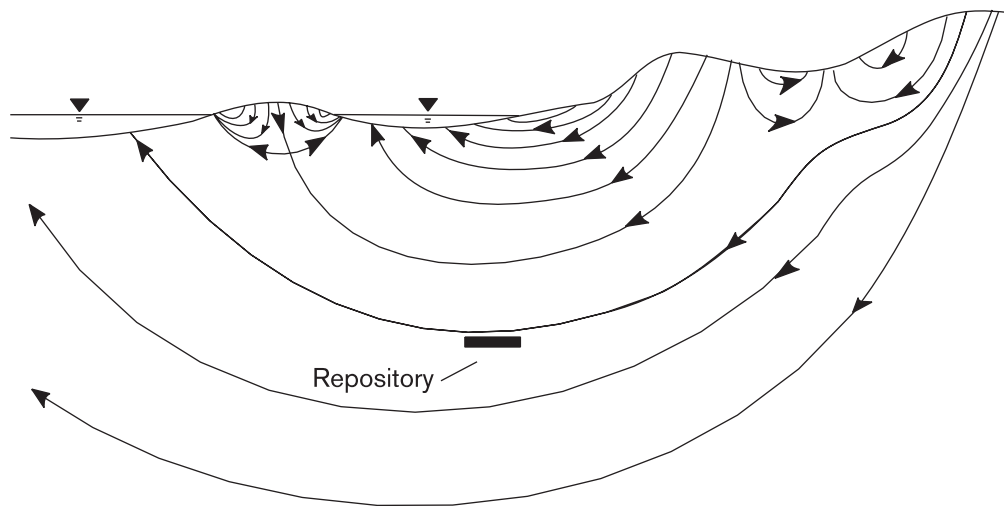


Figure 5-5. Schematic diagram of topographically induced flow pattern. Both the gradient and the groundwater flow normally diminish with depth. The occurrence of water-conducting fractures and fracture zones can, however, result in a much more complicated flow pattern than the one shown in the figure.

Heating of the water causes its density to decrease. A local heating of the water, for example by spent fuel in the deep repository, can give rise to density changes that create large-scale circulatory water movements /Claesson, 1992; Probert, 1998/. If the topographical gradient lies at typical values for Swedish conditions, however, this effect will have a limited influence on the flow pattern /Thunvik and Braester, 1980/.

A flowing groundwater also affects the temperature field via advective heat transport. Due to the normally low groundwater flows, however, the heat flow is mainly controlled by the heat conduction properties of the rock, and the heat transport due to flowing groundwater can be neglected, see section 5.4.1.

Situations where density variations cannot be neglected entail more complicated model calculations. In these cases the calculations must also take into account transport of salt and/or heat.

Flow properties of the pore structure

The flow properties of the pore structure in loose deposits are well described in, for example, de Marsily /1986/ and are not described here.

The flow properties of the pore structure in crystalline rock are determined by the fracture structure. The flow properties are dependent both on the flow properties of each fracture and on how the fractures are interconnected. The flow properties of a fracture are dependent above all on its aperture, but also its surface structure. The permeability according to equation 5-1 cannot normally be directly obtained for a fractured medium; rather, it is necessary to assign approximate flow properties to individual fractures or rock blocks, see the section "Model studies/experimental studies" below.

The rock outside the fractures is called the rock matrix. It normally contains microfractures with very small apertures. The water flow in the rock matrix is therefore usually very low at normally occurring hydraulic gradients. The permeability of a large rock block is therefore determined virtually completely by the open and interconnected fractures in the block.

The frequency of fractures, their spatial distribution, size distribution, shape and orientation distributions determine how hydraulically connected the fractures are. Extensive, elongated formations with a markedly increased fracture density in relation to the country rock are called fracture zones. Such fracture zones often constitute dominant flow paths for the groundwater. Fracture fillings in the form of clay can, however, result in low permeability in a zone despite the presence of many fractures. The width of the fracture zones can vary within wide limits, from a decimetre to tens of metres. Normally the transition from “rock” to “fracture zone” is diffuse, since the fracture frequency often increases in towards the fracture zone.

In the case of individual fractures and fracture zones, both of which can be regarded as two-dimensional bodies, the water-conducting capacity is given by the transmissivity.

Hydraulic experiments in the field have shown that fractures and fracture zones exhibit considerable spatial variations in water-conducting capacity, i.e. the system is hydraulically heterogeneous. Their water-conducting capacity can vary by several powers of ten. Variations within a given rock type are generally greater than the differences between the mean values for the different rock types. Models devised for prediction/analysis of groundwater flow (and thereby also solute transport) must in one way or another take this heterogeneity into account.

The transmissivity of an individual fracture is roughly proportion to the cube of the aperture according to the cubic law. This means that transmissivity can vary several powers of ten for a relatively small change in aperture. The cubic law, which applies to flow between two parallel discs, cannot be applied directly to natural fractures, however. Due to the surface structure of the fracture, some parts of the fracture are impervious when the fracture sides lie up against each other or due to the fact that the fracture is partially filled with clay and rock fragments. This limits the available space for flow, compared with the ideal case. Further, the fracture aperture can vary in the open part of the fracture /National Research Council, 1996; Hakami, 1995/.

Since the aperture varies, the flow in a fracture tends to vary in the fracture plane. Most of the flow is concentrated along winding channels in the plane. This means that only a portion of the fracture’s open volume is utilized for a large part of a flow that is created by a constant gradient. If the direction of the gradient changes, the pattern of the channels in which most of the flows take place is altered.

Several factors can influence the fracture’s transmissivity. If the mechanical load (effective stress) on the fracture increases, the aperture decreases and the portion of the fracture surface that lies up against the opposite fracture surface increases. This leads to a decrease in the fracture’s transmissivity. The transmissivity change per stress change is greatest at low effective stresses. If the mechanical load becomes too great, existing fracture planes may be displaced relative to each other, the rock may fracture further along existing fracture planes, or new fractures may be created. Movements that displace one fracture plane relative to the other may also occur. These mechanical phenomena may increase or decrease the local permeability of the rock. Heating or cooling of the rock is another process that can cause changes in apertures and affect the permeability of the rock.

If the water pressure in the fracture changes, for example because pumping is started in a nearby borehole, the whole fracture becomes hydraulically activated as long as the pressure change persists. The water pressure change causes deformation of the fracture and a volume change of the water in the fracture. This leads to the abstraction or infusion of a certain volume of water from or into the fracture, depending on whether the pressure decreases or increases. It is a relatively rapid sequence of events, owing to the fact that the water and the fractures have high compressibility and that the total fracture porosity is low. The volume of water per unit volume of the geosphere that is released from the fracture at a pressure change under closed conditions is usually termed the specific storage. If the fractures are open to the atmosphere (open conditions), the fractures are not compressed appreciably and are therefore drained. The volume of water per unit horizontal area that is released is normally termed the specific yield in this case. Much more water can be released at a given pressure change under open conditions than in fractures deep down in the rock. The specific storage and yield influence how long it takes for the groundwater table to reach the undisturbed level after a drawdown, caused for example by the construction of a deep repository. The time is also influenced by the permeability of the rock, the pore volume in tunnels, the proportion of precipitation that percolates, and infiltration from streams, lakes and seas.

The fracture surfaces are normally coated with various fracture-coating minerals. If precipitations occur on the fracture surface, the aperture decreases and transmissivity decreases. Certain fractures may be more or less healed by fracture-coating minerals and are then virtually impermeable. If fracture-coating minerals dissolve, transmissivity increases.

Flow properties of the water

The flow properties of the water depend on its viscosity. The viscosity is above all related to the temperature, but also to the salinity. The pressure has very little influence on the viscosity /Earlougher, 1977/. Increased temperature reduces viscosity and thereby increases K , see equation 5-5. At normal temperature gradients in Swedish bedrock (around 15 degrees/km) the viscosity is halved at 2,000 m depth compared with the expected viscosity near the ground surface. Near a canister the water temperature may approach 100°C, which makes the viscosity about one-fourth of the viscosity at undisturbed water temperature at 500 m depth. If the salinity is a few percent it only has a minor influence on the viscosity /de Marsily, 1986; Earlougher, 1977/. In general the influence of temperature and salinity on viscosity can be disregarded.

Influence of gas flow

The quantity and composition of the gas that is always present naturally in groundwater varies. In Sweden, geogases normally consist mainly of nitrogen and helium. Gas is also expected to be produced in the repository, section 4.5.3. The quantity of gas produced in the repository is expected to be low and probably will not appreciably affect the groundwater flow.

The gas may be dissolved or in the form of gas bubbles. Dissolved gas does not influence the water's flow properties. If the water pressure in water containing dissolved gas is lowered below a given level, gas bubbles will form in the fracture system. The water-conducting capacity of the fractures will then be reduced where the bubbles form. This can mainly be expected to occur near open tunnels (in contact with the atmosphere) and near boreholes, where a sharp pressure fall can occur if the borehole is flooded or pumped.

Experience from several tunnel investigations has shown that the radial hydraulic conductivity appears to diminish nearest the tunnel walls when the tunnels are open towards the atmosphere. Explanations for this phenomenon have been sought in stress redistributions and chemical precipitations. Another explanation is that the conductivity decrease may be a phase boundary phenomenon between air or other gas and water. The process is then described by a two-phase flow system. Knowledge of two-phase flow can be essential in evaluation of hydraulic field tests and for the resaturation process for buffer/backfill. When the deep repository is closed and sealed, the backfill material in the tunnels and the surrounding rock will gradually become water-saturated. This leads to an increase in the water-conducting capacity due to dissolution of the gas, and the water-conducting capacity of the rock nearest the tunnel may become higher than in surrounding rock due to the elevated fracture frequency /Emsley et al, 1997; Olsson, 1994; Jarsjö, 1998/.

Influence of land uplift

During the most recent glaciation, the ice cap depressed the bedrock several hundred metres. When the ice retreated, the earth's crust began resuming its original form, and this process of land uplift is still going on, causing displacement of the coastline along most of Sweden's coast. This is causing the boundary conditions for groundwater flow to change with time in near-coast areas. When sea becomes land, some of today's discharge areas will become recharge areas during the next thousand years. These dynamic boundary conditions influence the large-scale flow pattern, and some flow arises in the deep-lying saline groundwater /Voss and Andersson, 1993/.

Influence of climate change

In a long time perspective, considerable climate change is expected to take place, which influences the boundary conditions in groundwater flow models. From the viewpoint of groundwater flow, future cold periods with growing glaciers are probably the most important. A transition to a colder climate is expected within 5,000 to 10,000 years in different parts of Sweden. By defining different climate scenarios, effects on the groundwater flow can be studied in calculation models. Examples of scenarios are given below. The scenarios are described more thoroughly in Boulton et al /1999/.

From a hydraulic point of view, there is a great difference between an advancing glacier and a glacier that is retreating due to melting. An advancing glacier is expected to be cold, with a frozen bottom at the front. Permafrost exists in front of the glacier. The rock volume encompassed by the permafrost should exhibit a much lower water-conducting capacity than the unfrozen rock. The permafrost might possibly influence fracturing and the water chemistry in and near the frozen rock mass. During the first few thousand years of glacial growth, the above conditions should prevail within the area of glacial advance. A few kilometres from the front of the glacier, the lower part of the glacier melts and the water pressure under the ice is high, causing the meltwater to infiltrate into the bedrock. The permafrost in front of the glacier and the frozen rock mass ought to make the flow paths of the water from infiltration to discharge areas relatively long. Some of the infiltrated water is probably diverted to glacier streams under the ice that discharge at the glacier front. These glacier streams are responsible for the formation of eskers. Furthermore, the groundwater pressure declines locally near the glacier streams. The load from the ice can cause an increase in effective stress, which should cause the fracture aperture to decrease, at least locally.

A glacier that retreats as it melts probably has no or little permafrost under its front part and none ahead of the glacier front. This means that large gradients can arise nearest the front, and many of the potential flow paths from infiltration under the ice to the discharge areas are shorter than for the advancing glacier. The groundwater flows in the area near the glacier front may be large compared with other times. Some of the infiltrated water is probably diverted in glacier streams under the ice, which discharge at the glacier front in this case as well. The front edge of the glacier may be highly fractured, and under such conditions the groundwater level is controlled by the topography in the fractured area. The slope of the glacier front is probably also greater than that of an advancing glacier. This means that the mechanical load of the ice may create displacements in the bedrock and alter the effective stress, which can in turn alter the permeability in the rock.

The global sea level is probably also changed during the glaciation. The depth of the sea and the coastline displacement are dependent on the global sea level change and the downwarping of the ground surface due to the advancing glacier and the subsequent land uplift when the glacier retreats. This influences the potential differences that drive the groundwater flow.

Influence by humans

Future human intrusions can change the boundary conditions and thereby the flow conditions at repository level. Rock-drilled wells for water supply are sunk in water-bearing portions of the rock, which can sometimes be major permeable fracture zones. If these zones are hydraulically connected to the flow system around the repository, pumping-out of groundwater will probably have an effect on the flow conditions through the repository. Similar interventions with perhaps even a greater influence on flow conditions are deep tunnelling projects or other activities that involve the abstraction of large groundwater quantities in the vicinity of a deep repository.

Local changes in groundwater recharge can occur as a consequence of, for example, construction of dams, drainage of wetlands and urbanization. Human influence is described more thoroughly in Morén et al /1999/.

Model studies/experimental studies

Predictive modelling of water flow and transport in fractured rock is complex in comparison with in porous geological media. To describe the groundwater flow in the bedrock, it is necessary that the heterogeneous nature of the rock be represented in the models and that the scale on which the calculation problem is considered be taken into account. Different approaches are used, representing different idealizations of how the groundwater flows. The idealized approaches for calculating groundwater flow can be divided into discrete models and continuum models. In discrete models the water flows through networks composed of discrete fracture planes /National Research Council, 1996, Dershowitz et al, 1995; Nordqvist, 1995; Long et al, 1985; Cacas, 1990/. In continuum models, the properties of the rock vary continuously /Norman, 1992; National Research Council, 1996; Follin 1992/. Then there are channel network models /Gylling ,1997/, which are, however, to be regarded as continuum models from a groundwater flow viewpoint, while the transport hypotheses may be different compared with other continuum models, see section 5.8. The choice of model depends on the purpose of the analysis in question, what geometric scale is to be studied, and available data.

Regardless of the chosen model concept, the models must include the processes which, according to the above, significantly influence the groundwater flow. The hydraulic driving forces come in as boundary conditions in the models, and these have a great influence on the results. It is primarily a question of whether the dominant contribution to groundwater movements at repository depth comes from regional groundwater systems or from local topography in combination with steeply-dipping structures /e.g. Voss and Andersson, 1993/. If the modellings take into account density differences in the groundwater caused by salinity variations and/or temperature differences, boundary and initial conditions for temperature and salinity must also be determined /Follin, 1995/.

A large number of experimental studies have been conducted during the past 20 years at, among other places, Stripa Mine /Fairhurst et al, 1993; Gnirk, 1993; Gray, 1993; Olsson, 1992/, the Äspö HRL /Wikberg et al, 1991; Rhén et al, 1992; Emsley et al, 1997; Rhén et al, 1997/ and at Finnsjön in Sweden /Ahlbom et al, 1991; 1992/. A number of important experimental studies have been conducted at Grimsel in Switzerland and at URL in Canada as well. Modelling concepts have been tested and developed within SKB, and a number of international projects have been carried out such as Stripa, Decovalex /Stephansson et al, 1996/, Intraval /Larsson et al (Eds.), 1997/ and within the Task Force at the Äspö HRL /for example: Gustafson and Ström, 1995; Svensson, 1997a,b/.

Time perspective

After the deep repository has been closed, the groundwater table above the repository will gradually be restored to original levels. The restoration is, as previously mentioned, dependent on a number of factors. Local conditions are important. It will probably take tens of years to perhaps 100 years for the groundwater to reach its original, undisturbed level. The time required to restore the groundwater level is, however, short compared with other processes that can influence the performance of the deep repository. In near-coast areas, the construction of the final repository will result in the intrusion of deeper-lying more saline waters into the tunnel system. How long it will take to obtain a saline water distribution similar to the original is unclear.

Climate change and land uplift are constantly ongoing processes. Land uplift before the next cold period with glacier advance is expected to continue for several thousand years. A cold climate with altered precipitation conditions, permafrost and glaciers will probably influence conditions in large parts of Sweden during the period between approximately 10,000 and 100,000 years from now. This will lead to slow changes in the size and pattern of groundwater recharge.

The time perspective for solute transport is discussed under transport processes, section 5.8.

Natural analogues

Geochemical, hydrochemical, palaeogeological and palaeohydrological studies can provide an insight into long-term and large-scale flow patterns, see e.g. Wallin /1995/. By studying the distribution and composition of fracture-filling minerals and the composition of the groundwater, certain conclusions can be drawn or judgements made regarding flow patterns and flow conditions. The consistency between the chemical information and the hydrogeological information can be analyzed, which strengthens confidence in site-specific descriptions of the geosphere.

Summary of uncertainties

Predictions of the properties of the geosphere contain several uncertainties. One reason for this is reliance on limited site investigations and the fact that it is not possible to completely describe the entire rock volume in detail. Due to uncertainties regarding the existence, direction, size and properties of conductive structures, many flow paths from the repository to the biosphere are conceivable. The existence, direction, size and properties of major conductive structures may be known with great certainty within certain well-investigated rock volumes, while uncertainty regarding the same structures, and others, may be great in rock volumes with low investigation intensity. Spatial variability can be expected to be great within both identified major fracture zones and the rock mass between these zones. The variability can in practice only be described statistically, since the number of measurement points will be limited. The number of measurement points and measurement methods must be chosen so that a satisfactory statistical basis is obtained for the description of the geosphere.

A considerable uncertainty lies in the determination of the interconnected network of conductive structures. The connection between geologically interpreted structures and hydraulic structures is not clear-cut, and cross-hole tests are generally required to establish connectivity on a larger scale with certainty, while a large number of single-hole tests are required to obtain statistical measures of the flow properties of the rock. The evaluated water-conducting properties obtained from field measurements also exhibit a scale dependence that must be taken into account when assigning properties in a groundwater flow model. There are several suggestions on how scale transformation can be done, but uncertainties still exist concerning how it should be done in a correct or acceptable manner. Uncertainties in the models can, however, be reduced by measurements in the field. By measuring pressure and flow in the rock mass under different conditions, data are obtained that can be utilized to test and calibrate models.

By means of studies of existing glaciers and structures of the existing quaternary geology, large advances have been made during the past ten years in our understanding of what happens beneath a glacier and near its front. Large uncertainties concerning the boundary conditions on the ground surface under and near a glacier during a glacial period still remain, however. Large uncertainties also exist regarding what the next glaciation will look like in quantitative terms, such as the ice's rate of advance, thickness, etc.

Handling in the safety assessment

In modelling groundwater movements in the safety assessment, it is very important to examine what different uncertainties mean for the performance of the rock barrier. Assessments of uncertainty intervals within the framework of a site description make it possible to define different variation cases in the safety assessment, which can be used to study the consequences of the uncertainties. In a similar manner, different temporal changes – such as climate changes, land uplift, etc. – can be illuminated by variation analyses.

Base scenario: In the base scenario it is of interest to study flows at repository level and the inward transport to the repository of solutes in the groundwater. These factors can influence the chemical environment and evolution of the repository. Groundwater flow models can form an important component in these analyses, or alternatively approximate mass balance calculations can be carried out to determine the quantity of solutes that can be transported to the repository. This latter alternative is chosen in SR 97.

Groundwater flow models are also used to describe how the pre-closure repository can attract saline water due to pumping of the tunnels (upconing) and how resaturation of the tunnels proceeds once pumping ceases. Transient simulations are required for this type of calculation. A saline water at the repository can influence the function of the bentonite negatively. A slow resaturation entails retardation of the establishment of reducing conditions at the repository. However, these two processes are only judged to have marginal effects on total safety and are dealt with approximately in SR 97.

Canister defect scenario: This is the main scenario in SR 97 as regards analysis of radionuclide transport in groundwater. Releases from defective canisters result in groundwater transport of radionuclides through the geosphere to release points in the biosphere. Since the canister defect scenario is based on present-day conditions, non-transient simulation is used, i.e. any changes in the geosphere with time are neglected.

The primary quantity to calculate is flow of radionuclides to the recipient (biosphere) with a given flow of nuclides from the buffer/backfill. To carry out these calculations, flow models on a regional and local scale are used in SR 97. The regional models provide an overall understanding of large-scale groundwater flow patterns and direct boundary conditions for the local models. Density-driven flow is incorporated in the regional models as needed, i.e. the composition of the groundwater affects the flow.

The local models provide the magnitude of the flow at repository level plus flow paths through the geosphere to the recipient. Density-driven flow is not incorporated in the local models in SR 97. The results from the local models are used for further calculation of radionuclide transport. The code HYDRASTAR /Norman, 1992/ is used for modelling of local groundwater flow in SR 97. Due to the natural variability of the geosphere and the limited availability of data, a stochastic approach is applied. This means that multiple realizations – all equally probable – are generated in the flow models so that distributions rather than individual values of the relevant parameters are obtained. The distributions reflect an uncertainty caused by the spatial variability.

Input parameter values that define the flow models – such as the underlying statistical model for hydraulic conductivity, the existence of well-defined conductive structures (fracture zones) or boundary conditions – can be burdened with uncertainties. This parametric uncertainty is often analyzed via variation cases in the safety assessment. The variation cases can be viewed as sensitivity analyses where the response of the geosphere models to changes in input parameter values are systematically studied.

Climate change: Climate change can have important consequences for the barrier performance of the geosphere. Climate change may entail changes in both conductivity distribution and boundary conditions as well as altered chemical conditions. Both transient simulation and approximate calculations are used in SR 97 to shed light on these effects.

Earthquake: Earthquakes can lead to a more or less instantaneous change in fracture structure and resulting conductivity distribution. However, this aspect of earthquakes is not addressed in SR 97; instead, quantitative analyses are made of what magnitude of earthquake would be required to cause damage to the canisters in the repository. The mechanical effects on the repository are thus deemed to be more important than mechanical or hydraulic/hydrological effects on the geosphere.

5.5.2 Gas flow/dissolution

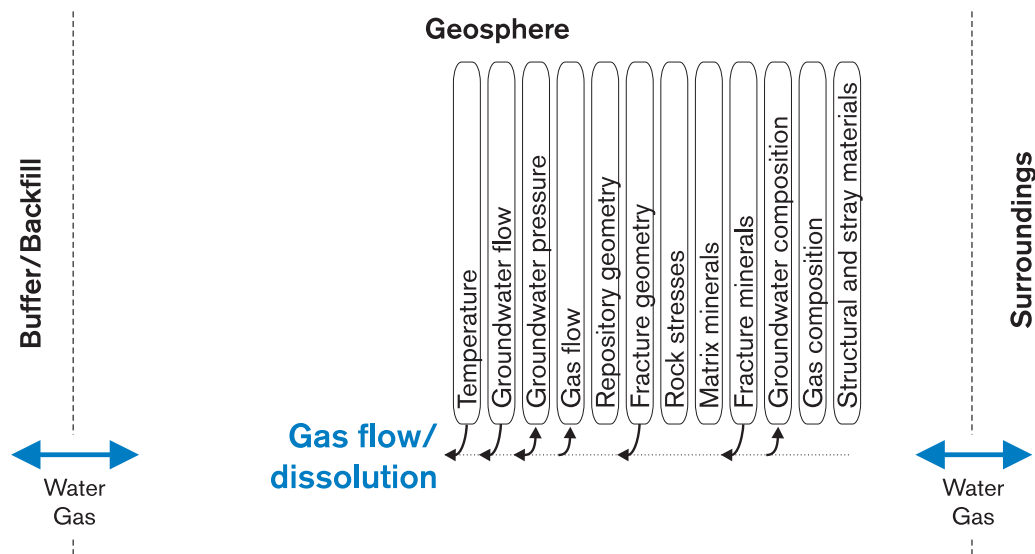


Figure 5-6. Gas flow/dissolution.

Overview

Gas from the repository can be transported through the fracture system in the bedrock up to the biosphere. Flows of water and gas influence each other in the fracture system. Further, gas can be dissolved in the groundwater and thereby be transported like other solutes with the water.

Gas transport can be significant because it influences the groundwater flow and because certain radionuclides can be transported in the gas phase.

General description

Gas that is generated in the waste can entail increased loading of and possible fracturing in the barriers in the near field, and may also affect the water flow. Gas that leaks out through the near-field barrier will pass through the tunnel area and the excavation-disturbed zone (EDZ) surrounding the tunnel. It is possible that the EDZ has higher permeability than the surrounding rock, and that it thereby constitutes a preferential transport pathway for the gas, see section 5.5.1. Eventually the gas is transported further out into the rock in the far field.

Gas can also enter the repository via air that enters during construction, and then remains after backfilling. The backfill material may also contain considerable quantities of air. When the repository is closed and the water pressure increases, this may lead to dissolution of the gas in the water /Olsson, 1994/.

Gas dissolved in water follows the groundwater flow. The flow of separate gas and water phases in the rock can generally be described as a two-phase flow. The forces that influence the flow of gas and water are mainly gravity and the pressure for each phase. Since gas is as a rule lighter than water, gravity generally leads to an upward force for the gas flow. The pressure distribution in each phase (gas or water) is highly dependent on how strongly the phase is bound by capillary forces to the solid medium and therefore on how large a fraction of gas and water is present in the pore spaces. As a rule, the capillary binding forces for water are much stronger than those for gas, giving the water a tendency to adhere to the rock. This means that the driving force for water transport tends to be directed from “wet” to more “dry” areas. The relationship between degree of saturation and pressure for gas and water is strongly dependent on the fracture and pore geometry of the rock. In general, the capillary forces are stronger the smaller the pores and fractures the rock contains. Experimental data are required for calculations. The two-dimensional nature of the rock fractures may entail a greater channelling of the water flow compared with the two-phase conditions in three-dimensional media /Jarsjö, 1998; National Research Council, 1996/.

The size of the gas and water flow is also dependent on the conductivity for the phase in question. The conductivity is also strongly dependent on the degree of saturation for the phase. This is particularly true for water, where the conductivity decreases rapidly with even a small presence of gas in the system. This is due to the fact that the large fractures and pores, which represent the greatest conductivity, are rapidly emptied since the water is not so tightly bound by capillary forces there. The gas, on the other hand, rapidly occupies the large pores, so that the conductivity of the gas rises rapidly at even a moderate degree of saturation. The dependence of the conductivity on the degree of saturation for the phase in question is determined experimentally if quantitative calculations are to be made.

Model studies/experimental studies

Experiments have been conducted both in the laboratory environment and in the field. Field studies have, for example, been conducted at the Äspö HRL /Jarsjö 1998/, at Stripa /Olsson (Ed.), 1992/ and at Grimsel /Finsterle and Pruess, 1995/. The results of laboratory studies are reported in Jarsjö /1998/.

Calculations that have been performed /Wikramaratna et al, 1993/ show that it is possible that the geosphere has great capacity to transport gas from the repository up to the surface. The natural fracture system can thus constitute a rapid transport pathway for the gas.

Time perspective

The timescale for gas transport from the repository to the atmosphere is considerably shorter than the timescale for water transport.

Natural analogues

Not applicable.

Summary of uncertainties

A realistic description of gas flow in the geosphere would be burdened with great uncertainties. The uncertainties can be handled in the safety assessment by treating the process pessimistically, see below.

Handling in the safety assessment

Base scenario: Where gas is present in the fracture system, this leads to reduced groundwater flow. It is therefore pessimistic from the perspective of the safety assessment to neglect gas transport when modelling groundwater flow.

Canister defect scenario: To the extent radionuclides can occur in the gas phase, it is pessimistic to regard the geosphere as short-circuited for the gas, i.e. the gas immediately reaches the biosphere on release from the buffer. This is dealt with in detail in section 5.8.

5.6 Mechanical processes

5.6.1 Introduction

General

One of the fundamental safety functions of the bedrock is to give the repository's engineered barriers a mechanically stable environment in both the short and long term. This means that the functions of the buffer and the canister may not be altered significantly by deformations in the rock. Another safety function of the bedrock is to retard the transport of radionuclides to the biosphere, which from a mechanical viewpoint means that the retention properties of the rock may not be seriously degraded by large movements along fractures and fracture zones, or by extensive formation of new fractures.

In general, the Swedish bedrock offers an environment that can protect and secure the repository functions. Sweden's crystalline basement comprises a part of the Baltic Shield, which extends from the Kola Peninsula and Karelia over Finland and Sweden to southern Norway. The rock types that occur in different provinces of the Baltic Shield are approximately 900 to 2,500 million years old.

Deformation and strength properties of the rock mass

In a mechanical sense, the rock mass is composed of intact rock (rock blocks) and discontinuities (mainly fractures and fracture zones). When the rock mass is loaded, it is deformed by deformation of the intact rock (possibly with formation of new fractures), and by displacement, compression or widening of the discontinuities. The deformation properties of the rock mass are thus dependent not only on the strength and deformation properties of the constituent rock types, but also on the frequency, orientation and mechanical properties of the discontinuities. The deformation and strength properties of the rock mass are scale-dependent: large rock volumes are more likely to be intersected by large fracture zones.

The deformation and strength properties of the individual discontinuities and the intact rock can be adequately described with the aid of stress-deformation relationships and failure criteria. Provided that the considered rock volume is sufficiently large to contain a representative set of fractures from typically four or more fracture sets, this can also be said to apply to the composite system, i.e. the rock mass. There are no general and simple relationships for small rock volumes with a small number of fractures.

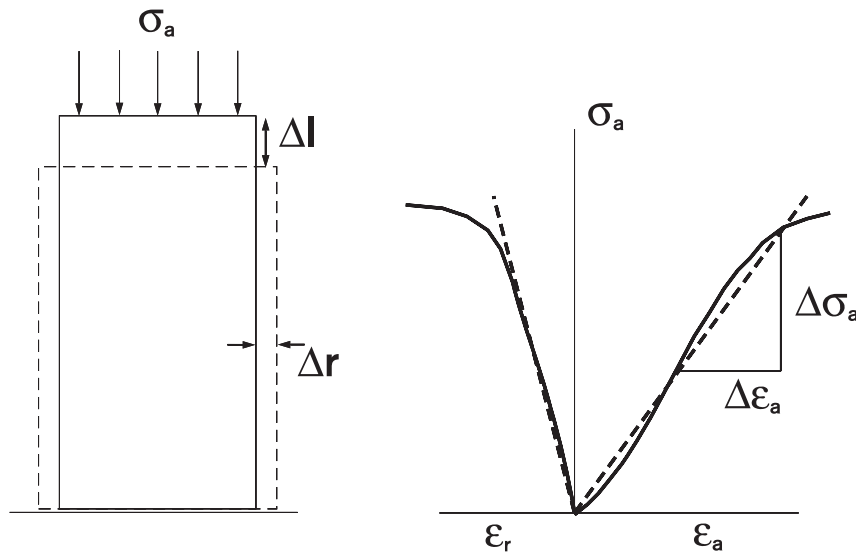


Figure 5-7. Determination of Young's modulus and Poisson's ratio by uniaxial loading of rock specimens, where the axial strain ϵ_a and the radial strain ϵ_r are determined for different axial loads σ_a . At small deformations, the stress-strain relationships are approximately linear, and Young's modulus (the modulus of elasticity) is obtained according to $E = D\sigma/\Delta\epsilon_a$. Poisson's ratio n is the ratio between radial and axial strain under uniaxial compression: $\nu = \epsilon_r/\epsilon_a$.

Deformation properties: The stresses that are generated in connection with certain types of deformations such as compression, shearing and tensile strain can be estimated with the aid of stress-strain relationships.

In the case of small deformations, the process is largely reversible and can be characterized using elastic parameters: Young's modulus, Poisson's ratio (intact rock) and shear stiffness, normal stiffness (discontinuities). Figure 5-7 schematically illustrates the significance of Young's modulus and Poisson's ratio.

Young's modulus has the dimension stress, while Poisson's ratio is dimensionless.

For small deformations of fractures, the normal stiffness $K_n = \Delta\sigma_n/\Delta u_n$ and the shear stiffness $K_s = \Delta\sigma_s/\Delta u_s$, given in a similar way to the relationship between stress and displacement in the normal and shear direction, respectively. K_n and K_s both have the dimension stress/length.

For the composite system, i.e. for the rock mass, there are different methods to estimate elastic parameters that correspond to the ones used for intact rock. Several expressions have, for example, been proposed for the modulus of elasticity where rock quality indices, such as the Rock Mass Rating (RMR) is weighed in /Brady and Brown, 1993/.

An irreversible or plastic contribution is included in large deformations of intact rock, fractures and rock masses. Failure generally occurs, i.e. a maximum stress is reached which, under the given conditions, defines the strength of the system (e.g. the uniaxial compressive strength of a rock specimen or the shear strength of a fracture at a given normal compression).

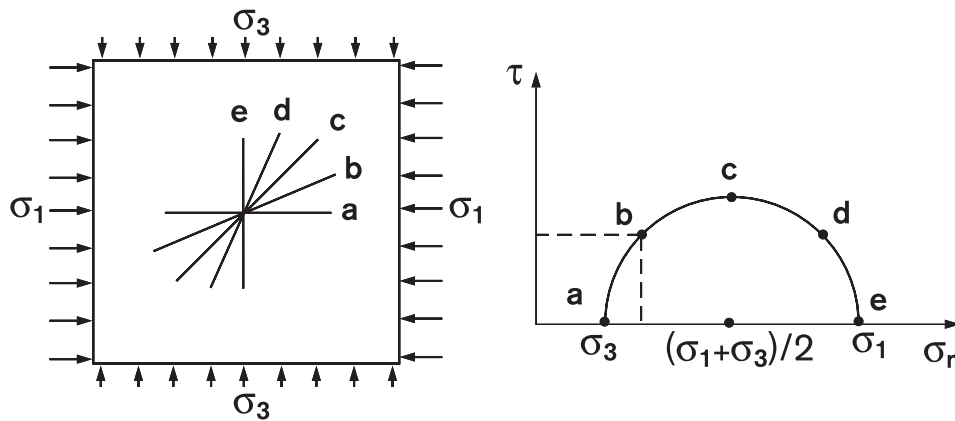


Figure 5-8. State of stress illustrated by Mohr's circle. If the signs of the shear stresses are disregarded, the problem is symmetrical and half the circle is enough. The intersection of the dashed lines with the coordinate axes gives the normal stress and the shear stress in planes oriented as the plane b.

State of stress: The state of stress in the rock is a variable for all mechanical processes. States of stress are tensors and are characterized by three mutually perpendicular principal directions, each of which corresponds to a principal stress. If all three principal stresses, σ_1 , σ_2 and σ_3 , are equal, the state of stress is isotropic and the principal directions are indefinite. If the principal stresses are unequal, the state of stress is anisotropic or deviatoric. To simplify, the intermediate principal stress σ_2 is often disregarded. The state of stress can then be illustrated by Mohr's circle as illustrated schematically in Figure 5-8. All points on the circle correspond to planes, or orientations of planes, in a medium with the major and minor principal stresses σ_1 and σ_3 . The horizontal coordinate gives the normal stress σ_n which acts in the plane, the vertical coordinate gives the shear stress τ . If σ_1 and σ_3 are equal, no shear stresses exist and the semicircle degenerates to a point. The maximum shear stress $(\sigma_1 - \sigma_3)/2$ acts in the plane c in the figure (45° to the principal stress directions). The normal stress in plane c is equal to the mean compressive stress $(\sigma_1 + \sigma_3)/2$. No shear stresses act in the planes a and e, which are the principal stress planes.

The stresses that act in the bedrock before any disturbance in the form of rock removal or heating has taken place are called the primary or natural rock stresses. For Swedish bedrock it is usually assumed that one of the primary principal stresses (usually the smallest one) is approximately vertical and corresponds to the weight of the overlying rock, which means approximately 13.5 MPa at 500 m depth. The major and intermediate principal stresses are then both approximately horizontal. Both general and site-specific regression relationships between primary horizontal stresses and depth exist, but the variations are great, both between different sites and locally within smaller areas. For Beberg and Ceberg, the relationships give a maximum horizontal stress at 500 m depth of 23 MPa and 20 MPa, respectively /Ljunggren et al, 1998/. Horizontal stresses in the order of 35–40 MPa and considerable anisotropies in the horizontal plane have been measured in Aberg /Leijon, 1995/.

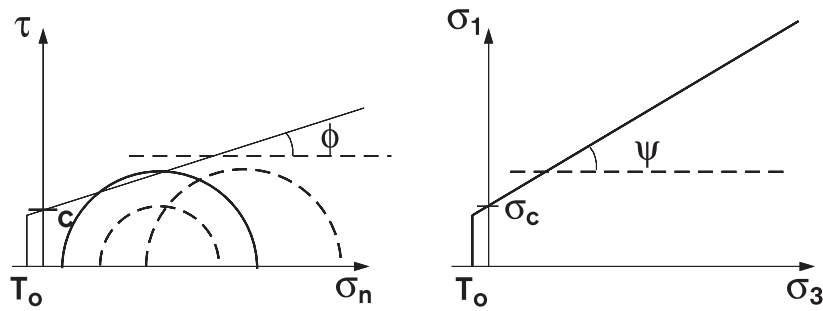


Figure 5-9. Failure envelope according to Coulomb in terms of a) shear and normal stresses and b) principal stresses. c = cohesion, ϕ = friction angle, σ_c = uniaxial compressive strength, T_o = uniaxial tensile strength. The slope of the envelope in the principal stress representation is given by $\tan\psi = (1+\tan\phi)/(1-\tan\phi)$. The solid Mohr circle represents, as opposed to the two dashed ones, a state of stress for which the strength is exceeded.

Strength properties: The strength of rock-mechanical systems is dependent on the load conditions. Idealized relationships, failure criteria, give the dependence as ratios between the principal stresses σ_1 , σ_2 and σ_3 , or between the shear stress t and the normal stress σ_n that act on some special plane. For the criteria that are normally applied to rock, i.e. Coulomb's criterion and Hoek-Brown's criterion, it is assumed that the influence of the intermediate principal stress σ_2 can be disregarded.

Figure 5-9 shows failure envelopes, based on Coulomb's criterion. The criterion gives a good representation of the shear strength of individual discontinuities, but because of its simplicity is often applied to intact rock and rock masses as well, despite the fact that it is based on assumptions that are rarely met. A simple strength analysis at a given state of stress can then be done by comparing the envelope with Mohr's circle. Two independent parameters are included: cohesion and friction angle.

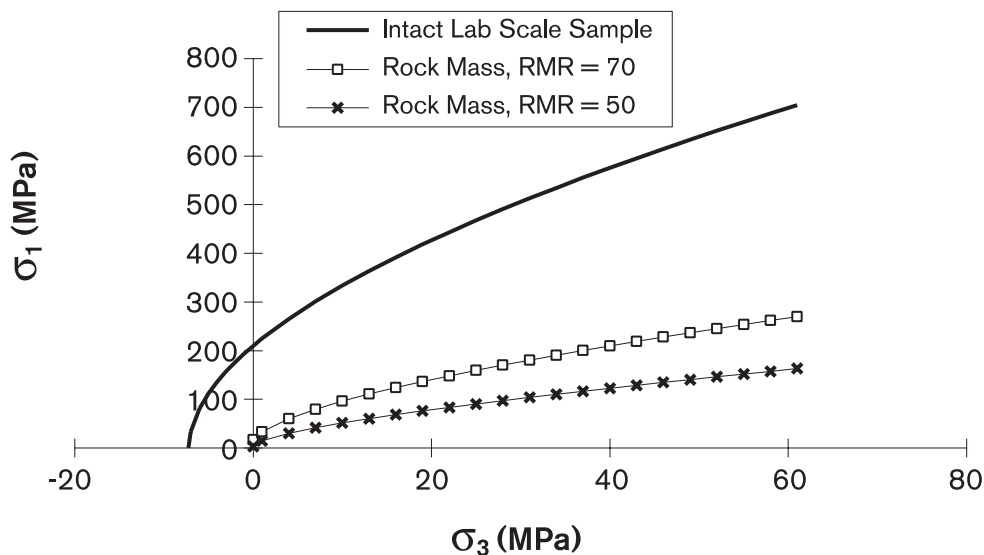


Figure 5-10. Failure envelopes according to Hoek-Brown.

Coulomb's criterion is primarily applicable to individual fractures. For intact rock and for rock masses with at least 4 arbitrarily oriented fracture sets, Hoek-Brown's failure criterion gives a better strength estimate. Figure 5-10 shows failure envelopes according to Hoek-Brown, with parameter values typical for intact granite and with parameter values adjusted to apply to rock masses with different RMR indices /Brady and Brown, 1993/.

Even though the result of the application to the rock mass must be interpreted with caution, Figure 5-10 illustrates a fundamentally important fact: the decisive importance of the fractures for the strength of the rock mass.

Stability: The rock, or the rock mass, is a mechanical system that is normally in static equilibrium under the prevailing loads, i.e. no unbalanced forces exist. The equilibrium can, however, be more or less stable. If small disturbances of the equilibrium lead to a sudden decrease in the system's potential energy and large changes in its geometry, the equilibrium is not stable. Disturbances of equilibrium may be due to load changes or changes in the strength properties, for example due to changes in groundwater pressure or due to hydrothermal changes of the material in filled fractures.

Instability in the host rock requires that the rock mass, locally or globally, is near the failure state, i.e. that the state of stress corresponds to a point near the failure envelope. The failure state as such does not, on the other hand, have to entail serious instability: small deformations, of no consequence for performance and safety, can be sufficient for the system to regain its equilibrium if failure should occur.

Processes in the safety assessment

All mechanical processes in the host rock have to do with deformations, and all deformations have to do with loads and stresses. These fundamental concepts link together the components of the rock mass, the intact rock and the discontinuities, in such a way that there is no truly logical and at the same time expedient subdivision of the geosphere's mechanics into individual processes. Fracture propagation, for example, involves at the same time ongoing plastic deformation of intact rock and movement in an existing fracture. The following subdivision into processes has nevertheless been deemed expedient:

1. Movement in intact rock.
2. Thermal movement.
3. Reactivation – movements along existing discontinuities.
4. Fracturing (formation and propagation).
5. Time-dependent deformations.

By "movement in intact rock" is meant the mainly elastic movements that occur in rock without visible fractures at moderate loads, i.e. at loads that do not cause failure.

By "thermal movement" is meant a fundamental thermomechanical process in intact rock: volume expansion caused by increased heat-induced movements in the crystal matrix in response to temperature increase. The effects of the volume expansion in the form of movements along fractures or failure and fracturing in constrained, heated rock fall under the headings "reactivation – movements along existing discontinuities" and "fracturing".

By “reactivation - movements along existing discontinuities” is meant all types of movements, elastic and inelastic, which take place along discontinuities of various kinds.

By “fracturing” is meant failure in intact rock, both by formation of new fractures and growth of existing fractures.

All deformations in the repository are time-dependent in the sense that all load changes, instantaneous and continuous, are distributed over time. The continuous mechanical processes, which take place more or less simultaneously with the load changes and in accordance with the same stress-deformation relationship that is assumed to apply to the different components of the rock mass, are regarded here as non-time-dependent. By “time-dependent deformations” is meant delayed deformations that occur due to the fact that the rock in the long time perspective has, or may have, time-dependent material properties. There are classification problems: The process “fracturing”, for example, contains an inherent time dependence that has to do with initiation and propagation of microfractures at loads that are lower than the laboratory-determined strength, and which can after some time lead to failure, for example spalling next to chamber walls. The same type of phenomenon could conceivably take place at a slow rate at many places and at different distances from the repository’s cavities, for example in small areas around strained asperities, and then contribute to the exhibition by the rock mass of time-dependent deformation properties.

The rock mass is made up of intact rock and of discontinuities. That is why “movement in intact rock”, “reactivation” and “fracturing” are fundamental and general processes. All load changes are accompanied by movement in intact rock. Furthermore, if there are suitably oriented fractures, the movements occur preferentially along them. At large loads fracturing also sometimes occurs, especially if suitably oriented fractures along which the movements can take place are not present. “Thermal movement” is also a fundamental process, but unlike the other three it is not caused by load changes. On the contrary, the process causes load changes and therefore drives the other three processes. Finally, “time-dependent deformations” comprise delayed movements in intact rock and delayed reactivation and fracturing, and are therefore not strictly speaking a separate process. Our knowledge of delayed deformations is poor and it is therefore expedient to regard the aggregate effect of all such deformations and simultaneous changes in the material properties of the rock mass as a special process.

Initial state

After deposition and closure, the host rock is in what is termed in the safety assessment the initial state. Mechanically, the initial state is characterized by the fact that the rock around tunnels and deposition holes has been affected by the disequilibrium, with subsequent deformations and stress redistributions, that has resulted from excavation of the various cavities. The processes “movement in intact rock” and “reactivation” have thus already occurred, and possibly “fracturing” as well. When it comes to stress redistribution, the range of its influence is a few tunnel diameters counting from the tunnel wall (Figure 5-11). Furthermore, the rock nearest the walls of the cavities has been directly affected, or damaged, by the blasting or boring procedure. This excavation-damaged zone (EDZ) has a depth of from a cm or so up to 50 cm, depending on the tunnelling method used /Olsson et al, 1996; Autio, 1997/.

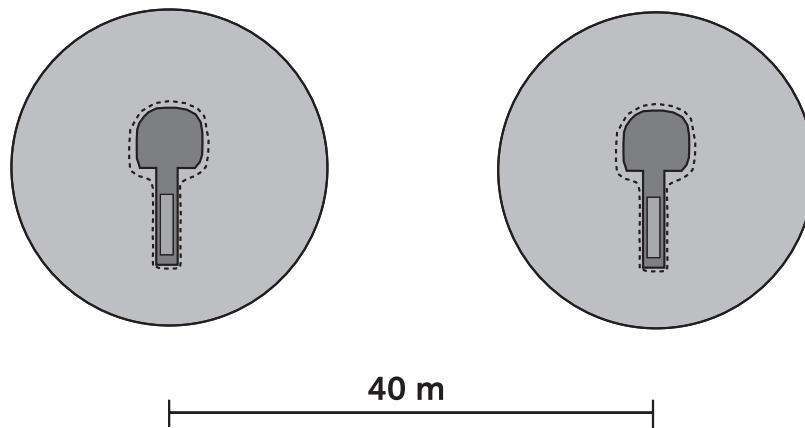


Figure 5-11. Schematic illustration of EDZ (inside dotted curve) and stress-affected zone.

During the construction and deposition phase the rock is drained. In the initial state, the pore water pressure in the fractures nearest the excavated cavities is therefore reduced in relation to the natural groundwater pressure. Mechanically, this means that the shear strength of the fractures is higher than it will be when the groundwater pressure is subsequently restored.

The primary rock stresses are still active outside the stress-affected zone. Inside the zone secondary stresses prevail, which are characterized by large tangential stresses and small radial stresses, i.e. large stress anisotropies and therefore large shear stresses. The magnitude and anisotropy of the secondary stresses are highly dependent on the primary stresses and the direction of the tunnels in relation to the primary stresses. If the tunnels are perpendicular to the major primary principal stress, such large tangential compressive stresses can arise in a small area around the intersection between the tunnel and the deposition hole that the rock there will very probably be in a state of failure / Hökmark, 1996/.

5.6.2 Movements in intact rock

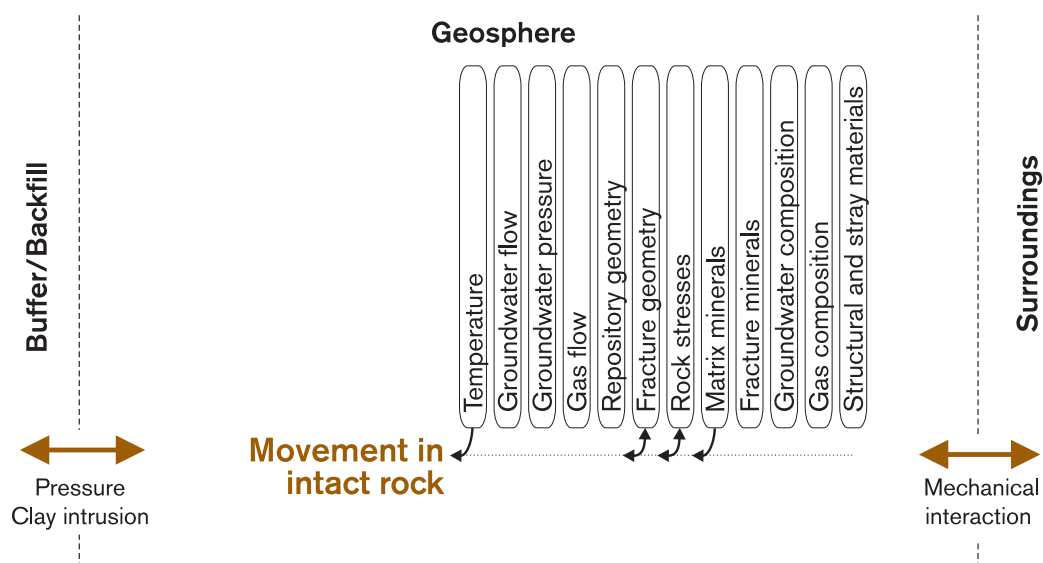


Figure 5-12. Movement in intact rock.

Overview, general description

No mechanical processes in the geosphere can take place without movements also occurring in the intact rock. However, the process does not really have any direct impact on safety.

In the case of intact crystalline rock, linear-elastic relationships for homogeneous isotropic media apply. At a given load, the movements are therefore determined by two elastic parameters, e.g. Young's modulus and Poisson's ratio.

Influence of rock stresses, influence on rock stresses: The coupling to the rock stresses is given by linear-elastic stress-strain relationships and by the elastic parameters.

Influence of fracture geometry, influence on fracture geometry: The fractures and the intact rock influence each other via the rock stresses.

Influence of temperature: Within the temperature range 0 – 150 °C the temperature dependence of the elastic parameters is negligible /Lau et al, 1991/. Temperature changes are on the other hand crucial for the thermal movements in intact rock.

Influence of matrix properties: Mineral composition and grain size influence the elastic properties.

Summary of uncertainties

There are no conceptual uncertainties when it comes to describing movements in intact rock. There is some data uncertainty when it comes to Young's modulus and Poisson's ratio. Firstly there is a statistical variation in values determined in the laboratory, and secondly there is a variation due to the sampling technique. Furthermore, there is a variation between rock types, i.e. between rocks of differing matrix composition. For the rock types that occur in the Äspö HRL, Young's modulus lies between 60 and 80 GPa /Rummel, 1997; Stille and Olsson, 1996/. Poisson's ratio lies between 0.18 and 0.27.

Model studies/experimental studies

The intact rock is included in all numerical studies of stresses and deformations in the host rock. The mechanical structure of the rock mass is, however, such that all essential displacements take place along discontinuities of various kinds.

The intact rock is approximately linear-elastic, and it is therefore possible to get an idea of how the geometry of the repository cavities would be affected by load changes if the rock mass were entirely composed of intact rock by applying analytical expressions, *Kirsch Equations* for stresses and deformations around circular cavities, to hypothetical load cases. All reasonable load cases then give negligible deformations of the deposition hole geometry.

Handling in the safety assessment

The contribution made to change of the geometry of deposition holes by movements in intact rock is without importance for safety and performance.

5.6.3 Thermal movement

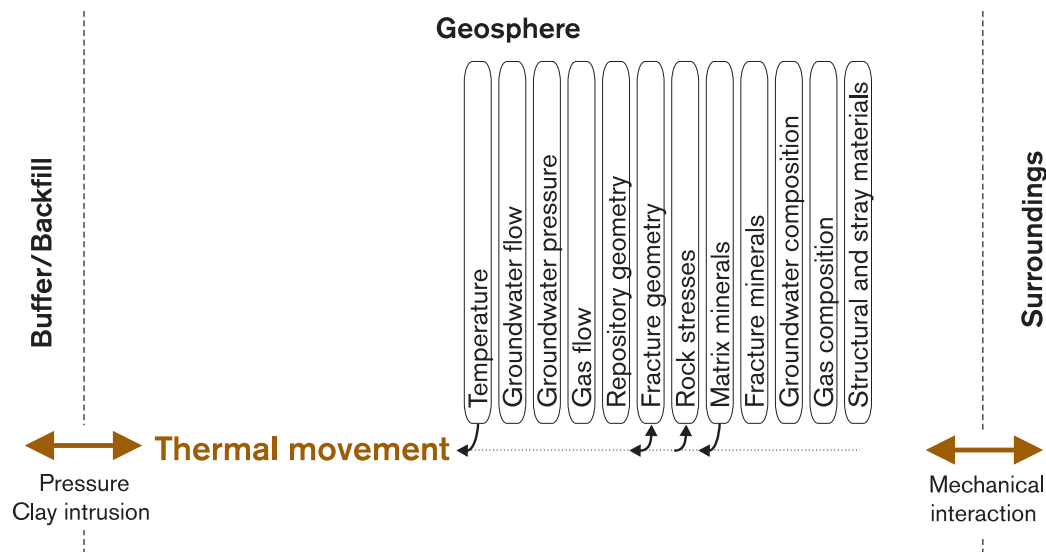


Figure 5-13. Thermal movement.

Overview

When canisters of spent fuel are deposited in the bedrock, the temperature of the rock will increase due to the fuel's residual power or decay heat. For a free volume of intact rock, a uniform temperature increase would result in a volume expansion that depends solely on the coefficient of thermal expansion. Since the rock in the repository is constrained, the expansion is completely or partially suppressed and thermal stresses are generated around the canister holes and the repository. The size of the volume expansion and the thermal stresses is dependent on the coefficient of thermal expansion and the compression properties of the rock.

General description

Influence on rock stresses: the heated rock is constrained by the surrounding unheated rock, which keeps the thermal movement small while the thermal stresses are instead high. The thermal stresses correspond to the load that would be needed to compress a freely expanded rock element to the volume the element actually occupies at the given temperature, and are therefore dependent on the rock's deformation properties.

Influence of temperature: Temperature changes are the reason the process takes place at all. The rock temperature at different points, both in the near field and at great distance from the deposition holes, can be calculated analytically /Claesson and Probert, 1996/. If it is assumed that the initial temperature is 15°C, the maximum temperature at the boundary of the deposition holes is about 70°C. Within this temperature range the coefficient of thermal expansion for granite is virtually independent of the temperature /Swan, 1978/.

Influence of fracture geometry, influence on fracture geometry: The general rule, as for movement in intact rock, is that fractures are influenced via the stresses. The existence of fracture zones with small normal stiffness in the host rock means that the equivalent modulus of elasticity is small, which means that the thermal stresses may be reduced. The existence of compressible fracture zones outside the host rock means that a larger volume expansion is allowed, which also would reduce the thermal stresses.

Influence of matrix composition: The coefficient of thermal expansion is in principle dependent on the rock type, but the variations are not great and the values that are generally used are reasonable mean values.

Time perspective

The maximum temperature is reached about 50 years after deposition. After approximately 5,000 years the temperature in the host rock is about 15°C above the original temperature. The greatest thermal stresses are obtained around deposition holes between 50 and about 200 years after deposition /Hökmark, 1996/.

Model studies/experimental studies

Probert and Claesson /1997/ made analytical thermomechanical calculations where the bedrock was assumed to be a semi-infinite elastic continuum with elastic parameters roughly as for intact rock. The maximum global thermal stress was approximately 17 MPa. Hakami et al /1998/ made numerical calculations that showed that the maximum global thermal stresses were halved if it was assumed that the repository rock was intersected by a number of compressible fracture zones. Hökmark /1996/ conducted numerical near-field studies with an elastic model that showed that the thermal stresses in the intersection between deposition hole and tunnel are between 20 and 40 MPa, depending on what constraint condition is assumed.

Summary of uncertainties

Uncertainties in understanding: There are no conceptual uncertainties regarding the process.

Uncertainties in data: The data uncertainty is small. The coefficient of thermal expansion varies for different types of granite between $6.7 \cdot 10^{-6}$ and $8.4 \cdot 10^{-6}$ per °C /Swan, 1978/. The greatest uncertainty concerns the degree of restraint, i.e. what volume expansion of the host rock will actually be allowed, and what compression properties the host rock has.

Handling in the safety assessment

The thermal movements as such have no direct effects on safety. The thermal load contribution can, however, together with the loads already acting in the initial state, cause the strength of intact rock and of individual fractures to be exceeded. The effects of the thermal load contribution are dealt with in the processes “reactivation” and “fracturing”.

5.6.4 Reactivation – Movement along existing fractures

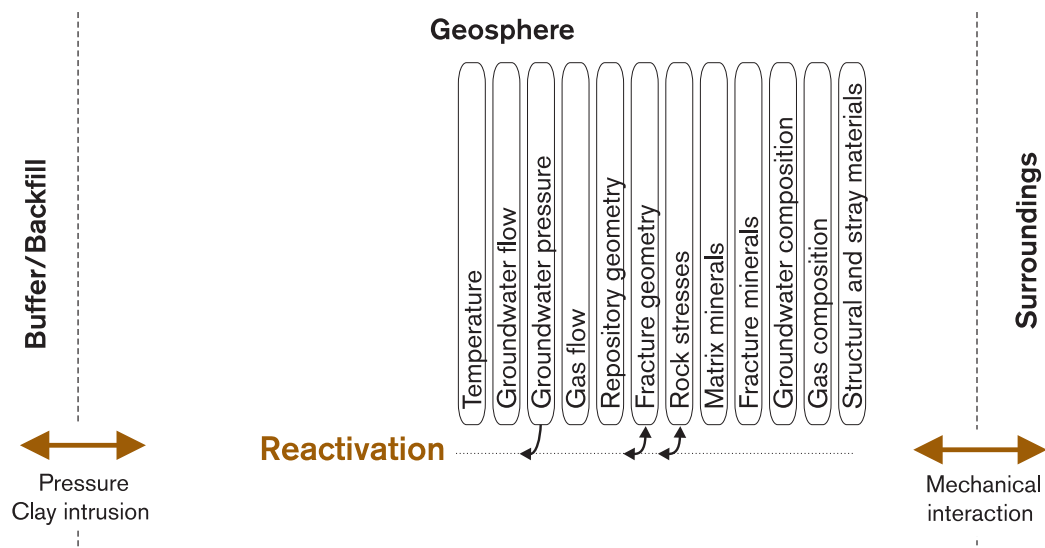


Figure 5-14. Reactivation – Movement along existing fractures.

Overview

The most fundamental mechanical process in the geosphere from the safety viewpoint is movements in large discontinuities. Discontinuities of all types, from millimetre-sized fractures to composite fracture zones extending several kilometres, are mechanical systems whose behaviour is controlled by the loads to which they are subjected, by the prevailing groundwater pressure and by their own inherent mechanical properties. There are two main types of deformations: shear movements and normal movements. In reality the two types of deformation occur simultaneously.

General description

On the near-field scale, and possibly on the tunnel scale as well, large fracture zones hardly appear as discrete discontinuities but rather in the form of an elevated frequency of individual fractures or as areas with deviant mechanical properties. On the repository scale, however, it is expedient to regard large fracture zones as discrete discontinuities. Single fractures in the rock mass outside the large fracture zones contribute to the average properties of the rock mass, but do not appear on the repository scale as individual units. Our state of knowledge regarding deformation and strength properties differs considerably for single fractures and large fracture zones.

Normal movements: Movements in the normal direction can take place due to changes in the effective normal stress (e.g. increased or decreased compression, increased or decreased water pressure in the fracture), and due to far-reaching shear deformations where irregularities force the fracture surfaces to separate (dilatancy).

In the case of pure normal loads, the greater the normal stiffness of the discontinuity is, the less mechanical importance the discontinuity has. Infinite normal stiffness is equivalent to non-existence of the discontinuity. In the case of single fractures, the normal stiffness is strongly dependent on the normal stress, which means that the stiffness is great for fractures in high compression and less for fractures in low compression /Hökmark, 1991; Barton et al, 1985/. The normal stress dependence of large fracture zones is small, however /Leijon, 1993/. In the case of large zones, it can be assumed for normal stresses of approx. 10 MPa that the normal stiffness is around two orders of magnitude smaller than for single unfilled fractures.

The fracture spacings for fractures not situated within fracture zones are great, which, together with large normal stiffness and small mechanical apertures, means that purely normal movements in individual single fractures are generally of little importance for the mechanical properties of the rock mass. Fracture zones with small normal stiffness, on the other hand, can absorb large compressions and thereby influence the mechanical properties of the rock mass.

Shear movements: The deformation and strength properties of single fractures are complexly dependent on, among other things, the strength of the material in the fracture surfaces and the topography of the fracture surfaces. With Barton's system /Barton et al, 1985/, empirically based stress-deformation relationships can be developed for both shear movements and normal movements. The system is based on laboratory determination of values for a small number of fundamental fracture parameters according to a standardized procedure. These are the fracture's residual friction angle ϕ_r , the fracture's surface roughness JRC (Joint Roughness Coefficient) and the fracture's surface strength JCS (Joint Compressive Strength).

In the case of single fractures, elaborated material models thus exist which well describe the type and size of fracture movements under given loading conditions, provided that the assigned parameter values are representative of the fracture in its entirety. In practice, e.g. in numerical simulation of rock-mechanical problems, the parameter values are not known and estimates have to be used, for example based on comparisons with cases where systematic laboratory determinations have actually been done. In analysis of movements of individual fractures in a rock mass, the greatest problem is actually not that the material properties of the fracture are not known with sufficient accuracy, but that assumptions must be made concerning the fracture's position, orientation, extension and interaction with other fractures. These geometric parameters are usually more important than details in the material properties, which is why in practice simpler and more robust material models are used which nevertheless possess the basic features of more sophisticated models. Figure 5-15 shows as an example a comparison between Barton's model for shear movement and an ideal elastoplastic model with failure criterion according to Coloumb.

The elastic part of the deformation can amount to a millimetre or so /Barton and Vik, 1988; Olsson, 1998/. Shear movements of such size that they are of importance for safety are therefore mainly friction-controlled.

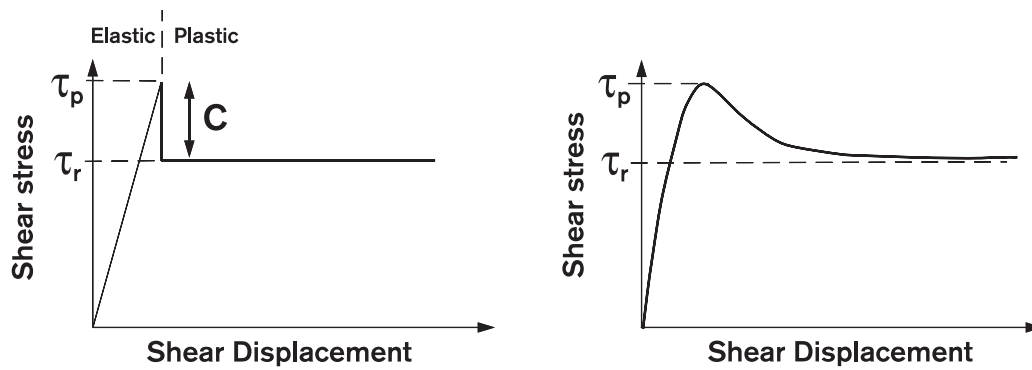


Figure 5-15. Stress – deformation relationship for single fracture. τ_p = strength at failure, τ_r = residual strength, ϕ = friction angle, σ_n = normal stress, c = cohesion, JCS = Joint Compressive Strength, JRC = Joint Roughness Coefficient.

There are no empirically based general material models for fracture zones, i.e. structures composed as systems of single fractures. Width and fracture frequency, plus degree and nature of interaction between constituent fractures, can vary within wide limits for one and the same fracture zone. If the fracture zone is conceived as a discrete discontinuity, mechanical properties must be assumed that represent the aggregate influence of the constituent fractures. No knowledge or experience exists similar to that that exists for the description of the mechanical properties of single fractures, but it is generally assumed that movements in the shear direction are controlled by friction.

Influence of fracture geometry: In general, the geometry of the fracture system influences the movements of the individual fracture via its influence on the deformation properties of the rock mass. The extension of a fracture or fracture zone along its own plane has a particularly great importance for the largest shear deformation that can occur at a given load /Turcotte, 1992/. The maximum deformation of a fracture in an elastic medium can be determined analytically /Pollard and Segall, 1987/ and is dependent on the extension and friction angle of the fracture and the elastic properties of the rock. If it is pessimistically assumed that the fracture’s friction angle is zero, the largest shear deformation that can be obtained in fractures of different extension in the host rock can be defined for different load cases. Figure 5-16 shows such an analytical relationship between fracture extension and maximum possible shear movement. The relationship is pessimistic and pertains to the theoretical case that the fracture has an infinite extension perpendicular to the plane of the figure. In order to get a displacement of 0.1 m in this two-dimensional geometry and with a maximum shear stress of 20 MPa, an at least 100 m long friction-free fracture is required. For a fracture with a friction angle of 30°, an approximately 400 m long fracture is needed. The deformation for actual fractures, with finite extension in all directions, will be less.

Influence on fracture geometry: Normal movements affect the aperture of individual fractures.

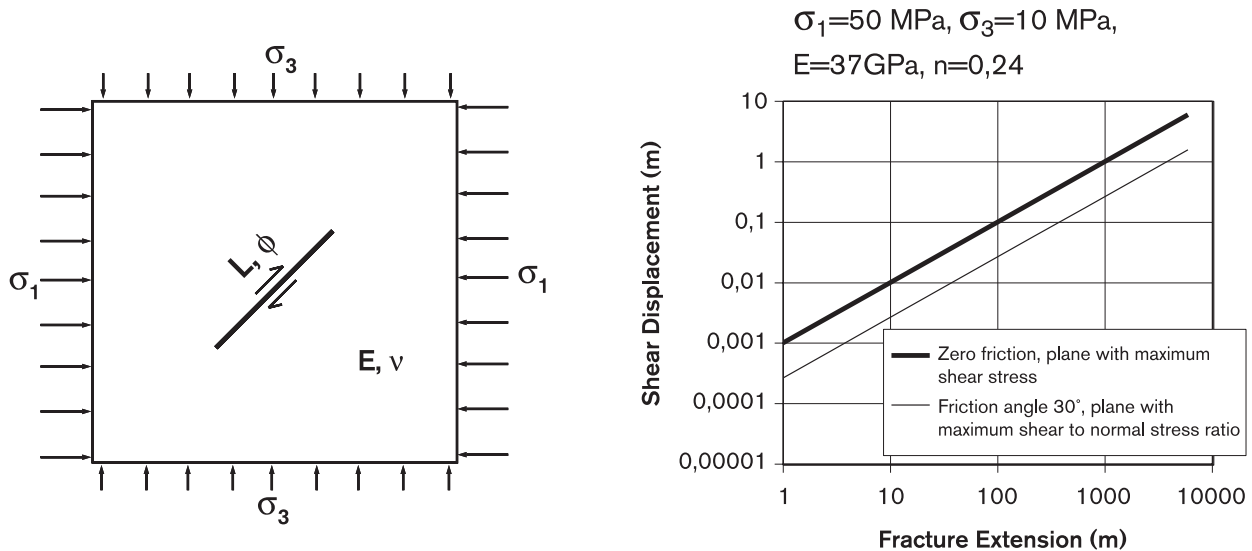


Figure 5-16. Fracture with extension L and friction angle ϕ in elastic medium with the elasticity parameters E and ν . The shear deformation is maximal at the centre of the fracture and zero at the edges. The graph shows the relationship between maximum displacement and fracture extension for a pessimistic 2D case.

Influence of rock stresses: The rock stresses are of great importance for the process. If the state of stress is strongly anisotropic, i.e. if the difference between the major and minor principal stress is great, there will be fracture planes with large shear stresses and small normal stresses, which entails great risks for shear failure in connection with future changes in the rock stresses. Large primary principal stress differences can also result in strengthened stress anisotropy around tunnels and deposition holes, which means greater shear movements in fractures in the near field.

Influence on rock stresses: The idea that the state of stress in the earth's crust is partially determined by friction in large fracture zones has been put forward by, among others, Jaimson and Cook /1978/. In summary, the ratio between shear stress and mean compressive stress is upwardly limited, and future load changes that would cause the limit to be exceeded will give rise to friction-controlled shear movements so that the stress ratio is restored. This line of reasoning, which entails that the bedrock is always in an unstable state, can only be applied on the largest scale /Leijon, 1993/. In the near field, movements along discontinuities that are tangentially oriented in relation to cavities result in increased tangential stresses between cavity and fracture. Movements along discontinuities that intersect the cavity periphery at an oblique angle can reduce the tangential stresses. Normal movements in single fractures are small and have little effect on the state of stress. Large fracture zones limit the thermal stresses due to temperature increase by allowing large normal deformations.

Influence of groundwater pressure: At elevated groundwater pressures, the effective normal stress is reduced in all discontinuities that are hydraulically connected to the groundwater system, which means that their shear strength decreases. In the case of discontinuities that are loaded with large shear stresses, movements can be triggered as a consequence of shear failure.

Model studies/experimental studies

A number of methods exist for numerical analysis of the mechanics of rock masses made up of discrete blocks, for example DEM (Distinct Element Method) and DDA (Discontinuous Deformation Analysis). Several rock-mechanical studies of movements and stresses around the final repository have been done with the DEM programs UDEC (2D) and 3DEC (3D). The studies have been done on both the tunnel and repository scales.

Tunnel scale: Hökmark /1990/ and Hökmark and Israelsson /1991/ simulated excavation of the BMT tunnel at Stripa with UDEC and 3DEC. The fractures were 10 m – 20 m in length, with mechanical properties in accordance with laboratory determinations done previously on fracture specimens from the Stripa Mine /Barton and Vik, 1988/. A complicated material model similar to Barton's model was used in the UDEC study. An ideal elastoplastic model with Coloumb's fracture criterion was used in the 3DEC study. Excavation of a half-scale deposition hole was also simulated in the 3DEC study. The calculated shear movements amounted to 2–3 mm at most. Johansson et al /1991/ performed similar calculations with UDEC and 3DEC for a hypothetical repository in the Finnish bedrock, but assumed a larger strength in the fractures and furthermore analyzed the thermomechanical effects of the deposited fuel. The maximum shear movements amounted to 3 mm. Shen and Stephansson /1990a/ obtained a maximum shear movement of 1.2 mm in similar calculations.

Repository scale: Shen and Stephansson (1990b) conducted a 3DEC study of a repository in rock with small (1–3 km length), medium-sized (2–8 km length) and large fracture zones (> 8 km length). The maximum shear movement, 5.5 cm, was obtained at the ground surface for a large fracture zone during glaciation with a 3 km ice cover. The thermal pulse gave maximum shear movements of approximately 1 cm. In a more recent 3DEC study, the maximum shear movement of large fracture zones was approximately 2 cm for the thermal pulse and approximately 8 cm for glaciation /Hansson et al, 1995/.

Rosengren and Stephansson /1990/ analyzed the effect of an ice load above a hypothetical repository in Finnsjön with UDEC. The maximum shear movement amounted to approximately 3 cm.

Israelsson /1996/ performed thermomechanical 3DEC calculations for a hypothetical repository in Äspö with nine steeply-dipping, large fracture zones intersecting the hypothetical repository area. The maximum shear movement was about 2 cm for pessimistic assumptions regarding the thermal power. Down to a maximum depth of about 200 m below the surface, the aperture of the zones increased.

La Pointe et al /1997/ analyzed the effect of occasional quakes of different magnitudes at different distances from a hypothetical repository with a fracture structure in accordance with a fracture structure model for the Äspö HRL. The analysis was performed with the Displacement Discontinuity programme POLY3D for the pessimistic assumption that the fractures are friction-free. For quakes of magnitude 6.1 that occur at a distance of 2 km from the repository, the greatest shear deformation in the repository area was around 2 mm (Figure 5-17). In order to induce a 0.1 shear displacement in the host rock, a quake of magnitude 7.5 must occur at a distance of less than 100 m and a quake of magnitude 8.2 at a distance of less than 1,000 metres.

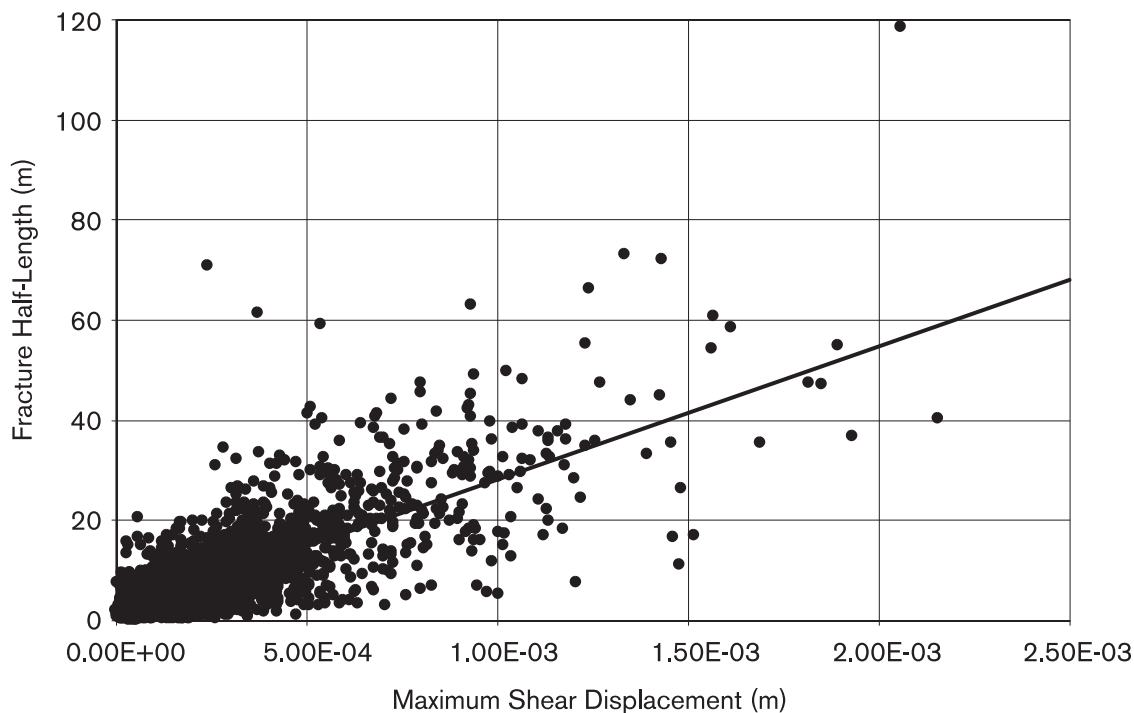


Figure 5-17. Shear displacement of fractures in the repository caused by quake of magnitude 6.1 at a distance of 2 km from the repository as a function of the length of the fractures. The scatter around the regression line is due to the distance of the individual fractures from the quake and their orientation /La Pointe et al, 1997/.

Natural analogues

In the international literature, as well as in SKB's studies, reports and compilations are found of observable displacements in the field. A relatively modern database deals with displacement movements in conjunction with earthquakes /see La Pointe et al, 1997 after Wells and Coppersmith, 1994/. SKB's efforts have been focused on postglacial displacements and neotectonics.

The earthquake database contains compilations for different types of faults. Figure 5-18 shows such a compilation. It can be seen from the figure that the relationship between displacement sum and fracture size is of the same type as the theoretically derived relationship shown in Figure 5-16.

Postglacial fault movements have been studied in northern Sweden in the Lansjärv Fault, among others. The structures are interpreted to be very old (hundreds of millions of years) and their extension in length can be followed over 100 km. The faults are considered to be caused by reactivations in the already existing structures. The displacement sums amount to 5 to 10 metres /see further Bäckblom and Stanfors, 1989; Stanfors and Ericsson, 1993/. Similar observations have been made for normal faults in Hanöbukten and on the North Sea that have been interpreted from marine seismic investigations /see Wannäs and Flodén, 1994; Muir-Wood, 1995/.

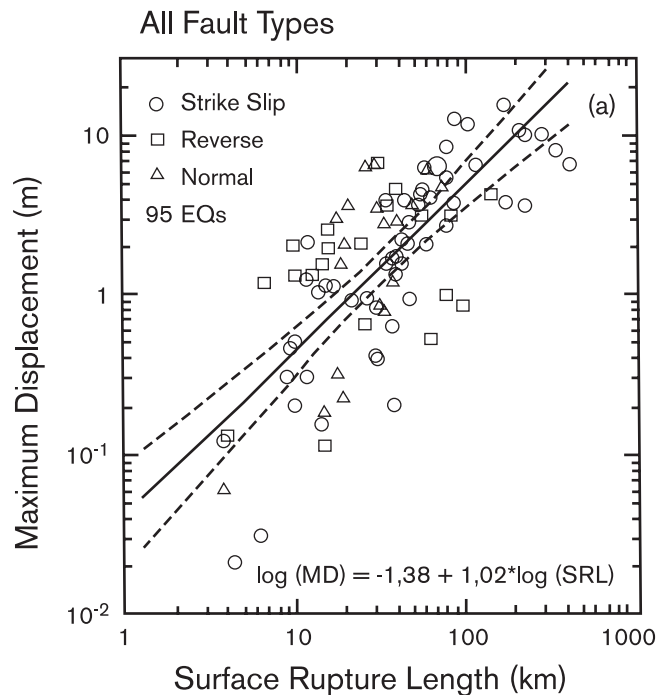


Figure 5-18. Empirical relationship between maximum displacement and observable length of fault structure that has been active in conjunction with an earthquake. The database consists of 95 earthquakes /from La Pointe et al, 1997/.

Other studies are based on observable displacements in geological structures (e.g. shore-lines) or fossils that cross faults. A special study of shears in individual fractures has been carried out on outcrops in limestone on Öland. The limestone contains partially sheared-off fossils. The fracture lengths vary, but are in the order of 10 to 100 m. The maximum and cumulative displacement sums that have been observed are approximately 0.10 m. The displacements have taken place during a period of approximately 450 million years. /se Mihes and Gee, 1992/.

In summary, it can be concluded that clear correlations exist between the measured displacement sums (shear) and the lengths of the structures where these displacements have taken place.

Time perspective

The process is linked to changes of the load and the groundwater pressure and takes place during the period the thermal load varies (approx. 0–5,000 years) and during the period a future ice cover advances and retreats. The time perspective for seismic movements depends on the statistical magnitude/frequency relationships that apply to the candidate host rocks.

Summary of uncertainties

Uncertainties in data: A considerable uncertainty exists when it comes to assessing the loads to which the host rock will be subjected. This does apply to the thermal load, where uncertainties exist regarding which effective modulus of elasticity is applicable to the repository and the surrounding rock.

Uncertainties in understanding: As regards effects of a coming glaciation, uncertainty prevails as to which is the most appropriate way to describe the interaction between ice load and bedrock. The loads on the host rock are, for example, different if the earth's crust is modelled as an elastic plate on a viscous medium /Rehbinder and Yakubenko, 1998/ compared with the loads that have been assumed in the analyses done thus far.

There is an uncertainty regarding how the topography of the individual discontinuity on different scales influences its mechanical properties. Models for scale dependence exist, but no results from large-scale tests with non-planar fractures in constrained rock. The method that is generally applied, namely to regard discontinuities as completely planar, is presumably pessimistic.

For large fracture zones, conceptual uncertainties exist above all when it comes to stress-deformation relationships in the shear direction. What is generally assumed – namely that the movements are determined by friction and that the friction angle is small and the same over the entire extension plane of the zone – entails that the shear deformation of the fracture zone is overestimated.

Handling in the safety assessment

The process can be of importance for safety in two ways:

- 1) Shear movements in discontinuities that intersect deposition holes are of direct importance for safety if the movement is so great that buffer and canister are damaged. For each load case it is possible, by applying relationships between length (extension) and shear deformation, to determine how long a fracture has to be in order for a shear deformation to exceed the safety criterion. Statistically generated fracture network models exist for the candidate repository sites that can show how many canister hole positions are intersected by such fractures. A limit can therefore be set on the number of damaged canisters. The relationship between extension and maximum shear deformation that is shown in Figure 5-16 is, however, pessimistic. In order not to set unnecessarily pessimistic limits, more realistic relationships that take into account the fact that all fractures have a finite extension in all directions should therefore be used.
- 2) Normal movements can in principle be of importance for safety due to the fact that the transmissivity of fractures changes when the aperture changes. The transmissivity of individual fractures is sensitive to variations in normal stress, but the permeability of the rock mass is dependent on the influence on many fractures with different orientations and complex connectivity conditions. If different fractures in the system are compressed or widened only marginally in response to load changes, the effect of large transmissivity changes in other fractures on the permeability of the rock mass may be small. Based on the mechanical analyses that have been done of fracture movements in the near field, the general conclusion can be drawn that the influence on the fractures in the near field that is obtained in the various scenarios is of the same order of magnitude as the one previously caused by boring/blasting of tunnels and deposition holes /see e.g. Shen and Stephansson 1996a/. The permeability change that has already occurred in the initial state in the near-field rock in comparison with the undisturbed rock can therefore serve as an estimate of the permeability changes in the near field that may be obtained in the various scenarios. Theoretical studies indicate permeability changes of no more than 1 or 2 orders of magnitude

around cavities in rock /see e.g. Case and Kelsall, 1987/. In the ZEDEX experiment in the Äspö HRL, no experimental evidence has been found for permeability increases caused by stress redistributions in response to tunnel excavation /Olsson and Winberg, 1996/. In SR 97, the M-H coupling is therefore judged to be such that it is not necessary to take into account the influence of the mechanical processes on the retention properties of the near-field rock. Furthermore, the load cases taken into account in SR 97 generally entail that the stress level in the near field increases, i.e. the aperture of the fractures is more likely to decrease than increase. The situation is slightly different in the rock between the ground surface and down to a depth of about 200 m. Here a systematic reduction of the horizontal stresses is obtained during the thermal pulse, resulting in increased permeability in the vertical direction. The distance to the repository is, however, so great that this is not taken into account either in SR 97. It should nevertheless be emphasized that the hydro-mechanical coupling in the rock has not been sufficiently systematically investigated to enable it to be definitively dismissed.

Criteria can be set up for direct shear movements across deposition holes. At present, the criterion is that shear movements exceeding 0.1 m should be avoided to prevent canister damages, see section 3.6.2. There are no equivalent general criteria for permeability changes.

Base scenario: In the base scenario, fracture movements occur for three reasons: the thermal load, load changes in the near field due to the bentonite's swelling pressure, and due to the fact that the effective stress in the rock's fractures declines when the groundwater pressure is restored.

The thermomechanical numerical calculations that have been done have not shown any shear movements in excess of 0.1 m. The largest shear movements have furthermore occurred along fracture zones of such size that they will not be permitted to intersect deposition holes /Almén et al, 1996/. The analytical calculations that have been done to determine the thermal stresses show that the maximum shear stress contribution obtained in a thin horizontal disc after about 50 years will not exceed approximately 7 MPa /Probert and Claesson, 1997/. This is consistent with, and one of the reasons for, the small displacements obtained in the numerical thermomechanical analyses. The shear stresses around cavities are greater, but in such small areas that only small fractures or parts of larger fractures can be affected.

The swelling pressure of the bentonite has a small local effect on the state of stress and therefore has a negligible effect on the movement of the fractures /Shen and Stephansson, 1996a; Hökmark, 1996/.

The effect of effective stress reduction as a result of restoration of the groundwater pressure has not been analyzed specifically, but limits can in principle be determined with the aid of the relationship fracture extension – shear deformation for friction-free fractures. The friction-free part of the fracture is so small that the effect can be neglected.

The above conclusions are cited in SR 97, i.e. that the studies performed show that no shear movements in fractures that intersect canister hole positions are expected to be greater than 0.1 m in the base scenario.

Climate change (Glaciation): Several different possibilities exist for describing the interaction between bedrock and ice cover, both directly below the ice cover and in the marginal areas. All descriptions give different loads on the host rock.

In the static load cases analyzed so far in numerical models, no fracture movements big enough to damage canisters have been obtained. This is consistent with the relatively small shear stress contribution obtained in these load cases. The shear component of the stress contribution is approximately 14 MPa at repository level, but with such an orientation that the stress anisotropy is actually reduced /Hansson et al, 1995/. By considering extension–deformation relationships of the type shown in Figure 5-16, it is possible for other reasonable static load cases as well to make the assessment that no shear movements in fractures that intersect canister hole positions will be great enough to damage the canister. This is true even if it is assumed that the shear strength of the fractures has been reduced due to the fact that the groundwater has been pressurized with a water column equal to the thickness of the ice load.

Dynamic effects that arise when the ice retreats are included in the earthquake scenario.

Reference is made in SR 97 to the above conclusions, i.e. that the completed studies show that no shear movements in fractures that intersect canister hole positions are expected to be greater than 0.1 m.

Earthquake: Estimates of the expected frequency of quakes of different magnitudes in different parts of Sweden can be found in the literature /Kijko et al, 1993/ and can be translated to frequency per unit area around the candidate repository sites.

In the earthquake analyses in SR 97, the centre of the quake is distributed statistically (small quakes) and deterministically (medium-sized and large quakes) around the host rocks /La Pointe et al, 1998/. Statistical fracture network models /Follin and Hermanson, 1997/ are created for the different host rocks that show the number and size distribution of the fractures that will intersect deposition holes.

By applying relationships (obtained with the program POLY3D as described above under model studies) between magnitude, distance to quake centre, fracture extension and shear deformation to a representative selection of canister-intersection fractures, statistics are obtained that show displacements along these fractures. If the relationships are applied repeatedly in accordance with the earthquake statistics that are established as described above for the different repository sites, the cumulative effects of all earthquakes expected within the next 100,000 years can be calculated. The result is then used in SR 97 to estimate the number of canisters that may be damaged by earthquakes.

5.6.5 Fracturing

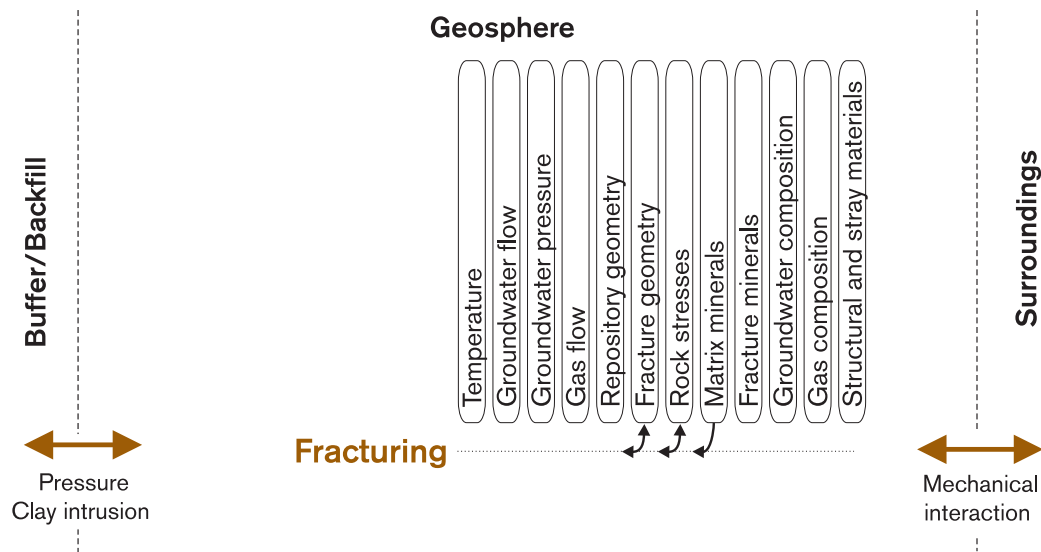


Figure 5-19. Fracturing.

Overview and general description

When specimens of intact rock are loaded gradually, i.e. subjected to increasing stresses, deformations are obtained which are elastic to begin with, but as the load increases also exhibit an irreversible (plastic) element. At far-reaching deformation, a maximum stress is reached which is the strength of the specimen under the given conditions. After further deformation, the specimen may be fragmented so that its remaining loadbearing capacity, its residual strength, is dependent solely on friction between the fragments.

The fundamental mechanism in the process, the growth of microfractures, has been described by A. A. Griffith /Griffith, 1924/. The application of Griffith's original failure theory presupposes the existence of arbitrarily oriented elliptical cavities in a continuous elastic medium. The theory then says that the tensile strength is one-eighth of the uniaxial compressive strength, which is roughly true for most crystalline rock types. The theory is otherwise difficult to apply in describing failure in intact rock on a macroscopic level under general stress assumptions, which is why empirical failure criteria are generally used, e.g. Hoek-Brown's criterion.

The fracturing process is thus dependent on the state of stress, but in fact starts at lower loads than the actual failure load. Rock in a state of stress equivalent to approximately 80 percent of the failure load may, without further load increase, be fragmented after some time if the stress level is retained /Martin, 1994/. The phenomenon can be observed when tunnels and other cavities are excavated in rock at great depth where the primary stresses give rise to large stress concentrations. Next to the cavity walls, the tangential stresses are large and the radial constraint small, which can cause rock breakout due to fracturing parallel to the cavity wall (spalling).

The mechanisms that control the growth of microfractures in principle also control the propagation of existing fractures. In constrained rock, an individual fracture can propagate by spreading in its own plane by means of shear failure, and by fracturing at an angle to its own plane by tensile failure at the periphery of the fracture, so-called “splay cracks” /Scholz 1990/.

Influence of rock stresses: The process is directly coupled to the state of stress as described above.

Influence on rock stresses: Failure in intact rock entails that the load that cannot be taken by the plasticized portions is redistributed. Around cavities, this means that stress maxima are displaced from the periphery out into the rock.

Influence on fracture geometry: The process entails by definition that the fracture geometry is affected.

Influence of fracture geometry: In the areas where the process takes place on any appreciable scope, namely next to deposition holes and tunnels, the local fracture geometry can be crucial. Tangentially oriented fractures can give rise to stress concentrations between fracture and cavity, increasing the risk of failure. Fractures that intersect the periphery of the cavities at oblique angles can cause stress reductions, reducing the risk of failure.

Influence of matrix composition: The rock type is of importance for strength. For the rock types that have been investigated in Äspö, the uniaxial tensile strength determined in the laboratory varies between 170 MPa and 260 MPa /Stille and Olsson, 1996/.

Model studies/experimental studies

The sequence of initial and then growing plasticization, failure and continued deformation until the residual strength of the specimen has been reached are stages in the fracturing process in intact rock and have been described in studies by, among others, Martin /1994/ and Li /1993/. In the initial elastic phase, the specimen's microfractures are first compressed. Then a stable growth of the microfractures occurs in the direction of the largest principal stress. Before failure occurs, i.e. before the limit of the strength of the specimen has been reached, a phase takes place with unstable growth of the microfractures, either as before in the direction of the largest principal stress, or where shear fractures form by the interaction and fusing of several growing microfractures. The way in which fracture growth occurs is dependent on the rock properties and the load: at uniaxial load the unstable growth and the macroscopic fragmentation occur axially, i.e. in the direction of the largest principal stress. In constrained specimens, shear fractures can form.

Whether an existing fracture propagates, and in what direction this propagation occurs, depends on the local stress field at the fracture periphery /Scholz, 1990/. Numerical models for prediction of propagation in elastic media, based on application of strain energy criteria, have been tested in 2-dimensional near-field analyses /Shen and Stephansson, 1996b/. The results showed that the process presupposes high stress levels and strong stress anisotropy. If the ratio between the largest and smallest primary principal stress was greater than 4, propagation and fusion of individual fractures around circular cavities occurred.

Johansson et al /1995/ studied the state of stress after excavation of tunnel and deposition hole in the area around the intersection of tunnel and deposition hole for different assumptions concerning the local primary rock stresses. The study was done numerically with a 3D continuum program, where the rock was assumed to be elastic. The area around the deposition hole was then divided into categories with respect to how the state of stress was related to the different stages in the evolution of brittle failures that had been identified at the URL /Martin, 1994/. The results showed that for primary stresses roughly corresponding to conditions at 1,000 m depth, only insignificant areas were in direct failure states, while slightly larger areas (max. depth approx. 150 mm from deposition hole wall) were in a state of unstable fracture growth, i.e. with the possibility of spalling. A slightly larger area still (to a max. depth of approx. 400 mm) was in a state where fracturing had been initiated (stable fracture growth). At stresses corresponding to a depth of 500 m, stress levels corresponding to direct failure or unstable fracture growth were not obtained anywhere. In all analyses, the least favourable tunnel orientation was assumed, i.e. with the tunnel axis perpendicular to the largest primary principal stress.

Hökmark /1996/ performed thermomechanical elastic 3D calculations of the state of stress around deposition holes. The analysis showed that the areas that were in a potential failure state after heating were restricted to small volumes in the intersection tunnel/ deposition hole and to even smaller areas along the sides of the boreholes. The maximum depth from the deposition hole border was about 300 mm.

At the URL in Canada, brittle failures with rock breakout were obtained along nearly vertical lines in two vertical 600 mm holes bored in the floor of a tunnel in fracture-poor rock with large primary stresses. However, no failures were obtained in the uppermost part of the holes, on a level with the tunnel's EDZ. In a subsequent heating phase with peak temperatures of between 80 and 90°C at the borehole walls, the failures widened to become continuous all the way down to the borehole bottoms, still with the exception of the portion belonging to the tunnel's EDZ /Martino and Read, 1995/. The depth of the brittle failures was about 50 mm, counting from the borehole walls.

Time perspective

See the process "Reactivation – movement along existing fractures".

Summary of uncertainties

A large and important uncertainty exists when it comes to assessing the loads to which the host rock will be subjected. See corresponding section under the process "Reactivation – movement along existing fractures".

It is uncertain whether laboratory-determined strength values are at all applicable *in situ* to intact rock next to e.g. tunnel walls. Owing to the stress history undergone by the rock when the tunnel face passes, the process of microfracture initiation may follow a different course than in the laboratory. This may lead to an overestimation of the strength /Martin, 1994/. Even though the true failure loads can be estimated, our conceptual understanding of progressive brittle failures is poor and we can therefore not make predictions of the scope of failure, for example next to deposition hole walls, on the basis of calculations.

The programs for modelling of fracture propagation that have been tested are 2-dimensional, which presumably means that the scope of the process is overestimated. It is also uncertain what potential for large displacements a fracture created by fusion of two imperfect coplanar fractures may have. The fracture extension that sets the limit for the possible displacement along such a fracture can reasonably be assumed to be less than the sum of the extensions of the two original fractures.

The fracture-mechanical models that are used in the programs to describe fracture propagation have been developed for application to other types of materials than rock, e.g. metals, and do therefore not taken into account the possible presence of inherent weaknesses.

Handling in the safety assessment

The process can be of importance for safety in three ways:

1. Fractures that intersect deposition holes propagate and fuse with other fractures so that fractures of such large extension are formed that current or future loading can generate shear deformations. In order for the shear deformation to be able to affect a canister, the canister hole must be located near the centre of the fracture. At the edges of the fracture the shear deformation is zero, regardless of the size of the fracture.
2. Failure at the boundary of the deposition hole causes mechanical effects in the form of volume expansion of the plasticized rock so that the buffer is compressed and damages the canister. It should be observed that both the generation of the failure and the effects, in the form of volume expansion, are inhibited by the bentonite's swelling pressure. This has not been taken into account in the model studies and experimental studies described above.
3. Failure (formation of fractures) next to the deposition hole wall causes permeability changes in the area between deposition hole and deposition tunnel. Such permeability changes presumably already exist in the initial state, especially if the tunnels are perpendicular to the largest primary principal stress. This possible hydromechanical coupling is not taken into account in SR 97 (see corresponding under the process "reactivation").

Base scenario: The studies that have been done show that the stresses that are required for propagation of existing fractures will not occur other than in small areas nearest tunnels and deposition holes /Shen and Stephansson, 1996/. The number of fractures of sufficiently large extension to give shear displacements greater than 0.1 m (the criterion for avoidance of canister damages) and with canister holes near the fracture centre will therefore not be affected.

The thermal load causes a widening of the areas around the intersection between tunnel and deposition hole that are already in or near a failure state. The studies performed show that the increase will be small and the effect, in the form of compression of the buffer, can presumably be neglected.

The judgement is made in SR 97, with reference to the above studies, that no canisters will be damaged due to fracture propagation or due to failure in the rock nearest the deposition holes in the base scenario.

Climate change (Glaciation): If the stresses and the stress anisotropy generated by an ice load are sufficiently great, the consequence could in principle be that even fractures at great distances from the repository's cavities can propagate and fuse. In the analyses

done to date, however, the stress contributions generated by ice loads have not led to increased stress anisotropy other than near the cavities /see Rosengren and Stephansson, 1990; Hansson et al, 1995/. In SR 97, glaciations are therefore not judged to lead to an increase in the number of canister-intersecting fractures of great extension and with canister holes near the centre of the fracture.

The scope of failures with fracturing near the canister hole will presumably be less than for the base scenario /Shen and Stephansson, 1996a/. The calculated or estimated scope depends, however, on how the ice load is represented. Johansson and Hakala /1995/ looked at the effects of very great stresses. At stress levels that greatly exceed those that are assumed to be created by a glaciation in the above studies, the area around the intersection between tunnel and deposition hole was in a failure state. In the tunnel floor, the area between the deposition holes was in a state of unstable fracture growth. At the level of the canisters, parts of the deposition hole walls were in a state of stress corresponding to stable fracture growth. It can be presumed that if a failure had occurred, it would have reached a scope roughly like the one that arose in a similar stress situation at the URL in Canada (see above under experimental studies), i.e. brittle failures up to a limited depth. Failures of this scope are not judged to compress the buffer in a way that damages the canister.

The judgement is made in SR 97, with reference to the above studies, that no canisters will be damaged due to fracture propagation or due to failure in the rock nearest the deposition holes in the event of a glaciation.

Earthquake: Frequency/magnitude relationships exist (see the process “reactivation – movement along existing discontinuities”), but no results are available from studies that show consequences in the form of fracturing for quakes of different magnitudes and at different distances from the repository. It can, however, be assumed that the mechanical impact on the canisters caused by fracturing is subordinate to the impact obtained due to movements in existing fractures. The judgement is therefore made in SR 97 that the earthquake scenario is sufficiently well covered by the fracture movement analysis described under the process “reactivation”.

5.6.6 Time-dependent deformations

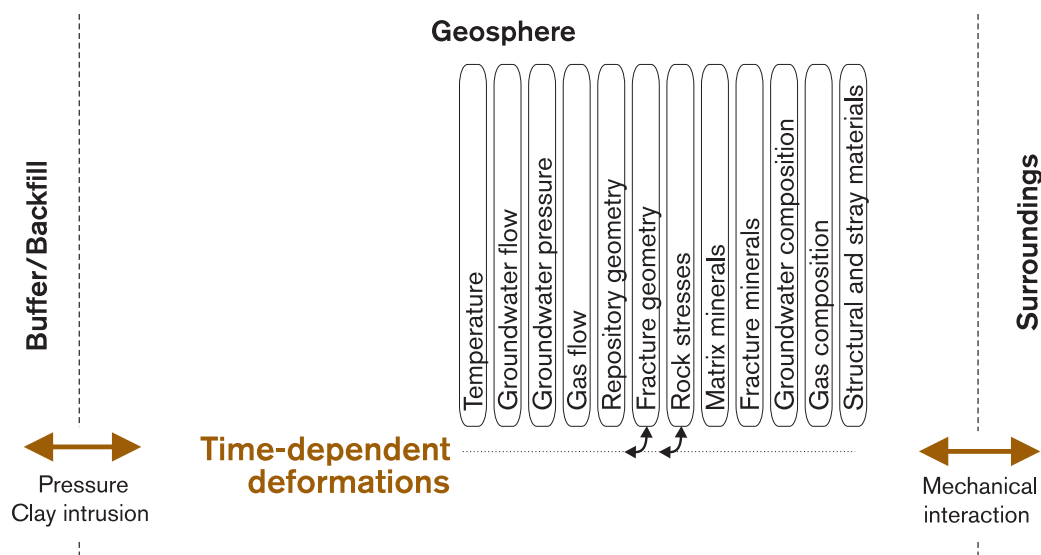


Figure 5-20. Time-dependent deformations.

Overview

All movements in the rock are included in the processes described above and consequently influence and are influenced by the same variables. Time-dependent deformations are therefore not separate processes in a true sense, but the aggregate effect of simultaneously occurring load changes, changes in material properties, movement in intact rock, movements along existing fractures and fracturing.

General description

Time-dependent deformations in the host rock can be of two main types:

- 1) The loads on the host rock change due to displacements generated at great distance from the host rock. The tectonically caused compression of the interior of the Baltic Shield can be assumed to correspond to a strain of 10^{-11} /year, while the strain due to the still-ongoing land uplift may amount to 10^{-9} /year /Muir-Wood, 1993/. A strain of 10^{-9} /year corresponds to a stress growth of 5 MPa in 100,000 years if the strain is approximated as uniaxial compression and the modulus of elasticity is set at 50 GPa. The time dependence applies to the load change, so the deformations that occur in the host rock are not time-dependent in the true sense (see overview).
The processes, fracture movement and fracturing, that can have direct importance for safety take place in the same way as in other load cases. Owing to the small stress growth and the long time perspective, effects of tectonic displacements are not taken into account in SR 97.
- 2) The mechanical properties of the host rock change with time so that movements take place due to already active stresses (creep movement). It is this type of movement that is really meant by the use of the term “time-dependent deformations” above. The changes may be directly dependent on the state of stress, e.g. unstable growth of microfractures in intact rock. Uneven distribution of shear stresses along fracture planes on all scales can lead to initiation and growth of microfractures and eventually to local plasticization in connection with stress concentrations at irregularities in fracture surfaces /Pusch and Hökmark, 1993/. The changes can also relate to the occurrence and properties of fracture-filling minerals.

The driving force behind creep movements is the occurrence of shear stresses. The deformation therefore proceeds either until no shear stresses remain, or until the shear stresses have been reduced and redistributed to parts of the system that are not plasticized.

Model studies/experimental studies

The movement in the dome in SFR has been measured with extensometers since the blasting was concluded in 1985. The measured movements are however unsystematic and so small in relation to the accuracy of the extensometers that interpretation, as well as prediction of possible continued movement, is difficult. Furthermore, the dome is reinforced with bolts and shotcrete.

Results from plate loading tests on rock show that the creep strain at constant load declines logarithmically with time /Pusch and Hökmark, 1993/.

A numerical model of a circular tunnel where the rock material nearest the tunnel periphery was assumed to have time-dependent deformation properties gave a maximum radial creep movement of 0.3 mm after approximately 2,000 years /Pusch and Hökmark, 1993/. Eloranta et al /1992/ found that it would take about 10^9 years for the deposition hole wall to move 10 mm radially, provided that the rock around the deposition hole is of good quality. Pusch /1996/ estimated the possible time-dependent deformation of deposition holes by assuming that the creep properties of the rock can be represented as a modulus of elasticity that decreases logarithmically with time. The estimate gave a maximum diameter decrease of 12 mm after 10,000 years.

Natural analogues

Natural analogues show maximum shear movements of 0.1 m for 10–100 m long fractures during a timespan of 450 years (see section under “reactivation”).

Summary of uncertainties

The uncertainties are great and pertain to both assessment of the loads that will act on the host rock and the conceptual description of delayed deformations in intact rock, along fractures and in the rock mass.

There are several different types of rheological models for continuous models that could theoretically be used for the rock mass or for the intact rock. However, the different models give essentially different outcomes, and there is no really valid justification for any specific model, even though the experimental results suggest that the deformation diminishes rapidly with time.

There are no relationships for time-dependent deformations in fractures, which means there is no model for how time-dependent deformations are distributed between discontinuities and intact rock.

Handling in the safety assessment

If it is assumed that all significant movements take place along fractures, then the ultimate consequence of an extensive creep movement that has taken place over a long period of time is that no fractures can take any shear stresses anymore. The assessment of the number of damaged canisters then depends solely on how many canister holes are intersected by fractures of sufficiently great extension for the maximum shear deformation without friction to exceed 0.1 m. Nothing is known about the timescale for such a hypothetical evolution, but the state of stress in the rock today suggests that the fractures can take shear stresses and that the evolution, if it exists at all, is therefore extremely slow. According to the above, the timescale for the natural analogues is hundreds of millions of years.

If it is pessimistically assumed that the rock around the canister holes is deformed in its entirety like a continuum according to a rheological model that gives movement as long as there are shear stresses, the movement will not cease until the buffer has been compressed so that the swelling pressure is as great as the rock's mean compressive stress. If the mean compressive stress at the canister hole is 20 MPa, which is slightly more than the mean compressive stress at Aberg, Beberg and Ceberg today, the pressure on the canister will therefore increase to be equally great. This pressure increase is not enough to damage the canister. In fact, the mean compressive stress at repository depth will be less than 20 MPa if the rock mass is really deformed as described above, i.e. as a viscous fluid. The state of stress will then be hydrostatic, with a mean compressive stress equivalent to the dead weight of the rock, i.e. about 14 MPa.

If the same assumption is made for the rock around the backfilled tunnels, i.e. that the deformations continue for as long as any shear stresses remain, in principle the same thing applies as for the deposition holes. When the pressure in the backfill is equal to the mean compressive stress in the rock and all the arch effect around the tunnel periphery is lost, the movements will stop. The difference is that the backfill cannot, like the compacted bentonite buffer, mobilize counter-pressure in the form of a swelling pressure that increases rapidly in response to compression. In the backfill the swelling pressure is negligible and the convergence is therefore limited by the pure compression properties of the backfill, which are dependent on composition and degree of compaction. The compression properties in highly compressed backfill under high pressures have not been systematically investigated, but it is presumably pessimistic to assume that the backfill can be compressed by 10 percent, which would mean that the porosity of the backfill is reduced by approximately one-third. A ten-percent volume reduction entails a five-percent reduction in tunnel radius, i.e. about 10 cm.

The assumption that the rock can be deformed like a viscous medium until all arch effect has been lost and all shear stresses have been equalized must be regarded as very pessimistic. If this type of movement takes place at all, it is more likely that it ceases as soon as some fraction of the shear stresses around the cavities has been relaxed, and that convergence will therefore be little. The effects on the fracture system around the cavities and thereby the permeability of the near-field rock have not been systematically investigated, but in general terms it can be presumed that axially oriented fractures close, since the radial pressure increases, and that radially oriented fractures open, since the tangential stresses decrease. The scope and effect of these fracture width changes is unknown but can, until more accurate analyses have been done, be assumed to be approximately equivalent to the disturbance that already exists due to the EDZ.

Limits can be set on the consequences of creep movements in the rock mass for the loads that will exist in connection with a glaciation as well. If it is hypothetically assumed that the creep movements that take place during the glaciation are larger enough that the shear stresses in the rock mass disappear, the same line of reasoning as above can be applied. The state of stress will then be hydrostatic, i.e. the stresses are equal in all directions and are determined by the dead weight of the rock mass (about 14 MPa) and the ice load (about 30 MPa). The pressure on the canister thus increases to about 44 MPa. This is of the same order of magnitude as the pressure that is found if it is assumed that no creep movements take place. Without creep movements, the canister holes do not converge, which means that the bentonite buffer is not compressed and therefore retains its original swelling pressure (about 7 MPa). The ice load then acts instead on the canister via an elevated pore water pressure (total about 37 MPa) so that the total pressure on the canister is about 44 MPa.

With reference to the completed studies, the natural analogues and the above rough calculations, the effects of creep movements are not judged to have any significance for the safety of the repository in SR 97.

5.7 Chemical processes

5.7.1 Introduction

The chemical situation in Swedish bedrock is generally very stable. Reaction and transport processes proceed continuously but generally lead to changes only in a very long time perspective. Reactions occur between different components in the groundwater, between water and fracture minerals, and between water and rock matrix. The groundwater flow accounts for transport of reactants and reaction productions to and from the

reactions. The flowing groundwater also leads to a mixing of different groundwater types from different areas in the geosphere.

The frames for the evolution of the chemical situation are given by inflow and outflow of water from/to the biosphere, and by exchange with very deep-lying groundwater. The evolution is thereby controlled by, among other factors, precipitation amounts and near-surface chemical conditions. The geochemical evolution on a repository site is thus determined by:

- Present-day geochemical situation.
- Transport and reaction processes in the geosphere.
- Interaction with the surroundings, mainly inflows and outflows from/to the biosphere, which are in turn dependent on the climate.

Present-day geochemical situation is similarly the result of previous climatic conditions, and transport and reaction processes.

Large changes in the chemical composition of the groundwater are caused primarily by long-term climate change, which leads to altered precipitation and above all flow conditions, which can in turn lead to noticeable effects on the composition of the groundwater. Effects of climate change are discussed in the climate scenario. In the base scenario, land uplift in particular causes effects on flow pattern and thereby groundwater composition.

Historical evolution

In order to be able to provide a good description of geochemical conditions in the future, it is necessary to have an understanding of the historical evolution, i.e. the conditions that have given rise to today's situation. Much of the research on the geochemical evolution is therefore aimed at understanding the historical evolution.

Importance for repository safety

In combination with the groundwater flow, the composition of the groundwater is of great importance for repository performance, both in the short and long term. The interaction between the engineered barriers and the groundwater determines how long the spent fuel will remain isolated. Even in a situation where the isolation has been broken, the groundwater is of crucial importance for the dissolution and transport of radionuclides in the fuel /SKB, 1995/.

The quantity of dissolved oxygen in the water and the quantity of sulphide that can come into direct contact with the copper canister are of importance for copper corrosion. These substances corrode the canister in different ways. An attack of oxygen causes pitting, while sulphide corrosion is distributed evenly over the whole surface. Reducing conditions in the groundwater are therefore a requirement for the deep repository site, i.e. there must not be any dissolved oxygen in the water. Other constituents in the groundwater do not affect the canister's integrity, except for a combination of extremely high salinities and low pH.

For the buffer (bentonite), it is necessary that the groundwater contain a minimum of dissolved salts. The presence of divalent cations is essential for the bentonite not to form colloids. The sum of the calcium and magnesium concentrations should exceed 4 mg/l. Very high salinities can eliminate the swelling capacity of the bentonite and thereby disable its function as a diffusion barrier between the canister and the rock.

This effect is noticeable at a salinity of around 50,000 mg/l. For the backfill, which consists of a mixture of uncompacted bentonite and sand or crushed rock, lower salinities are also of importance. Bentonite/aggregate proportions are therefore chosen with reference to prevailing salinities, see section 4.1.1.

The water's variables pH and Eh are important for radionuclide transport. Under reducing conditions (no dissolved oxygen), many of the most harmful nuclides occur in a reduced form with very low solubility. The solubility is lower at neutral pH than under acid or alkaline conditions. In typical groundwaters, reducing conditions prevail and the pH is neutral. The total salinity of the water influences the retention of weakly sorbing nuclides.

The water's content of colloids and microbes is also of great importance for nuclide transport, since these particles can act as carriers for radionuclides. At high concentrations, strongly sorbing nuclides will be able to adhere to colloids and microbes instead of to the fracture surfaces and thereby be transported with the groundwater flow. In investigated groundwaters, the concentration of colloids has been so low that this transport mechanism has been of no importance.

Time perspective

In simplified terms, three timescales can be distinguished in the geochemical evolution around a deep repository.

In a short time perspective, 10–100 years, the chemical conditions are determined by disturbances in the natural situation caused by the repository itself.

In a longer time perspective, up to tens of thousands of years, today's natural conditions of groundwater flow and mixing are dominant.

In a very long time perspective, longer than tens of thousands of years, the composition of the groundwater is also affected by its reactions with the rock's minerals and by climate change.

Equilibrium water/rock mineral

The hypothetical composition of the water, if it were in equilibrium with the rock, can be calculated with thermodynamic data. Data exist for most mineral phases, even though they are sometimes burdened with great uncertainties. The uncertainties are, however, often overshadowed by the fact that the chemical environment in the rock seldom exhibits equilibrium, since most reactions are very slow. In general, equilibrium is a situation which the groundwater/mineral system strives for but never achieves. The deviation from equilibrium is completely dependent on the water's flow and mixing conditions /Plummer et al, 1991; Laaksoharju and Wallin, 1997/. Not even in stagnant volumes, where diffusion dominates over flow as a transport process, will all reactions achieve equilibrium /Gascoyne et al, 1987; Frape and Fritz, 1987/.

Mixing conditions

Due to the great heterogeneity in the rock's hydraulic conductivity and time-dependent changes in the pressure conditions, the water flow in the bedrock can vary widely in time and space. This is generally of greater importance for the composition of the water than previous reactions between water and rock minerals. A water sample can contain a fraction that has been isolated from the atmosphere for over one million years and a

fraction that has infiltrated the rock in modern time /Laaksoharju et al, 1995/. The water thus exhibits a spectrum of origin types (end-members) that have been mixed in different proportions. The mixtures are not in chemical equilibrium; reactions between components in solution and precipitation and dissolution of solid phases occur constantly. To be able to describe and quantify these reactions, it is necessary to be familiar with the conditions that prevailed when different water types were formed and the chemical composition they have had /Laaksoharju and Wallin, 1997/. It is very difficult to describe conditions millions of years back in time, whereas events that have occurred since the most recent glaciation can be traced in the water composition /Laaksoharju and Wallin, 1997; Rhen et al, 1997/.

Bacterial processes

Many types of microbes are found at repository depth, but only those that can survive in the prevailing chemical environment are active /Kotelnikova and Pedersen, 1998/.

Bacterial processes are of great importance for the composition of the groundwater. This is particularly true of pH and Eh. Bacteria contribute to the consumption of dissolved oxygen in infiltrating surface waters, reduce trivalent iron in fracture minerals and reduce sulphate in sulphate-rich old sea water /Laaksoharju (Ed.), 1995, Banward (Ed.), 1995; Pedersen and Karlsson, 1995/.

Uncertainties

There are uncertainties regarding the importance of the various processes for the chemical evolution of the repository in both the short and long term. In many cases it is not uncertainties in the understanding of the actual processes that are most important, but rather uncertainties regarding the circumstances under which the different processes are active. The water chemistry, for example, will evolve quite differently during an ice age compared with the case without an inland ice sheet, even though the same chemical processes are involved.

In general, uncertainty increases with time. It is possible to give a good description of the expected conditions one thousand to ten thousand years ahead in time, whereas the conditions that will exist 10,000–100,000 years in the future must be considered speculative, based on expected or possible climatic conditions.

How can the processes be handled in the safety assessment?

The different processes can be treated qualitatively (by discussion in general terms) or quantitatively (in calculations), depending on how much is known about them and how important the process is for repository evolution. It is desirable to perform calculations for the processes that are most important for the evolution of the repository, regardless of whether this is critical for the safety assessment or not. Owing to the great natural variability in flow rate and residence time and the complex mixing conditions, the evolution of the water chemistry can only be calculated along typical flow paths. However, this should be adequate for showing that a good understanding exists of the mechanisms that influence the composition of the water under the conditions that are expected to prevail at repository depth.

With today's level of knowledge, the chemical composition of the groundwater can be quantified for a time period up to the next expected ice age. The composition during the time from repository operation until just after closure can be quantified if site-specific conditions and quantities and types of engineering materials are known. What is most important is to describe chemical stability with reference to pH and Eh conditions and concentrations of the most important ionic species that affect the engineered barriers, see the sections on bentonite and canister.

5.7.2 Advection/mixing

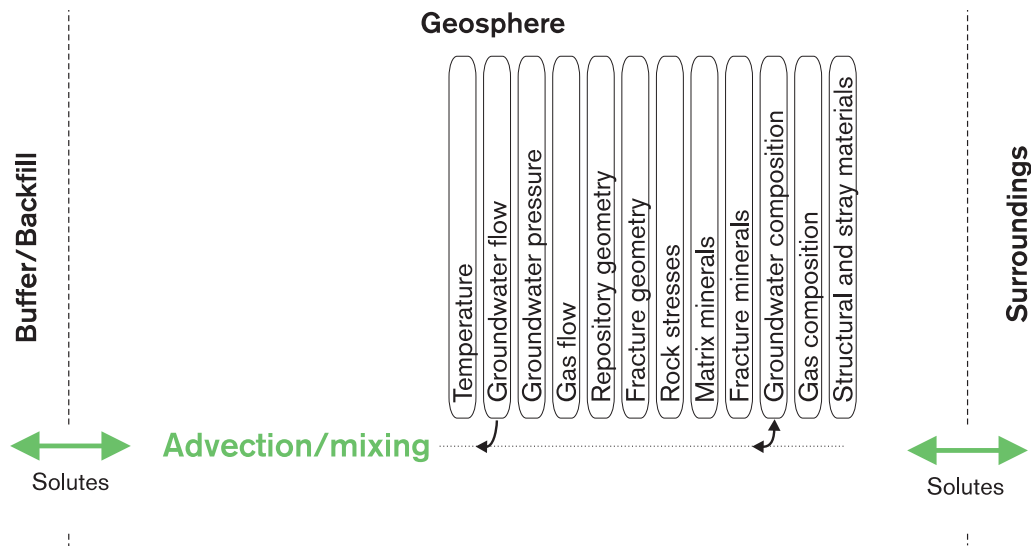


Figure 5-21. Advection/mixing.

Overview

Advection, transport with the flowing water, is the most important transport process for dissolved substances (solutes) in the groundwater. The process is of central importance for the chemical evolution of the repository, partly because it is responsible for transport of substances that influence bentonite and canister to the repository, and partly because any releases of radionuclides from the repository can be transported to the biosphere by advection. Furthermore, advection is responsible for transport of substances to and from nearly all chemical reactions in the geosphere.

The exchange of solutes with the biosphere, with remote parts of the geosphere and with buffer/backfill in the repository comprise boundary conditions for the process. Climate change will lead to changes in the composition of the water entering the repository, which will in turn lead to large-scale and long-term changes in water composition. Advection thereby leads to a situation where different water types replace each other and/or are mixed.

A detailed description of the mathematical modelling of advection is given in the section on radionuclide transport.

Studies of the historical evolution of advection/mixing that have been made to obtain a better understanding of the future evolution are described below.

General description

The factors that influence groundwater flow have been described in section 5.5 on hydraulic processes in the geosphere. The groundwater moves in the rock's fracture system, most of the flow will be concentrated to flow paths with good permeability. These meet to a greater or lesser extent so that water from different conductive fractures is mixed. Under static conditions with constant driving forces, the difference in the composition of the waters that are mixed will be small. On the other hand, large differences will exist when the groundwater flow changes direction and water of another type comes down into the flow paths.

Inflow and outflow of groundwater, the geographic location of the highest and lowest groundwater table and the magnitude of the pressure head difference are the factors that determine the flow conditions. An example of contrasts in this respect is the great potential which a thick ice cover at a glacier margin can create in comparison with the complete equilibrium that prevails in the rock under a very large lake or a sea.

Evolution since the most recent ice age: After the most recent ice age, the different evolutionary stages of the Baltic Sea have influenced the mixing of the groundwater to a varying degree depending on the location in relation to the coastline. As the continental ice sheet retreated, glacial water penetrated down into the bedrock, displaced the previous water and mixed with it in the boundary layer. It is impossible to set a limit today for how deep the glacial water reached, but large proportions of water originating from colder climatic conditions are generally found down to a level of 100–300 metres. Traces of such water are also found at greater depths. It is, however, unclear whether this water has the same origin, or whether it may derive from a previous deglaciation.

At sites that have at some time been covered by the sea since the last glaciation, traces of old sea water are generally seen. The driving force for the infiltration of sea water is the higher density which has caused the water to penetrate down into the rock to the depth where the salinity was once equally high. The process of land uplift has since brought previously sea-covered sites above sea level, exposing them to inflow and outflow controlled by precipitation and topography.

Conditions at great depth: Highly saline water is usually encountered at great depth. The depth to the saline water varies from site to site. The salinity of the water exceeds that of the sea water, showing that its origin is a brine, i.e. a very saline water where the salt has been leached out of the rock over millions of years.

Mixing is thus a process which is essentially controlled by external (climatic) conditions and which is of crucial importance for what changes can be expected to occur in the composition of the groundwater in the future. The obvious changes in composition, above all in coastal areas but also perhaps in other parts of the country, are transitions between glacial meltwater, marine salt water, fresh water from precipitation (meteoric water) and brackish water under permafrost. Each type of water can displace the previous groundwater, alter equilibria, form or dissolve fracture-filling minerals, etc.

There have been ten or so glaciations during the past million years, and thereby probably some forty or so far-reaching changes of this kind. Each of these changes has left traces in the low-conductive parts of the rock where water exchange is slower than in the conductive zones, see further under uncertainties.

Model studies/experimental studies

The importance of mixing for the observed chemical changes has long been a qualitative type of knowledge. It has been possible via statistical multivariate analysis to conclude that a water sample contained, for example, both a modern and a very old component simultaneously.

Model development during the evaluation of the hydrochemical conditions on Äspö has made it possible to calculate the proportions of different identified water types by means of the components sodium, potassium, calcium, magnesium, chloride, sulphate, carbonate, deuterium, tritium and oxygen-18 /Laaksoharju and Wallin, 1997; Rhén et al, 1997/. The results indicate that mixing has occurred in several phases as a result of varying flow conditions. Since the most recent ice age the following mixing processes have been identified and quantified:

- 1) Glacial meltwater penetrated to a depth of several hundred metres and mixed there with saline groundwater which was at least partly isolated from the atmosphere for millions of years.
- 2) Subsequently, Baltic Sea water from the Littorina stage (7,000 years ago) sank down, due to its higher density, until it reached a saline water with the same density. At this inversion, the glacial meltwater was pushed up into the conductive zones, but also remained in the low-conductive rock.
- 3) Meteoric water then gradually penetrated down to a depth of 100–200 m after rain-water started to infiltrate when Äspö rose above sea level about 3,000 years ago.

A hydrodynamic simulation of these conditions has been carried out by /Svensson, 1999/. All the different water types that have occurred since the most recent deglaciation have been introduced under the pressures and other boundary conditions considered relevant. The transient simulation shows how different water types successively replace each other. At 450 m depth below Äspö, the sequence of dominant waters is: glacial meltwater (at the start), Yoldia Sea water, Ancylus Lake water, Littorina Sea water and, finally, today's meteoric water. This simulation includes neither mixing nor penetration in stagnant low-conductive parts of the rock. There are therefore no traces of the previous water types that can *de facto* be traced in the water chemistry. Other analyses which include dispersion show that a remnant can be expected, which agrees well with the hydrochemical picture /Voss and Andersson, 1993; Löfman and Taivassalo, 1995/.

The comparison suggests that it is necessary to include all of the processes that influence water exchange in order to obtain a correct description. Interaction with low-conductive volumes and isolated water reservoirs is of importance for the water's exchange rate.

Time perspective

The timescale is determined by the timescale for climate change and by how long such change continues to influence the hydrogeochemical situation.

Conditions during an ice age, for example, are dependent on the nature, duration etc. of the ice. An effect of the most recent ice age is, for example, the ongoing land uplift, which can lead to replacement of non-saline surface water with saline water. This exchange process can proceed for thousands of years after a glaciation at repository depth (500 m).

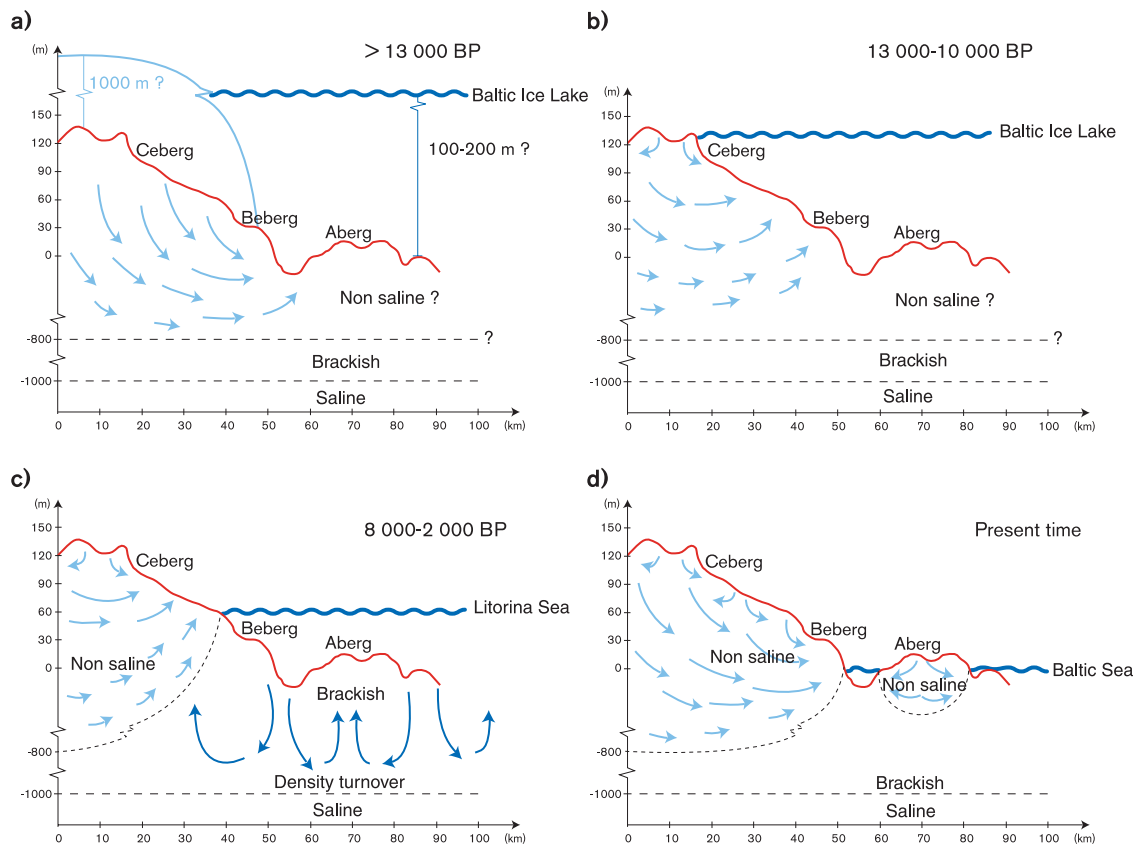


Figure 5-22. Evolution of Aberg, Beberg and Ceberg from the retreat of the ice after the most recent ice age until today. The different stages of the Baltic Sea are of great importance for the large-scale groundwater flux on the three sites. The difference between the sites is greatest during the period from the Littorina stage up to the present-day situation.

In a short time perspective, about 100 years, the groundwater disturbance caused by the repository will influence the groundwater chemistry to some extent.

The timescale for advection as regards radionuclide transport from the repository to the surface is dealt with in the section on radionuclide transport.

Natural analogues

A computer model for evaluation of hydrochemical data called M3 has been developed with the aid of the data gathered in and around the Äspö HRL. The model has also been used to describe the hydrochemical mixing conditions in the analogue studies in Oklo and Palmottu /Laaksoharju et al, 1999; Gurban et al, 1998/. In both of these cases, as on Äspö, it has been possible to distinguish the effects of mixing from the effects of chemical reactions. In the model study in Oklo, the described flow conditions could subsequently be verified by hydrogeological models.

Summary of uncertainties

Uncertainties in fundamental understanding: The conceptual uncertainties around advection/dispersion are small. Advection and dispersion are two well-defined model terms that are used in calculating radionuclide transport in groundwater. They are dealt with in section 5.8.1.

The models that are used for hydrochemical modelling are limited to the site from which the data derive. The predictive capacity of the models used is thereby limited to the same geographic area or similar areas where similar processes are active. The mixing model for Aberg can, for example, only be applied in Beberg and Ceberg if it can be assumed that these sites have undergone a similar evolution as Aberg.

There are, however, such similarities in the data quantities that the reliability of the models can be considered good. In very generalized terms, it can be said that the groundwater chemistry exhibits a mean residence time of around ten to a hundred years in the uppermost 100 m of the rock, while the residence time at 500 m depth lies in the range of thousands to tens of thousands of years. At greater depths, more than 1,000 m, the residence times are much longer.

Mixing is in the strict sense not a process but an aggregate result of advection and diffusion. Mixing is evaluated by means of inverse modelling, which involves starting from known results (data) and attempting to quantify the underlying processes, in this case mixing. The sequence in which different mixings have occurred comprises a fundamental uncertainty in the interpretation of the mixing process. To this is added the degree of mixing (disturbance) caused by borehole drilling and sampling, which further complicates the situation (data uncertainty).

The mixing phenomena that have occurred recently can be quantified better and with greater certainty than those that occurred a long time ago. It is, for example, relatively simple to trace meteoric water that has infiltrated on Äspö since the island rose above the surface of the sea approximately 3,000 years ago. On the other hand, it is impossible to determine whether meltwater from the most recent ice age has reached down to a depth of only a few hundred metres, or much deeper.

Uncertainties in data: Waters from different parts of the fracture network are sometimes mixed during drilling and subsequent sampling. This mixing can be incorrectly interpreted as being representative of the point in the rock where the sample was taken. Under unfavourable conditions, the water may derive from a different site entirely or be mixed with different water types from many different sites. By marking the drilling water, it is possible to make corrections for the quantity of water that has been injected. It is more difficult to correct for any disturbances caused by water from a fracture system flowing into the borehole and out into another fracture system. Careful evaluations have been carried out for the purpose of ascertaining how representative the water samples are (Smellie et al, 1985; 1987, Smellie and Laaksoharju, 1992; Laaksoharju and Skårman, 1995; Laaksoharju et al, 1995b). A positive trend can be seen in these evaluations. Study site investigations carried out prior to the KBS-3 report in the early 1980s gave about 15 percent representative sampling points, Klipperås gave 40 percent and Äspö 60 percent representative water samples.

In addition to the uncertainty in representativeness, there is a smaller uncertainty in measurements and analyses. These vary depending on analysis method and constituent. The greatest uncertainties concern redox- and pH-sensitive components such as sulphide, iron, manganese and hydrogen carbonate, where the uncertainty may be 50 percent. The uncertainty for other analyses is less than 10 percent.

Handling in the safety assessment

Base scenario: The process is included as an integral part of the hydrogeochemical evolution.

Canister defect scenario: See base scenario.

Climate change: The hydrogeochemical situation and the evolution of the geosphere are modelled with respect to the expected climatic evolution. This is based largely on the knowledge that has been obtained by reconstruction of previous chemical and hydrological conditions. The descriptions can be divided up into the time intervals 0–100 years, 100–1,000 years, 1,000–10,000 years and 10,000–100,000 years after closure.

In the time interval 10,000–100,000 years, assumptions concerning the ice age scenario will also determine the hydrochemical conditions. As a consequence of wide variations in the hydraulic driving forces, groundwaters of various types will be mixed and thereby lead to dissolution and precipitation of e.g. calcite.

Qualitative descriptions should be made with extreme hydrochemical conditions. During an ice age, a water with low ionic content may be brought down that causes the bentonite to form colloids. The opposite extreme is that a very saline water is brought up to repository level and thereby reduces the buffer's swelling capacity. There must be a discussion of the conditions required for this to take place. This type of question is discussed in SR 97 in Boulton et al /1999/.

Of special importance in the ice-age scenario is a possible transport of oxygenated water down to repository level. The conditions then differ from today's in that there may not be any soil cover that can contribute organic degradable material which bacteria can use to consume dissolved oxygen. Calculations have been carried out within SR 97 /Guimera et al, 1999/ showing that the groundwater flow is of decisive importance for how long it takes for oxygenated water to reach down to repository level. The calculations also show that the quantity of oxygen that can be transported in this way is limited and that the rock has the capacity to consume this oxygen.

Earthquake: Flow paths can be influenced and thereby advection. The influence on water chemistry can be considered negligible in comparison with other uncertainties in this scenario.

5.7.3 Diffusion

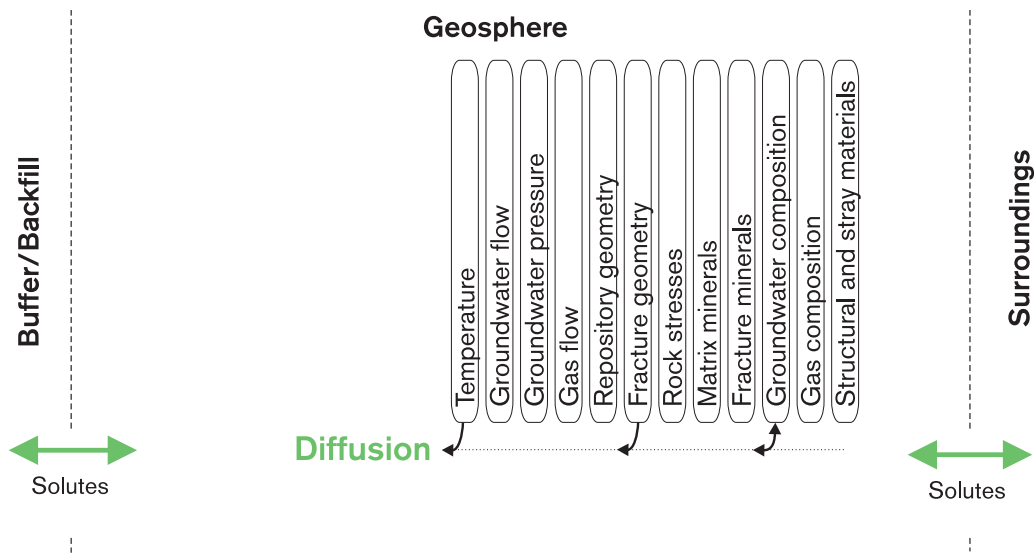


Figure 5-23. Diffusion.

Overview, general description

Solute in the groundwater can move by diffusion from areas of higher to areas of lower concentration in the bedrock's fracture system. The diffusion rate is determined by the properties of the water and the solutes, as well as by the temperature.

Diffusion as a transport mechanism takes on importance where transport with the flowing water, advection, is small, i.e. under stagnant conditions. Such conditions can prevail at great depths or in impervious rock volumes. Diffusion is also significant due to the fact that solutes can diffuse between the flowing water in fractures and stagnant water in the pores of the rock matrix, a phenomenon known as matrix diffusion. This aspect of diffusion is above all important for calculating radionuclide transport, see section 5.8.

Model studies/experimental studies

In a stagnant situation that has existed for a long time, diffusion might be expected to have had a pronounced influence on the conditions. Calculations have been carried out on the basis of the salinity profile in the KLX02 borehole at Laxemar, west of Äspö. The results agree fairly well with measured values if a diffusion time of one million years is assumed /Laaksoharju and Wallin, 1997/. As is evident from the section on uncertainties, it is not clear how much of the profile derives from diffusion and how much may be due to disturbances in the borehole /Rhén et al, 1997/.

Time perspective

Matrix diffusion can be important in connection with nuclide transport, see section 5.8.3.

Summary of uncertainties

Diffusion is basically a simple process that can well be described and modelled, even for water-bearing parts of the rock. The difficulty in practice is distinguishing the effects of diffusion from the effects of reactions and mixing.

Conceptual uncertainties surrounding matrix diffusion are discussed under the section “Radionuclide transport”.

Handling in the safety assessment

Base scenario: To explain the slow change from e.g. saline to non-saline (fresh) water at great depth, it is necessary to describe the diffusion process qualitatively. However, there is no evidence that diffusion has been or will be significant for the groundwater composition at repository depth. Effects of diffusion in the geosphere are therefore not analyzed in the base scenario.

Canister defect scenario: Matrix diffusion comprises an important retention factor in the calculation of radionuclide transport, see section 5.8.

Climate change: There is reason to assess the importance of diffusion in connection with recurrent glaciations. In SR 97, for example, penetration of oxygen (oxidized water) after a glaciation and how this affects underlying saline groundwater is analyzed. In order for this oxygen to be consumed by minerals in the rock, the water must diffuse into the matrix. See further section 5.7.5 for a discussion of this process.

Earthquake: See base scenario.

5.7.4 Reactions groundwater/rock matrix

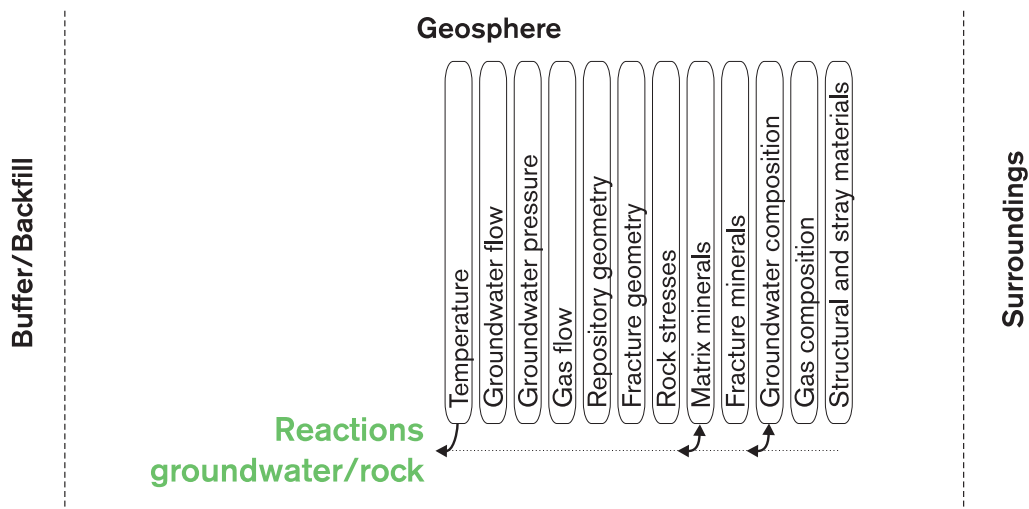


Figure 5-24. Reactions groundwater/rock matrix.

Overview

Stagnant groundwater will eventually approach a chemical equilibrium by reactions with the different minerals in the bedrock. Most reactions between water and minerals are, however, so slow that complete equilibrium will never be reached, even if the water’s flux in the bedrock is very slow.

The groundwater’s many reactions with the rock matrix are of importance for the chemical evolution of the groundwater in general. However, only some of these are of importance for the chemical evolution of the repository in a million-year perspective.

General description

Ever since the rocks were formed nearly two billion years ago, chemical reactions have transformed and affected the rock and its fracture system. During rock formation, water was released which also contains other residual products that did not fit into the crystal lattice, such as chloride, sodium and calcium. This water is called juvenile and has always existed down in the rock and usually contains large quantities of dissolved salts. If the salinity of the water exceeds 10 percent, i.e. 100 g/l TDS, it is called a brine /Frape and Fritz, 1987/. Such a water is stagnant due to its high density, which furthermore increases with time as more salt is leached out of the rock matrix.

The chemical reactions that take place in the groundwater/mineral system have widely varying reaction rates. It is thereby possible to some extent to use known reaction rates to assess the residence time for the groundwater in the rock. The degree of equilibrium gives a rough idea of the residence time. Bruno has compiled reaction rates for different kinds of reactions /Grenthe och Puigdomenech, 1997/. The fastest are metal hydrolysis reactions, with half-lives ranging from microseconds to tenths of seconds. Then follows complexation between metals and organic ligands, with half-lives of hundredths of a second to minutes, while fulvic and humic binding reactions proceed about ten times slower. Redox reactions with an electron transfer take from tens of minutes to several years, while redox reactions, which require changes in molecular structure, have half-lives of several to thousands of years.

Reactions which include solid phases (minerals) are generally much slower than reactions that only take place in the aqueous phase. (Exceptions are ion exchange reactions, which proceed just as quickly as reactions in the aqueous phase.) Dissolving haematite in water takes tens to tens of thousands of years, and dissolution of aluminium silicate takes tens of thousands to millions of years. There are, however, reactions between solid phase and water that are considerable faster, e.g. dissolution and precipitation of calcite, which have half-lives of seconds to days.

However, the reaction rate is also strongly dependent on the chemical environment where the reaction occurs. Precipitation of iron(oxy)hydroxide takes from picoseconds up to tens of years, depending on the pH and iron concentrations in the groundwater.

At very high pH, which can occur in contact with concrete, the reaction rates for dissolution of silicate minerals in granitic bedrock are significant. The silicate minerals are dissolved as a consequence of hydrolysis reactions, after which secondary reaction products are precipitated. Valuable knowledge concerning the reaction has been obtained from the hyperalkaline sources in Maqarin in Jordan /Smellie (Ed.), 1998/. Not very much is known about the reaction rate, but it is assumed that the reaction can reduce the pH to 10–11 and that it is presumably an extremely thin layer of minerals that react. At high pH, these secondary phases consist of calcium silicate hydrates (CSH), which are common in concrete. Zeolites form at lower pH.

Very saline groundwaters (brines) occur and are encountered everywhere drilling has been done to great depths. The depth varies widely from a few hundred metres to several km. This thereby shows how deep the superficial circulation cells have reached at one time after the brine was formed, which is often millions of years ago. The absence of brine therefore does not necessarily mean that recent circulations of surface water have occurred, but it does show that water exchange has occurred at this depth at some time since the rocks were formed.

Brines can also be formed by the dissolution of evaporites (salts deriving from a dried-up sea far back in time) by infiltrating groundwater. In general, brines of evaporitic origin can be considered to be common in sedimentary rocks, while leaching is the probable source of brines in crystalline bedrock. In both cases, however, the occurrence is a clear indication that the water is stagnant.

The effect of the various aforementioned reactions between water and mineral is also evident in the rock. Since the rock was formed, conversion of primary minerals to secondary (clay) minerals has proceeded constantly. The effects have been greatest under so-called hydrothermal conditions, when hot aggressive water has passed through the flow paths in the rock, preferably the major fracture zones. Hydrothermal conditions ceased to exist in the Fennoscandian shield several hundred million years ago, and the water that passed through the rock at that time has disappeared. The effects in the rock are that material has been dissolved and cavities called druses have formed, while at other places large quantities of fracture-filling minerals have been deposited. Afterwards, these fracture systems have been subjected to reactivation on several different occasions, so that the water's previous flow paths in the rock are difficult to trace, even in the large water-bearing fracture zones.

In saline groundwater as well, an increasing degree of chemical equilibrium is an indication that the water is stagnant. How such waters will evolve in the future is a more difficult question. In this case as well, one may assume that the conditions are constant and from there analyze how changes in the hydrological conditions affect the situation, see further under "mixing".

The minerals in the rock have a varying tendency to be altered or dissolved in groundwater. The same reactions probably take place on a microscale in the rock matrix as those that take place on a macroscale in water-bearing fracture zones. The difference is mainly that the water in the matrix is stagnant and transport of reactants and reaction products only takes place by diffusion. There is no sharp borderline between water-bearing fractures and the rock matrix. So far only modest attempts have been made to characterize the chemistry in the rock's pore water. Studies in the URL in Canada show that the rock matrix contains very saline water even if the water in the water-bearing rock has insignificant salinities.

Influence on pH: The rock's minerals are of importance for the groundwater's pH. There is a direct influence that is dependent on the interaction between the water and readily soluble minerals such as calcite, and an indirect influence that is controlled by slow weathering, the chemistry of the water and microbial conditions. There is a clear tendency for the pH to increase with depth, i.e. with the residence time, for non-saline waters, with extreme values of up to 10 pH units. The pH values for saline waters lie within a narrower range and seldom exceed 8.5. pH values below 7 and as low as 5.2 do, however, occur at great depth (more than 1,000 m) in extremely saline Canadian brines /Frape and Fritz, 1987/. There is a hypothetical relationship between hydrolysis reactions and their importance for the pH level. This has been verified for several granitic rock types /Tolhuat et al, 1992/.

Influence on redox conditions: The bedrock mineral's contents of reducing substances such as sulphide, divalent iron and manganese are vital for maintaining reducing conditions in the groundwater. The capacity to resist an attack by oxidizing substances – such as oxygen trapped in the repository on closure, or oxygen-rich water that infiltrates down on melting of a glacier – exists in the minerals. The redox level, or Eh, and the kinetics of the reactions are determined by the dominant redox pairs in solution along with the variety and quantity of microbes.

Model studies/experimental studies

It is possible with the aid of thermodynamic calculation tools to figure out which mineral alterations can be expected under different conditions. The accuracy of data and reactions is sufficient, whereas knowledge of the reaction kinetics is less satisfactory, which makes it difficult to get an idea of what time spans need to be postulated to achieve equilibrium.

Time perspective

Very saline water, brine, will remain unchanged during the short (geologically speaking) period of time needed for safe disposal of nuclear waste. The fact that brines still exist is attributable to their stability in time. This is also true of the primary minerals in the rock. The conditions that prevail today will remain relevant during the entire life of the repository.

Chemical reactions that influence the composition of the water occur in a timeframe of thousands to hundreds of thousands of years. Producing a water with extremely high salinity (brine) requires much longer periods. The prevailing chemical groundwater composition is the result of many different ongoing reactions. Because they have been going on for a long time, they have reached a static situation where the effects of different reactions balance each other. The composition can thereby be regarded as static, i.e. it will remain as it is unless changes in the flow conditions cause changes in the mixing proportions between different water types.

Summary of uncertainties

Many different mineral alteration reactions lie behind the evolution of the water chemistry, and in extreme cases the formation of brines. The end result of these reactions is generally well known. The uncertainty relates to the kinetics of the reactions, where it is known that many are extremely slow. It is therefore also unreliable to regard the water/mineral system as if it were in equilibrium and thereby capable of being described with the aid of thermodynamic data. Due to the inertia in the system, i.e. its slow kinetics, small changes caused by dissolution and precipitation in the rock matrix can be expected in the geologically short timespan needed for disposal of the spent nuclear fuel.

Handling in the safety assessment

Base scenario: The process is not deemed to cause appreciable changes in groundwater composition or matrix porosity in the base scenario. Changes in pH caused by cement are dealt with in section 5.7.7.

Canister defect scenario: See base scenario.

Climate change: See base scenario.

Earthquake: See base scenario.

5.7.5 Dissolution/precipitation of fracture-filling minerals

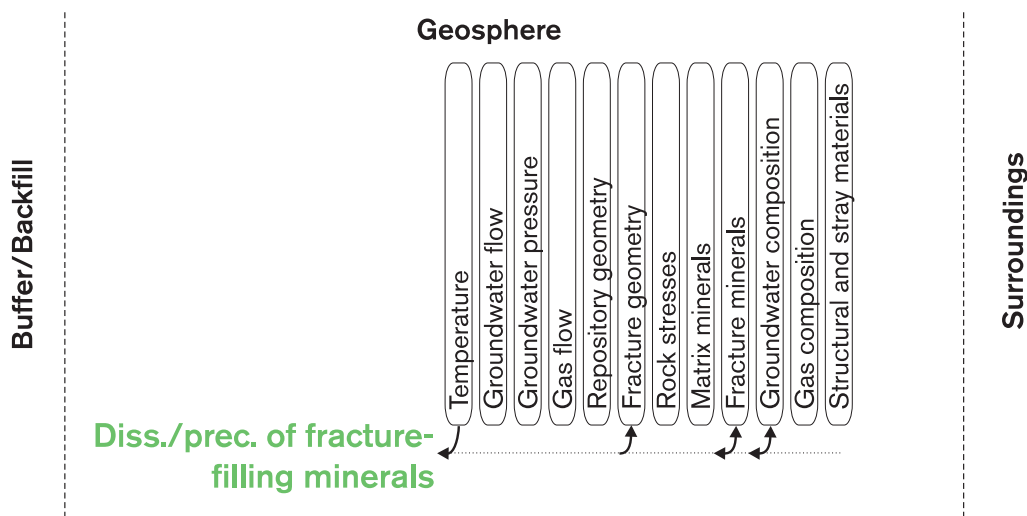


Figure 5-25. Dissolution/precipitation of fracture-filling minerals.

Overview

Minerals on fracture surfaces can dissolve in the groundwater. And conversely, solutes in the groundwater can precipitate on the fracture surfaces.

Under steady-state conditions, these processes are as a rule very slow. In the case of transient processes, e.g. infiltration (inflow) of acid or oxygenated water in the bedrock, the capacity of the fracture-filling minerals to buffer (counteract) chemical changes is important. In the case of radionuclide transport, the interaction between dissolved nuclides and fracture surfaces is important.

General description, model studies/experimental studies

Reactions between water and fracture-filling minerals give rise to conversion (alteration) of primary mineral phases to secondary ones. The phenomenon is called chemical weathering, and the secondary mineral phases consist of different kinds of clay minerals. In crushed volumes, where both mechanical and chemical influences have occurred at different times since the rock was formed, there are large quantities of different secondary fracture-filling minerals. The sequence in which they have been formed can be revealed by a careful mapping /Tullborg et al, 1991/. However, it is usually difficult to determine when and under what conditions this has taken place. Most fracture-filling minerals have originated under hydrothermal conditions (temperatures above 100°C and pressures well above 1 bar) far in the past. Subsequently, they have been subjected to alterations on several different occasions.

Precipitated minerals formed by mixing of waters of different compositions are also present on individual fracture surfaces. Such precipitations are calcite, gypsum, siderite, pyrite, fluorite and certain iron oxides. The existence of these mineral phases makes it possible to draw qualitative conclusions concerning the water chemistry that prevailed when the minerals were formed. By contrast, the opposite reactions, dissolution of

fracture-filling minerals, can neither be identified or quantified. A rapid transport of a carbon dioxide-rich water can, for example, dissolve calcite in a flow path relatively rapidly, and on mixing with another water precipitate calcite on the fracture surfaces. Calcite mineral in the same fracture has been investigated at different depths to provide information on the dissolution rate and thereby the groundwater flux /Landström and Tullborg, 1995/.

Co-precipitation of radionuclides: Precipitation and dissolution reactions are of great importance for nuclide transport and understanding of retention processes for radionuclides. Small amounts of nuclides may be entrained in e.g. the calcite lattice in connection with the precipitation of different mineral phases. This process is called co-precipitation and can be described quantitatively. Other trace substances that occur in the groundwater system have been able to be modelled via co-precipitation, and it is likely that radionuclide concentrations in groundwater could also be controlled by this process /Bruno et al, 1996/.

Influence on sodium and calcium concentration: Meteoric recharging water that contains calcium gains sodium with depth, while infiltrated seawater loses sodium in exchange for calcium. The reason is ion exchange which takes place in clay minerals along with weathering and precipitation reactions. As a result of these reactions, the water, regardless of whether it is fresh or saline, will have certain concentrations and proportions of sodium and calcium. Very dilute groundwaters are unusual at great depths, and the calcium concentration generally exceeds 10 mg/l at repository depth. This is important, since calcium destabilizes colloidal particles at a concentration in excess of about 4 mg/l.

Influence on magnesium and potassium concentration: The cations magnesium and potassium are common in groundwater, but their concentration is kept down by uptake in smectite clays and precipitation reactions. This is clearly evident on sites where seawater has infiltrated the rock and the concentrations have fallen from a high level to below 150 mg/l for magnesium and 12 mg/l for potassium.

Influence on pH: The groundwater's pH normally lies in the range 6.5–9.5. Of greatest importance for the pH in the infiltrating groundwater are reactions between carbon dioxide dissolved in the water and calcite mineral in the rock's fracture system. The carbonate system quickly reaches a state of equilibrium and determines the water's pH, which will then lie around 8.5 /Stumm and Morgan 1981/. The total carbonate concentration often varies within the range 100 to 300 mg/l and seldom exceeds 600 mg/l. Extremely high carbonate concentrations can occur as a result of biological activity. Concentrations of 1,000 mg/l have been recorded on isolated occasions. The biological processes that drive up the carbonate concentration also cause the pH to fall to below 7.

With increasing depth, the carbonate concentration usually decreases and the salinity increases. Saline groundwaters that have been isolated for a long time generally have a lower pH than non-saline stagnant waters. The reason may be that hydrogen ions located in the mineral layers can be replaced by cations in the water so that more protons come out into solution and the pH thereby becomes lower than in non-saline groundwaters /Toulhoat et al, 1992/.

The carbonate content of non-saline deep waters also declines with increasing residence time as an effect of increasing pH. The increasing pH is a result of feldspar weathering,

which releases calcium which, by precipitation of calcite, further lowers the carbonate concentration. The pH-buffering capacity which exists in the carbonate system in the groundwater, and which determines the pH, is however small in comparison with the buffering capacity in the minerals. The amount of calcite that coats the fracture surfaces is of greater importance for buffering against acidification than the carbonates in the aqueous phase. Equally large capacity exists in feldspars, which can also buffer against acidification. A quantitative example of the capacity of feldspar was given in a study in Poços de Caldas /Chapman et al, 1993/, where a superficial groundwater with a pH of 3 was changed to 6–7 by reaction with feldspar /Nordström, 1992/.

Calcite minerals are a useful indicator of inflow of recently-infiltrated groundwater. In areas where carbon dioxide-rich groundwater has infiltrated the bedrock, calcite dissolution can be seen to have occurred down to a depth of about 100 metres. The proportion of calcites in fracture-filling minerals in the water-bearing fractures can be estimated at 5 to 40 percent. The calcite minerals thereby constitute an effective buffer against infiltrating acid groundwater. Various analyses have been performed for the purpose of describing how an acidification will affect the groundwater composition at repository level /Wersin et al, 1994/. The conclusion is that the capacity of the minerals in the rock is sufficient to buffer against any acidification that can reasonably be expected.

Influence on redox conditions: Under the undisturbed conditions which prevail before the repository is built and which are expected to be reinstated some time after closure, it can be assumed that conditions are reducing and that the Eh of the groundwater coincides with iron and sulphide minerals in the rock and lies at a level such that uranium (technetium, neptunium and plutonium) in solution occurs in reduced, poorly soluble form. The Eh is linked to the pH and varies within the range -100 to -400 mV for pH values in the range 7–9.

The redox buffering capacity will lie in the available iron and sulphide minerals in the fractures. Numerous experiments have been conducted to explore both the reaction kinetics /Malmström et al, 1995/ and the capacity /Pirhonen and Pitkänen, 1991/ of iron-bearing minerals.

Influence on fracture geometry: Due to the relatively rapid dissolution and precipitation reaction with calcite, the flow paths in the rock will be changed if the chemistry of the infiltrating groundwater is changed. Open fractures will be healed and previously healed fractures may be opened due to changes in water chemistry. Only in the event of major climate changes is the effect expected to be pronounced.

An idea can be obtained of the effect of fracture opening/closing by comparing the occurrence of healed and open calcite fractures near the ground surface and at greater depths. The proportion of healed fractures is estimated to be one-third at depths down to 100 m and two-thirds at depths greater than 100 m. There are, however, great local variations due to site-specific hydrological conditions.

Time perspective

The dissolution and precipitation reactions in the fracture systems are fast in comparison with the weathering of the primary minerals. These reactions are therefore of importance in a repository perspective. It is necessary to take into account the consequence for fracture minerals of keeping the repository open, and the fact that it takes some time before the initial undisturbed conditions have been restored.

Natural analogues

In the Poços de Caldas project, the effects of co-precipitation were evaluated for analogues to radionuclides. The importance of co-precipitation as a retention process could be verified /Bruno et al, 1996/.

Summary of uncertainties

There is in general high certainty regarding the formation and kinetics of the fracture-coating minerals that have formed at low temperatures, i.e. those that have been precipitated due to supersaturation in the groundwater. The difficulty is to find these minerals and get an idea of their quantities and occurrence among the much larger quantity of fracture-filling minerals that have arisen under hydrothermal conditions. There is also an uncertainty regarding the origin of certain iron oxides, where it is of importance whether they have arisen under hydrothermal conditions or by oxidation of oxygenated groundwater. The variability, co-existence and spatial distribution of different minerals is poorly understood.

Co-precipitation reactions are known for certain solid phases and trace substances. There is great uncertainty as to whether these reactions apply generally.

Handling in the safety assessment

Base scenario: With knowledge of the hydrochemical conditions on different sites, the equilibrium situation should be calculated for the most common fracture-filling minerals calcite, gypsum, siderite, fluorite, barite, pyrite and iron sulphide. These calculations can be used to describe the stability of the groundwater system and can give an indication of what direction its evolution will take.

Canister defect scenario: See base scenario. For the influence of co-precipitation on radionuclide transport, see section 5.8.

Climate change: A qualitative analysis should be made of the clogging of present-day flow paths and opening of others by precipitation and dissolution of calcite. This requires knowledge of the occurrence and variability of the calcites on the analyzed sites. Sufficient knowledge exists for Aberg, but not for Beberg and Ceberg.

When a glacier melts, oxygenated water could possibly penetrate down to repository depth. This is dealt with in SR 97 by groundwater modelling /Svensson, 1999/ and by calculation of the reactions of the oxygen during transport down in the rock /Guimera et al, 1999/. The groundwater modelling yields travel times, while the oxygen calculations answer the question of whether the oxygen is consumed during the descent of the water.

Earthquake: See base scenario.

5.7.6 Microbial processes

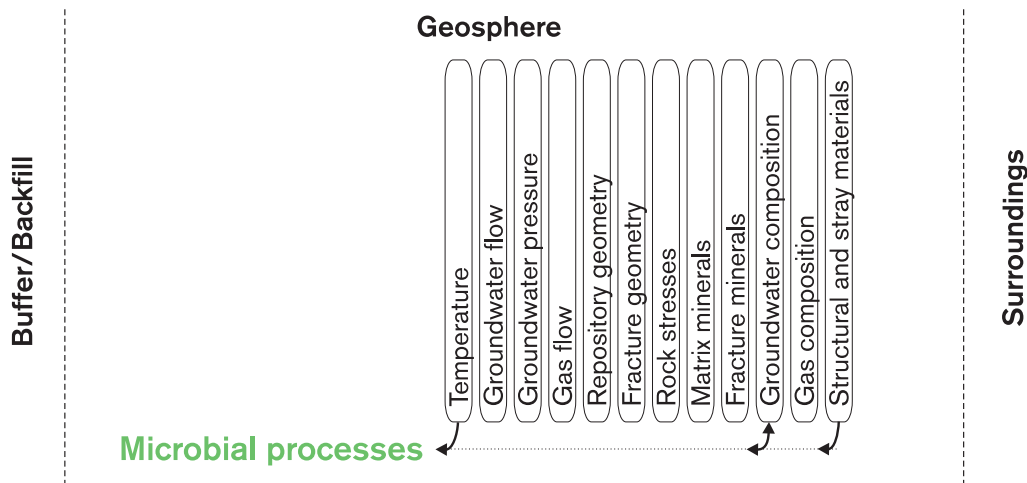


Figure 5-26. Microbial processes.

Overview

Bacteria in the groundwater can act as catalysts for:

- reactions where oxygen oxidizes organic matter,
- oxidation of divalent iron and sulphide with oxygen,
- reduction of trivalent iron to divalent (via oxidation of organic matter),
- reduction of sulphate to sulphide (via oxidation of organic matter),
- reduction of carbon dioxide to organic matter (via oxidation of hydrogen),
- reduction of carbon dioxide to methane (via oxidation of hydrogen or certain organic compounds).

The organic engineering and stray materials present in the repository can serve as nutrients for microbes in the vicinity of the repository. Even in the absence of organic matter, the bacteria can utilize methane and hydrogen dissolved in the water.

Consumption of oxygen influences the redox conditions in the groundwater around the repository, one of the more important variables in the hydrogeochemical environment. Sulphide can contribute to corrosion of copper, so the sulphide concentrations in the groundwater around the repository are of importance for the canister's isolating function.

General description

The importance of microbes for groundwater composition has recently received greater attention and been examined in greater detail than before /Pedersen, 1997/. It has also been found that microbes have, in special contexts, significantly altered the chemistry of the water. Bacteria can be beneficial, for example by participating in the chemical reduction of dissolved oxygen, or unfavorable, for example by reducing sulphate to sulphide /Pedersen and Karlsson, 1995/.

Oxygen consumption: Bacteria are of great importance when it comes to consuming the dissolved oxygen present in infiltrating surface water. Organic matter is the principal reducing agent and bacteria play a key role as catalysts in the rock's fracture system as well /Banwart (Ed.) 1995/. Previously it has been believed that this reaction only takes place in the soil layer, but this is not the case. This process can be expressed in simplified terms as follows:



During the construction and operating phases, the inflow of groundwater to the facility will influence the redox conditions. The increasing groundwater flux in the rock above the repository is not expected to influence the water's redox properties appreciably, however. The reason is that the increased flow of superficial oxygenated water will be balanced by the microbes so that all oxygen is consumed anyway. Stoichiometrically, 4 mg/l of organic carbon is sufficient to reduce 10 mg/l of dissolved oxygen. If the organic matter content is higher, trivalent iron and sulphate will also be oxidized after all oxygen has been consumed /Banwart et al, 1995/.

During repository construction, atmospheric oxygen will come into contact with minerals on tunnel walls and with water entering the facility. The oxygen will in all likelihood be consumed by bacteria after closure, provided there is some organic matter left in the repository.

Most groundwaters contain methane, which is degassed at the ground surface or when the water reaches a tunnel system. Methane-oxidizing bacteria are very common. They oxidize methane with oxygen, thereby contributing to oxygen consumption in a repository. Methane is thus an important complement to organic matter in microbial oxygen consumption. In contrast to the organic matter content, the methane content is often constant or increases with depth.

Reduction of iron: When all dissolved oxygen has been completely consumed, the concentrations of divalent iron in the groundwater often rise. The divalent iron is formed via reduction of trivalent iron in various minerals by iron-reducing bacteria, which utilize organic matter as a reducing agent /Chapelle and Lovley 1992/. The highest concentrations of divalent iron, 1–10 mg/l, often occur in the depth interval down to 100 m, after which the iron concentration drops to 0.01–0.1 mg/l at repository level. The reason is that sulphate-reducing bacteria that compete with iron-reducing bacteria for the nutrients are more efficient when the supply diminishes. At greater depths, the supply of both organic matter and nutrients is lower. The reduction of sulphate generates sulphide, which precipitates iron as iron sulphide or pyrite. This explains the reduction in iron concentration often seen towards greater depth. Both of these processes have a beneficial influence on the available redox capacity in the flow paths. Precipitation of iron and sulphide minerals in the flow paths make these minerals available for situations when the redox capacity may be needed, e.g. to reduce oxygen dissolved in the water.

Reduction of sulphate: The occurrence of bacterial sulphate reduction is concentrated to sites where the supply of organic matter, nutrients and sulphate is plentiful. This is particularly true beneath bottom sediments in the Baltic Sea, where the hydrological

evolution has resulted in infiltration of sulphate-rich seawater into the rock's fracture system on one or more occasions since the most recent ice age /Laaksoharju and Wallin 1997; Rehn et al, 1997/. An analysis of the prerequisites for extensive sulphate reduction has shown that salinity is also of importance /Laaksoharju (Ed.), 1995/. The most favourable range was in this case 3,000–6,000 mg/l of chloride, i.e. the salinity of the Baltic Sea.

On other sites there are sulphate-reducers that have optimal conditions at other salinities, indicating that the bacteria have adapted to prevailing conditions through mutations.

Unusually low pH values (6.8–7.0) have also been recorded in conjunction with extensive sulphate reduction in the tunnel section out to Äspö.

Reduction of carbon dioxide: Methanogenic microorganisms reduce carbon dioxide to organic matter and methane, using hydrogen as an energy source. Certain methanogens can utilize acetate and many can utilize compounds with only one carbon atom, such as formate, methanol, methylamine, etc. Methane occurs generally in most investigated groundwaters. One group of bacteria that is of particular interest is homoacetogenic bacteria. They reduce carbon dioxide to organic matter, including acetate, using hydrogen as an energy source and thus constitute a link between hydrogen and acetate-utilizing microbes (methanogens, iron- and sulphate-reducing bacteria). Homoacetogenic bacteria have been encountered in large quantities both in the rock around the Äspö HRL and in deep Finnish groundwaters.

Carbon dioxide-reducing bacteria have a favourable impact on a repository, since they convert hydrogen to methane and organic matter, which can in turn be utilized by methane-, iron- and sulphur-oxidizing bacteria, as described above.

Model studies/experimental studies

Besides the above-mentioned studies, great efforts have been made to demonstrate – both by means of models and experimentally – that reducing conditions exist at repository depth. An experiment was carried out during the construction phase of the Äspö HRL for the purpose of clarifying what happens with dissolved oxygen that rapidly infiltrates an open facility /Banwart et al, 1995/. Another is now under way, aimed at increasing our knowledge of what happens with the oxygen that is left when the repository has been closed /Puigdomenech, 1998/. In both of these studies, the importance of the microbes has been conclusively demonstrated and even quantified /Kotelnikova and Pedersen, 1998/.

Summary of uncertainties

Uncertainties in understanding: Our knowledge of what effects the different microbes have and the preconditions for their existence is good.

Uncertainties in data: Great variability exists in where and to what extent the different microbial processes occur. Bacterial reduction of oxygen in the superficial rock is, however, widely occurring and well-supported.

A special situation that ought to be taken into account concerns the precipitations of bacteria and iron hydroxide that are formed when reduced groundwater meets atmospheric oxygen in tunnels. If this precipitation proceeds for a long time, large quantities of organic matter will be deposited on the tunnel walls and remain after closure. How large these quantities are, and what consequences this may have, are still unknown.

Handling in the safety assessment

Base scenario: Mass balance calculations can show how different kinds of residual materials remaining in the repository will react. It is assumed that all organic matter will be able to serve as nutrients for microbes. Furthermore, the availability of hydrogen will be decisive for microbial activity in the long term. This means that an increased effect of microbial activity must be expected until all organic matter has been consumed, and subsequently an activity that is controlled by the supply of hydrogen. This means that oxygen, iron, sulphate and carbon dioxide will be reduced. The scope of these reactions is dependent on mass flows. Qualitative discussions of these processes are presented in SR 97.

Canister defect scenario: See base scenario. The bacteria can also function as carriers of nuclides and thereby be of some importance for nuclide transport, see section 5.8.

Climate change: The absence of a soil layer with oxygen-consuming bacteria can lead to increased penetration of oxygenated water. See “Reactions groundwater/rock matrix” above for effects of this.

Earthquake: See base scenario.

5.7.7 Decomposition of inorganic engineering material

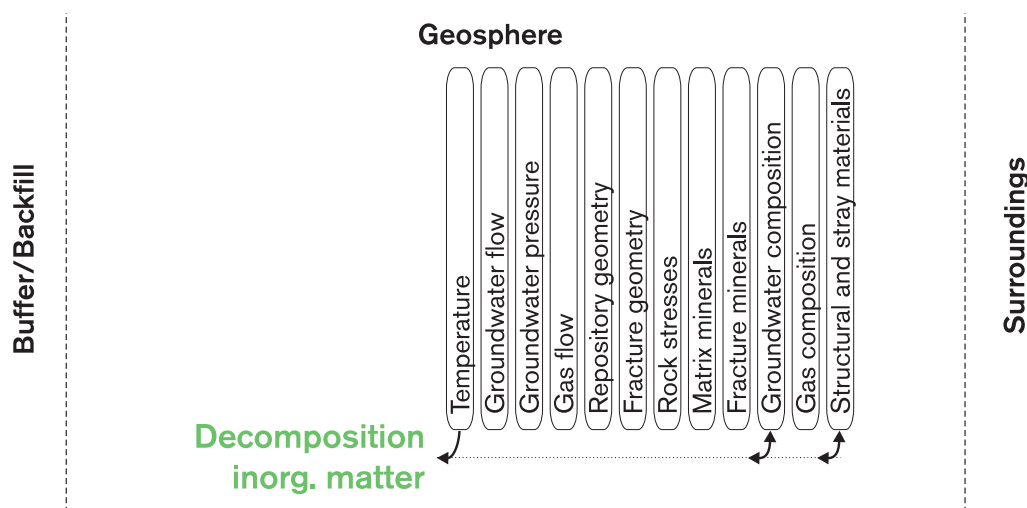


Figure 5-27. Decomposition of inorganic engineering material.

Overview

Inorganic materials that are not chemically stable in a deep repository will decompose and will mainly affect the water composition. Iron and steel will corrode with hydrogen formation, while dissolution of cement and concrete locally can affect the pH of the water.

General description

Steel corrosion: $\text{Fe} + \text{H}_2\text{O} = \text{FeO} + \text{H}_2$. Steel corrodes with hydrogen formation and has no appreciable effects on the water chemistry.

Dissolution of cement and concrete: Cement and concrete can theoretically influence the pH of the water, but are presumably of no importance since concrete dissolution is expected to proceed slowly and the quantities in the repository are expected to be small. Cement is also used to seal water-conducting rock in access tunnels. Experience from the groutings done in the Äspö tunnel also shows that large quantities of cement mortar cause small and short-lived changes in the pH of the groundwater /Rhén et al, 1997/.

Natural analogues

Silicate minerals in granitic bedrock react with hydroxide ions, which may derive from cement. The silicate minerals dissolve as a consequence of hydrolysis reactions, after which secondary reaction products are precipitated. The course of the reaction has been studied at the hyperalkaline springs in Maqarin, Jordan /Smellie (Ed.), 1998/. The reaction rate is unknown, but it is estimated that the reaction can reduce the pH from about 13 to 10–11 and that it is presumably an extremely thin layer of minerals that reacts.

Summary of uncertainties

The uncertainties pertain to the quantities of materials that remain and where in the repository they are. Approximate total quantities can be estimated today. Where they are concentrated and how in relation to each other may be of importance to the analysis.

Handling in the safety assessment

Base scenario: The process is neglected in view of the fact that the quantities are small.

Canister defect scenario: See base scenario.

Climate change: See base scenario.

Earthquake: See base scenario.

5.7.8 Colloid formation

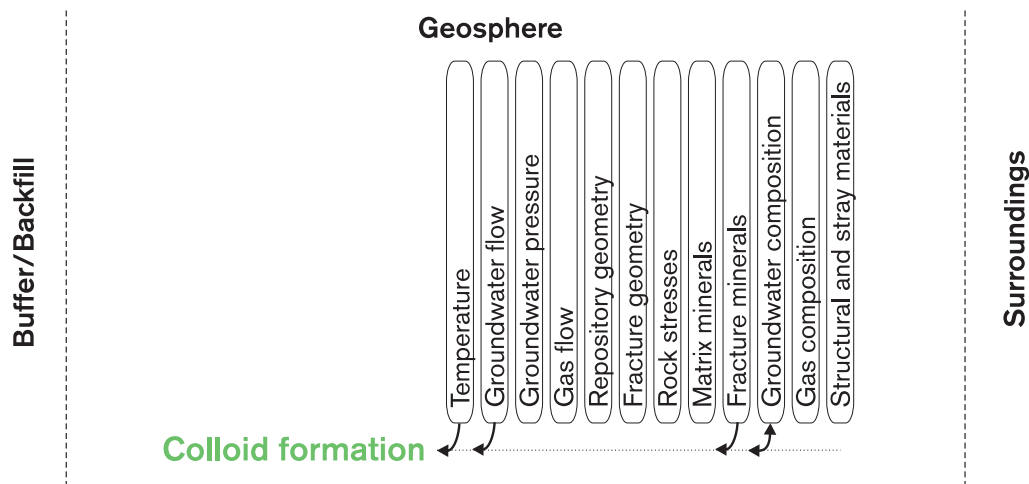


Figure 5-28. Colloid formation.

Overview

Colloidal particles can form in the groundwater as a result of chemical reactions, for example due to supersaturation when two different types of water are mixed. They can also form as a result of erosion. Radionuclides can sorb (adhere) to colloidal particles and be transported with them. It is therefore important to estimate to what extent such particles can occur or be formed in the groundwater.

General description

Colloid formation can take place as a consequence of supersaturation in water or due to interaction between solid materials and aqueous solution. The concentrations in deep-living waters are very low, so that it can be assumed that colloids, if they form, are not stable under these chemical conditions.

Colloids can be transported in water-conducting fractures in the same way as solutes, the difference being that colloidal particles are not affected by matrix diffusion.

Colloids are tiny particles that do not sediment. A practical definition of colloidal material is the fraction that passes through a 0.45μ filter, i.e. has a diameter less than 450 nm. These tiny particles can be conglomerates of molecules and compounds, such as iron hydroxides, or single large organic molecules. Bacteria comprise a special group of "colloids". There is no lower limit for the size of colloids. The borderline between dissolved hydrated substances and colloids is thereby diffuse.

Colloids occur generally and plentifully in superficial water, but are rare in deep groundwaters. The concentrations of colloidal material are so low (less than 0.05 mg/l) that it can be said that mixing and precipitation, as well as chemical weathering, do not generate stable colloids in concentrations of any importance /Laaksoharju et al, 1993/.

In contrast, the slightest admixture of atmospheric oxygen in a reducing groundwater gives rise to extensive colloid formation. After closure of the repository, the water may contain high concentrations of colloidal material during a transitional period, in the order of several to several tens of ppm /Wikberg, 1987/.

Model studies/experimental studies

Colloids have been modelled and investigated experimentally in many different contexts, including as a separate EU project with participants from a number of research institutes /Kim et al, 1996/. No *in situ* experiments are known, however. Under the reducing conditions in the bedrock, the concentrations are usually so low that they cannot be measured. A value of 0.05 mg/l has been estimated on the basis of an evaluation of measured concentrations and an estimate of the uncertainties inherent in these values. The value is pessimistically high. The evaluation is based on an experimental study conducted in cooperation between SKB and TVO at Olkiluoto /Laaksoharju et al, 1993/.

Time perspective

Extensive colloid formation can be expected in conjunction with closure of the repository, when mixing of oxidizing and reducing water occurs. The time this takes is determined by the groundwater flow and is expected to be no more than a few years.

Summary of uncertainties

Formation of colloids is dependent on several factors that are not fully understood today. In contrast to solutes, it is not possible to stipulate equilibrium conditions for colloids.

Handling in the safety assessment

Base scenario: Extensive colloid formation is expected to occur temporarily in connection with the closure of the repository. Shortly after closure and from then on, the concentration of colloids is expected to be less than 0.5 mg/l /Laaksoharju et al, 1998/. Colloids are of no importance in the base scenario.

Canister defect scenario: Previous calculations have shown that the expected colloid concentrations are of no importance for radionuclide transport /Allard et al, 1991/. For further discussion, see section 5.8.

Climate change: Water with an extremely low concentration of dissolved salts can erode the bentonite buffer, which could give rise to colloid formation. Such water could enter the repository in conjunction with the melting of an inland ice sheet. This is dealt with in section 4.7.7.

Earthquake: See base scenario.

5.7.9 Gas formation/dissolution

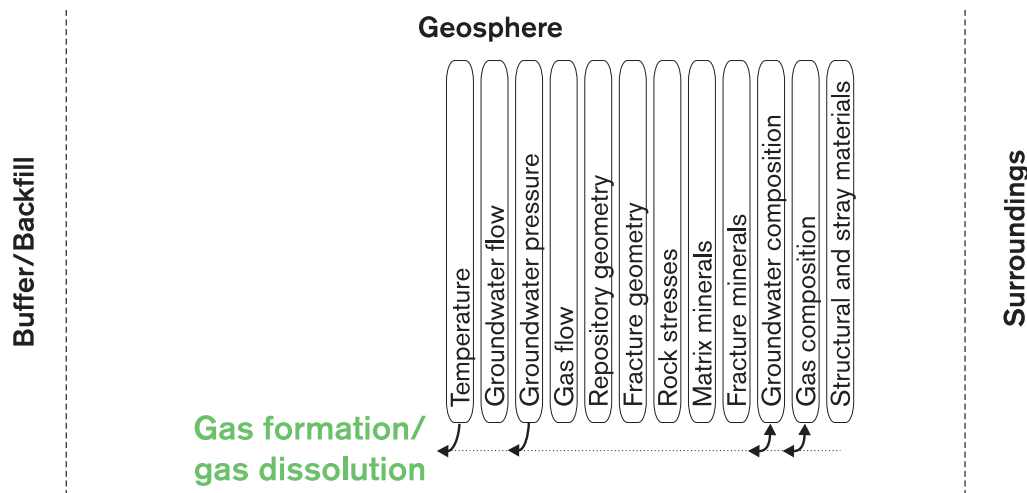


Figure 5-29. Gas formation/dissolution.

Overview, general description, model studies/experimental studies

All gaseous substances can dissolve in water. The solubility of different gases varies and is dependent on both hydrostatic pressure and temperature. Solubility is often given at 25°C and a pressure of 1 atmosphere (NTP = normal temperature and pressure) in the gas in question. If several gases together contribute to the total pressure, the solubility of the individual gases is proportional to their partial pressure, i.e. the portion of the pressure contributed by the individual gas. In a gas mixture at 1 atmosphere that consists of equal parts nitrogen and hydrogen, the partial pressure of each gas is 0.5 atmosphere. In an aqueous solution in equilibrium with such a gas mixture, the concentration of the dissolved gases is then only half of the concentration that is soluble with a pure gas phase.

Solubility increases in proportion to the hydrostatic pressure, i.e. the solubility at a depth of 500 m is 50 times higher than at the same temperature on the ground surface. If several gases are dissolved, their partial pressures contribute to the total pressure. If the aggregate partial pressure of the gases exceeds the hydrostatic pressure, a separate gas phase is formed. This gas phase then consists of a mixture of all the dissolved gases in proportion to their partial pressures. Such a degassing takes place, for example, when deep-lying groundwater is pumped up to the ground surface for sampling.

The groundwater contains varying quantities of dissolved gas. Nitrogen usually dominates, followed by methane, carbon dioxide, helium, argon, hydrogen, etc. Sometimes high concentrations of hydrogen and methane occur. The total quantity of dissolved gas varies around 5 volume-percent (NTP) and is generally higher towards greater depth. There are also sites where very high gas concentrations have been encountered, up to 1,000 ml of gas per litre of groundwater, and where the composition has been completely different with hydrogen and/or methane as the dominant components /Sherwood et al, 1993; Pitkänen et al, 1998/.

There are different hypotheses concerning the origin of gas dissolved in groundwater. Low concentrations can be explained by the fact that infiltrated groundwater has been saturated with respect to the gas components present in the air. The oxygen has then been consumed by reactions, while the other components are found in the same proportion as in air. Very high concentrations of hydrogen and methane encountered locally are assumed to derive from upflowing from the interior of the earth, or to be the result of extensive bacterial activity /Pedersen, 1997/.

Summary of uncertainties

Uncertainties in understanding: Our fundamental understanding of the process is very good.

Uncertainties in data: The reaction constants that are needed to describe the process are in general well known.

The quantity of dissolved gas varies greatly, as previously mentioned. The large variation that has been measured on various sites is probably linked to the varying occurrence of microbes. Furthermore, some of the variation may be due to the fact that some gas comes from great depth and has been generated in the rock, while other gas comes from the ground surface.

Handling in the safety assessment

Base scenario: No gas formation/dissolution of importance for the evolution of the repository is expected in the base scenario. Concentrations of dissolved gases are expected to remain the same as those that exist now.

Canister defect scenario: Hydrogen gas from a corroding cast iron insert complements the situation in the base scenario, see further section 4.5.3. Possible radionuclide transport in a separate gas phase is dealt with in section 5.8.

Climate change: See base scenario and section 5.7.10.

5.7.10 Methane ice formation

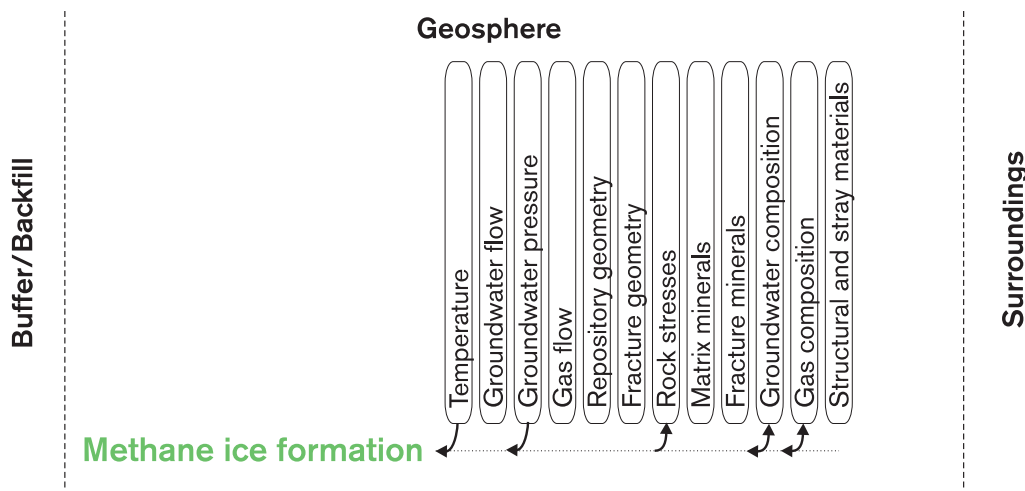


Figure 5-30. Methane ice formation.

Overview, general description

At the pressures and temperatures that prevail during a glaciation, water and methane can combine to form a solid phase known as methane ice, involving small energy fluxes. The transformation from the solid methane ice phase to water and methane gas can give rise to a volume change that affects the rock, especially if large quantities are transformed at the same time.

Methane ice formation can take place at the ground surface directly beneath a thick glacier, or under a permafrost that reaches down to a depth of 150 m or deeper. It can be assumed that it is only in highly conductive fracture systems that an upward transport and enrichment of methane is possible. This means that it is only there that methane ice can form. In nature, methane ice has been observed in marine sediments and underneath permafrost. It is unlikely that methane ice formation will occur in a deep repository on a scale of importance to the safety of the repository. In order for this to happen, methane must be present in the gas phase at a depth of 500 m in order to combine with water and form methane ice. The solubility of methane is 4 g/l at normal pressure and 20°C. To occur in the gas phase at repository level at the hydrostatic pressures prevailing there, a concentration of over 200 g/l of dissolved methane is needed, or very high concentrations of other dissolved gases. Actual concentrations of dissolved gas are always much lower (Hermansson et al, 1991a, b).

Summary of uncertainties

Uncertainties in understanding: Methane ice formation is a physically well understood process.

Uncertainties in data: Computer uncertainties concern the necessary conditions for the formation of methane ice in connection with a deep repository, and above all the combination of a permafrost that reaches down to repository level at the same time as methane occurs in the gaseous phase at repository level.

Handling in the safety assessment

Base scenario: Not applicable.

Canister defect scenario: See base scenario.

Climate change: Present-day knowledge suggests that this process is of no importance for the safety of the deep repository during a glaciation.

Earthquake: See base scenario.

5.7.11 Salt exclusion

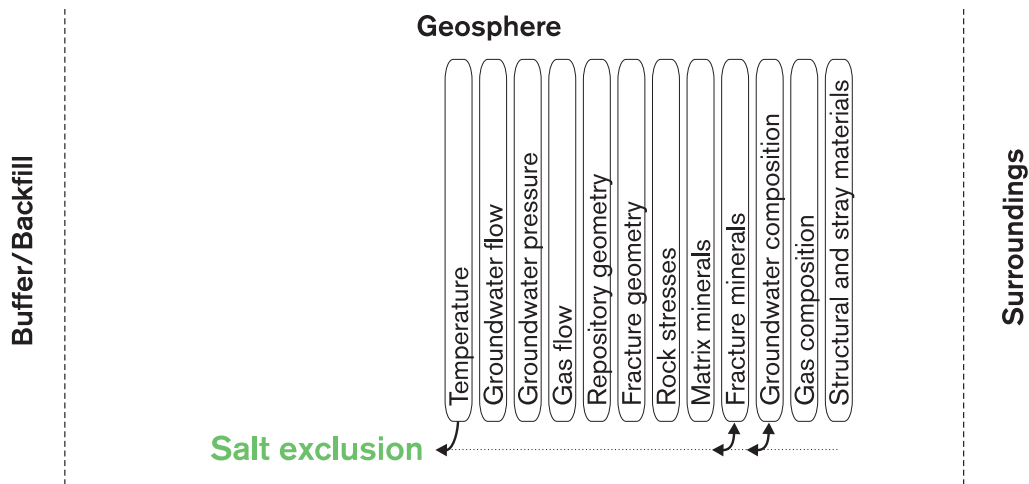


Figure 5-31. Salt exclusion.

Overview and General description

As water freezes slowly, the solutes present in the water will not be incorporated in the crystal lattice of the ice. All salt that has been present in the water will then be pushed in front of the glacier. It is assumed that this can also occur in connection with permafrost, provided that freezing proceeds slowly and continuously. This process could, if repeated a number of times, give rise to a relatively sharp borderline between fresh and saline water at the depth to which the permafrost has reached.

Summary of uncertainties

It is doubtful whether salt exclusion occurs to an extent that makes the process significant for the distribution of saline and fresh water.

Handling in the safety assessment

Base scenario: Not applicable.

Canister defect scenario: See base scenario.

Climate change: Salt exclusion is a process that is probably of no importance for the safety of the repository and is therefore not taken into account in the assessment.

Earthquake: See base scenario.

5.8 Radionuclide transport

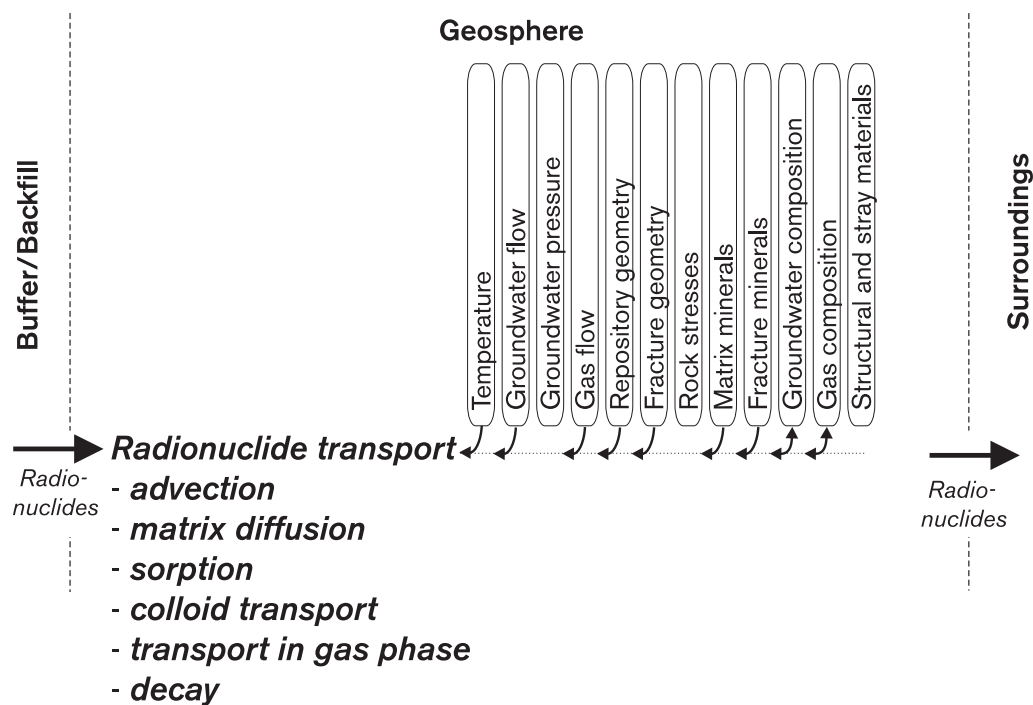


Figure 5-32. Radionuclide transport.

Overview

Radionuclides can be transported with the flowing groundwater, *advection*. Another process that can be important under stagnant conditions is *diffusion*. An important aspect of this is *matrix diffusion*, i.e. radionuclides diffuse into the stagnant water in the micropores of the rock and are thereby retained and transported more slowly than the flowing water. The timescale for advection relative to the timescale for matrix diffusion determines the relative importance of the latter process. *Sorption*, where radionuclides sorb (adhere) to the surfaces of the fracture system and the rock matrix, is also crucial for radionuclide transport. Matrix diffusion and sorption are the two most important retention processes for radionuclides in the geosphere. Another factor that can be of importance for retention is sorption on *colloidal particles* and transport with them. The chemical environment in the water determines what *speciation* (chemical form) the radionuclides will have, which is crucial particularly for the sorption phenomena. Some nuclides can be transported in the *gas phase*. Finally, *radioactive decay* influences the groundwater's content of radionuclides and must therefore be included in the description of transport phenomena.

5.8.1 Advection and dispersion

General description

Section 5.5.1 describes the processes that control the groundwater flow through the fractured rock in the geosphere, and how to calculate an integrated flow, the Darcy flow rate, through the rock. Section 5.7 describes how the processes of advection and dispersion can lead to mixing of groundwater, and how the hydrogeochemical environment is affected by these mixing conditions. How the processes of advection and dispersion influence radionuclide transport is described below.

Only a small portion of the volume of the rock is taken up by cavities such as fractures and porous structures in the intact rock. The groundwater flows in these cavities, but only through fractures that are hydraulically connected and through that portion of the fracture volume that is open to flow. The flow porosity, which is smaller than the total porosity of the rock, is the portion of the rock that is taken up by flowing groundwater. The total groundwater flow per unit area is called the Darcy velocity. The mean transport velocity of the water particles is obtained as the Darcy velocity divided by the flow porosity. This resultant transport process describes the groundwater's bulk movement and is called advection.

The Darcy velocity is defined on a macroscopic scale. On smaller scales, velocity differences occur for the flow within a fracture and between different fractures. These velocity variations lead to mixing phenomena called hydrodynamic dispersion. During transport in fractured rock, the dispersion is usually dominated by velocity variations between different flow paths.

The division of transport into an advective and a dispersive component is dependent on the scale studied and is relatively arbitrary. The advective component describes the mean transport, while the dispersive component takes into account effects of heterogeneity in the rock and velocity variations on scales smaller than that described by advection. Dispersion also contains a component that describes pure molecular diffusion in water. Dispersion is a model concept rather than an actual process.

Model studies/experimental studies

The so-called advection-dispersion concept is often used in the modelling of tracer tests. This concept expresses in its simplest one-dimensional formulation that the mass flow is proportional to the advective velocity multiplied by the concentration in the aqueous phase and to a dispersion coefficient multiplied by the concentration gradient. The dispersion coefficient is often expressed as a constant (longitudinal dispersivity) multiplied by the advective velocity.

A number of combined studies have been done where experiments have been conducted in the field and modelled at the same time. In Sweden, experiments have, for example, been conducted in the Stripa Mine /Gnrík 1993; Olsson and Gale 1995/, in Finnsjön /Ahlbom et al, 1992/ and at the Äspö HRL /Gustafson and Ström, 1995; Elert, 1999/.

In modelling with the advection-dispersion concept, it has often turned out to be difficult to estimate parameters *a priori* for the advective and dispersive transport based solely on hydraulic data such as flowrates and pressures. For the advective component, the problem involves determining a relevant flow porosity for calculation of the mean velocity of the water. Further, it has turned out that the dispersivity concept does not work generally at high spatial variability in fractured rock; among other things, a scale dependence has been observed for the dispersion. The importance of these aspects is touched upon below under "Handling in the safety assessment".

Time perspective

In modelling studies, advective travel times from repository sites up to the biosphere of the order of tens to hundreds of years have typically been obtained /SKB 91, 1992; Svensson, 1997/. Dispersion does not significantly influence these timespans. It is important to note that these advective travel times are pure model results without any counterpart in the actual systems; an actual "water particle" is subjected to both diffusion and matrix diffusion (see below) and thereby has longer travel times. Furthermore, the travel times cited above are proportional to the assumed porosity, which is not well known in fractured rock (see "Summary of uncertainties" below).

Summary of uncertainties

The conceptual uncertainties surrounding advection can be regarded as very small. The process in itself is well understood, but the naturally occurring spatial variability in hydraulic conductivity entails that groundwater flow and advective velocities also vary in space. In modelling, this variability can entail an uncertainty for transport predictions. Difficulties in estimating the flow porosity (see above) also entail an uncertainty in determination of the final advective velocity. For transport of sorbing radionuclides, however, the advective velocity is of secondary importance (see “Sorption and Matrix diffusion” below); the resulting uncertainty in advection is therefore not of major importance.

The conceptualization of velocity variations as a dispersion process is more problematical; other approaches may be necessary in order to achieve an adequate description. Alternative approaches are described in greater detail below under “Handling in the safety assessment”.

Handling in the safety assessment

Base scenario: No radionuclide transport is expected in the base scenario. If the analysis of the base scenario should nevertheless result in canister damages, radionuclide transport is handled as in the canister defect scenario below.

Canister defect scenario: In SKB’s safety assessment SR 97, three different conceptualizations are used for groundwater flow and transport: Discrete fracture model, channel network model, and stochastic continuum description. In all models, a large-scale mixing is obtained by means of explicit modelling of variation in advective velocity between different transport pathways. In the discrete models, individual fractures comprise transport pathways, while a spatial conductivity distribution comprises the basis for pathlines with varying velocity in the continuum models. This large-scale mixing is the dominant component in what is known as dispersion. The explicit modelling of these velocity variations thus serves to minimize the use of the somewhat problematical concept of dispersion to small-scale velocity variations (i.e. velocity variations on scales smaller than the explicitly modelled scale). The individual pathlines comprise a basis for a collection of one-dimensional streamtubes by means of which radionuclide transport is described in SR 97.

Dispersion/mixing along the individual streamtube is normally modelled by means of a dispersion term where the dispersive mass flow is proportional to a dispersion coefficient. As described above, the dispersion coefficient is given by the velocity of the groundwater and a coefficient called longitudinal dispersivity (dispersion length). The dispersion lengths can be very uncertain to estimate, due to the difficulty of conducting tracer tests in fractured rock over suitable length scales. Transverse dispersion is often very much less than longitudinal dispersion. The scale dependency of the dispersion coefficient that has been determined in the field is sometimes simulated by the use of a dimensionless constant, called the Peclet number. The Peclet number represents the ratio between advective and dispersive transport. The parameter is included in the advection-dispersion formulation for particle transport in rock that is used in SR 97 /Norman and Kjellbert, 1990/. Uncertainties in dispersion are handled in SR 97 by the use of a range for the Peclet number /Andersson et al, 1998; Andersson, 1999/. The effect of this uncertainty is small, however.

Climate change and earthquake: The influence of these scenarios on groundwater flow and transport is described in section 5.5.1. If there is a need for radionuclide calculations, the same transport models are used as for the canister defect scenario, but with flow paths and velocities representing the relevant scenario. For SR 97, however, there is the limitation that transport is described with streamtubes. The definition of these is based on a groundwater flow that does not change in time. Thus, it is necessary within each scenario to define time periods with roughly constant flow conditions.

5.8.2 Sorption

General description

The term “sorption” includes a number of different retention processes/mechanisms which result in a substance (radionuclide) that is transported dissolved in groundwater being immobilized (adhering) to the solid surfaces of the rock. The most important mechanisms are ion exchange and surface complexation /Carbol and Engkvist 1995/. Sorption for some radionuclides can be irreversible in practice and then results in permanent immobilization of the nuclide. In these cases, the nuclide is incorporated in the mineral lattice. For the quantities of radionuclides that have the potential to be immobilized, the sorption capacity of the geosphere can be considered to be unlimited, i.e. the sorption will not be weakened as the amount of sorbed material increases.

Sorption can take place directly on the surfaces of the water-bearing fractures or on the surfaces of the microfractures inside the rock matrix, where the water is more or less stagnant. Furthermore, sorption can take place on other material, such as clay minerals, which may be present on the surfaces of the water-bearing fractures.

Depending on the process in question, the strength of the sorption is highly dependent on the chemical properties of the ions and the presence of possible complexing agents. It is therefore essential to know the redox conditions, and the groundwater’s pH and content of complexing agents such as humic and fulvic acids (section 5.7.5). The chemical form of the nuclide (speciation) is controlled by the prevailing redox conditions. Complexation in the aqueous phase can reduce the sorption for some of the radionuclides. The amount of the reduction depends on the form and charge of the radionuclide and on the groundwater’s content of humic substances. In connection with ion exchange, the salinity of the water is also of great importance. High salinity reduces e.g. the sorption of Cs^+ and Sr^{2+} /Carbon and Engkvist, 1997/.

The minerals that serve as the substrate for sorption have different capacities for taking up radionuclides. Some minerals are, for example, good ion exchangers, while others are not. Clay minerals and iron oxyhydroxides have a large capacity to bind nuclides.

A number of other processes besides ion exchange and surface complexation also influence the distribution of nuclides between aqueous phase and solid phase. Precipitation reactions and co-precipitation (mineralization) have been identified as important processes that can contribute to the retention of radionuclides /Grenthe and Puigdomenech 1997/. These processes, which are highly dependent on the speciation of the radionuclides and the saturation of the water with respect to the species in question, are however not usually regarded as sorption reactions.

Model studies/experimental studies

A large number of experimental, nuclide-specific studies of sorption have been carried out /Carbol and Engkvist 1995/. These tests are usually conducted as batch tests where a specimen containing the nuclide in question in aqueous solution is allowed to come to equilibrium with the solid rock material. Minerals and water compositions are used that are typical for the repository site and the important parameters – such as pH, ionic strength and concentration of radionuclides – are then varied. The change in the aqueous concentration of the nuclide provides a measure of the sorption. Column tests with flowing water can also be used to estimate the sorption. In the field, attempts have been made to estimate the sorption directly by determining the distribution of tracer between fracture surfaces and equivalent groundwater in boreholes /Landström and Tullborg, 1990/. Transport experiments with sorbing tracers in the field can also be used to estimate the strength of the sorption process /Frick et al, 1992; Winberg et al, in prep/.

If the sorption is linear, completely reversible and in equilibrium, a distribution coefficient for the particular water chemistry in question, K_d , can be estimated. The assumption of linearity is usually met at the low concentrations that are of interest, while the assumption of equilibrium is met if the sorption has a timescale that is much shorter than the timescale for transport with advection and dispersion. The use of K_d entails a simplification of the relatively complex sorption processes. Models that take into account non-linear sorption and/or non-equilibrium conditions exist, but are seldom used in safety assessments.

Time perspective

For most nuclides, the sorption process, particularly ion exchange, is considered to be fast compared with the timescale for advective transport in fractured rock. This means that equilibrium between rock material and aqueous phase usually prevails under natural conditions.

Processes such as incorporation of nuclides in the mineral lattice are much slower than ion exchange and cannot be considered to be in equilibrium with the rock. However, since these processes are not utilized in the safety assessment (see below), this slow rate is not worrisome.

Natural analogues

Dealt with below under the process “Matrix diffusion”.

Summary of uncertainties

Since sorption is a collective term for several processes, it can be claimed that our conceptual understanding varies. The use of the simplification with the distribution coefficient K_d is conceptually and practically attractive; but the validity of this approach can be questioned under certain specific conditions when the prerequisites of the concept are not fulfilled. As discussed above, however, both the linearity and equilibrium conditions are met for the conditions that apply in the safety assessment. Thus, the validity of the concept does not in itself entail an uncertainty factor, given the purpose of the safety assessment.

The greatest single uncertainty factor that affects the K_d value is the variability of the groundwater chemistry /Bruno and Duro, 1997/. Given all uncertainties, the K_d values

that are used in safety assessments (see below) are chosen so that the retention capacity in radionuclide transport is not overestimated, i.e. cautiously pessimistic values are used.

Sorption by means of surface complexation can theoretically also be described with surface complexation models. These models are general and well-founded, but require a large quantity of thermodynamic data for the sorbing substances. Furthermore, they require surface complexation constants, which are difficult to measure for all possible combinations of nuclides and minerals. The results of different experiments with surface complexation models have therefore not been used to replace the distribution coefficients (the K_d values), but rather to further our understanding of the sorption mechanisms and determine what they are dependent on, i.e. how reliable the sorption can be considered to be /Carbol and Engkvist, 1995; Olin and Lehtikoinen, 1997/.

Handling in the safety assessment

Base scenario: No radionuclide transport is expected in the base scenario. If the analysis of the base scenario should nevertheless result in canister damages, radionuclide transport is handled as in the canister defect scenario below.

Canister defect scenario: Models based on the assumption that sorption in the rock matrix can be simplified and modelled with the linear equilibrium model (utilization of K_d) are used in the safety assessment. This means that retention processes such as mineralization are not used for the safety assessment.

In order not to overestimate sorption in connection with changes in water chemistry, cautiously pessimistic distribution coefficients are assigned /Carbol and Engkvist, 1995; Carbol and Engkvist, 1997/. In SR 97, for example, different values of K_d are used for non-saline and saline water, and in relevant cases for different redox forms. In principle, K_d can also be compensated for a decrease in sorption caused, for example, by humic and fulvic acids /Grenthe et al, 1992/. This is not done in SR 97, however, since the concentrations of organic matter in the deep groundwaters in question are relatively low /Carbol and Engkvist, 1997/. Furthermore, an uncertainty span for K_d is used in SR 97 that includes both experimental uncertainty and uncertainties regarding the natural chemical environment. For further discussion of parameters values in SR 97, the reader is referred to Andersson /1999/.

Climate change and earthquake: The influence of these scenarios on groundwater flow and transport is described in section 5.5.1. If there is a need for radionuclide transport calculations, the same transport models are used as for the canister defect scenario, but with flow paths, chemical conditions and thus also K_d values representing the relevant scenario.

5.8.3 Molecular diffusion and matrix diffusion

General description

Transport by molecular diffusion takes place when solutes move from areas of high concentration to areas of low concentration. Molecular diffusion in the flowing water is generally considered to be subordinate to the effect of advection and dispersion. Under stagnant conditions in the fractures in the rock, however, the process can be important. Molecular diffusion is also important in conjunction with matrix diffusion in the rock's water-filled microfractures.

Matrix diffusion in the rock's system of interconnected microfractures can be important since the water there is virtually stagnant compared with the water moving in the fractures. The existence of an interconnected system of microfractures in granitic rock has been verified by experiments both in the laboratory /Skagius and Neretnieks, 1985; Skagius, 1986/ and in the field /Birgersson and Neretnieks 1988/. In water with low ionic strength, anions have lower diffusion into the matrix than equivalent uncharged particles with otherwise identical properties. This is due to an ion exclusion effect, where the negatively charged anions are repelled from the negatively charged pore surfaces and thus have a smaller effective volume disposable for diffusion /Ohlsson and Neretnieks, 1997/. In the case of cations that undergo ion exchange, this diffusion can be reinforced by a phenomenon called surface sorption. In this case the radionuclides also diffuse in the sorbed solid phase /e.g. Skagius, 1986/.

For many nuclides, transport through the rock will be strongly restricted by sorption on the fracture surfaces in the rock (see sorption above). Matrix diffusion further increases the available surface area for sorption by exposing the surfaces of the microfractures to the radionuclides. The transport of weakly sorbing and non-sorbing radionuclides will also be retarded by matrix diffusion to some extent. In the stagnant water in the rock matrix, transport is only possible by means of diffusion and is therefore very slow. When the concentration of the nuclides in the water-conducting fractures becomes lower than in the matrix, they diffuse back from the matrix to these water-conducting fractures. Thus, matrix diffusion is not an irreversible process, but merely a retardation mechanism.

Besides by the diffusion and sorption properties of the matrix, the importance of matrix diffusion for radionuclide transport is also determined by the geometry of the fractures and the magnitude of the flow (the advective velocity) in the fractures. At high advective velocities, the transport-retarding effect of matrix diffusion decreases; the diffusive timescale for transport into the matrix becomes longer in relation to the timescale for advective transport. In a similar manner, the transport-retarding effect of matrix diffusion increases at lower advective velocities, which can be achieved for example when a given total flow is distributed over larger fracture surfaces. For this given total flow, the contact surface area (flow-wetted surface area) between radionuclides in aqueous solution and rock has increased at the same time as the advective velocity has decreased.

With the assumption of a simplified flow geometry, for example flow through rectangular channels, the controlling groups of parameters for matrix diffusion can be expressed as the flow-wetted surface area divided by the flow through the channel plus a group of parameters including the K_d value, the diffusion coefficient and the porosity. The flow-wetted surface area divided by the water flow is a critical parameter here for sorbing nuclides and is of great importance for the resulting mass flow of nuclides in the mobile groundwater.

For a more detailed discussion of this subject, the reader is referred to /Neretnieks 1980; Elert et al, 1992; Olsson et al, 1994; Moreno et al, 1995; Elert, 1997/.

Model studies/experimental studies

The group of parameters that control the sorption capacity can be determined relatively simply in the laboratory. Diffusion coefficients are primarily determined with diffusion cells. A compilation of values for use in SR 97 has recently been done /Ohlsson and Neretnieks 1997/. Determination of K_d values is discussed above in the section on sorption.

Different methods have been proposed for estimating the flow-wetted surface area, for example tracer tests, tunnel observations, measurements in boreholes, geochemical studies and numerical experiments. The different methods yield a wide range of variation in the estimated values, often between two and three orders of magnitude /Elert, 1997/. This is in part dependent on the method in question and in part on different properties in the rock. Furthermore, it is the ratio between the flow-wetted surface area and the flow along transport pathways that is of interest for retention, not the flow-wetted surface area in itself. This further complicates measurements in the field.

Time perspective

Matrix diffusion is a slow process. It is primarily the combination of matrix diffusion and sorption that gives the geosphere its retarding capacity. Even with advective travel times of a few tens of or hundred years for transport from the repository to the recipient, most radionuclides arrive retarded by several orders of magnitude in relation to the advective travel time.

Natural analogues

Fracture surfaces can be reddened as a result of hydrothermal changes /Elert, 1997/. This reddening could be used as an indication of the contact surface area (flow-wetted surface area) between flowing water and rock. The problem is that this reddening took place a long time ago under conditions of which we have no knowledge today, among other things the boundary conditions for the water flow are unknown. Since the contact surface area is highly dependent on the flow situation, extrapolating reddening results to today's flow-wetted surface areas is associated with great uncertainties. Further, as previously mentioned it is the ratio of the flow-wetted surface area and the flow that controls retention; it is not enough just to know the flow-wetted surface area under previous, perhaps different flow conditions.

Natural analogues in the form of geological formations with elevated natural radioactivity can be used to verify matrix diffusion as a process that took place over long timespans. Analogues of this type – found for example at Palmottu in Finland, Alligator Rivers in Australia and Cigar Lake in Canada – offer an opportunity to achieve better process understanding /Miller et al, 1994/. By measuring concentration profiles *in situ* and comparing with model simulations with relevant data, it is possible to get an idea of the effects of matrix diffusion /Rasilainen, 1997/. Agreement between measured and simulated profiles indicates that the matrix diffusion models used are realistic. Since the applied models include sorption processes, it can be claimed that the analogue studies also verify the fact that combined matrix diffusion and sorption are active processes *in situ*.

Summary of uncertainties

Matrix diffusion is a process that is difficult to quantify and thereby burdened with relatively great uncertainties. Even if it has been possible to demonstrate diffusion into the rock material (matrix diffusion) in laboratory experiments, it is much more difficult to show this under field conditions. However, the natural analogues offer evidence for the fact that matrix diffusion takes place (see above). Further, the concept of flow-wetted surface area (contact surface area, specific surface area, wet surface area, etc.) is burdened with considerable conceptual uncertainties. The concept is obvious in a geometrically simplified flow model, but the question is whether these models can

realistically describe the effect of matrix diffusion under natural flow conditions. Further development of the model concepts and the concept of flow-wetted surface area itself is needed to answer this question satisfactorily.

Handling in the safety assessment

Base scenario: No radionuclide transport is expected in the base scenario. If the analysis of the base scenario should nevertheless result in canister damages, radionuclide transport is handled as in the canister defect scenario below.

Canister defect scenario: The model FARF31 is utilized in SR 97 /Norman and Kjellbert, 1990/ to describe transport through the rock. The model solves the transport equations along one-dimensional streamtubes (see “Advection and dispersion” above) and is based on a double porosity description with advection-dispersion in the mobile phase (flowing water) and diffusion in the immobile rock matrix. An exchange term between the two media is included in the calculations. The penetration depth of radionuclides in the matrix can be described in the model. If, for example, the fractures in the rock are closely spaced, the extent of the matrix between the fractures is smaller. In the matrix, the nuclides can also be subjected to sorption described with the K_d concept.

Nuclide-specific diffusion coefficients /Ohlsson and Neretnieks, 1997/ and K_d values /Carbol and Engkvist, 1997/ are utilized for FARF31 in SR 97. For the sorption values, assessments of ion exclusion have been included, whereas surface sorption has not been taken into account. The specific values used in SR 97 are discussed further in Andersson /1999/.

As described above, the advective component of transport (i.e. transport pathway and non-reactive travel time) is obtained from a groundwater flow model. In the continuum models, no information is obtained on the flow-wetted surface area, inasmuch as the medium is described by means of conductivity values rather than by means of an explicit geometry. In the channel network model, the flow-wetted surface area is included in the actual model formulation and can be based directly on actual borehole measurements. In the discrete fracture models, the contact surface area between flowing water and rock can be calculated. Even though the result in this case is controlled by which input data are used for fracture statistics, this method offers yet another means to verify the concept and use of the flow-wetted surface area for use in the safety assessment. In the safety assessments for fractured rock that have been carried out to date, values within the range 0.01–1 m²/(m³ rock) have been utilized for the flow-wetted surface area /Elert, 1997/.

The continuum model HYDRASTAR /Norman, 1992/ is mainly used in SR 97 for description of groundwater flow. The transport pathways/streamtubes obtained from HYDRASTAR and a span of values for the flow-wetted surface area based on estimation of conductive fracture frequency are used in FARF31 /Andersson et al, 1998/.

Climate change and earthquake: The influence of these scenarios on groundwater flow and transport is described in section 5.5.1. If there is a need for radionuclide calculations, the same transport models are used as for the canister defect scenario, but with flow paths, flow-wetted surface area and other relevant conditions representing the relevant scenario.

5.8.4 Colloid transport

General description

Colloid formation is described in section 5.7.8. Sorbing radionuclides could in principle be transported more or less unretarded with the velocity of the water if they adhered to colloidal particles in the groundwater /Laaksoharju et al, 1995b/. The colloids can consist either of inorganic particles such as silicon, iron hydroxide and clay, or of organic particles such as bacteria. The median concentration of colloids in the groundwater is less than 0.05 mg/l /Laaksoharju et al, 1995b/. If the uptake of radionuclides on colloidal particles is reversible, this process will be manifested as a reduction of the K_d value, where the reduction is inversely proportional to the concentration of colloids and the sorption tendency on the colloids. This reduction is, however, negligible given the maximum colloid concentrations in Swedish rock /Allard et al, 1991/.

If, on the other hand, the nuclide should adhere irreversibly, the situation may be another one. In this case, the nuclide will be transported with the particle and at worst not be delayed at all by sorption and/or matrix diffusion in the rock. However, calculations show that the consequences in this case as well are of no importance for safety, due to the fact that the natural concentration of colloids is so low. The evaluation is summarized by Allard et al /1991/.

As far as colloids in deep groundwaters are concerned, the concentration of colloids could theoretically increase in connection with the melting of a glacier following an ice age. However, studies show that the low concentrations may persist even then, since the expected dilution does not result in the low calcium concentrations that are required for stable colloids to form /Laaksoharju et al, 1995b/.

In summary, it can be said that radionuclides in the groundwater can occur sorbed on colloids, and that the possibility that a small fraction will be bound irreversibly to mobile natural colloidal particles cannot be entirely excluded. However, the overall consequence of this for the safety of the repository is negligible.

Model studies/experimental studies

Laboratory tests confirm that radionuclides can sorb on colloids and that the sorption on these mineral colloids is largely reversible. The strength of the sorption is roughly equivalent to the measured K_d for the corresponding minerals and nuclides /Christiansen-Sätmark, 1995/.

Time perspective

The same time perspective can be considered applicable as for advective transport.

Summary of uncertainties

The process of sorption on colloidal material is burdened with relatively great uncertainties. These uncertainties concern whether the process is reversible or not, and what actual concentrations of colloidal material are present in the groundwater. However, the relevance of the process for the overall safety of the repository is of a subordinate character, inasmuch as the concentrations of colloidal material that are required for the process to make a difference never occur naturally in the groundwaters in question. Consequently, these uncertainties are not problematical from the perspective of the safety assessment.

Handling in the safety assessment

For the reasons given above, SKB has not found reason to develop a special transport model for this mechanism.

5.8.5 Speciation

General description

The chemical conditions in the water (pH, redox conditions, etc.) determine what speciation (chemical form) the radionuclides will have. This speciation mainly influences the sorption properties dealt with above under "Sorption".

5.8.6 Transport in gas phase

General description

The flow of gas in the geosphere is described in section 4.5.3. How radionuclides can be transported with a gas phase is described below.

At the pressure prevailing in a deep repository, some radionuclides that would exist in gaseous form under atmospheric pressure will be dissolved in the aqueous phase. These nuclides are then transported as solutes whose transport has been described above. The following treatment applies solely to radionuclides that can exist in gaseous form at the relevant pressures.

The groundwater down at repository level contains dissolved gases, e.g. nitrogen and helium. A gas phase can form if the sum of the partial pressures of all constituent substances in the water exceeds the water pressure. This gas phase contains the individual substances in proportion to their individual partial pressures and solubilities. The natural concentrations of dissolved gases are, however, so low that they are not sufficient to form a gas phase at the water pressure prevailing at the depths in question /SKB 91, 1992/.

Higher gas concentrations could arise locally at a canister if it is so damaged that water has entered up to the cast iron insert. Hydrogen gas is generated by oxygen-free corrosion of iron, and in this case the water could become supersaturated with dissolved gas so that bubbles are formed, i.e. the sum of the partial pressures exceeds the water pressure. Since gas bubbles are lighter than water, they strive upward towards the biosphere. Only radionuclides that can exist in the gas phase can be transported directly with the bubbles. This applies only to a few nuclides. The gas's content of these nuclides is controlled by the partial pressures and solubilities of the nuclides.

Colloidal particles can also be transported with gas bubbles /Wan and Wilson, 1994a/. The concentration of colloids in deep groundwaters is low and of no importance in this context, but experiments show that bentonite particles can also accompany gas bubbles /Wan and Wilson, 1994b/. If this is correct, it means that bentonite particles, including contaminated bentonite particles, could accompany gas bubbles. There is thus a possibility of indirect transport of radionuclides with gas bubbles from a damaged canister.

Model studies/experimental studies

No model or experimental studies have been conducted on transport of radionuclides with a separate gas phase. This is justified mainly by the way in which the process is dealt with in the safety assessment (see below).

A model study has been carried out to ascertain the importance of radionuclide transport with gas and particles /Neretnieks and Ernstson, 1997/. In the study it was assumed that all gas from a damaged canister is released in the form of small bubbles covered with montmorillonite particles from the bentonite buffer. The clay was further assumed to have sorbed radionuclides from the leaching of the fuel. The particles were assumed to remain irreversibly bound to the bubbles, while all gas was assumed to reach the ground surface. The actinides remained irreversibly bound to the clay particles, while caesium and strontium desorbed from the bentonite clay and underwent matrix diffusion combined with sorption during transport through the rock. The results of the calculations showed that the releases to the biosphere were very limited for all nuclides even with these very pessimistic assumptions.

Time perspective

The transport of gas bubbles through the geosphere can be much faster than advective transport.

Summary of uncertainties

The process for transport of gaseous nuclides in gas bubbles is well understood. By contrast, sorption of colloids on gas bubbles is burdened with considerable uncertainties. However, this process is of subordinate importance for overall safety.

Handling in the safety assessment

Base scenario: No radionuclide transport is expected in the base scenario. If the analysis of the base scenario should nevertheless result in canister damages, radionuclide transport is handled as in the canister defect scenario below.

Canister defect scenario: In the safety assessment, transport in the gas phase is treated pessimistically as a short circuit of the repository with the biosphere, i.e. transport through the geosphere is neglected /SKB, 1995/.

Transport via colloidal material that is transported with gas bubbles is not taken into account in the safety assessment. This is based on the model studies described above.

If necessary, transport in the gas phase can be treated in a similar manner for other scenarios.

5.8.7 Radioactive decay

General description

The radionuclides undergo decay during their transport through the geosphere. The ratio of the nuclides' half-lives to the total travel time (i.e. the result of both advective transport and matrix diffusion and sorption) determines how large a fraction of the nuclide content reaches the biosphere. Radioactive decay is discussed in section 2.3.1.

Summary of uncertainties

The half-lives of the nuclides are known with great certainty.

Handling in the safety assessment

Base scenario: No radionuclide transport is expected in the base scenario. If the analysis of the base scenario should nevertheless result in canister damages, radionuclide transport is handled as in the canister defect scenario below.

Canister defect scenario: The transport code FARF31 /Norman and Kjellbert, 1990/ handles both chain decay and decay for individual nuclides.

5.9 References

- Ageskog L, Jansson P, 1998.** Prototype repository. Finite element analyses of heat transfer and temperature distribution in buffer and rock. SKB PR HRL-98-20, Svensk Kärnbränslehantering AB.
- Ahlbom K, Tirén S, 1991.** Overview of geologic and geohydrologic conditions at the Finnsjön site and its surroundings. SKB TR 91-08, Svensk Kärnbränslehantering AB.
- Ahlbom K, Andersson J-E, Andersson P, Ittner T, Ljunggren C, Tirén S, 1992.** Finnsjön study site. Scope of activities and main results. SKB TR 91-08, Svensk Kärnbränslehantering AB.
- Alexander R (ed.), 1992.** A natural analogue study of the Maqarin hyperalkaline groundwaters. NAGRA Technical Report 91-10. Nagra Switzerland.
- Allard B, Karlsson F, Neretnieks I, 1991,** Concentrations of particulate matter and humic substances in deep groundwaters and estimated effects on the adsorption and transport of radionuclides. SKB TR 91-50, Svensk Kärnbränslehantering AB
- Almén K-E, Stanfors R, Svemar C, 1996.** Nomenklatur och klassificering av geologiska strukturer vid platsundersökningar för SKB's djupförvar. SKB PR D-96-29, Svensk Kärnbränslehantering AB.
- Andersson J, Hermansson J, Elert M, Gylling B, Moreno L, Selroos J-O, 1998.** Derivation and treatment of the flow wetted surface and other geosphere parameters in the transport models FARF31 and COMP32 for use in safety assesment. SKB R-98-60, Svensk Kärnbränslehantering AB.
- Andersson J, 1999.** SR 97 – Data and data uncertainties. Compilation of data and evaluation of data uncertainties for radionuclide transport calculations. SKB TR-99-09, Svensk Kärnbränslehantering AB.
- Autio J, 1997.** Characterization of the excavation disturbance caused by boring of the experimental full scale deposition holes in the research tunnel at Olkiluoto. SKB TR 97-24, Svensk Kärnbränslehantering AB.
- Banwart S (ed.), 1995.** The Äspö redox investigations in block scale. Project summary and implications for repository performance assessment. SKB TR 95-26, Svensk Kärnbränslehantering AB.

Banwart S (ed.), Laaksoharju M, Skårman C, Gustafsson E, Pitkänen P, Snellman M, Landström O, Aggeryd I, Mathiasson L, Sundblad B, Tullborg E-L, Wallin B, Pettersson C, Pedersen K, Arlinger J, Jahromi N, Ekendahl S, Hallbeck L, Degueldre C, Malmström M, 1995. The Redox experiment in block scale. Final reporting of results from the Three Year Project. SKB PR 25-95-06, Svensk Kärnbränslehantering AB.

Barton N, Bandis S, Bakhtar K, 1985. Strength, deformation and conductivity coupling of rock joints. *IJRM*, Vol. 22, No 3, pp. 121–140.

Barton N, Vik G, 1988. Stage I joint characterization and stage II preliminary prediction using small Core Samples. Stripa Project IR 88-08, Svensk Kärnbränslehantering AB.

Birgersson L, Neretnieks I, 1988. Diffusion in the Matrix of Granitic Rock. Field Test in the Stripa Mine. Final Report. SKB TR 88-08, Svensk Kärnbränslehantering AB.

Boulton G S, Wallroth T, Kautsky U, Morén L, 1999. Impact of long-term climate change on a deep geological repository for spent nuclear fuel. SKB TR-99-05, Svensk Kärnbränslehantering AB.

Brady B, Brown E T, 1993. Rock mechanics for underground mining. Second edition, Chapman & Hall, London.

Bruno J, Duro L, Jordana S and Cera E, 1996. Revisiting Poços de Caldas. Application of the co-precipitation approach to establish realistic solubility limits for performance assessment. SKB TR 96-04, Svensk Kärnbränslehantering AB.

Bruno J, Duro L, 1997. Discussion of data uncertainties, Review of selected sorption data of radionuclides in granitic rock. SKB PR U-98-06, Svensk Kärnbränslehantering AB.

Bäckblom G (ed.), Stanfors R (ed.), 1989. Interdisciplinary study of post-glacial faulting in the Lansjärv area Northern Sweden. SKB TR 89-31, Svensk Kärnbränslehantering AB.

Cacas M C, Ledoux E, de Marsily G, Tillie B, Barbereau A, Durand E, Fuega B, Peudecerf P, 1990. Modeling fracture flow with a stochastic discrete fracture network: Calibration and validation, 1. The flow model, *Water Resour. Res.* 26(3), 479–489.

Carbol P, Engkvist I, 1995. Sorption och sorptionsmodeller. Tillämpningar och begränsningar i säkerhetsanalys. SKB AR 95-26 (in Swedish), Svensk Kärnbränslehantering AB.

Carbol P, Engkvist I, 1997. Compilation of radionuclide sorption coefficients for performance assessment. SKB R-97-13, Svensk Kärnbränslehantering AB.

Case J B, Kelsall P C, 1987. Modification of Rock Mass Permeability in the Zone surrounding a shaft in Welded Tuff. Nevada Nuclear Waste Storage Investigation Project, Contractor Report SAND86, 7001, Albuquerque, Nevada, USA.

Chapelle F, Lovley D, 1992. Competitive exclusion of sulphate reduction by Fe(III) reducing bacteria. *Ground Water*, vol. 30, 29–36.

Chapman N A, McKinley I G, Shea M E, Smellie J A T (editors), 1993. The Poços de Caldas project: Natural analogues of processes in a radioactive waste repository. Elsevier, Amsterdam, p. 234.

Christiansen-Sätmark B, 1995. Transport of radionuclides and colloid through quartz sand columns. Doctoral thesis, Dept of Nuclear Chemistry, Chalmers University of Technology, Göteborg, Sweden.

Claesson J, 1992. Buoyancy flow in fractured rock with a salt gradient in the groundwater – An initial study. SKB TR 92-05, Svensk Kärnbränslehantering AB.

Claesson J, Probert T, 1996. Temperature field due to time dependent heat sources in a large rectangular grid – Derivation of analytical solution. SKB TR 96-12, Svensk Kärnbränslehantering AB.

Dershowitz W G, Lee J, Geier J, Foxford T, La Pointe P, Thomas A, 1995. FracMan User manual, Golder Associates Inc. Seattle.

Earlougher R C, 1977. Advances in well test analysis. SPE monograph Volume 5 of Henry L. Doherty Series.

Elert M, Neretnieks I, Kjellbert N, Ström A, 1992. Description of the transport mechanisms and pathways in the far field of a KBS-3 type repository. SKB TR 92-09, Svensk Kärnbränslehantering AB.

Elert M, 1997. Retention mechanisms and the flow wetted surface – implications for safety analysis. SKB TR 97-01, Svensk Kärnbränslehantering AB.

Elert M, 1999. The Äspö task force on modelling of groundwater flow and transport of solutes. Evaluation of modelling of radially converging and dipole tests with conservative tracers (TRUE-1 Tasks 4C and 4D). SKB TR-99-04, Svensk Kärnbränslehantering AB.

Eloranta P, Simonen A, Johansson E, 1992. Creep in crystalline rock with application to high level nuclear waste repository. Report YJT-92-10. Nuclear Waste Commission of Finnish Power Companies, Helsingfors, Finland.

Emsley S, Olsson O, Stenberg L, Alheid H-J, Falls S, 1997. Zedex – A study of damage and disturbance from tunnel excavation by blasting and tunnel boring. SKB TR 97-30, Svensk Kärnbränslehantering AB.

Fairhurst C, Gera F, Gnirk P, Gray M, Stillborg B, 1993. OECD/NEA International Stripa Project. Overview volume I. Executive summary. Svensk Kärnbränslehantering AB.

Finsterle S, Pruess K, 1995. Solving the estimation-identification problem in two-phase flow modelling. Water Resour. Res., 31, 913–924.

Follin S, 1992. Numerical calculations of heterogeneity of groundwater flow. SKB TR 92-14, Svensk Kärnbränslehantering AB.

Follin S, 1995. Geohydrological simulation of a deep coastal repository. SKB TR 95-33, Svensk Kärnbränslehantering AB.

Follin S, Hermanson J, 1997. A Discrete Fracture Network Model of the Äspö TBM Tunnel Rock Mass. SKB AR D-97-001, Svensk Kärnbränslehantering AB.

Frape S K, Fritz P, 1987. Geochemical trends for groundwaters from the Canadian shield. In: Fritz P and Frappe S K, Saline water and gases in crystalline rocks. Geol. Assoc. of Canada Spec. Pap., 33:19–38.

Frick U, Alexander W R, Baeyens B, Bossart P, Bradbury M H, Bühler Ch, Eikenberg J, Fierz Th, Heer W, Hoehn E, McKinley I G, Smith P A, 1992. Grimsel Test Site. The radionuclide migration experiment – Overview of investigations 1985–1990, PSI-Bericht Nr. 120 NAGRA NTB 91-04, Switzerland.

Gascoyne M, Davison C C, Ross J D, Pearson R, 1987. Saline groundwaters and brines in plutons in the Canadian shield. In: Fritz P and Frappe S K, Saline water and gases in crystalline rocks. Geol. Assoc. of Canada Spec. Pap., 33.

Gnirk P, 1993. OECD/NEA International Stripa Project. Overview volume II. Natural barriers. Svensk Kärnbränslehantering AB.

Gray M, 1993. OECD/NEA International Stripa Project. Overview volume III. Engineered barriers. Svensk Kärnbränslehantering AB.

Grenthe I, Stumm W, Laaksoharju M, Nilsson A-C, Wikberg P, 1992. Redox potentials and redox reactions in deep groundwater systems. Chemical Geology, vol. 98 (1992), pp. 131–150.

Grenthe, I, Puigdomenech, I (ed.), 1997, Modelling in Aquatic Chemistry (chapter by Bruno, J, Trace Element Modelling), p 573, OECD/NEA, Paris, France.

Griffith A A, 1924. Theory of rupture. Proc. 1st Int. Congr. Appl. Mech., Delft.

Guimera J, Duro L, Jordana S, Bruno J, 1999. Effects of ice melting and redox front migration in fractured rocks of low permeability, SKB TR-99-xx, Svensk Kärnbränslehantering AB (in preparation).

Gurban I, Laaksoharju M, Ledoux E, Madé B, Salignac AL. 1998. Indication of uranium transport around the reactor zone at Bagombe. SKB TR-98-06, Svensk Kärnbränslehantering AB.

Gustafson G, Ström A, 1995. The Äspö Task Force on modelling of groundwater flow and transport of solutes. Evaluation report on Task No 1, the LPT2 large scale field experiments. SKB ICR 95-05, Svensk Kärnbränslehantering AB.

Gylling B, 1997. Development and applications of the channel network model for simulations of flow and solute transport in fractured rock. Doctoral Thesis, Dep. of Chemical Eng. and Tech. TRITA- KET R72, Royal Institute of Technology, Stockholm, Sweden.

Hakami E, 1995. Aperture distribution of rock fractures. Doctoral Thesis. Div. of Engineering Geology, Department of Civil and Environmental Engineering, Royal Institute of Technology, Stockholm, Sweden.

Hakami E, Olofsson S-O, Hakami H, Israelsson J, 1998. Global thermomechanical effects from a KBS-3 type repository. Summary Report. SKB TR-98-01, Svensk Kärnbränslehantering AB.

Hansson H, Stephansson O, Shen Baotang, 1995. SITE-94. Far-field rock mechanics modelling for nuclear waste disposal. SKI Report 95:4, Swedish Nuclear Power Inspectorate, Stockholm, Sweden.

Hermansson H-P, Sjöblom R, Åkerblom G, 1991a. Geogas in Crystalline Bedrock. SKN (National Board for Spent Nuclear Fuel) Report 52, Stockholm, Sweden.

Hermansson H-P, Åkerblom G, Chyssler J, Lindén A, 1991b. Geogastransport i berg, förstudie. SKN (National Board for Spent Nuclear Fuel) Rapport 43, Stockholm, Sweden.

Hökmark H, 1990. Distinct element method modeling of fracture behavior in near-field rock. Stripa Project TR 91-01, Svensk Kärnbränslehantering AB.

Hökmark H, Israelsson J, 1991. Distinct element modelling of joint behavior in nearfield rock. Stripa Project TR 91-22, Svensk Kärnbränslehantering AB.

Hökmark H, 1996. Canister Positioning. Stage 1 Thermomechanical Nearfield Rock Analysis. SKB AR D-96-014, Svensk Kärnbränslehantering AB.

Israelsson J, 1995. Global Thermo-Mechanical Effects from a KBS-3 Type Repository. Phase 1: Elastic analyses. SKB PR D-95-008, Svensk Kärnbränslehantering AB.

Israelsson J, 1996. Global Thermo-Mechanical Effects from a KBS-3 Type Repository. Phase 2: Three dimensional modelling with major fracture zones – base. SKB PR D-96-006, Svensk Kärnbränslehantering AB.

Jaimson B, Cook N G, 1978. An analysis of measured values for the state of stress in the Earth's crust. Report LBL-7071, SAC-07, Lawrence Berkeley Laboratory, Berkeley, California.

Jarsjö J, 1998. Hydraulic conductivity relations in soil and fractured rock: Fluid component and phase interaction effects. Doctoral Thesis, Dep. of Civil and Environmental Eng. TRITA- AMI PHD 1019, Royal Institute of Technology, Stockholm, Sweden.

Johansson E, Hakala M, Lorig L, 1991. Rock mechanical, thermomechanical and hydraulic behaviour of the near field for spent nuclear fuel. Report YJT-91-21. Nuclear Waste Commission of Finnish Power Companies, Helsingfors, Finland.

Johansson E, Hakala M, 1995. Rock mechanical aspects on the critical depth for a KBS-3 type repository based on brittle rock strength criterion developed at URL in Canada. SKB AR D-95-014, Svensk Kärnbränslehantering AB.

Kijko A, Skorda E, Wahlström R, Mäntyniemi P, 1993. Maximum likelihood estimation of seismic hazard for Sweden. Natural Hazards, Vol. 7, 41–57.

Kim J I, Delakowitz B, Zeh P, Probst T, Lin X, Ehrlicher U, Schauer C, Ivanovich M, Longworth G, Hasler S. E, Gardiner M, Fritz P, Klotz D, Lazik D, Wolf M, Geyer S, Alexander J L, Read D, Thomas J B, 1996. Colloid migration in groundwaters: geochemical interactions of radionuclides with natural colloids. EUR 16754 EN.

Knutsson G, Morfeldt C-G, 1995. Grundvatten. Teori & tillämpning, Svensk Byggtjänst, Stockholm, Sweden.

- Kotelnikova S, Pedersen K, 1998.** Microbial oxygen consumption in Äspö tunnel environments. SKB PR HRL-98-11, Svensk Kärnbränslehantering AB.
- Kukkonen I, Lindberg A, 1995.** Thermal conductivity of rocks at the TVO investigation sites Olkiluoto, Romuvaara and Kivetty. Report YJT-95-08, Nuclear Waste Commission of Finnish Power Companies, Helsinki, Finland.
- La Pointe P, Wallmann P, Thomas A, Follin S, 1997.** A methodology to estimate earthquake effects on fractures intersecting canister holes. SKB TR 97-07, Svensk Kärnbränslehantering AB.
- La Pointe P, Cladouhos T, Follin S, 1998.** Calculation of displacements on fractures intersecting canisters induced by earthquakes: Aberg, Beberg and Ceberg Examples (in preparation).
- Laaksoharju M, Vuorinen U, Snellman M, Allard B, Pettersson C, Helenius J, Hinkkanen H, 1993.** Colloids or artefacts? A TVO/SKB co-operation project in Olkiluoto, Finland. SKB TR 93-32, Svensk Kärnbränslehantering AB.
- Laaksoharju M (ed.), 1995.** Sulphate reduction in the Äspö HRL tunnel. SKB TR 95-25, Svensk Kärnbränslehantering AB.
- Laaksoharju M, Degueldre C, Skårman C, 1995a.** Studies of colloids and their importance for repository performance assessment. SKB TR 95-24, Svensk Kärnbränslehantering AB.
- Laaksoharju M, Skårman C, 1995.** Groundwater sampling and chemical characterization of the Äspö HRL tunnel in Sweden. SKB PR 25-95-29, Svensk Kärnbränslehantering AB.
- Laaksoharju M, Smellie J, Nilsson A-C, Skårman C, 1995b.** Groundwater sampling and chemical characterization of the Laxemar deep borehole KLX02. SKB TR 95-05, Svensk Kärnbränslehantering AB.
- Laaksoharju M, Wallin B, 1997.** Evolution of the groundwater chemistry at the Äspö Hard Rock Laboratory. Proceedings of the second Äspö International Geochemistry Workshop, June 6–7, 1995. SKB ICR 97-04, Svensk Kärnbränslehantering AB.
- Laaksoharju M, Gurban I, Skårman C, 1998.** Summary of hydrochemical conditions at Aberg, Beberg and Ceberg. Intera KB, Sollentuna, Sweden.
- Laaksoharju M, Gurban I, Andersson C, 1999.** Indications of the origin and evolution of the groundwater at Palmottu. The EU Palmottu natural analogue project. SKB TR-99-xx-xx, Svensk Kärnbränslehantering AB (in print).
- Landström O, Tullborg E-L, 1990.** The influence of fracture mineral/groundwater interaction on the mobility of U, Th, REE and other trace elements. SKB TR 90-37, Svensk Kärnbränslehantering AB.
- Landström O, Tullborg E-L, 1995.** Interactions of trace elements with fracture filling minerals from the Äspö Hard Rock Laboratory. SKB TR 95-13, Svensk Kärnbränslehantering AB.
- Larsson A, Pers K, Skagius K, Dverstorp B (eds.) 1997.** The International INTRAVAL Project. Phase 2, Summary report. OECD/NEA – SKI.

- Lau J O S, Jackson R, Gorski B, 1991.** The effects of temperature and pressure on the mechanical properties of Lac du Bonnet grey granite. In Roegiers (ed.): *Rock Mechanics as a Multidisciplinary Science*, Balkema, Rotterdam.
- Leijon B, 1993.** Mechanical properties of fracture zones. SKB TR 93-19, Svensk Kärnbränslehantering AB.
- Leijon B, 1995.** Summary of rock stress data from Äspö. SKB PR 25-95-15, Svensk Kärnbränslehantering AB.
- Li Chunlin, 1993.** Deformation and failure of brittle rocks under compression. PhD Thesis, Division of Rock Mechanics, Luleå University of Technology, Luleå, Sweden.
- Ljunggren C, Klasson H, Leijon B, 1998.** Valuation of rock stress measurements at Aberg, Beberg and Ceberg. Svensk Kärnbränslehantering AB.
- Long J C S, Gilmour P, Witherspoon P A, 1985.** A model for steady state flow in random three-dimensional networks of disc-shaped fracture. *Water Resour. Res.* 21(8), 1105–1115.
- Löfman J, Taivassalo V, 1995.** Simulations of pressure and salinity fields at Äspö. SKB ICR 95-01, Svensk Kärnbränslehantering AB.
- Malmström M, Banwart S, Duro L, Wersin P, Bruno J, 1995.** Biotite and chlorite weathering at 25 °C. SKB TR 95-01, Svensk Kärnbränslehantering AB.
- de Marsily G, 1986.** Quantitative hydrogeology. *Groundwater hydrology for engineers*, Academic Press, Inc., New York.
- Martin D, 1994.** TVO & SKB Workshop on Brittle Rock Strength. SKB AR 94-59, Svensk Kärnbränslehantering AB.
- Martino J B, Read R S, 1995.** Mine-By Experiment Phase III – Heated Failure Tests. Technical Progress Report and Summary of Stage 3. AECL, Whiteshell Laboratories, Pinnawa, Manitoba.
- Miller W, Alexander A, Chapman N, McKinley I, Smellie J, 1994.** Natural analogue studies in the geological disposal of radioactive wastes, Elsevier, Amsterdam.
- Milnes A G, Gee D G, 1992.** Bedrock stability in southeastern Sweden. Evidence from fracturing in the ordovician limestones of northern Öland. SKB TR 92-23, Svensk Kärnbränslehantering AB.
- Morén L, Ritchey T, Stenström M, 1998.** Scenarier baserade på mänskliga handlingar. SKB R-98-54, Svensk Kärnbränslehantering AB.
- Moreno L, Gylling B, Neretnieks I, 1995.** Solute transport in fractured media. The important mechanisms for performance assessment. SKB TR 95-11, Svensk Kärnbränslehantering AB.
- Muir-Wood R, 1993.** A review of the seismotectonics of Sweden. SKB Technical Report TR 93-13, Svensk Kärnbränslehantering AB.
- Muir-Wood R, 1995.** Reconstructing the tectonic history of Fennoscandia from its margins: The past 100 million years. SKB TR 95-36, Svensk Kärnbränslehantering AB.

- National Research Council, 1996.** Rock fractures and fluid flow. Contemporary understanding and applications. National Academy Press, Washington, D.C., U S A.
- Neretnieks I, 1980.** Diffusion in the rock matrix: An important factor in radionuclide retardation?, *J. Geophysical Research*, vol. 85, no. B8, pp. 4379–4397.
- Neretnieks I, Ernstson M-L, 1997.** A note on radionuclide transport by gas bubbles, *Mat. Res. Soc. Symp. Proc.*, vol. 465, pp. 855–862.
- Nordqvist A W, 1995.** Discrete modeling of solute transport in rocks with variable aperture fractures. Doctoral Thesis, Dep. of Civil and Environmental Eng. TRITA-AMI PHD 1004, Royal Institute of Technology, Stockholm, Sweden.
- Nordstrom D K, McNutt R H, Puigdomènech I, Smellie J A T, Wolf M, 1992.** Ground water chemistry and geochemical modeling of water-rock interactions at the Osamu Utsumi mine and the Morro do Ferro analogue study sites, Poços de Caldas, Minas Gerais, Brazil. *Journal of Geochemical Exploration*, 45 (1992) 259–287, Elsevier Science Publishers B V, Amsterdam.
- Norman S, Kjellbert N, 1990.** FARF31 – A far field radionuclide migration code for use with the PROPER package. SKB TR 90-01, Svensk Kärnbränslehantering AB.
- Norman S, 1992.** HYDRASTAR – a code for stochastic simulation of groundwater flow. SKB TR 92-12, Svensk Kärnbränslehantering AB.
- Ohlsson Y, Neretnieks I, 1997,** Diffusion data in granite, Recommended values. SKB TR 97-20, Svensk Kärnbränslehantering AB.
- Olin M, Lehikoinen J, 1997.** Application of surface complexation modelling: Nickel sorption on quartz, manganese oxide, kaolinite and goethite, and thorium on silica, POSIVA 97-10, Helsinki, Finland.
- Olsson O (ed.), 1992.** Site characterization and validation – Final report. SKB TR 92-22, Svensk Kärnbränslehantering AB.
- Olsson O, 1994.** Test plan for degassing of groundwater and two phase flow. Release 1.0. SKB PR 25-94-34, Svensk Kärnbränslehantering AB.
- Olsson O, Neretnieks I, Cvetkovic V, 1994.** Deliberations on radionuclide transport and rationale for tracer transport experiments to be performed at Äspö. A selection of papers. SKB PR 25-95-01, Svensk Kärnbränslehantering AB.
- Olsson O, Gale J E, 1995.** Site assessment and characterization for high-level nuclear waste disposal: results from the Stripa Project, Sweden. *Quarterly Journal of Engineering Geology*, vol. 28, suppl. 1, pp. S17–S30.
- Olsson O, Emsley S, Bauer C, Falls S, Stenberg L, 1996.** ZEDEX – a study of the zones of disturbance for blasted and bored tunnels. SKB ICR 96-03, Svensk Kärnbränslehantering AB.
- Olsson O, Winberg A, 1996.** Current understanding of extent and properties of the excavation disturbed zone and its dependence of excavation method. In: J.B. Martino and C.D. Martin (eds.): *Proceedings of the Excavation Disturbed Zone Workshop*. Canadian Nuclear Society, Toronto, Ontario, Canada.

- Olsson R, 1998.** Mechanical and hydromechanical behavior of hard rock joints. PhD Thesis, Chalmers University of Technology, Göteborg, Sweden.
- Pedersen K, Karlsson F, 1995.** Investigation of subterranean micro-organisms. Their importance for performance assessment of radioactive waste disposal. SKB TR 95-10, Svensk Kärnbränslehantering AB.
- Pedersen K, 1997.** Investigations of subterranean microorganisms and their importance for performance assessment of radioactive waste disposal. Results and conclusions achieved during the period 1995 to 1997. SKB TR 97-22, pp 1-280, Svensk Kärnbränslehantering AB.
- Pirhonen V, Pitkänen P, 1991.** Redox capacity of crystalline rocks. Laboratory studies under 100 bar oxygen gas pressure. SKB TR 91-55, Svensk Kärnbränslehantering AB.
- Pitkänen P, Lukkonen A, Ruotsalainen P, Leino-Forsman H, Vuorinen U, 1998.** Geochemical modelling of groundwater evolution and residence time at Olkiluoto site. Helsinki, Finland: Report POSIVA 98- (to be published).
- Plummer L N, Prestemon E C, Parkhurst D L, 1991.** An interactive code (NETPATH) for modelling NET geochemical reactions along a flow path. US Geological Survey, Water-Resources Investigation Report 91-4078.
- Pollard D D, Segall P, 1987.** Theoretical displacements and stresses near fractures in rock: with applications to faults, joints, veins, dikes, and solution surfaces. Fracture Mechanics of Rock, Academic Press Inc. Ltd., London.
- Probert T, Claesson J, 1997.** Thermoelastic stress due to a rectangular heat source in a semi-infinite medium. Application for the KBS-3 Repository. SKB TR 97-26, Svensk Kärnbränslehantering AB.
- Probert T, 1998.** The underground as a storage facility. Modelling of Nuclear Waste Repositories and Aquifer Thermal Energy Stores. Doctoral Thesis, Lund-MPh-98/02, Department of Mathematical Physics. Lund Institute of Technology, Lund, Sweden.
- Puigdomenech I, Banwart S A, Bateman K, Milodowski A E, West J M, Griffault L, Gustafsson E, Hama K, Yoshida H, Kotelnikova S, Pedersen K, Lartigue J-E, Michaud V, Trotignon L, Morosini M, Rivas Perez J, Tullborg E-L, 1998.** Redox experiment in detailed scale (REX). First project status report. SKB-ICR-99-01-SE, Svensk Kärnbränslehantering AB.
- Pusch R, Hökmark H, 1993.** Mechanisms and consequences of creep in the nearfield rock of a KBS-3 repository. SKB TR 93-10, Svensk Kärnbränslehantering AB.
- Pusch R, 1996.** JADE, Jämförelse av bergmekaniska funktionssätt hos KBS3-V, KBS3-H och MLH. Underlagsrapport för konceptjämförelse. Clay Technology AB, Lund, Sweden.
- Rasilainen K, 1997.** Matrix diffusion model. In situ tests using natural analogues, VTT Publications 331, Technical Research Centre of Finland, Espoo, Finland.
- Rehbinder G, Yakubenko P A, 1998.** Displacements and flexural stresses of a loaded elastic plate on a viscous liquid. SKB PR U-98-04, Svensk Kärnbränslehantering AB.

- Rhén I, Svensson U, Andersson J-E, Andersson P, Eriksson C-O, Gustafsson E, Ittner T, Nordqvist R, 1992.** Äspö Hard Rock Laboratory. Evaluation of the combined longterm pumping and tracer test (LPT2) in borehole KAS06. SKB TR 92-32, Svensk Kärnbränslehantering AB.
- Rhén I (ed.), Gustafsson G, Stanfors R, Wikberg P, 1997.** Äspö HRL – Geoscientific evaluation 1997/5. Models based on site characterization 1986–1995. SKB TR 97-06, Svensk Kärnbränslehantering AB.
- Rosengren L, Stephansson O, 1999.** Distinct element modelling of the rock mass response to glaciation at Finnsjön, central Sweden. SKB TR 90-40, Svensk Kärnbränslehantering AB.
- Rummel F, 1997.** Determination of rock mechanics parameters of the granite at the Äspö Hard Rock Laboratory, Sweden. Äspö Hard Rock Laboratory Technical Note TN-97-13z.
- Scholz C H, 1990.** The mechanics of earthquakes and faulting. Cambridge University Press, Cambridge.
- Shen B, Stephansson O, 1990a.** Modelling of rock mass response to repository excavations, thermal loading from radioactive waste and swelling pressure of buffer material. SKI Technical Report 90:12, Swedish Nuclear Power Inspectorate, Stockholm, Sweden.
- Shen B, Stephansson O, 1990b.** 3DEC mechanical and thermomechanical analysis of glaciation and thermal loading of a waste repository. SKI Technical Report 90:3, Swedish Nuclear Power Inspectorate, Stockholm, Sweden.
- Shen B, Stephansson O, 1996a.** SITE-94. Modelling of rock fracture propagation for nuclear waste disposal. SKI Report 96:18, Swedish Nuclear Power Inspectorate, Stockholm, Sweden.
- Shen B, Stephansson O, 1996b.** SITE-94. Near-field rock mechanical modelling for nuclear waste disposal. SKI Report 96:17, Swedish Nuclear Power Inspectorate, Stockholm, Sweden.
- Sherwood Lollar B, Frapé S K, Fritz P, Macko S A, Welhan J A, Blomqvist R, Lahermo P W, 1993.** Evidence for bacterially generated hydrocarbon gas in Canadian shield and Fennoscandian shield rocks. *Geochimica et Cosmochimica Acta* (57) 5073–5085.
- Skagius K, Neretnieks I, 1985.** Porosities and diffusivities of some non-sorbing species in crystalline rocks. SKB TR 85-03. Svensk Kärnbränslehantering AB
- Skagius K, 1986.** Diffusion of dissolved species in the matrix of some Swedish crystalline rocks, PhD Thesis. Department of Chemical Engineering, Royal Institute of Technology, Stockholm, Sweden.
- SKB 91, 1992.** Final disposal of spent nuclear fuel. Importance of the bedrock for safety. SKB TR 92-20, Svensk Kärnbränslehantering AB.
- SKB, 1995.** SR 95 Template for safety reports with descriptive example. Svensk Kärnbränslehantering AB.

SKB, 1995. R&D-Programme 95, Parts I-II. Treatment and final disposal of nuclear waste. Programme for encapsulation, deep geological disposal and research, development and demonstration. Svensk Kärnbränslehantering AB.

Smellie J, Larsson N-Å, Wikberg P, Carlsson L, 1985. Hydrochemical investigations in crystalline bedrock in relation to existing hydraulic conditions: Experiences from the SKB test sites in Sweden. SKB TR 85-11, Svensk Kärnbränslehantering AB.

Smellie J A T, Laaksoharju M, 1992. The Äspö Hard Rock Laboratory. Final evaluation of the hydrogeochemical pre-investigations in relation to existing geologic and hydraulic conditions. SKB TR 92-31, Svensk Kärnbränslehantering AB.

Smellie J (ed.), 1998. Maqarin natural analogue study: Phase III. SKB TR-98-04, Swedish Nuclear Fuel and Waste Management Co.

Stanfors R, Ericsson L O, 1993. Post-glacial faulting in the Lansjärv area, northern Sweden. Comments from the expert group on a field visit at the Molberget post-glacial fault area. SKB TR 93-11, Svensk Kärnbränslehantering AB.

Stephansson O, Jing L, Tsang C F (eds.), 1996. Coupled Thermo-Hydro-Mechanical Processes of Fractured Media Developments in Geotechnical Engineering, Vol. 79, Elsevier Science B. V., Amsterdam.

Stille H, Olsson P, 1996. Summary of rock mechanical results from the construction of Äspö Hard Rock Laboratory. SKB PR HRL 96-07, Svensk Kärnbränslehantering AB.

Stumm W, Morgan J, 1981. Aquatic Chemistry, 2nd ed. Wiley Interscience Publishers.

Sundberg J, 1995. Termiska egenskaper för kristallint berg i Sverige. Kartor över värmekonduktivitet, värmeflöde och temperatur på 500 m djup. SKB PR D-95-018, Svensk Kärnbränslehantering AB.

Sundberg J, Gabrielsson A, 1998. Field measurements of thermal properties of the rocks in the prototype repository at Äspö HRL. SKB PR HRL-98-28, Svensk Kärnbränslehantering AB.

Svensson U, 1997a. A regional analysis of groundwater flow and salinity distribution in the Äspö area. SKB TR 97-09, Svensk Kärnbränslehantering AB.

Svensson U, 1997b. A site scale analysis of groundwater flow and salinity distribution in the Äspö area. SKB TR 97-17, Svensk Kärnbränslehantering AB.

Svensson U, 1999. Subglacial groundwater flow at Äspö as governed by basal melting and ice tunnels. SKB R-99-38, Svensk Kärnbränslehantering AB.

Swan G, 1978. The Mechanical Properties of Stripa Granite. Swedish American Program on Radioactive Waste in Mined Caverns in Crystalline Rock. Report SAC-03, Lawrence Berkeley Laboratories, Berkeley, California.

Thunvik R, Braester C, 1980. Hydrothermal conditions around a radioactive waste repository. SKBF/KBS TR 80-19. Svensk Kärnbränsleförsörjning AB.

Thunvik R, Braester C, 1991. Heat propagation from a radioactive waste repository. SKB TR 91-61, Svensk Kärnbränslehantering AB.

- Toulhoat P, Beaucaire C, Michard G, Ouzounian G, 1992.** Chemical evolution of deep groundwater in granites, Information acquired from natural systems. Paleohydrogeological methods and their applications. Proceedings from an NEA workshop 9–10 November, 1992.
- Tullborg E-L, Wallin B, Landström O, 1991.** Hydrogeochemical studies of fracture minerals from water conducting fractures and deep groundwaters at Äspö. SKB PR 25-90-01, Svensk Kärnbränslehantering AB.
- Turcotte D L, 1992.** Fractals and chaos in geology and geophysics. Cambridge University Press, Great Britain.
- Voss C I, Andersson J, 1993.** Regional flow in the Baltic shield during Holocene coastal regression. *Groundwater*, Vol. 31, No. 6, p 989-1006.
- Wallin B, 1995:** Paleohydrological implications in the Baltic area and its relation to the groundwater at Äspö, south-eastern Sweden – A literature study. SKB TR 95-06, Svensk Kärnbränslehantering AB.
- Wan J, Wilson J L, 1994a.** Colloid transport in unsaturated porous media. *Water Resources Research*, vol. 30, no. 4, pp. 854–864.
- Wan J, Wilson J L, 1994b.** Visualization of the role of gas-water interface on the fate and transport of colloids in porous media. *Water Resources Research*, vol. 30, no. 1, pp. 11–23.
- Wannäs K, Flodén T, 1994.** Tectonic framework of the Hanö Bay area, southern Baltic Sea. SKB TR 94-09, Svensk Kärnbränslehantering AB.
- Wersin P, Bruno J, Laaksoharju M, 1994.** The implication of soil acidification on a future HLW repository. SKB TR 94-31, Svensk Kärnbränslehantering AB.
- Wikberg P, Axelsen K, Fredlund F, 1987.** Deep groundwater in crystalline rock. SKB TR 87-07, Svensk Kärnbränslehantering AB.
- Wikberg P (ed.), Gustafson G, Rhén I, Stanfors R, 1991.** Äspö Hard Rock Laboratory. Evaluation and conceptual modelling based on the pre-investigations. SKB TR 91-22, Svensk Kärnbränslehantering AB.
- Wikramaratna R S, Goodfield M, Rodwell W R, Nash P J, Agg P J, 1993.** A preliminary assessment of gas migration from the Copper/Steel Canister. SKB TR 93-31, Svensk Kärnbränslehantering AB.
- Winberg A (ed.), Andersson P, Hermansson J, Byegård J, Cvetkovic V, 1999.** Final report of the First stage of the Tracer Retention Understanding Experiments. SKB TR-99-XX, Svensk Kärnbränslehantering AB (in preparation).

ISSN 1404-0344

Norstedts Tryckeri, 1999